Axiomatic/Asymptotic Analysis and Best Theory Diagrams for Laminated Plates/Shells Loaded by Mechanical, Thermal and Electrical Loadings

Politecnico di Torino

PhD dissertation

Axiomatic/Asymptotic Analysis and Best Theory Diagrams for Laminated Plates/Shells Loaded by Mechanical, Thermal and Electrical Loadings

Author:
Alessandro Lamberti

Supervisors:
Prof. Erasmo Carrera
Dr. Maria Cinefra
Dr. Marco Petrolo

Contents

List of Figures

List of Tables

Summary

A structural model can be defined as accurate if its response is in accordance with the reality. The accuracy of a model depends on the initial hypotheses which, in general, are related to the geometry, the displacement field and to the material response to the external loads.

In the field of geometrical approximations, a plate or shell model can be employed when a structure has two dimensions prevalent on the third dimension. The use of a shell model is necessary when the curvature of a bidimensional structure is significant, as a matter of fact a plate can be considered as a shell with infinite curvature. The definition of the displacement field for a plate or a shell plays and important role in the accuracy of a model. A number of theories are available, which are based on different assumptions. In the scientific literature Kirchoff's, Reissner-Mindlin's models are addressed as classical theories for plate analysis while Love's models is addressed as classical model for shell analysis.

In the last decades, the use of non-conventional materials such as carbon fiber reinforced laminates, metallic foams or layered ceramic-metallic structures has become very common in several engineering sectors. These particular materials make it possible to obtain very light and resistant structures: these characteristics are really appreciated in the aerospace sector. A plate/shell can be made of several layers of non-conventional materials: in this case, the plate /shell is defined as multilayered. The classical models can be profitably employed to analyze thin one-layered structures, but the same models are not proper to analyze the mechanical behavior of multilayered plates/shells since the complicated effects that take place in a multilayered structure are not considered in the classical models.

A further complication in the analysis of multilyered structures, comes from the different nature of the loads that can act on a structure. As an example, a space vehicle can be subjected to a mechanical and thermal load in the same time, or a structure can be subjected to a thermal and electric loads combined together. In this case, an accurate structural model should be able to incorporate the combined action of different type of

loads: these type of problems are referred as multifield problems.

A possibility to overcome the limitations of classical models and to take into account multifield problems can come from the use the Carrera Unified Formulation (CUF). According to the CUF, the unknown variables are described via expansions of the thickness coordinate of the plate/shell. The expansion order is a free parameter of the analysis. Stiffness, mass and loading arrays are obtained through a set of fundamental nuclei whose form does not depend on either the expansion order nor on the choice made for the base functions. The CUF has been employed according to the Equivalent Single Layer (ESL) and Layer Wise (LW) schemes: the former scheme analyze a plate/shell as an equivalent single layer, the former approach considers separately each layer. Analytical models have been implemented and considered in this work.

The equilibrium equations for plates and shells can be obtained by means of two different variational statements: the Principle of Virtual Displacement (PVD) and the Reissner Mixed Variational Theorem (RMVT). The PVD assumes a displacement field and puts the 3D indefinite equilibrium and the related equilibrium conditions at the boundary surfaces into a variational form. Refined bidimensional models can be obtained by means of this variational statement. Multifiled problems can be obtained by adding the thermal and electrical contributions to the PVD for the pure-mechanical case. Mixed plate/shell models can be obtained if some variables which cannot be obtained correctly via post-processing (e.g transverse shear/normal stresses and normal electric displacement) are assumed a-priori. The RMVT is obtained from the PVD by adding opportune Lagrange multipliers and coherently rewriting the constitutive equations. A description of the classical plate and shell models, of the CUF and the variational statements is reported in the first part of this thesis.

In general, better accuracy can be obtained in the field of plates and shells analysis by employing higher expansion order. As a drawback, higher computational cost is required with respect to classical formulations. The possibility to lower the computational cost without loosing in accuracy can come from the use of the axiomatic/asymptotic technique which aims to retain the non-relevant terms from a refined model. This technique makes it possible to analyze the relevance of a model variable by computing the error introduced with its suppression. The error is measure with respect to a reference solution. The relevance of a term depends on the displacement/stress component considered, on the geometry of the plate/shell and on the type of material. The axiomatic/asymptotic technique and the results related to the plate/shell models for multifield cases are described in the second part of this thesis.

A number of parameters affect the number of the retained variables, in particular the level of accuracy of the model. As the accuracy of a bidimensional model varies, the number of the retained terms may differ. A synthetic information of this fact is provided

by the Best Theory Diagram, which reports in a "error vs term-number" (E/NDOFs) Cartesian plane the effectiveness of a given theory in terms of accuracy and computational cost. The BTD represents the best theory for a given error, that is the least cumbersome theory for a specific case. This type of graph is obtained by means of the axiomatic/asymptotic technique, but differently from the previous cases the effectiveness of an entire sequence of active/non-active terms is considered. A genetic algorithm is employed to obtain the term combination for a specific plate/shell case without computing the error of all possible terms combination. The third and last part of this thesis is devoted to introduce and comment BTDs for multifield problems.

Part I

Plate and shell analysis

Chapter 1

Introduction

Plate and shell analysis is based on several models which exhibit different level of accuracy. A number of assumptions can be adopted which can be proper or not depending on the problem analyzed. In general, less restrictive assumptions offer the possibility to perform an accurate analysis. An accurate bidimensional model should be able to consider a multilayered plate/shell and multifield problems. Plates and shells can be made of different layers, in this case these structures are defined as multilayered. In general the material properties can be different form one layer to another one, since homogeneous isotropic, orthotropic and piezoelectric materials can be employed. In this case, refined models offer better accuracy than the classical formulations. A plate or shell structure can be subjected to different loads, as a mechanical transverse pressure, a temperature distribution (thermal load) or, in the case piezoelectric materials are employed, an electric potential distribution (piezoelectric load).

A structural analysis can be performed by assuming some hypothesis on the solid under exam. In general, these assumptions regard about, for example, the geometry and the material behavior. In the field of geometric assumptions, plates and shells configurations can be assumed. A shell can be defined as a three-dimensional body bounded by two closely spaced curved surfaces [1]; in this case two dimensions are prevalent with respect to the remaining third dimensions which can be defined as the distance between the two surfaces. Shells are defined on the basis of a reference curved surface, which can be described as the locus of points which lie midway between these surfaces. An example of shell is reported in Fig. 1.1(a) where the midsurface is Ω and its boundary is denote as Γ. The reference system used to analyze the shell is denoted as $\alpha - \beta - z$, α and β belong on the surface Ω. The third coordinate z is normal to the surface Ω. The thickness of the shell is equal to h and it is measured along the z axis.

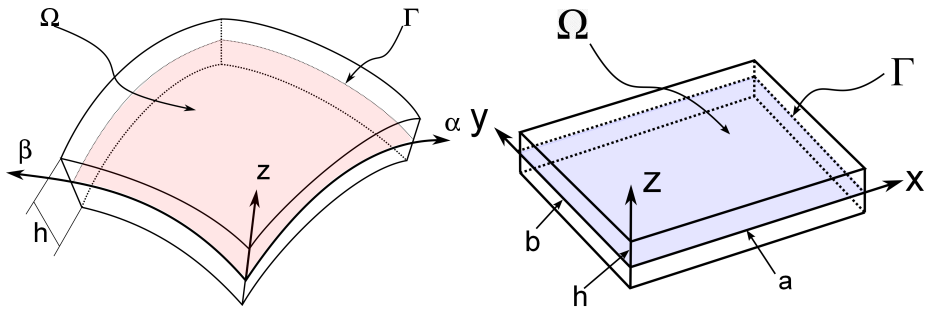

(a) Shell geometry (b) Plate geometry

Figure 1.1: Shell and plate geometry and notation.

A plate can be considered as a special case of shell, that is a shell with no curvature. An example of plate is reported in Fig. 1.1(b). The midsurface is denoted as Ω and its boundary as Γ. A Cartesian reference system is employed to describe the plate, the reference axes x and y belong to the surface Ω and the third coordinate is normal to Ω. The length and the width of the plate are denoted as a and b respectively, the thickness is denoted as

1.1 Shell/plate structural models

The analysis of the deformation process for a plate/shell is based on the definition of the displacement field. In the field of classical models, it is possible to mention the so-called Love First Approximation Theories (LFAT) which will be discussed in the following. These assumptions are based on the well-known Cauchy, Poisson, Kirchhoff and Love thin shell assumptions ([2], [3], [4], [5]). An improvement of the LFAT can be obtained if at least one or more hypotheses are removed. This is the case of the Love Second Approximation Theories (LSAT). These models were developed considering single-layer isotropic structures. In the recent years new materials were employed in shells and plates structures. In particular, multilayered plates and shells became common in use: these structures are made of several layers whose material properties can be different from one to another. An example of multilayered plate is reported in Fig. 1.2.

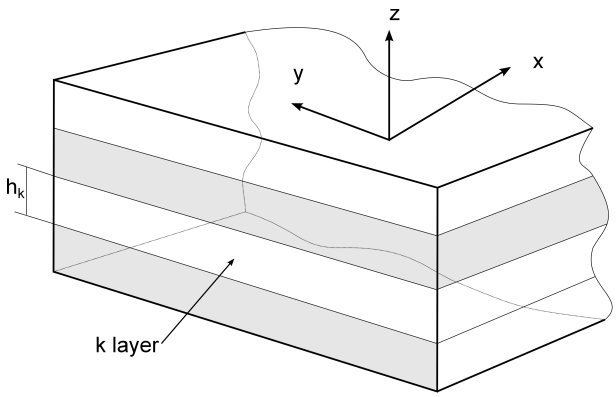

Figure 1.2: Multilayered plate configuration.

The thickness of layer k is denoted as h_k. The evaluation of transverse stresses can be relevant for the analysis of failure of such a structure. Classical models are not efficient for the analysis of such structures since they do not take into account these stresses. In a multilayered shell/plate structure, transverse stress and displacement components are continuous functions with z direction; these significant peculiarities of layered structures were defined as C_z^0-requirement in [6]: the zig-zag form of the displacement components along the thickness coordinate is defined as Zig-Zag effect (ZZ) and the transverse stresses continuity at the interfaces is defined as Interlaminar-Continuity (IC).

A complete overview on laminated shell structures contributions can be found in the many survey articles and books available in the scientific literature, among them the works of Ambartsumin [7, 8, 9], Grigolyuk and Kogan [10], Kapania [11], Grigolyuk and Kulikov [12], Norr and alii [13], Fettahlioglu and Steele [14], Berdichevsky [15], Berdichevskyand and Misyura [16] , Carrera [17, 18, 19, 20] and the book by Reddy [21]. In addition an in-depth analysis of plate models can be found in the excellent works written by Ambartsumian [22], Librescu and Reddy [23] and Noor and Burton [24].

It has to be highlighted that a distinction among plate models can be considered. As reported in the work of J. Reddy [21] it is possible to define the Equivalent Single Layer (ESL) and the Layer Wise (LW) approaches. According to the ESL approach a plate/shell model can be analyzed considering it as a single equivalent lamina. In this case the number of unknown is independent of the number of layers of the plate/shell. In the LW approach the displacement field is defined as a continuous function with the thickness direction. In this case the number of unknown depends on the number of the layer of a plate/shell.

1.2 Multifield problems

The deformation of a structure can be caused by several factors, such as a pressure distribution. In some case, a temperature distribution or piezoelectric effects may be the cause of the deformation state of a plate/shell. The inclusion of such phenomena into the structural analysis is referred as a multifield problem. These problems are of extreme interest since they are commonly present on the most recent and advanced industrial sector, such as aerospace and nuclear industries. In the following thermal and piezoelectric problems are discussed.

1.2.1 Thermal stress analysis

Whenever the operative temperature of a structure presents a significant differences in space and/or in time it is recommended to take into account the effect of the thermal stresses. As most critical case, it is possible to mention the effect of the temperature distribution on the blades of a turbine, on the external surface of hypersonic vehicles or on the walls of a nuclear reactor. In some other case the computation of thermal-mechanical response of a structure is desired since the thermal deformation can alter significantly the layout of a structure as can happen for optical mirrors or space reflector antennas. In the case a shape memory alloy is employed a correct evaluation of thermal - mechanical behavior is fundamental.

The analysis of such a phenomenon is a typical problem of the thermoelasticity. This branch of the applied mechanics is relatively young, as noted in [25]. The first paper on thermoelasticity was written by J.M.C. Duhamel, [26]. In that work, the author reported the formulation of boundary value problems and also obtained the equations for the coupling of the temperature field and the body's deformation. In the further years, other works on thermoelasticity were published. Navier's and Fouries's works should be mentioned ([27], [28]), and also F. Neumann [29] in 1885, to E. Almansi [30] in 1897, to O. Tedone [31] in 1906, and W. Voigt [32] in 1910.

Research on the thermoelasticity has been conducted in the recent years, examples are reported in [33], [34] and in [35]. In [33], the author conducted a survey on the response of flat plates to thermal loadings. Isotropic homogeneous, as well as anisotropic or heterogeneous plates were considered. The author in [34] focused on the hierarchy of composite models, predictor-corrector procedures, the effect of temperature-dependence of material properties on the response, and the sensitivity of the thermomechanical response to variations in material parameters. The work presented in [35] describes the developments of the nonlinear thermostructural analysis of laminated composite plates and shells of arbitrary geometry. Another author which

covered the thermo mechanical analysis of plate is Reddy, his book [21] can be consulted. Another interesting work is reported in [36], where the authors present an exact solution of the three-dimensional equilibrium equations for a plate under a given distributed temperature.

An important note that should be considered whenever it is intended to develop a structural model able to describe the thermal-mechanical response of a multilayered plate comes from Murakami and it is reported in [37]: "the results indicate the need for adopting a plate theory with a cubic variation of in-plane displacements in *each* layer to improve the prediction of transverse normal displacement". In other words due to the intrinsic through-the-thickness variation of the variation of the thermal loading, the author suggests to employ a Layer-Wise approach to correctly detect the deformation and stress state of a layered plate.

1.2.2 Piezo mechanic stress analysis

Piezoelectric materials when subjected to a pressure load generate a positive or negative charge distribution. This phenomenon was discovered in 1880-1881 by Curie brothers (Jacques and Pierre Curie, [38]) for some kind of natural crystals. The known material which exhibit piezoelectric properties are quartz and tourmaline (natural crystals) and some synthetic crystals such as lithium sulfate, and several kinds of polymers and polarized ceramics. The most common piezoelectric materials are the piezoceramic barium titanate ($BaTiO_3$) and piezo lead zirconate titanate (PZT).

It is possible to distinguish into direct and inverse effect: the direct effect means the generation of a distribution of charge when the piezoelectric material is subjected to a pressure load. Inverse effect, instead, means the deformation of the piezoelectric material when a electric charge is applied to it. It is worthy to note that piezoelectric materials can be used at the same time as actuators and sensors. In this case this kind of material are defined as self-sensing piezoelectric actuator.

The piezoelectric phenomenon can be explained in terms of distortion of the crystal lattice. The application of a mechanical load alters the the position of the atoms of the crystal lattice generating a charge distribution. Instead when an electric charge is applied to a piezoelectric material the heavier atoms move to the lower energy position causing the deformation of the crystal. This phenomena can occur only if the temperature is below a certain limit, called Curie temperature. Above this temperature, the piezoelectric effect disappears due to high thermal agitation. Further details on piezoelectricity can be found in the books [39], [40] and [41].

In the last 20 years the piezoelectric material were considered for the creation of *smart structures*. The direct and inverse effects of such materials can be exploited in

order to operate and as sensors (e.g. to monitor the health status of a structure) and as actuators. This kind of structures are defined as *smart structures*. In 1988 a definition of a definition of smart systems/structures was proposed ([42]):

> A system or material which has built-in or intrinsic sensor(s), actuator(s) and control mechanism(s) whereby it is capable of sensing a stimulus, responding to it in a predeterminated manner and extent, in a short/appropriate time, and reverting to its original state as soon as the stimulus is removed.

Example of application pf piezoelectric materials can be found in the monitoring of the health status of structures. The strain measure of some location can offer vital informations on the integrity status of a structure, such as a bridge. Another field of extreme interest for the application of such devices is the aeronautical and space sector, where a continuous detection of the health of a structure can help in the conduction of the maintenance operations and in avoiding the crack propagation.

The actuation of structures is another field of application of piezoelectric materials. The inverse piezoelectric effect can be used to deform piezoelectric patches embedded in a structure, as a consequence the structure itself can deform. In this case this process is defined as shape morphing. This kind of actuation offers several advantages such as the abscense of complex mechanisms and the possibility to obtain very complex shapes. The aeronautic sector can take advantage of such kind of actuation since this technology can offer the possibility to create hingeless flight surfaces with a consequent improvement of the aerodynamic of the vehicle. This can lead to increase the efficiency requirements and reduce emissions. Anyway, this technology has yet to be applied on a commercial vehicle, it has to be studied in order to verify its safety and effective advantages. Another field of application is the attenuation of vibrations thanks to their their high strain sensitivity ([43]).

Interested readers can be addressed to the paper written by Saravanos and Heyliger [44] and by Benjeddou [45] for a more complete discussion on electromechanical analysis of multilayered plates embedding piezo-layers.

Chapter 2

Preliminaries

The response of a body to applied loads can be evaluated by assuming some hypotheses. In the following it is assumed a linear elastic behavior of the materials and infinitesimal deformations are considered. The displacement state for a body is described and the strain distribution is introduced. Then, constitutive equations are reported: generalized Hooke's law is described for several type of materials.

2.1 Deformation state of an elastic body.

The displacement field of a body under the effect of a load can be defined as

$$\mathbf{u}(x_1, x_2, x_3, t) = \begin{cases} u_{x_1}(x_1, x_2, x_3, t) \\ u_{x_2}(x_1, x_2, x_3, t) \\ u_{x_3}(x_1, x_2, x_3, t) \end{cases} \tag{2.1}$$

Vector displacement $\mathbf{u}$ defines the displacement of a point P_0 in the undeformed configuration into P_0' in the deformed configuration. In Fig. 2.1 deformed and undeformed configurations of a body are reported. In addition points P_0 and P_0' are reported. The components of the displacement $\mathbf{u}$ are defined according to the Cartesian reference system reported in the same figure. If the static or quasi-static response is considered the time dependency is removed, that is

$$\mathbf{u}(x_1, x_2, x_3) = \begin{cases} u_{x_1}(x_1, x_2, x_3) \\ u_{x_2}(x_1, x_2, x_3) \\ u_{x_3}(x_1, x_2, x_3) \end{cases} \tag{2.2}$$

It is assumed that the displacement field does not show any discontinuity, i.e. no laceration and no material overlapping are present; this is the congruence condition.

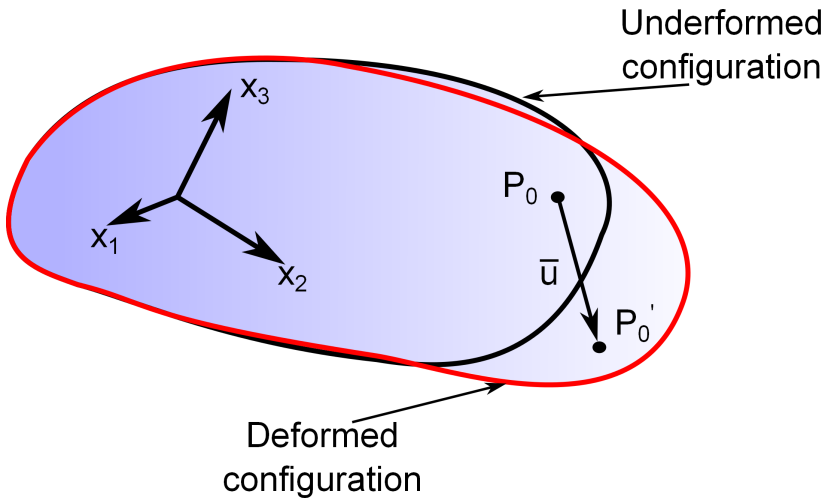

Figure 2.1: Undeformed and deformed configuration.

If the displacements are small it is possible to defined the *infinitesimal strain tensor* as

$$\epsilon_{ij} = \frac{1}{2}\left(\frac{\partial u_i}{\partial x_j} + \frac{\partial u_j}{\partial x_i}\right) \qquad i,j = 1,2,3 \tag{2.3}$$

In the following the geometrical relations for shells and plates are introduced.

2.1.1 Geometrical relations for shells

A shell is defined as a three-dimensional body bounded by two closely spaced curved surfaces [1]; in this case two dimensions are prevalent with respect to the remaining third dimensions which can be defined as the distance between the two surfaces. Shells are defined on the basis of a reference curved surface, which can be described as the locus of points which lie midway between these surfaces. An example of shell is reported in Fig. 2.2. The reference surface is denoted as Ω and its boundary as Γ. On the surface Ω the reference system $\alpha - \beta - z$ is defined. The curvature are R_α and R_β.

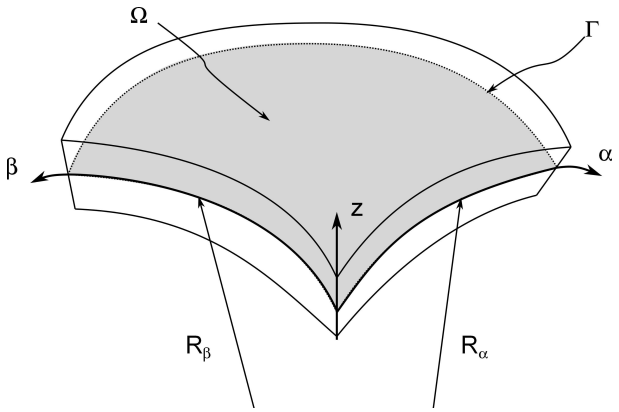

Figure 2.2: Shell configuration and notation.

The mathematical description of the deformation of a shell is based on the differential geometry relations. A complete review on this topic is reported in the book [1]. In the following few fundamental concepts are reported.

Differential relation for surfaces; first and second fundamental form The deformation of a point of the shell can be completely described once the deformation of its reference surface is known. Firstly, the displacement of the points of a generic surface has to be described. Let us consider a generic surface Ω_0, as reported in Fig. 2.3.

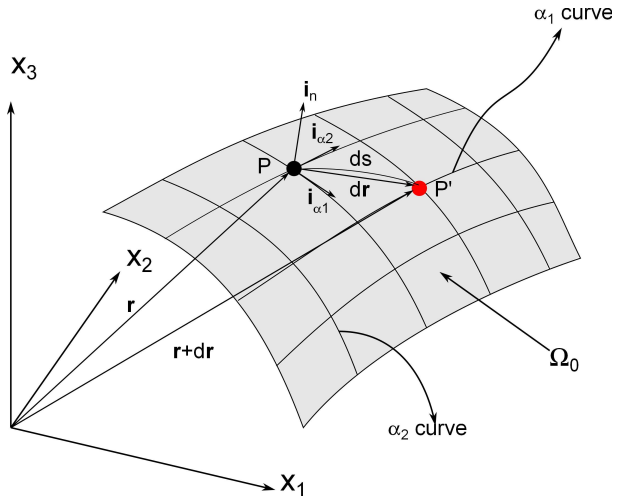

Figure 2.3: Middle surface coordinates.

Its undeformed configuration can be described by the vector $\mathbf{r}$ and two independent parameters α_1 and α_2:

$$\mathbf{r} = \mathbf{r}(\alpha_1, \alpha_2) = r_1(\alpha_1, \alpha_2)\mathbf{e}_1 + r_2(\alpha_1, \alpha_2)\mathbf{e}_2 + r_3(\alpha_1, \alpha_2)\mathbf{e}_3 \tag{2.4}$$

where $[\mathbf{e}_1\ \mathbf{e}_2\ \mathbf{e}_3]$ are an orthogonal basis for the reference system $x_1 - x_2 - x_3$ depicted in Fig. 2.3. On the surface Ω_0 it is possible to define a family of curves by fixing one parameter in turn. In Fig. 2.3 these curves are reported. These curves are defined as *parametric curves of the surface*. The vector $\mathbf{r}$ denotes a point P on the surface. A point P' located in the neighborhood of point P can be identified by the vector $\mathbf{r} + d\mathbf{r}$ as reported in Fig. 2.3. Vector $d\mathbf{r}$ can be defined as

$$d\mathbf{r} = \mathbf{r}_{,\alpha_1} d\alpha_1 + \mathbf{r}_{,\alpha_2} d\alpha_2 \tag{2.5}$$

where we have introduced the notation

$$\mathbf{r}_{,\alpha_i} = \frac{\partial \mathbf{r}}{\partial \alpha_i} \qquad i = 1, 2 \tag{2.6}$$

Vectors $\mathbf{r}_{,\alpha_1}$ and $\mathbf{r}_{,\alpha_2}$ are tangent to the parametric curves defined for α_1 and α_2 and their length is

$$|\mathbf{r}_{,\alpha_1}| = A \qquad |\mathbf{r}_{,\alpha_2}| = B \tag{2.7}$$

In this case the unit vectors tangent to the coordinate curves α_1 and α_2 can be defined as

$$\frac{\mathbf{r}_{,\alpha_1}}{A} \qquad \frac{\mathbf{r}_{,\alpha_2}}{B} \tag{2.8}$$

and it is

$$\frac{\mathbf{r}_{,\alpha_1}}{A} \cdot \frac{\mathbf{r}_{,\alpha_2}}{B} = \cos(\chi) \tag{2.9}$$

where χ is the angle between the coordinate curves α_1 and α_2. In this case an orthogonal local reference system can be defined as

$$\mathbf{i}_\alpha = \frac{\mathbf{r}_{,\alpha_1}}{A} \qquad \mathbf{i}_\beta = \frac{\mathbf{r}_{,\alpha_2}}{B} \qquad \mathbf{i}_n = \frac{\mathbf{i}_\alpha \times \mathbf{i}_\beta}{\sin(\chi)} \tag{2.10}$$

The distance of the points P and P' can be computed considering the relation above reported. Let the position of point P defined by the parameters (α_1, α_2) and the position of the point P' by $(\alpha_1 + d\alpha_1, \alpha_2 + d\alpha_2)$. The distance of the two points is

$$d\mathbf{r} = \mathbf{r}_{,\alpha_1} d\alpha_1 + \mathbf{r}_{,\alpha_2} d\alpha_2 \tag{2.11}$$

and the length is

$$\begin{aligned} d\mathbf{r} \cdot d\mathbf{r} =& (\mathbf{r}_{,\alpha_1} d\alpha_1 + \mathbf{r}_{,\alpha_2} d\alpha_2) \cdot (\mathbf{r}_{,\alpha_1} d\alpha_1 + \mathbf{r}_{,\alpha_2} d\alpha_2) \\ =& d\mathbf{r}_{,\alpha_1} \cdot d\mathbf{r}_{,\alpha_1} d\alpha_1^2 + d\mathbf{r}_{,\alpha_1} \cdot d\mathbf{r}_{,\alpha_2} d\alpha_1 d\alpha_2 + d\mathbf{r}_{,\alpha_2} \cdot d\mathbf{r}_{,\alpha_2} d\alpha_2^2 \end{aligned} \tag{2.12}$$

remembering the definition of the unit tangent vector proposed in eq. 2.8 it is possible to write

$$d\mathbf{r} \cdot d\mathbf{r} = ds^2 = A^2 \, d\alpha_1^2 + 2AB \cos(\chi) \, d\alpha_1 d\alpha_2 + B^2 d\alpha_2^2 \tag{2.13}$$

The relation reported in eq. 2.13 is defined as the *first quadratic form of the surface*. Quantities A^2, $AB\cos(\chi)$ and B^2 are called *first fundamental quantities*; it is possible to defined by means of the relation reported in eq. 2.13 the infinitesimal lengths, the angle between the curves, and the area on the surface, in other words the intrinsic geometry of the surface. In order to find the curvature of a curve which lies on the surface, the *second quadratic form of the surface* has to be introduced. A curve on a surface Ω_0 ca be defined according to the equation

$$\mathbf{r} = \mathbf{r}(s) \tag{2.14}$$

where s is the arc length from a certain origin. The unit tangent vector τ along the curve s can be defined as

$$\tau = \frac{d\mathbf{r}}{ds} = \mathbf{r}_{,\alpha_1} \frac{d\alpha_1}{ds} + \mathbf{r}_{,\alpha_2} \frac{d\alpha_2}{ds} \tag{2.15}$$

The derivation of the vector τ can be obtained by means of the Frenet's formula which states that

$$\frac{d\tau}{ds} = \frac{\mathbf{N}}{\rho} \tag{2.16}$$

where $\mathbf{N}$ is the unit vector of the principal normal to the curve and $1/\rho$ is curvature of the curve. It is

$$\begin{aligned}\frac{d\tau}{ds} =&\frac{\partial}{\partial s}\left(\mathbf{r}_{,\alpha_1}\frac{\partial\alpha_1}{\partial s}+\mathbf{r}_{,\alpha_2}\frac{\partial\alpha_2}{\partial s}\right)\\ =&\mathbf{r}_{,\alpha_1\alpha_1}\left(\frac{\partial\alpha_1}{\partial s}\right)^2+\mathbf{r}_{,\alpha_1}\frac{\partial^2\alpha_1}{\partial s^2}+\mathbf{r}_{,\alpha_1\alpha_2}\frac{\partial\alpha_1}{\partial s}\frac{\partial\alpha_2}{\partial s}+\\ &+\mathbf{r}_{,\alpha_2\alpha_2}\left(\frac{\partial\alpha_2}{\partial s}\right)^2+\mathbf{r}_{,\alpha_2}\frac{\partial^2\alpha_2}{\partial s^2}+\mathbf{r}_{,\alpha_2\alpha_1}\frac{\partial\alpha_2}{\partial s}\frac{\partial\alpha_1}{\partial s}\\ =&\mathbf{r}_{,\alpha_1\alpha_1}\left(\frac{\partial\alpha_1}{\partial s}\right)^2+\mathbf{r}_{,\alpha_2\alpha_2}\left(\frac{\partial\alpha_2}{\partial\, s}\right)^2+\mathbf{r}_{,\alpha_1}\frac{\partial^2\alpha_2}{\partial\, s^2}+\mathbf{r}_{,\alpha_2}\frac{\partial^2\alpha_1}{\partial s^2}+\\ &+2\,\mathbf{r}_{,\alpha_1\alpha_2}\frac{\partial\alpha_1}{\partial s}\frac{\partial\alpha_2}{\partial s}\end{aligned}\tag{2.17}$$

where

$$\mathbf{r}_{,\alpha_i\alpha_j}=\frac{\partial\mathbf{r}}{\partial\alpha_i\partial\alpha_j}\qquad i,j=1,2\tag{2.18}$$

In this case it is

$$\frac{\mathbf{N}}{\rho}=\mathbf{r}_{,\alpha_1\alpha_1}\left(\frac{\partial\,\alpha_1}{\partial\,s}\right)^2+\mathbf{r}_{,\alpha_2\alpha_2}\left(\frac{\partial\alpha_2}{\partial\,s}\right)^2+\mathbf{r}_{,\alpha_1}\frac{\partial^2\alpha_2}{\partial\,s^2}+\mathbf{r}_{,\alpha_2}\frac{\partial^2\alpha_1}{\partial s^2}+2\,\mathbf{r}_{,\alpha_1\alpha_2}\frac{\partial\alpha_1}{\partial s}\frac{\partial\alpha_2}{\partial s}\tag{2.19}$$

Let's define φ as the angle between the vector $\mathbf{i}_n$ and the normal $\mathbf{N}$. It is possible to write:

$$\mathbf{i}_n\cdot\mathbf{N}=\cos(\varphi)\tag{2.20}$$

If both member of equation 2.19 are scalar-multiplied by $\mathbf{i}_n$ it is

$$\frac{\cos(\varphi)}{\rho}=\frac{L\,d\alpha_1^2+2M\,d\alpha_1\,d\alpha_2+N\,d\alpha_2}{ds^2}\tag{2.21}$$

where

$$\begin{aligned}L=&\mathbf{r}_{,\alpha_1\alpha_1}\mathbf{i}_n\\ M=&\mathbf{r}_{,\alpha_1\alpha_2}\mathbf{i}_n=\mathbf{r}_{,\alpha_2\alpha_1}\mathbf{i}_n\\ N=&\mathbf{r}_{,\alpha_2\alpha_2}\mathbf{i}_n\end{aligned}\tag{2.22}$$

It is remembered that $\mathbf{r}_{,\alpha_1}\mathbf{i}_n = \mathbf{r}_{,\alpha_1}\mathbf{i}_n = 0$ since $\mathbf{r}_{,\alpha_1}$ and $\mathbf{r}_{,\alpha_2}$ are normals to $\mathbf{i}_n$. The expression $L\,d\alpha_1^2 + 2M\,d\alpha_1\,d\alpha_2 + N\,d\alpha_2$ is defined as the *second quadratic form of the surfaces*. It is possible to calculate the curvature ρ of the curves obtained by intersecting the surface with normal plan. The vectors $\mathbf{i}_n$ and $\mathbf{N}$ are either parallel ($\varphi = 0$) or have opposite directions ($\varphi = \pi$). The normal $\mathbf{i}_n$ it is considered as outer pointing, and the normal $\mathbf{N}$ Since a "plane" curve always leaves its tangent in the direction of vector $\mathbf{N}$ and if one takes its outer normal as the positive normal to the surface, $\varphi = \pi$ results. Thus the normal curvature is

$$\frac{1}{\rho} = \frac{L\,d\alpha_1^2 + 2M\,d\alpha_1\,d\alpha_2 + N\,d\alpha_2}{A^2\,d\alpha_1^2 + 2AB\cos(\chi)\,d\alpha_1 d\alpha_2 + B^2 d\alpha_2^2} \tag{2.23}$$

To obtain the curvatures of the α_1 curves and the α_2 curves take $\alpha_2 =$ constant and $\alpha_1 =$ constant respectively, thus

$$\frac{1}{R_{\alpha_1}} = -\frac{L}{A^2} \qquad \frac{1}{R_{\alpha_2}} = -\frac{N}{B^2} \tag{2.24}$$

Strain-displacement relation for shells The position of a point P in a thin shell can be defined according to the relation

$$\mathbf{R}(\alpha, \beta, z) = \mathbf{r}(\alpha, \beta) + z\mathbf{i}_n \tag{2.25}$$

where α and β express the position of the point P on the reference surface Ω, z is the distance of the point P from the reference surface Ω measured along $\mathbf{i}_n$ (see Fig. 2.2). z varies from $-h/2$ to $h/2$, where h is the thickness of the shell. The magnitude of the infinitesimal variation of the vector $\mathbf{R}$ is

$$\begin{aligned} d\mathbf{R}\cdot\, d\mathbf{R} =& (d\mathbf{r} + dz\,\mathbf{i}_n + z\,d\mathbf{i}_n)\cdot(d\mathbf{r} + dz\,\mathbf{i}_n + z\,d\mathbf{i}_n) \\ =& d\mathbf{r}\cdot d\mathbf{r} + dz d\mathbf{r}\cdot\mathbf{i}_n + z\,d\mathbf{r}\cdot\, d\mathbf{i}_n + \\ &+ dz\,\mathbf{i}_n\cdot d\mathbf{r} + dz^2\,\mathbf{i}_n\cdot\mathbf{i}_n + z\,dz\,\mathbf{i}_n\cdot d\mathbf{i}_n + \\ &+ z\,d\mathbf{i}_n\cdot d\mathbf{r} + z\,dz\,d\mathbf{i}_n\cdot\mathbf{i}_n + z^2\,d\mathbf{i}_n\cdot d\mathbf{i}_n \end{aligned} \tag{2.26}$$

Remembering the above mentioned definition of $\mathbf{i}_n$ and the chain rule derivation it is possible to state that

$$\mathbf{i}_n = \frac{\partial \mathbf{i}_n}{\partial \alpha} d\alpha + \frac{\partial \mathbf{i}_n}{\partial \beta} d\beta \tag{2.27}$$

It is possible to write

$$ds^2 = g_1 d\alpha^2 + g_2 \beta^2 + g_3 dz^2 \tag{2.28}$$

where

$$g_1 = \left[A\left(1 + \frac{z}{R_\alpha}\right)\right] \qquad g_2 = \left[B\left(1 + \frac{z}{R_\beta}\right)\right] \qquad g_3 = 1 \tag{2.29}$$

The strain - displacement relations for a shell then are

$$\begin{aligned}
\epsilon_{ii} =& \frac{\partial}{\partial \alpha_i}\left(\frac{u_i}{\sqrt{g_i}}\right) + \frac{1}{2g_i}\sum_{k=1}^{3}\frac{\partial g_i}{\partial \alpha_k}\frac{u_k}{\sqrt{g_k}} \qquad i = 1,2,3 \\
\gamma_{ij} =& \frac{1}{\sqrt{g_i g_j}}\left[g_i \frac{\partial}{\partial \alpha_j}\left(\frac{u_i}{\sqrt{g_i}}\right) + g_j \frac{\partial}{\partial \alpha_i}\left(\frac{u_j}{\sqrt{g_j}}\right)\right] \qquad i,j = 1,2,3 \;\; i \neq j
\end{aligned} \tag{2.30}$$

where ϵ_{ii} are the normal strains, γ_{ij} are the shear strains and u_i are the displacement components. The indices 1, 2 and 3 replace the coordinate reference system α, β and z. For a shell the explicit components of the metric tensor are

$$\begin{aligned}
\epsilon_{\alpha\alpha} =& \frac{1}{1+\frac{z}{R_\alpha}}\left(\frac{1}{A}\frac{\partial u_\alpha}{\partial \alpha} + \frac{u_\beta}{AB}\frac{\partial A}{\partial \beta} + \frac{u_z}{R_\alpha}\right) \\
\epsilon_{\beta\beta} =& \frac{1}{1+\frac{z}{R_\beta}}\left(\frac{u}{AB}\frac{\partial B}{\partial \alpha} + \frac{1}{B}\frac{\partial u_\beta}{\partial \beta} + \frac{u_z}{R_\beta}\right) \\
\epsilon_{\alpha\beta} =& \frac{A\left(1+\frac{z}{R_\alpha}\right)}{B\left(1+\frac{z}{R_\beta}\right)}\frac{\partial}{\partial \beta}\left[\frac{u_\alpha}{A\left(1+\frac{z}{R_\alpha}\right)}\right] + \frac{B\left(1+\frac{z}{R_\beta}\right)}{A\left(1+\frac{z}{R_\alpha}\right)}\frac{\partial}{\partial \alpha}\left[\frac{u_\beta}{B\left(1+\frac{z}{R_\beta}\right)}\right] \\
\gamma_{\alpha z} =& \frac{1}{A\left(1+\frac{z}{R_\alpha}\right)}\frac{\partial u_z}{\partial \alpha} + A\left(1+\frac{z}{R_\alpha}\right)\frac{\partial}{\partial z}\left[\frac{u_\alpha}{A\left(1+\frac{z}{R_\alpha}\right)}\right] \\
\gamma_{\beta z} =& \frac{1}{B\left(1+\frac{z}{R_\beta}\right)}\frac{\partial u_z}{\partial \beta} + B\left(1+\frac{z}{R_\beta}\right)\frac{\partial}{\partial z}\left[\frac{u_\beta}{B\left(1+\frac{z}{R_\beta}\right)}\right] \\
\epsilon_{zz} =& \frac{\partial u_z}{\partial z}
\end{aligned} \tag{2.31}$$

2.1.2 Geometrical relations for plates

Plates can be considered as particular case of shells with no curvature. In this case the the geometrical relations can be considered as a particular case of those for shells. In Fig. 2.4 the geometry and the notation of a rectangular plate is reported. The reference surface is denoted as Ω and its boundary as Γ. The reference system axes which belong to the reference surface Ω are denoted as x, y, and z is the reference axis normal to the reference surface. The length side dimensions of the plate are indicated as a and b and the thickness of the plate is defined as h.

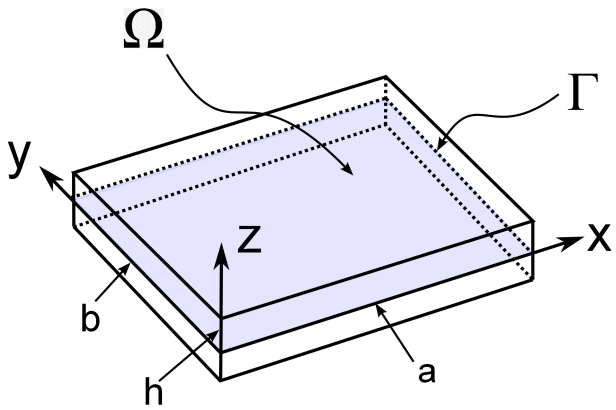

Figure 2.4: Plate configuration and notation.

Considering a Cartesian reference system as reported in Fig. 2.4, the strains can be defined as

$$\boldsymbol{\epsilon}^k = \mathbf{D}\mathbf{u}^k \tag{2.32}$$

where k denote the generic k layer of a plate and $\mathbf{D}$ is a differential operator whose components are

$$\mathbf{D} = \begin{bmatrix} \frac{\partial}{\partial x} & 0 & 0 \\ 0 & \frac{\partial}{\partial y} & 0 \\ 0 & 0 & \frac{\partial}{\partial z} \\ \frac{\partial}{\partial y} & \frac{\partial}{\partial x} & 0 \\ \frac{\partial}{\partial z} & 0 & \frac{\partial}{\partial x} \\ 0 & \frac{\partial}{\partial z} & \frac{\partial}{\partial y} \end{bmatrix} \tag{2.33}$$

Strain components can be grouped into in-plane (p) and out-of-plane (n) components, that is

$$\boldsymbol{\epsilon}_p^k = \begin{bmatrix} \epsilon_{xx}^k & \epsilon_{yy}^k & \epsilon_{xy}^k \end{bmatrix}^T \qquad \boldsymbol{\epsilon}_n^k = \begin{bmatrix} \epsilon_{xz}^k & \epsilon_{yz}^k & \epsilon_{zz}^k \end{bmatrix}^T \tag{2.34}$$

The upper script T denotes the transpose operation. In this case it is possible to write

$$\boldsymbol{\epsilon}_p^k = \mathbf{D}_p \mathbf{u}^k \qquad \boldsymbol{\epsilon}_n^k = \mathbf{D}_n \mathbf{u}^k \tag{2.35}$$

defining

$$\mathbf{D}_p = \begin{bmatrix} \frac{\partial}{\partial x} & 0 & 0 \\ 0 & \frac{\partial}{\partial y} & 0 \\ \frac{\partial}{\partial y} & \frac{\partial}{\partial x} & 0 \end{bmatrix} \tag{2.36}$$

$$\mathbf{D}_n = \begin{bmatrix} \frac{\partial}{\partial z} & 0 & \frac{\partial}{\partial x} \\ 0 & \frac{\partial}{\partial z} & \frac{\partial}{\partial y} \\ 0 & 0 & \frac{\partial}{\partial z} \end{bmatrix} = \overbrace{\begin{bmatrix} 0 & 0 & \frac{\partial}{\partial x} \\ 0 & 0 & \frac{\partial}{\partial y} \\ 0 & 0 & 0 \end{bmatrix}}^{\mathbf{D}_{n\Omega}} + \overbrace{\begin{bmatrix} \frac{\partial}{\partial z} & 0 & 0 \\ 0 & \frac{\partial}{\partial z} & 0 \\ 0 & 0 & \frac{\partial}{\partial z} \end{bmatrix}}^{\mathbf{D}_{nz}} \tag{2.37}$$

2.2 Stress - strain constitutive relations

The description of the material reaction to an applied load is obtained by means of the *constitutive equations*. In the following, elastic materials are considered that is, materials whose constitutive behavior is only a function of the current state of deformation. The material body can be divided into two categories: *heterogeneous* and *homogeneous*. The former category includes all materials whose properties vary throughout the body, the latter category includes all materials whose properties do not vary throughout the body. The material body can be defined *hyperleastic* if the work done by the stress distribution during the deformation process depends only on the initial state and the current configuration. It is possible to divide materials body as *anisotropic* if the material properties are directionally dependent, that is a material body property varies at a point according to a considered direction. A material body can be defined as *isotropic* if a material properties are not directionally dependent. A material body is defined as *ideally elastic* if it can recover its initial configuration under isothermal conditions. In this case it is possible to define a one-to-one relationship between the state of stress and the state of strain in the current configuration exists. Before introducing the constitutive relations for an elastic material let us define a material body reference system

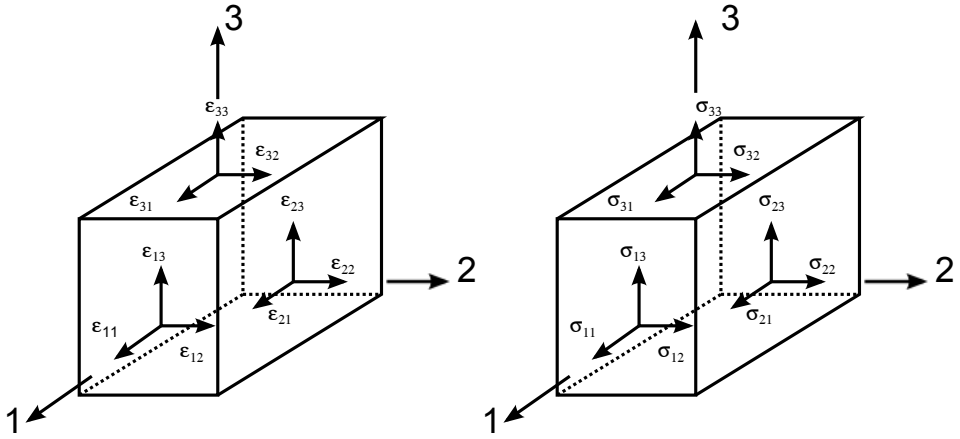

(a) Strain state (b) Stress state

Figure 2.5: Material reference system.

In Fig. 2.5 a material reference system $1-2-3$ is introduced, which can have a different orientation from the physical reference system $x_1 - x_2 - x_3$ (see Fig. 2.1). Stresses and strain are denoted as

$$\begin{aligned} \boldsymbol{\sigma}_m &= [\sigma_{11},\ \sigma_{22},\ \sigma_{33},\ \sigma_{23},\ \sigma_{13},\ \sigma_{12}] \\ \boldsymbol{\epsilon}_m &= [\epsilon_{11},\ \epsilon_{22},\ \epsilon_{33},\ \epsilon_{23},\ \epsilon_{13},\ \epsilon_{12}] \end{aligned} \tag{2.38}$$

The subscript m indicates that the stresses and strains are expressed in the material reference system. In the following he relation between the strain state and the stress state in defined according to the material reference system. For sake of brevity subscript m is omitted. The generalized Hooke's law relates the nine stress components with the nine strain components:

$$\sigma_{ij} = Q_{ijkl}\epsilon_{kl} \qquad \text{or} \qquad \boldsymbol{\sigma} = \mathbf{Q}\boldsymbol{\epsilon} \tag{2.39}$$

where Q_{ijkl} are the material elastic coefficients. Matrix $\mathbf{Q}$ is defined as *stiffness matrix*. In general 81 components have to be specified ($3^2 \times 3^2$); anyway the number of independent material elastic coefficients can be reduced if the symmetry of σ_{ij} and ϵ_{kl} is considered, as detailed in [21]. In this case the number of independent constants is reduced to 36 and it is

$$Q_{ijkl} = Q_{jikl} \quad Q_{ijkl} = Q_{ijlk} \tag{2.40}$$

In this case equation 2.39 can be written as

$$\begin{Bmatrix} \sigma_1 \\ \sigma_2 \\ \sigma_3 \\ \sigma_4 \\ \sigma_5 \\ \sigma_6 \end{Bmatrix} = \begin{bmatrix} Q_{11} & Q_{12} & Q_{13} & Q_{14} & Q_{15} & Q_{16} \\ Q_{21} & Q_{22} & Q_{23} & Q_{24} & Q_{25} & Q_{26} \\ Q_{31} & Q_{32} & Q_{33} & Q_{34} & Q_{35} & Q_{36} \\ Q_{41} & Q_{42} & Q_{43} & Q_{44} & Q_{45} & Q_{46} \\ Q_{51} & Q_{52} & Q_{53} & Q_{54} & Q_{55} & Q_{56} \\ Q_{61} & Q_{62} & Q_{63} & Q_{64} & Q_{65} & Q_{66} \end{bmatrix} \cdot \begin{Bmatrix} \epsilon_1 \\ \epsilon_2 \\ \epsilon_3 \\ \epsilon_4 \\ \epsilon_5 \\ \epsilon_6 \end{Bmatrix} \tag{2.41}$$

The equation 2.41 is written according to *contracted notation* or Voigt-Kelvin notation:

$$\sigma_1 = \sigma_{11} \quad \sigma_2 = \sigma_{22} \quad \sigma_3 = \sigma_{33} \quad \sigma_4 = \sigma_{23} \quad \sigma_5 = \sigma_{13} \quad \sigma_6 = \sigma_{12} \tag{2.42}$$

$$\epsilon_1 = \epsilon_{11} \quad \epsilon_2 = \epsilon_{22} \quad \epsilon_3 = \epsilon_{33} \quad \epsilon_4 = 2\epsilon_{23} \quad \epsilon_5 = 2\epsilon_{13} \quad \epsilon_6 = 2\epsilon_{12} \tag{2.43}$$

The number of independent elastic coefficient can be decreased if the material is considered as *hyperelastic*, that is a an strain energy density function exist which permits to state that $Q_{ijkl} = Q_{klij}$. The number of independent elastic coefficients is reduced to 21.

Monoclinic material The symmetry of the material body properties can offer a further reduction in the number of independent material coefficients. In this case, one or more material planes of symmetry exist. If the elastic coefficients have the same values for every pair of coordinate systems which are the mirror images of each other with respect to a plane, the material is defined as *monoclinic* material and it is

$$\begin{Bmatrix} \sigma_1 \\ \sigma_2 \\ \sigma_3 \\ \sigma_4 \\ \sigma_5 \\ \sigma_6 \end{Bmatrix} = \begin{bmatrix} Q_{11} & Q_{12} & Q_{13} & 0 & 0 & Q_{16} \\ Q_{21} & Q_{22} & Q_{23} & 0 & 0 & Q_{26} \\ Q_{31} & Q_{32} & Q_{33} & 0 & 0 & Q_{36} \\ 0 & 0 & 0 & Q_{44} & Q_{45} & 0 \\ 0 & 0 & 0 & Q_{45} & Q_{55} & 0 \\ Q_{16} & Q_{26} & Q_{36} & 0 & 0 & Q_{66} \end{bmatrix} \cdot \begin{Bmatrix} \epsilon_1 \\ \epsilon_2 \\ \epsilon_3 \\ \epsilon_4 \\ \epsilon_5 \\ \epsilon_6 \end{Bmatrix} \tag{2.44}$$

In this case the plane of symmetry is z and the number of independent elastic constant is equal to 13.

Orthotropic material When three mutually orthogonal symmetry plane exist the material is defined as *orthotropic*. In this case the number of independent parameters is equal to 9 and it is

$$\begin{Bmatrix} \sigma_1 \\ \sigma_2 \\ \sigma_3 \\ \sigma_4 \\ \sigma_5 \\ \sigma_6 \end{Bmatrix} = \begin{bmatrix} Q_{11} & Q_{12} & Q_{13} & 0 & 0 & 0 \\ Q_{21} & Q_{22} & Q_{23} & 0 & 0 & 0 \\ Q_{31} & Q_{32} & Q_{33} & 0 & 0 & 0 \\ 0 & 0 & 0 & Q_{44} & 0 & 0 \\ 0 & 0 & 0 & 0 & Q_{55} & 0 \\ 0 & 0 & 0 & 0 & 0 & Q_{66} \end{bmatrix} \cdot \begin{Bmatrix} \epsilon_1 \\ \epsilon_2 \\ \epsilon_3 \\ \epsilon_4 \\ \epsilon_5 \\ \epsilon_6 \end{Bmatrix} \tag{2.45}$$

The 9 independent material coefficients in 2.45 can be expressed by 9 independent material engineering constants:

$$E_1,\ E_2,\ E_3,\ G_{23},\ G_{13},\ G_{12},\ \nu_{12},\ \nu_{13},\ \nu_{23} \tag{2.46}$$

where

- $E_1,\ E_2,\ E_3$ are the Young's moduli in 1, 2 and 3 directions respectively;
- $\nu_{12},\ \nu_{13},\ \nu_{23} = \nu_{ij}$ are defined as the the ration of transverse strain in the jth direction to the axial strain in the ith direction when stressed in the ith direction $\nu_{ij} = \frac{\epsilon_j}{\epsilon_i}$;
- $G_{23},\ G_{13},\ G_{12}$ are the shear moduli in the $2-3$, $1-3$ and $1-2$ planes respectively.

The relation between the coefficients in the equation 2.45 are

$$\begin{aligned} Q_{11} &= \frac{1-\nu_{23}\nu_{32}}{E_2E_3\Delta}, Q_{12} = \frac{\nu_{21}+\nu_{31}\nu_{23}}{E_2E_3\Delta} = \frac{\nu_{12}+\nu_{32}\nu_{13}}{E_1E_3\Delta} \\ Q_{13} &= \frac{\nu_{31}+\nu_{21}\nu_{32}}{E_2E_3\Delta} = \frac{\nu_{13}+\nu_{12}\nu_{23}}{E_1E_2\Delta} \\ Q_{22} &= \frac{1-\nu_{13}\nu_{31}}{E_1E_3\Delta}, Q_{23} = \frac{\nu_{32}+\nu_{12}\nu_{31}}{E_1E_3\Delta} = \frac{\nu_{23}+\nu_{21}\nu_{13}}{E_1E_3\Delta} \\ Q_{33} &= \frac{1-\nu_{12}\nu_{21}}{E_1E_2\Delta}, Q_{44} = G_{23}, Q_{55} = G_{31}, Q_{66} = G_{12} \\ \Delta &= \frac{1-\nu_{12}\nu_{21}-\nu_{23}\nu_{32}-\nu_{31}\nu_{13}-2\nu_{21}\nu_{32}\nu_{13}}{E_1E_2E_3} \end{aligned} \tag{2.47}$$

For the Poisson's ratio the same relation is valid

$$\frac{\nu_{ij}}{E_i} = \frac{\nu_{ji}}{E_j} \tag{2.48}$$

Isotropic material A material is defined as isotropic if no preferred direction exists. In this case the engineering constants are

$$E_1 = E_2 = E_3 = E,\ G_{12} = G_{13} = G_{23} = G,\ \nu_{12} = \nu_{23} = \nu_{13} = \nu \tag{2.49}$$

with

$$G = \frac{E}{2(1+\nu)} \tag{2.50}$$

The Hooke's law is

$$\begin{Bmatrix} \sigma_1 \\ \sigma_2 \\ \sigma_3 \\ \sigma_4 \\ \sigma_5 \\ \sigma_6 \end{Bmatrix} = \Lambda \cdot \begin{bmatrix} 1-\nu & \nu & \nu & 0 & 0 & 0 \\ \nu & 1-\nu & \nu & 0 & 0 & 0 \\ \nu & \nu & 1-\nu & 0 & 0 & 0 \\ 0 & 0 & 0 & \frac{1}{2}(1-2\nu) & 0 & 0 \\ 0 & 0 & 0 & 0 & \frac{1}{2}(1-2\nu) & 0 \\ 0 & 0 & 0 & 0 & 0 & \frac{1}{2}(1-2\nu) \end{bmatrix} \cdot \begin{Bmatrix} \epsilon_1 \\ \epsilon_2 \\ \epsilon_3 \\ \epsilon_4 \\ \epsilon_5 \\ \epsilon_6 \end{Bmatrix} \tag{2.51}$$

where

$$\Lambda = \frac{E}{(1+\nu)(1-2\nu)} \tag{2.52}$$

2.2.1 Material coordinate transformation

The material elastic coefficients can be expressed according to a local reference system (material reference system $1-2-3$), while the problem is formulated according to a different reference system (physical reference system $x_1 - x_2 - x_3$), as discussed in [21]. In this case in order to solve the problem a coordinate transformation is needed. In general the stiffness matrix $\mathbf{Q}$ defined in the material reference system $1-2-3$ is transformed into the matrix $\mathbf{C}$ expressed according to the physical reference system $x_1 - x_2 - x_3$. A typical problem configuration is reported in Fig. 2.6

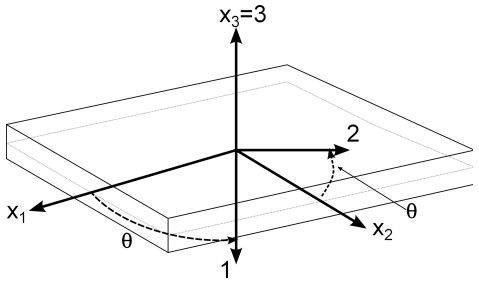

Figure 2.6: Material reference system transformation.

The material properties of a unidirectionally reinforced lamina are expressed according to the reference system $1-2-3$ which is aligned with the fibers orientation. The lamina lies on the 1-2 plane. The axis 3 of the material reference system and the axis x_3 of the physical reference system coincides: the material reference system can be transformed into the physical reference system by rotating the axes 1 and 2 by an angle θ about the x_3 axis. The transformation matrix in this case is

$$\mathbf{T} = \begin{bmatrix} \cos^2(\theta) & \sin^2(\theta) & 0 & 0 & 0 & -\sin(2\theta) \\ \sin^2(\theta) & \cos^2(\theta) & 0 & 0 & 0 & \sin(2\theta) \\ 0 & 0 & 1 & 0 & 0 & 0 \\ 0 & 0 & 0 & \cos(\theta) & -\sin(\theta) & 0 \\ 0 & 0 & 0 & -\sin(\theta) & \cos(\theta) & 0 \\ \sin(\theta)\cos(\theta) & -\sin(\theta)\cos(\theta) & 0 & 0 & \cos^2(\theta)-\sin^2(\theta) & \end{bmatrix} \tag{2.53}$$

The material stress $\boldsymbol{\sigma}_m$ can expressed according to the physical reference by means of the following transformation

$$\boldsymbol{\sigma} = \mathbf{T}\boldsymbol{\sigma}_m \tag{2.54}$$

In a similar manner it is possible to express the material strain state $\boldsymbol{\epsilon}_m$ according physical reference state as

$$\boldsymbol{\epsilon}_m = \mathbf{T}^T\boldsymbol{\epsilon} \tag{2.55}$$

$\boldsymbol{\sigma}$ and $\boldsymbol{\epsilon}$ are the stress and strain state expressed according to the physical reference system. Considering the Hooke's law it is possible to write

$$\boldsymbol{\sigma} = \mathbf{T}\boldsymbol{\sigma}_m = \mathbf{T}\mathbf{Q}\boldsymbol{\epsilon}_m = \mathbf{T}\mathbf{Q}\mathbf{T}^T\boldsymbol{\epsilon} \tag{2.56}$$

The transformed material stiffness matrix can be defined as

$$\mathbf{C} = \mathbf{T}\mathbf{Q}\mathbf{T}^T \tag{2.57}$$

2.3 Thermal constitutive relations

A temperature distribution can cause the deformation of a structure. The possibility to include the temperature effect in the stress computation can be performed considering the temperature as a primary variable, this is the approach followed in the fully coupled approach. On the contrary it is possible to consider the temperature distribution as an external load, this is the partially coupled approach. In this case the temperature distribution must be assumed a-priori or calculating it by solving the Fourier heat conduction equation. In the following the partially coupled approach is employed. Thermal stresses are computed as follows:

$$\boldsymbol{\sigma}_T = \mathbf{C}^k \boldsymbol{\epsilon}_T \tag{2.58}$$

where ϵ_T are the strains due to a temperature gradient, that is

$$\boldsymbol{\epsilon}_T = [\epsilon_{1T}\ \epsilon_{2T}\ \epsilon_{3T}\ \epsilon_{4T}\ \epsilon_{5T}\ \epsilon_{6T}] \tag{2.59}$$

The strains components are defined according to the reference system depicted in Figure 2.1. Considering the thermal expansion coefficient vector $\boldsymbol{\alpha}$, it is possible to write that:

$$\boldsymbol{\epsilon}_T = \{\alpha_1,\ \alpha_2,\ \alpha_3,\ 0,\ 0,\ 0\} \cdot \theta(x, y, z) = \boldsymbol{\alpha} \cdot \theta(x, y, z) \tag{2.60}$$

where $\theta(x, y, z)$ is the temperature distribution inside the body.

2.4 Piezoelectric constitutive relations

In a body, some piezoelectric layers can be present. These layers can act as sensors or as actuators. In the first case as a load is applied to the body and an electric potential distribution is originated. If the piezoelectric layers act as actuators, they deform all body as an electric potential distribution is applied. It is assumed that the linear elastic range of the materials and the physical limits of the piezoelectric layers, like Curie temperature and depolarization potential, are not exceeded by any deformations or loadings.

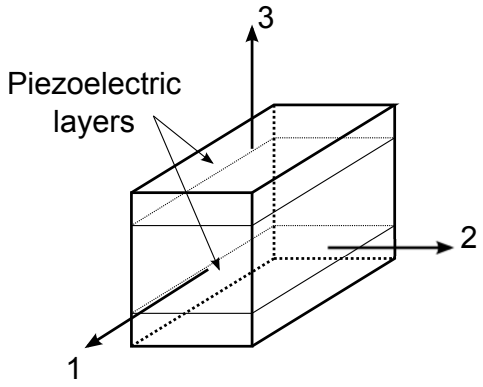

Figure 2.7: Material reference system - piezoelectric layers within the body.

For the sake of simplicity, the constitutive equations for the piezoelectric case are reported for the body depicted in Figure 2.7. In the followings, the engineering notation is used for stresses and strains with the indices 11, 22, 33, 13, 23, and 12. The directions of the piezoelectric material are named in the standard manner with 1-3, axis 3 being the polarization direction of the material (see Figure 2.7). In the following, an uniform modeling is implemented: all k layers are assumed piezoelectric, and the pure elastic layers are obtained by setting to zero the piezoelectric coefficients. Direct and converse piezoelectric effects define the coupling effect between stresses and electric field, the constitutive equations are defined according to the IEEE standard [46]:

$$\begin{aligned} \boldsymbol{\sigma}^k &= \mathbf{C}^k \boldsymbol{\epsilon}^k - \mathbf{e}^k \mathbf{E}^k \\ \tilde{\mathbf{D}}^k &= \mathbf{e}^k \boldsymbol{\epsilon}^k + \boldsymbol{\varepsilon}^k \mathbf{E}^k \end{aligned} \tag{2.61}$$

k is a generic layer of the body (see figure 2.7). The meaning of the operators indicated in eq. 2.61 are reported in the following list:

- $\mathbf{e}^k$ is the matrix of the piezoelectric constant:

$$\mathbf{e}^k = \begin{bmatrix} 0 & 0 & 0 & e^k_{14} & e^k_{15} & 0 \\ 0 & 0 & 0 & e^k_{24} & e^k_{25} & 0 \\ e^k_{31} & e^k_{32} & e^k_{36} & 0 & 0 & e^k_{33} \end{bmatrix} \tag{2.62}$$

- $\boldsymbol{\varepsilon}^k$ is the matrix of the permittivity coefficients of the k-layer:

$$\boldsymbol{\varepsilon}^k = \begin{bmatrix} \varepsilon_{11}^k & \varepsilon_{12}^k & 0 \\ \varepsilon_{21}^k & \varepsilon_{22}^k & 0 \\ 0 & 0 & \varepsilon_{33}^k \end{bmatrix} \tag{2.63}$$

- $\tilde{\mathbf{D}}^k$ is the dielectric displacement and $\mathbf{E}^k$ is the electric field:

$$\tilde{\mathbf{D}}^k = \left[\tilde{D}_1^k, \tilde{D}_2^k, \tilde{D}_3^k\right]^T \qquad \mathbf{E}^k = \left[E_1^k, E_2^k, E_3^k\right]^T \tag{2.64}$$

Superscript T represents the transposition operation. Matrix $\mathbf{C}^k$ is the matrix of the elastic constants of the generic k-layer previously introduced and $\boldsymbol{\epsilon}$ is vector of strains. The electric field strength $\tilde{\mathbf{E}}^k$ can be derived from the Maxwell equations:

$$\mathbf{E}^k = \mathbf{D}_e \Phi^k \tag{2.65}$$

where $\mathbf{D}_e$ is

$$\mathbf{D}_e = \begin{bmatrix} -\partial_{,x} & 0 & 0 \\ 0 & -\partial_{,y} & 0 \\ 0 & 0 & -\partial_{,z} \end{bmatrix} \tag{2.66}$$

(a Cartesian reference system is used) and Φ^k is the potential distribution for the generic k layer.

Chapter 3

Classical and refined plate models review

A brief review of the classical theories is presented in this chapter. In particular, the Kirchhoff and Mindlin plate theories are presented. In addition, a refined plate model is presented. It is shown that it is possible to construct a refined plate theory in a similar manner of the classical model, in particular it is demonstrated that is possible to define the governing equations of a plate in a unified manner.

3.1 Analysis of plate/shell structure

The solution of 3D elasticity equations for structure offers the most accurate evaluation of the elastic response but the computational cost can be significantly high. If a structure can be considered as a plate or a shell, a 2D approach is preferred. In this case, a 3D problem is reduced to a 2D problem: the problem defined in each point P of the 3D continuum is reduced into a problem defined in each point P_Ω which belong to the reference surface Ω (see Figure 2.4).

A number of models exist for the plate/shell analysis, which present different levels of accuracy. These models are based on some assumptions which are related to the displacement field and to the material behavior. In the following, the behavior of the material is considered as elastic. The definition of a 2D model can follow two different approaches: asymptotic or axiomatic.

According to the asymptotic approach, the analysis of a plate/shell can be performed by expanding the equilibrium equations in terms of a perturbation parameter δ. As an instance, in the case of a plate this parameter can be defined as the relation

between the thickness of the plate and the length of a side of the plate ($\delta = h/a$). The equilibrium equations $\mathbf{E}_\Sigma$ can be written as

$$\mathbf{E}_\Sigma \approx \mathbf{E}^1_\Sigma \delta^{p_1} + \mathbf{E}^2_\Sigma \delta^{p_2} + \mathbf{E}_\Sigma \delta^{p_3} + \cdots + \mathbf{E}^N_\Sigma \delta^{p_N} \tag{3.1}$$

where p_i are the exponents of the perturbation parameter δ (in general p_i are real numbers). This approach makes it possible to obtain the 3D solutions when $\delta \to 0$. It should be mentioned that this approach may give rise to further difficulties when applied to multilatered structure, since in this case the effect of other parameter should be taken into account, as the orthotropic ratio of the lamina E_L/E_T. An in-depth description of the asymptotic approach applied to shell analysis can be found in [47] and [48].

Another approach that can be followed is the axiomatic approach. In this case, the displacement/stress distribution along the thickness is postulated as

$$f(x_1, x_2 x_3) = \sum_{i=1}^{N} f_i(x_1, x_2) F_i(x_3) \tag{3.2}$$

where x_1, x_2 and x_3 are the coordinates of a point on the domain considered. In general, the function f can be the displacement components ($\mathbf{u} = [u_1\ u_2\ u_3]$), the strain or stress vector components. In these cases, displacement, strain or stress formulation are considered respectively. In addition, mixed formulation can be employed, that is formulation which consider the axiomatic expansion of different quantities, as displacement and stresses. It is possible to affirm that this type of approach is based on the intuition of the plate/shell behavior.

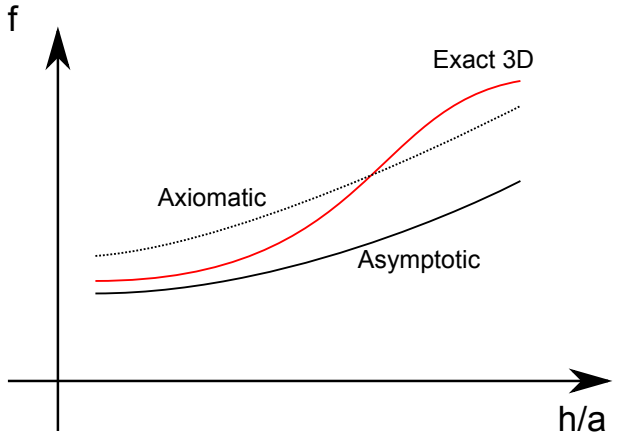

Figure 3.1: Representation of the accuracy for axiomatic and asymptotic process - 2D approaches and 3D exact solution.

In the Figure 3.1 the accuracy with respect to the 3D exact solution is represented for asymptotic and axiomatic solutions considering a generic function f. In the following, axiomatic models for plates are introduced.

3.2 Classical theories

The classical models have been developed for single-layer isotropic thin structures. It is possible to divide these theories into two groups: Love First Approximation Theories (LFAT) and Love Second Approximation Theories (LSAT). The LFAT models are base on the well-known thin plate/shell hypotheses, that is

1. transverse normals to the midsurface (Ω in Fig. 2.4) before deformation remain straight after deformation;

2. the transverse normals are inextensible;

3. the transverse normals rotate such that they remain perpendicular to the midsurface after deformation.

A second group of models can be obtained removing one of these hypotheses, in this case Love Second Approximation Theories (LSAT) theories are obtained. In general an hypothesis that can be removed is the perpendicularity of the transverse normals the midsurface after deformation.

3.3 Plate models review - Kirchhoff model for plates

A theory that can be employed for the multilayered plate analysis is the Classical Lamination Theory (CLT) which is based on the Kirchhoff hypothesis already introduced (for any detail, see the book [21]). According to Kirchhoff model, the initially plain transverse sections remain plain during the deformation process and normal to the reference surface Ω. A figure is presented:

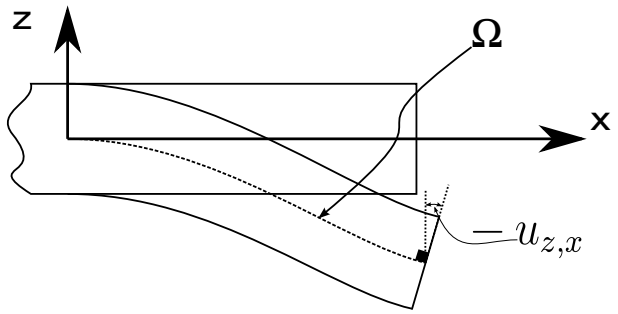

Figure 3.2: Deformation process according to Kirchhoff on $x - z$ plane.

Remembering the definition of strain it possible to write that:

$$\gamma_{xz} = 0 \rightarrow u_{x,z} + u_{z,x} = 0 \rightarrow u_{x,z} = -u_{z,x} \tag{3.3}$$
$$\gamma_{yz} = 0 \rightarrow u_{y,z} + u_{z,y} = 0 \rightarrow u_{y,z} = -u_{z,y} \tag{3.4}$$

In the following the operator $_{,\alpha}$ indicated the operation of derivation according to the generic coordinate α. The displacement field according to Kirchhoff is then

$$\begin{aligned} u_x &= u_{x0} + u_{x,z}\, z = u_{x0} - u_{z,x}\, z \\ u_y &= u_{y0} + u_{y,z}\, z = u_{y0} - u_{z,y}\, z \\ u_z &= u_{z0} \end{aligned} \tag{3.5}$$

The strain-displacement relations are reported in the following for the Kirchhoff model:

$$
\begin{aligned}
\epsilon_{xx} &= u_{x,x} = \overbrace{u_{x0,x}}^{\epsilon^0_{xx}} \overbrace{-u_{z,xx}\, z}^{\epsilon^1_{xx}} = \epsilon^0_{xx} + \epsilon^1_{xx} \\
\epsilon_{yy} &= u_{y,y} = \overbrace{u_{y0,y}}^{\epsilon^0_{yy}} \overbrace{-u_{z,yy}\, z}^{\epsilon^1_{yy}} = \epsilon^0_{yy} + \epsilon^1_{yy} \\
\gamma_{xy} &= 2\,\epsilon_{xy} = \overbrace{(u_{y0,x} + u_{x0,y})}^{\gamma xy^0} \overbrace{-2\, u_{z,xy}\, z}^{\gamma^1_{xy}} = \gamma^0_{xy} + \gamma^1_{xy} \\
\epsilon_{zz} &= 0 \\
\gamma_{xz} &= 2\,\epsilon_{xz} = 0 \\
\gamma_{yz} &= 2\,\epsilon_{yz} = 0
\end{aligned}
\tag{3.6}
$$

The material considered are governed by the Hooke' law.

3.3.1 Equilibrium equations

The application of the Principle of Virtual Displacement is used in order to determine the equilibrium equation of Kirchhoff plate model. A rectangular plate is considered, in order to explain the geometric configuration a picture is reported:

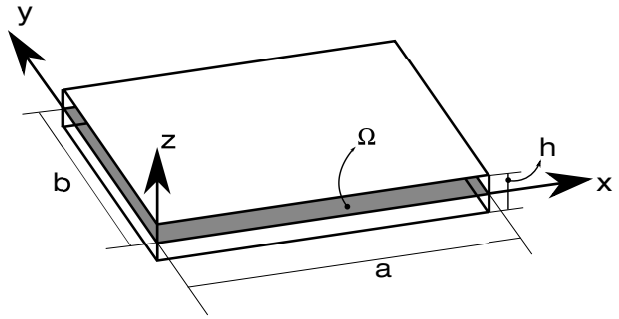

Figure 3.3: Rectangular plate configuration.

The sides of the rectangular plate are denoted as a and b. The thickness of the plate is constant and equal to h. According to the Principle of Virtual Displacement (PVD) the governing equation can be obtained solving

$$
\delta L_{int} = \delta L_{ext} \rightarrow \int_V \delta\boldsymbol{\epsilon}^T \cdot \boldsymbol{\sigma}\, dV = \int_V \delta\mathbf{u}^T\, \mathbf{p}\, dV \tag{3.7}
$$

where $\mathbf{p}$ is a transverse pressure load acts on the plate. It is possible to write for the equilibrium equations

$$\begin{array}{ll} \delta u_{x0}: & N_{xx,x} + N_{xy,y} = 0 \\ \delta u_{y0}: & N_{yy,y} + N_{xy,x} = 0 \\ \delta u_{z0}: & M_{xx,xx} + M_{yy,yy} + 2\, M_{xy,xy} + p = 0 \end{array} \tag{3.8}$$

with the related boundary conditions

$$\begin{array}{ll} \delta u_{x0}: & \overline{N}_{xx} n_x + \overline{N}_{xy} n_y = 0 \\ \delta u_{y0}: & \overline{N}_{yy} n_y + \overline{N}_{xy} n_x = 0 \\ \delta u_{z0,x}: & \overline{M}_{xx} n_x + \overline{M}_{xy} n_y = 0 \\ \delta u_{z0,y}: & \overline{M}_{yy} n_y + \overline{M}_{xy} n_x = 0 \\ \delta u_{z0}: & \overline{M}_{xx,x} n_x + \overline{M}_{yy,y} n_y + \overline{M}_{xy,y} n_y + \overline{M}_{xy,x} n_x = 0 \end{array} \tag{3.9}$$

The forces N_{xx}, N_{yy}, N_{xy} and moments M_{xx}, M_{yy}, M_{xy} are defined as

$$\left\{ \begin{array}{c} N_{xx} \\ N_{yy} \\ N_{xy} \end{array} \right\} = \int_A \left\{ \begin{array}{c} \sigma_{xx} \\ \sigma_{yy} \\ \sigma_{xy} \end{array} \right\} \qquad \left\{ \begin{array}{c} M_{xx} \\ M_{yy} \\ M_{xy} \end{array} \right\} = \int_A \left\{ \begin{array}{c} \sigma_{xx} \\ \sigma_{yy} \\ \sigma_{xy} \end{array} \right\} z\, dz \tag{3.10}$$

3.3.2 Evaluation of the equilibrium in terms of the displacement variables

The internal forces for an orthotropic plate can be evaluated in terms of the displacement variables. As first step, it is necessary to express the forces and momente reported in Equations and in terms of the strain components and of the components of the elastic matrix. Considering the definition of stresses, the fores and momenta $\mathbf{N}$ and $\mathbf{M}$ can be written as:

$$\left\{ \begin{array}{c} \mathbf{N} \\ \mathbf{M} \end{array} \right\} = \left[\begin{array}{cc} \mathbf{A} & \mathbf{B} \\ \mathbf{B} & \mathbf{D} \end{array} \right] \cdot \left\{ \begin{array}{c} \boldsymbol{\epsilon}^{(0)} \\ \boldsymbol{\epsilon}^{(1)} \end{array} \right\} \tag{3.11}$$

The above matrix can be expressed in a synthetic manner considering a multilayered plate:

$$(A_{ij}, B_{ij}, D_{ij}) = \sum_{k=1}^{N_L} \int_{z_k}^{z_{k+1}} C_{ij}^k \left(1, z, z^2\right)\, dz \tag{3.12}$$

N_L is the number of the layers and C_{ij}^k is the generic ij material parameter of the k-layer. The layers are enumerated starting from the bottom. Remembering the definition of strains, the internal actions (N_{xx}, N_{yy} and N_{xy} forces and M_{xx}, M_{yy} and M_{xy} moments) can be written in terms of the displacements:

$$\begin{bmatrix} K_{11} & K_{12} & K_{13} \\ K_{21} & K_{22} & K_{23} \\ K_{31} & K_{32} & K_{33} \end{bmatrix} \begin{Bmatrix} u_{x0} \\ u_{y0} \\ u_{z0} \end{Bmatrix} = \begin{Bmatrix} 0 \\ 0 \\ -p \end{Bmatrix} \tag{3.13}$$

where each term of the differential operator is:

$$\begin{aligned}
K_{11} =& A_{11}\,\partial_{,xx} + A_{16}\,\partial_{,yx} + A_{16}\,\partial_{,xy} + A_{66}\,\partial_{,yy} \\
K_{12} =& A_{12}\,\partial_{,yx} + A_{16}\,\partial_{,xx} + A_{26}\,\partial_{,yy} + A_{66}\,\partial_{,xy} \\
K_{13} =& -B_{11}\,\partial_{,xxx} - B_{12}\,\partial_{,yyx} - 2\,B_{16}\,\partial_{,xyx} - B_{16}\,\partial_{,xxy} - B_{26}\,\partial_{,yyy} - 2\,B_{66}\,\partial_{,xyy} \\
K_{21} =& A_{21}\,\partial_{,yx} + A_{26}\,\partial_{,yy} + A_{16}\,\partial_{,xx} + A_{66}\,\partial_{,yx} \\
K_{22} =& A_{22}\,\partial_{,yy} + A_{26}\partial_{,xy} + A_{26}\,\partial_{,yx} + A_{66}\partial_{,xx} \\
K_{23} =& -B_{21}\,\partial_{,xxy} - B_{22}\,\partial_{,yyy} - 2\,B_{26}\,\partial_{,xyy} - B_{16}\,\partial_{,xxx} - B_{26}\,\partial_{,yyx} - 2\,B_{66}\,\partial_{,xyx} \\
K_{31} =& -B_{11}\,\partial_{,xxx} - B_{16}\,\partial_{,yxx} - B_{21}\,\partial_{,xyy} - B_{26}\,\partial_{,yyy} - 2B_{16}\,\partial_{,xxy} - 2B_{66}\,\partial_{,yxy} \\
K_{32} =& -B_{12}\,\partial_{,yxx} - B_{16}\,\partial_{,xxx} - B_{22}\,\partial_{,yyy} - B_{26}\,\partial_{,xyy} - 2B_{26}\,\partial_{,yxy} - 2B_{66}\,\partial_{,xxy} \\
K_{33} =& -D_{11}\,\partial_{,xxxx} - D_{12}\,\partial_{,yyxx} - 2\,D_{16}\,\partial_{,xyxx} - D_{21}\,\partial_{,xxyy} - D_{22}\,\partial_{,yyyy} - \\
& - 2\,D_{26}\,\partial_{,xyyy} - 2D_{16}\,\partial_{,xxxy} - 2D_{26}\,\partial_{,yyxy} - 4\,D_{66}\,\partial_{,xyxy}
\end{aligned} \tag{3.14}$$

3.3.3 Closed form solution for Kirchhoff plate, Navier solution

In the following a closed form solution for simply supported rectangular plate is reported. In the following, it assumed that is the the coupling effect bending - stretching is not considered and the bending - twisting effect is ignored. This implies to set to zero all elements of the matrix $[B]$ and the coefficient D_{16} and D_{26}. In this case it is possible to write:

$$\begin{bmatrix} K_{11} & K_{12} & 0 \\ K_{21} & K_{22} & 0 \\ 0 & 0 & K_{33} \end{bmatrix} \begin{Bmatrix} u_{x0} \\ u_{y0} \\ u_{z0} \end{Bmatrix} = \begin{Bmatrix} 0 \\ 0 \\ -p \end{Bmatrix} \tag{3.15}$$

No in-plane force is considered and the thermal load is not computed. The Navier solution can be employed to analyze a simply supported plate, in this case the boundary conditions on Γ are

$$\begin{aligned} u_{z0}(0,y) = u_{z0}(a,y) = 0 \quad & u_{z0}(x,0) = u_{z0}(x,b) = 0 \\ u_{x0}(x,0) = u_{x0}(x,b) = 0 \quad & u_{y0}(0,y) = u_{y0}(a,y) = 0 \\ N_x(0,y) = N_x(a,y) = 0 \quad & N_y(x,0) = N_y(x,b) = 0 \\ M_{xx}(0,y) = M_{xx}(a,y) = 0 \quad & M_{yy}(x,0) = M_{yy}(x,b) = 0 \end{aligned} \tag{3.16}$$

The displacement u_{x0}, u_{y0} and u_{z0} can be described as:

$$\begin{aligned} u_{x0} &= \hat{U}_{x0} \cdot \cos(\alpha\, x) \sin(\beta\, y) \\ u_{y0} &= \hat{U}_{y0} \cdot \sin(\alpha\, x) \cos(\beta\, y) \\ u_{z0} &= \hat{U}_{z0} \cdot \sin(\alpha\, x) \sin(\beta\, y) \end{aligned} \tag{3.17}$$

where

$$\alpha = \frac{m\pi}{a} \qquad \beta = \frac{n\pi}{b} \tag{3.18}$$

The acting load is a pressure acting on the top surface of the plate:

$$p = p_0 \cdot \sin(\alpha\, x) \sin(\beta\, x) \tag{3.19}$$

It is worthy to note that if different load distribution are considered (e.g. constant pressure distribution) Fourier series have to be used for both load and displacement field. Let's substitute the displacement functions into the differential operator:

$$\begin{bmatrix} -\alpha^2 A_{11} - \beta^2 A_{66} & -\alpha\beta\ (A_{12} + A_{66}) & 0 \\ -\alpha\beta\ (A_{21} + A_{66}) & -\beta^2 A_{22} - \alpha^2 A_{66} & 0 \\ 0 & 0 & -\alpha^4 D_{11} - 2\,\alpha^2\beta^2\ (D_{12} + 2\,D_{66}) - \beta^4 D_{22} \end{bmatrix} \begin{Bmatrix} \hat{U}_{x0} \\ \hat{U}_{y0} \\ \hat{U}_{z0} \end{Bmatrix} = \begin{Bmatrix} 0 \\ 0 \\ -p_0 \end{Bmatrix} \tag{3.20}$$

The solution of this system permits the evaluation of the parameter $\hat{U}_{x0}$, $\hat{U}_{y0}$ and $\hat{U}_{z0}$. In particular it is

$$\hat{U}_{z0} = \frac{p_0}{\alpha^4 D_{11} + 2\,\alpha^2\beta^2\,\left(D_{12} + 2\,D_{66}\right) + \beta^4 D_{22}} \tag{3.21}$$

Momenta M_{xx}, M_{yy} and M_{xy} can be computed as well, remembering that

$$\left\{ \begin{array}{c} M_{xx} \\ M_{yy} \\ M_{xy} \end{array} \right\} = \left[\begin{array}{ccc} D_{11} & D_{12} & 0 \\ D_{21} & D_{22} & 0 \\ 0 & 0 & D_{66} \end{array} \right] \cdot \left\{ \begin{array}{c} \epsilon_{xx}^{(1)} \\ \epsilon_{yy}^{(1)} \\ \gamma_{xy}^{(1)} \end{array} \right\} \tag{3.22}$$

In an explicit form it is

$$\begin{aligned} M_{xx} =& D_{11}\epsilon_{xx}^{(1)} + D_{12}\epsilon_{xx}^{(1)} = \\ =& D_{11} z \cdot \hat{U}_{z0}\alpha^2 \cdot \sin(\alpha\, x) \cdot \sin(\beta\, y) + D_{12} z \cdot \hat{U}_{z0}\beta^2 \cdot \sin(\alpha\, x) \cdot \sin(\beta\, y) = \\ =& \left(D_{11}\alpha^2 + D_{12}\beta^2\right) \cdot \hat{U}_{z0} \cdot \sin(\alpha\, x) \cdot \sin(\beta\, y) \qquad (3.23) \\ M_{yy} =& D_{21}\epsilon_{xx}^{(1)} + D_{22}\epsilon_{xx}^{(1)} = \\ & D_{21} z \cdot \hat{U}_{z0}\alpha^2 \cdot \sin(\alpha\, x) \cdot \sin(\beta\, y) + D_{22} z \cdot \hat{U}_{z0}\beta^2 \cdot \sin(\alpha\, x) \cdot \sin(\beta\, y) \\ =& \left(D_{21}\alpha^2 + D_{22}\beta^2\right) \cdot \hat{U}_{z0} \cdot \sin(\alpha\, x) \cdot \sin(\beta\, y) \qquad (3.24) \\ M_{xy} =& D_{66}\gamma_{xy}^{(1)} = -2\, D_{66}\alpha\beta \cdot \hat{U}_{z0} \cdot \cos(\alpha\, x) \cdot \cos(\beta\, y) \qquad (3.25) \end{aligned}$$

It is possible to demonstrate that the boundary conditions are respected.

3.4 Plate models review - Mindlin model for plates

In this section an Mindlin theory is proposed and analyzed. The discussion start from the definition of the geometry and of the displacement field considered by this theory. Similarly to Kirchhoff approach, in FSDT the cross section during the deformation process remains plain but, differently, the same transverse section is not normal to the reference surface during the deformation process. A figure is presented:

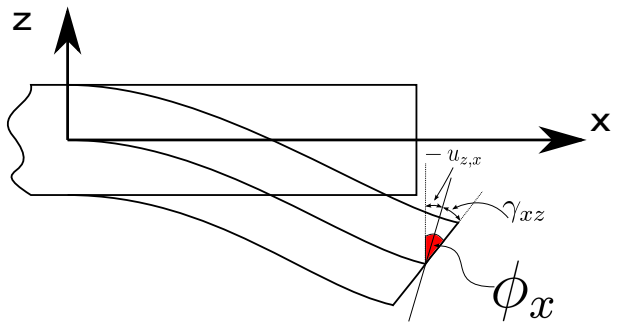

Figure 3.4: Deformation process according to Mindlin on $x - z$ plane.

The displacement field according to Mindlin is then

$$\begin{aligned} u_x &= u_{x0} + u_{x,z}\, z = u_{x0} + \phi_x\, z \\ u_y &= u_{y0} + u_{y,z}\, z = u_{y0} + \phi_y\, z \\ u_z &= u_{z0} \end{aligned} \tag{3.26}$$

Remembering the definition of strain it possible to write that:

$$u_{x,z} = \phi_x \rightarrow \gamma_{xz} = u_{x,z} + u_{z,x} = \phi_x + u_{z,x} \rightarrow \phi_x = -u_{z,x} + \gamma_{xz} \tag{3.27}$$

$$u_{y,z} = \phi_y \rightarrow \gamma_{yz} = u_{y,z} + u_{z,y} = \phi_y + u_{z,y} \rightarrow \phi_y = -u_{z,y} + \gamma_{yz} \tag{3.28}$$

In the following the operator $_{,\alpha}$ indicated the operation of derivation according to the generic coordinate α. The strain-displacement relations are reported in the follwing for the Mindlin model:

$$
\begin{aligned}
&\epsilon_{xx} = u_{x,x} = u_{x0,x} + \phi_{x,x}\, z \\
&\epsilon_{yy} = u_{y,y} = u_{y0,y} + \phi_{y,y}\, z \\
&\gamma_{xy} = 2\,\epsilon_{xy} = u_{x,y} + u_{y,x} = u_{x0,y} + \phi_{x,y}\, z + u_{y0,x} + \phi_{y,x}\, z \\
&\gamma_{xz} = 2\,\epsilon_{xz} = u_{x,z} + u_{z,x} = \phi_x + u_{z0,x} \\
&\gamma_{yz} = 2\,\epsilon_{yz} = u_{y,z} + u_{z,y} = \phi_y + u_{z0,y} \\
&\epsilon_{zz} = 0
\end{aligned}
\tag{3.29}
$$

that is

$$
\begin{aligned}
&\epsilon_{xx} = u_{x,x} = u_{x0,x} + \phi_{x,x}\, z \\
&\epsilon_{yy} = u_{y,y} = u_{y0,y} + \phi_{y,y}\, z \\
&\gamma_{xy} = 2\,\epsilon_{xy} = u_{x0,y} + u_{y0,x} + (\phi_{x,y} + \phi_{y,x})\; z \\
&\gamma_{xz} = 2\,\epsilon_{xz} = u_{z0,x} + \phi_x \\
&\gamma_{yz} = 2\,\epsilon_{yz} = u_{z0,y} + \phi_y \\
&\epsilon_{zz} = 0
\end{aligned}
\tag{3.30}
$$

3.4.1 Equilibrium equations

The application of the Principle of Virtual Displacement is used in order to determine the equilibrium equation of Mindlin plate model. The principle states that:

$$\delta L_{int} = \delta L_{ext} \tag{3.31}$$

The virtual internal work (δL_{int}) is made by the internal stresses while the external work (δL_{ext}) is made the applied external loads at the top, bottom and lateral surfaces. In this case the PVD becomes:

$$\int_V \delta\boldsymbol{\epsilon}^T \cdot \boldsymbol{\sigma}\, dV = \int_V \delta\mathbf{u}^T\, \mathbf{p}\, dV \tag{3.32}$$

It is possible to write for the equilibrium equations

$$
\begin{aligned}
\delta u_{x0}: &\quad N_{xx,x} + N_{xy,y} = 0 \\
\delta u_{y0}: &\quad N_{yy,y} + N_{xy,x} = 0 \\
\delta u_{z0}: &\quad Q_{x,x} + Q_{y,y} + p = 0 \\
\delta \phi_x: &\quad M_{xy,y} + M_{xx,x} - Q_x = 0 \\
\delta \phi_y: &\quad M_{xy,x} + M_{yy,y} - Q_y = 0
\end{aligned}
\tag{3.33}
$$

and the related boundary condtions are

$$\begin{array}{rl} \delta\, u_{x0}: & \overline{N}_{xx}n_x + \overline{N}_{xy}n_y = 0 \\ \delta\, u_{y0}: & \overline{N}_{yy}n_y + \overline{N}_{xy}n_x = 0 \\ \delta\, u_{z0}: & \overline{Q}_x n_x + \overline{Q}_y n_y = 0 \\ \delta\phi_x: & \overline{M}_{xx}n_x + \overline{M}_{xy}n_y = 0 \\ \delta\phi_y: & \overline{M}_{yy}n_y + \overline{M}_{xy}n_x = 0 \end{array} \tag{3.34}$$

where

$$\left\{ \begin{array}{c} N_{xx} \\ N_{yy} \\ N_{xy} \end{array} \right\} = \sum_{k=1}^{N_L} \int_{A_k} \left\{ \begin{array}{c} \sigma^k_{xx} \\ \sigma^k_{yy} \\ \sigma^k_{xy} \end{array} \right\} dz \quad \left\{ \begin{array}{c} M_{xx} \\ M_{yy} \\ M_{xy} \end{array} \right\} = \sum_{k=1}^{N_L} \int_{A_k} \left\{ \begin{array}{c} \sigma^k_{xx} \\ \sigma^k_{yy} \\ \sigma^k_{xy} \end{array} \right\} z\, dz \quad \left\{ \begin{array}{c} Q_x \\ Q_y \end{array} \right\} = \sum_{k=1}^{N_L} \int_{A_k} \left\{ \begin{array}{c} \sigma^k_{xz} \\ \sigma^k_{yz} \end{array} \right\} dz \tag{3.35}$$

3.4.2 Evaluation of the equilibrium in terms of the displacement variables

The internal forces and momenta can be expressed in a similar manner of the Kirchhoof theory:

$$\left\{ \begin{array}{c} \mathbf{N} \\ \mathbf{M} \end{array} \right\} = \left[\begin{array}{cc} \mathbf{A} & \mathbf{B} \\ \mathbf{B} & \mathbf{D} \end{array} \right] \cdot \left\{ \begin{array}{c} \boldsymbol{\epsilon}^{(0)} \\ \boldsymbol{\epsilon}^{(1)} \end{array} \right\} \qquad \{\mathbf{Q}\} = [\mathbf{A}] \cdot \{\gamma\} \tag{3.36}$$

Transverse shear stresses are constant since the transverse strain it is constant. In laminated plates the shear stresses at least vary quadratically. In order to evaluate a reasonable values of shear stresses through the FSDT theory it is necessary to correct the values of Q by means of a shear correction factor (K). It is

$$\left\{ \begin{array}{c} Q_{xz} \\ Q_{yz} \end{array} \right\} = K \cdot \int_{-h/2}^{h/2} \left\{ \begin{array}{c} \sigma_{xz} \\ \sigma_{yz} \end{array} \right\} dz \tag{3.37}$$

In this case it is possible to write

$$\{\mathbf{Q}\} = K\ [\mathbf{A}] \cdot \{\gamma\} \tag{3.38}$$

The components of the matrices $\mathbf{A}$, $\mathbf{B}$ and $\mathbf{D}$ are defined as in Equation 3.12. The equilibrium equation can be written considering a linear differential operator $\hat{\mathbf{K}}$:

$$\begin{bmatrix} K_{11} & K_{12} & K_{13} & K_{14} & K_{15} \\ K_{21} & K_{22} & K_{23} & K_{24} & K_{25} \\ K_{31} & K_{32} & K_{33} & K_{34} & K_{35} \\ K_{41} & K_{42} & K_{43} & K_{44} & K_{45} \\ K_{51} & K_{52} & K_{53} & K_{54} & K_{55} \end{bmatrix} \cdot \begin{Bmatrix} u_x \\ u_y \\ u_z \\ \phi_x \\ \phi_y \end{Bmatrix} = \begin{Bmatrix} 0 \\ 0 \\ -p \\ 0 \\ 0 \end{Bmatrix} \tag{3.39}$$

whose components are defined as follows

$$\begin{aligned}
K_{11} &= A_{11}\,\partial_{,xx} + A_{16}\,\partial_{,yx} + A_{16}\,\partial_{,xy} + A_{66}\,\partial_{,yy} \\
K_{12} &= A_{12}\,\partial_{,yx} + A_{16}\,\partial_{,xx} + A_{26}\,\partial_{,yy} + A_{66}\,\partial_{,xy} \\
K_{13} &= 0 \\
K_{14} &= B_{11}\partial_{,xx} + B_{16}\,\partial_{,yx} + B_{16}\partial_{,xy} + B_{66}\partial_{,yy} \\
K_{15} &= B_{12}\partial_{,yx} + B_{16}\,\partial_{,xx} + B_{26}\partial_{,yy} + B_{66}\partial_{,xy} \\
K_{21} &= A_{21}\,\partial_{,xy} + A_{26}\,\partial_{,yy} + A_{16}\,\partial_{,xx} + A_{66}\,\partial_{,yx} \\
K_{22} &= A_{22}\,\partial_{,yy} + A_{26}\,\partial_{,xy} + A_{26}\,\partial_{,yx} + A_{66}\,\partial_{,xx} \\
K_{23} &= 0 \\
K_{24} &= B_{21}\partial_{,xy} + B_{26}\,\partial_{,yy} + B_{16}\partial_{,xx} + B_{66}\,\partial_{,yx} \\
K_{25} &= B_{22}\partial_{,yy} + B_{26}\,\partial_{,xy} + B_{26}\partial_{,yx} + B_{66}\,\partial_{,xx} \\
K_{31} &= 0 \\
K_{32} &= 0 \\
K_{33} &= KA_{44}\,\partial_{,xx} + KA_{45}\,\partial_{,yx} + KA_{45}\,\partial_{,xy} + KA_{55}\,\partial_{,yy} \\
K_{34} &= KA_{44}\partial_{,x} + KA_{45}\partial_{,y} \\
K_{35} &= KA_{45}\partial_{,x} + KA_{55}\partial_{,y}
\end{aligned}$$

$$
\begin{aligned}
K_{41} &= B_{11}\,\partial_{,xx} + B_{16}\,\partial_{,yx} + B_{16}\,\partial_{,xy} + B_{66}\,\partial_{,yy} \\
K_{42} &= B_{12}\,\partial_{,yx} + B_{16}\,\partial_{,xx} + B_{26}\,\partial_{,yy} + B_{66}\,\partial_{,xy} \\
K_{43} &= -KA_{44}\,\partial_{,x} - KA_{45}\,\partial_{,y} \\
K_{44} &= D_{11}\partial_{,xx} + D_{16}\partial_{,xy} + D_{16}\,\partial_{,yx} + D_{66}\,\partial_{,yy} - KA_{44} \\
K_{45} &= D_{12}\partial_{,yx} + D_{16}\,\partial_{,xx} + D_{62}\partial_{,yy} + D_{66}\,\partial_{,xy} - KA_{45} \\
K_{51} &= B_{21}\,\partial_{,xy} + B_{26}\,\partial_{,yy} + B_{16}\,\partial_{,xx} + B_{66}\,\partial_{,yx} \\
K_{52} &= B_{22}\,\partial_{,yy} + B_{26}\,\partial_{,xy} + B_{26}\,\partial_{,yx} + B_{66}\,\partial_{,xx} \\
K_{53} &= -KA_{45}\partial_{,x} - KA_{55}\partial_{,y} \\
K_{54} &= D_{26}\,\partial_{,yy} + D_{21}\partial_{,xy} + D_{61}\partial_{,xx} + D_{66}\,\partial_{,yx} - KA_{45} \\
K_{55} &= D_{26}\,\partial_{,xy} + D_{22}\partial_{,yy} + D_{62}\partial_{,yx} + D_{66}\,\partial_{,xx} - KA_{55}
\end{aligned}
\tag{3.40}
$$

3.4.3 Closed form solution for Mindlin plate, Navier solution

In the following a closed form solution for the Mindlin plate model is presented. A simply supported plate is studied by taking into account the Navier solution. In this case, the boundary conditions on Γ are already defined in Equation 3.16. The displacement variables are defined as

$$
\begin{aligned}
u_x &= \hat{U}_{x0}\,\cos(\alpha\,x)\,\sin(\beta\,y) \\
u_y &= \hat{U}_{y0}\,\sin(\alpha\,x)\,\cos(\beta\,y) \\
u_z &= \hat{U}_{z0}\,\sin(\alpha\,x)\,\sin(\beta\,y) \\
\phi_x &= \hat{\phi}_{x0}\,\cos(\alpha\,x)\,\sin(\beta\,y) \\
\phi_y &= \hat{\phi}_{y0}\,\sin(\alpha\,x)\,\cos(\beta\,y)
\end{aligned}
\tag{3.41}
$$

where

$$
\alpha = \frac{m\,\pi}{a} \qquad \beta = \frac{n\,\pi}{b} \qquad m, n \in \mathbb{N} \tag{3.42}
$$

The Navier solution can exist if only

$$
A_{16} = A_{26} = A_{45} = B_{16} = B_{26} = D_{16} = D_{26} = 0
$$

that if only it is

$$
C^k_{16} = C^k_{26} = C^k_{36} = C^k_{45} = 0 \tag{3.43}
$$

Substituting the definition of the displacement component into Equation 3.40 it is possible to write

$$\begin{bmatrix} K_{11} & K_{12} & 0 & K_{14} & K_{15} \\ K_{21} & K_{22} & 0 & K_{24} & K_{25} \\ 0 & 0 & K_{33} & K_{34} & K_{35} \\ K_{41} & K_{42} & K_{43} & K_{44} & K_{45} \\ K_{51} & K_{52} & K_{53} & K_{54} & K_{55} \end{bmatrix} \cdot \begin{Bmatrix} \hat{U}_{x0} \\ \hat{U}_{y0} \\ \hat{U}_{z0} \\ \hat{\phi}_{x0} \\ \hat{\phi}_{y0} \end{Bmatrix} = \begin{Bmatrix} 0 \\ 0 \\ -p_z^0 \\ 0 \\ 0 \end{Bmatrix} \tag{3.44}$$

where

$$\begin{aligned}
K_{11} &= -\left(A_{11}\alpha^2 + A_{66}\beta^2\right)\hat{U}_{x0} & K_{12} &= -\left(A_{12} + A_{66}\right)\alpha\beta\,\hat{U}_{y0} \\
K_{13} &= 0 & K_{14} &= -\left(B_{11}\alpha^2 + B_{66}\beta^2\right)\hat{\phi}_{x0} \\
K_{15} &= -\left(B_{12} + B_{66}\right)\alpha\beta\hat{\phi}_{y0} & K_{21} &= -\left(A_{21} + A_{66}\right)\alpha\beta\,\hat{U}_{x0} \\
K_{22} &= -\left(A_{22}\beta^2 + A_{66}\alpha^2\right)\hat{U}_{y0} & K_{23} &= 0 \\
K_{24} &= -\left(B_{21} + B_{66}\right)\alpha\beta\hat{\phi}_{x0} & K_{25} &= -\left(B_{22}\beta^2 + B_{66}\alpha^2\right)\hat{\phi}_{y0} & K_{31} &= 0 \\
K_{32} &= 0 & K_{33} &= -\left(KA_{44}\alpha^2 + KA_{55}\beta^2\right)\hat{U}_{z0} \\
K_{34} &= -KA_{44}\alpha\hat{\phi}_{x0} & K_{35} &= -KA_{44}\beta\hat{\phi}_{y0}
\end{aligned}$$

$$\begin{aligned}
K_{41} &= -\left(B_{11}\alpha^2 + B_{66}\beta^2\right)\hat{U}_{x0} & K_{42} &= -\left(B_{12} + B_{66}\right)\alpha\beta\,\hat{U}_{y0} \\
K_{43} &= -KA_{44}\alpha\,\hat{U}_{z0} & K_{44} &= -\left(D_{11}\alpha^2 + D_{66}\beta^2 - KA_{44}\right)\hat{\phi}_{x0} \\
K_{45} &= -\left(D_{12} + D_{66}\right)\alpha\beta\hat{\phi}_{y0} & K_{51} &= -\left(B_{21} + B_{66}\right)\alpha\beta\,\hat{U}_{x0} \\
K_{52} &= -\left(B_{22}\beta^2 + B_{66}\alpha^2\right)\hat{U}_{y0} & K_{53} &= -KA_{55}\beta\,\hat{U}_{z0} \\
K_{54} &= -\left(D_{21} + D_{66}\right)\alpha\beta\hat{\phi}_{x0} & K_{55} &= -\left(D_{22}\beta^2 + D_{66}\alpha^2 + KA_{55}\right)\hat{\phi}_{y0}
\end{aligned} \tag{3.45}$$

The solution of the linear algebraic system 3.44 permits the definition of the unknowns $\hat{U}_{x0}$, $\hat{U}_{y0}$, $\hat{U}_{z0}$, $\hat{\phi}_{x0}$ and $\hat{\phi}_{y0}$. The boundary conditions can be verified as done for the Kirchhoof plate models.

3.5 Refined plate model

The introduction of higher order terms in a plate/shell model offers the possibility to improve the analysis of the plate/shell response. A comparison of the results obtained by means of the classical models with refined plate models is reported in [20].

In the following, it is shown how it is possible to obtain a refined plate model by introducing and additional term in the classical models described in the previous chapters. This example of refined theory is introduced in order to demonstrate that equilibrium equations obtained by means of a refined theory can be written in a unified and automatic manner. A non-classical displacement field can be defined as:

$$\begin{aligned} u_x(x,y,z) &= u_{x0}(x,y) + z u_{x1}(x,y) \\ u_y(x,y,z) &= u_{y0}(x,y) + z u_{y1}(x,y) \\ u_z(x,y,z) &= u_{z0}(x,y) + z u_{z1}(x,y) \end{aligned} \tag{3.46}$$

In this case, the strain-displacement relation can be defined synthetically as

$$\begin{aligned} \epsilon_{xx} &= \epsilon^0_{xx} + z\epsilon^1_{xx} \\ \epsilon_{yy} &= \epsilon^0_{yy} + z\epsilon^1_{yy} \\ \gamma_{xy} &= \gamma^0_{xy} + z\gamma^1_{xy} \\ \gamma_{yz} &= \gamma^0_{yz} + z\gamma^1_{yz} \\ \gamma_{xz} &= \gamma^0_{xz} + z\gamma^1_{xz} \\ \epsilon_{zz} &= \epsilon^0_{zz} \end{aligned} \tag{3.47}$$

where

$$\begin{aligned} \epsilon^0_{xx} &= u_{x0,x} & \epsilon^1_{xx} &= u_{x1,x} \\ \epsilon^0_{yy} &= u_{y0,y} & \epsilon^1_{yy} &= u_{y1,y} \\ \gamma^0_{xy} &= u_{x0,y} + u_{y0,x} & \gamma^1_{xy} &= u_{x1,y} + u_{y1,x} \\ \gamma^0_{yz} &= u_{z0,y} + u_{y1} & \gamma^1_{yz} &= u_{z1,y} \\ \gamma^0_{xz} &= u_{z0,x} + u_{x1} & \gamma^1_{xz} &= u_{z1,x} \\ \epsilon^0_{zz} &= u_{z1} & \epsilon^1_{zz} &= 0 \end{aligned} \tag{3.48}$$

In the following it is convenient to group the stress and strain quantities into two distinct sets, that is *in-plane*, denoted as p, and the *out-of-plane* quantities, denoted as n. In this case it is

$$\begin{aligned} \boldsymbol{\epsilon}_p &= \{\epsilon_{xx} \quad \epsilon_{yy} \quad \gamma_{xy}\} & \boldsymbol{\sigma}_p &= \{\sigma_{xx} \quad \sigma_{yy} \quad \gamma_{xy}\} \\ \boldsymbol{\epsilon}_n &= \{\epsilon_{xz} \quad \epsilon_{yz} \quad \gamma_{zz}\} & \boldsymbol{\sigma}_n &= \{\sigma_{xz} \quad \sigma_{yz} \quad \gamma_{zz}\} \end{aligned} \tag{3.49}$$

The in-plane and out-of-plane quantities are referred to the surface Ω depicted in Figure 2.4. Considering a generic k layer of a multilayered plate Hooke's law defines the stress-strain relation, othotropic materials are considered:

$$\boldsymbol{\sigma}_{pp}^k = \mathbf{C}_{pp}^k \boldsymbol{\epsilon}_p + \mathbf{C}_{pn}^k \boldsymbol{\epsilon}_n \tag{3.50}$$

$$\boldsymbol{\sigma}_{nn}^k = \mathbf{C}_{pn}^k \boldsymbol{\epsilon}_p + \mathbf{C}_{nn}^k \boldsymbol{\epsilon}_n \tag{3.51}$$

that is

$$\begin{aligned}
\left\{ \begin{array}{c} \sigma_{xx}^k \\ \sigma_{yy}^k \\ \sigma_{xy}^k \end{array} \right\} &= \left[\begin{array}{ccc} C_{11}^k & C_{12}^k & C_{16}^k \\ C_{21}^k & C_{22}^k & C_{26}^k \\ C_{16}^k & C_{26}^k & C_{66}^k \end{array} \right] \cdot \left\{ \begin{array}{c} \epsilon_{xx} \\ \epsilon_{yy} \\ \gamma_{xy} \end{array} \right\} + \left[\begin{array}{ccc} 0 & 0 & C_{13}^k \\ 0 & 0 & C_{23}^k \\ 0 & 0 & C_{36}^k \end{array} \right] \cdot \left\{ \begin{array}{c} \gamma_{xx} \\ \gamma_{yz} \\ \epsilon_{zz} \end{array} \right\} \\
\left\{ \begin{array}{c} \sigma_{xz}^k \\ \sigma_{yz}^k \\ \sigma_{zz}^k \end{array} \right\} &= \left[\begin{array}{ccc} 0 & 0 & 0 \\ 0 & 0 & 0 \\ C_{13}^k & C_{23}^k & C_{36}^k \end{array} \right] \cdot \left\{ \begin{array}{c} \epsilon_{xx} \\ \epsilon_{yy} \\ \gamma_{xy} \end{array} \right\} + \left[\begin{array}{ccc} C_{55}^k & C_{45}^k & 0 \\ C_{44}^k & C_{44}^k & 0 \\ 0 & 0 & C_{33}^k \end{array} \right] \cdot \left\{ \begin{array}{c} \gamma_{xx} \\ \gamma_{yz} \\ \epsilon_{zz} \end{array} \right\}
\end{aligned} \tag{3.52}$$

3.5.1 Governing equations

The governing equations for a plate are obtained by means of the Principle of the Virtual Displacement (PVD) which states

$$\delta L_{int} = \delta L_{ext} \tag{3.53}$$

that is

$$\sum_{k=1}^{N_L} \int_{\Omega_k} \int_{A_k} \left(\delta \boldsymbol{\epsilon}_p^T \boldsymbol{\sigma}_p^k + \delta \boldsymbol{\epsilon}_n^T \boldsymbol{\sigma}_n^k \right) dV = \sum_{k=1}^{N_L} \delta L_{ext}^k \tag{3.54}$$

N_L is the number of the layers of the plate under exam. Transverse plate section is denoted as A_k. The virtual variation of the external applied loadings is written as $\sum_{k=1}^{N_L} \delta L_{ext}?^k$ and the virtual variation of the internal strain energy is denoted as δL_{int}. Upper script T denotes the transposition operation. Internal forces and momenta can be defined as

$$\left\{ \begin{array}{c} N_{xx} \\ N_{yy} \\ N_{xy} \end{array} \right\} = \sum_{k=1}^{N_L} \int_{A_k} \left[\begin{array}{c} \sigma_{xx}^k \\ \sigma_{yy}^k \\ \sigma_{xy}^k \end{array} \right] dz \qquad \left\{ \begin{array}{c} N_{yz} \\ N_{xz} \\ N_{zz} \end{array} \right\} = \sum_{k=1}^{N_L} \int_{A_k} \left[\begin{array}{c} \sigma_{yz}^k \\ \sigma_{xz}^k \\ \sigma_{zz}^k \end{array} \right] dz \tag{3.55}$$

$$\left\{ \begin{array}{c} M_{xx} \\ M_{yy} \\ M_{xy} \end{array} \right\} = \sum_{k=1}^{N_L} \int_{A_k} z \left[\begin{array}{c} \sigma_{xx}^k \\ \sigma_{yy}^k \\ \sigma_{xy}^k \end{array} \right] dz \qquad \left\{ \begin{array}{c} M_{yz} \\ M_{xz} \end{array} \right\} = \sum_{k=1}^{N_L} \int_{A_k} z \left[\begin{array}{c} \sigma_{yz}^k \\ \sigma_{xz}^k \end{array} \right] dz \tag{3.56}$$

All passages are not reported in this chapter, further details can be found in the Appendix 10. Considering a transverse pressure distribution at the top surface of the place the equilibrium equations of the plate are:

$$\begin{array}{ll} \delta u_{x0}: & N_{xx,x} + N_{xy,y} = 0 \\ \delta u_{y0}: & N_{yy,y} + N_{xy,x} = 0 \\ \delta u_{z0}: & N_{yz,y} + N_{xz,x} + p = 0 \\ \delta u_{x1}: & M_{xx,x} + M_{xy,y} - N_{xz} = 0 \\ \delta u_{y1}: & M_{yy,y} + M_{xy,x} - N_{yz} = 0 \\ \delta u_{z1}: & M_{xz,x} + M_{yz,y} - N_{zz} + p\frac{h}{2} = 0 \end{array} \tag{3.57}$$

and the related boundary conditions are

$$\begin{array}{ll} \delta u_{x0}: & \overline{N}_{xx} n_x + \overline{N}_{xy} n_y = 0 \\ \delta u_{y0}: & \overline{N}_{yy} n_x + \overline{N}_{xy} n_y = 0 \\ \delta u_{z0}: & \overline{N}_{yz} n_x + \overline{N}_{xz} n_y = 0 \\ \delta u_{x1}: & \overline{M}_{xx} n_x + \overline{M}_{xy} n_y = 0 \\ \delta u_{y1}: & \overline{M}_{yy} n_x + \overline{M}_{xy} n_y = 0 \\ \delta u_{z1}: & \overline{M}_{yz} n_x + \overline{M}_{xz} n_y = 0 \end{array} \tag{3.58}$$

3.5.2 Internal forces and momenta in terms of displacement variables

The internal forces can be expressed in terms of the displacements, that is

$$\left\{ \begin{array}{c} \mathbf{N}_p \\ \mathbf{N}_n \\ \mathbf{M}_p \\ \mathbf{M}_n \end{array} \right\} = \left[\begin{array}{cccc} \mathbf{A} & \mathbf{B} & \tilde{\mathbf{A}} & \tilde{\mathbf{B}} \\ \mathbf{E} & \mathbf{F} & \tilde{\mathbf{E}} & \tilde{\mathbf{F}} \\ \mathbf{B} & \mathbf{D} & \tilde{\mathbf{B}} & \tilde{\mathbf{D}} \\ \mathbf{0} & \mathbf{0} & \tilde{\mathbf{H}} & \tilde{\mathbf{F}} \end{array} \right] \left\{ \begin{array}{c} \boldsymbol{\epsilon}_p^0 \\ \boldsymbol{\epsilon}_p^1 \\ \boldsymbol{\epsilon}_n^0 \\ \boldsymbol{\epsilon}_n^1 \end{array} \right\} \tag{3.59}$$

defining

$$\mathbf{A} = \sum_{k=1}^{N_L} \int_{A_k} \begin{bmatrix} C_{11}^k & C_{12}^k & C_{16}^k \\ C_{21}^k & C_{22}^k & C_{26^k} \\ C_{16}^k & C_{26}^k & C_{66}^k \end{bmatrix} dz \quad \mathbf{B} = \sum_{k=1}^{N_L} \int_{Ak} z \begin{bmatrix} C_{11}^k & C_{12}^k & C_{16}^k \\ C_{21}^k & C_{22}^k & C_{26}^k \\ C_{16}^k & C_{26}^k & C_{66}^k \end{bmatrix} dz$$

$$\tilde{\mathbf{A}} = \sum_{k=1}^{N_L} \int_{A_k} \begin{bmatrix} 0 & 0 & C_{13}^k \\ 0 & 0 & C_{23}^k \\ 0 & 0 & C_{36}^k \end{bmatrix} dz \quad \tilde{\mathbf{B}} = \sum_{k=1}^{N_L} \int_{Ak} z \begin{bmatrix} 0 & 0 & C_{13}^k \\ 0 & 0 & C_{23}^k \\ 0 & 0 & C_{36}^k \end{bmatrix} dz$$

$$\mathbf{E} = \sum_{k=1}^{N_L} \int_{A_k} \begin{bmatrix} 0 & 0 & 0 \\ 0 & 0 & 0 \\ C_{13}^k & C_{23}^k & C_{36}^k \end{bmatrix} dz \quad \mathbf{F} = \sum_{k=1}^{N_L} \int_{Ak} z \begin{bmatrix} 0 & 0 & 0 \\ 0 & 0 & 0 \\ C_{13}^k & C_{23}^k & C_{36}^k \end{bmatrix} dz$$

$$\tilde{\mathbf{E}} = \sum_{k=1}^{N_L} \int_{A_k} \begin{bmatrix} C_{44}^k & C_{45}^k & 0 \\ C_{45}^k & C_{55}^k & 0 \\ 0 & 0 & C_{33}^k \end{bmatrix} dz \quad \tilde{\mathbf{F}} = \int_{Ak} z \begin{bmatrix} C_{44}^k & C_{45}^k & 0 \\ C_{45}^k & C_{55}^k & 0 \\ 0 & 0 & C_{33}^k \end{bmatrix} dz$$

$$\mathbf{B} = \sum_{k=1}^{N_L} \int_{A_k} z \begin{bmatrix} C_{11}^k & C_{12}^k & C_{16}^k \\ C_{21}^k & C_{22}^k & C_{26}^k \\ C_{16}^k & C_{26}^k & C_{66}^k \end{bmatrix} dz \quad \mathbf{D} = \sum_{k=1}^{N_L} \int_{Ak} z^2 \begin{bmatrix} C_{11}^k & C_{12}^k & C_{16}^k \\ C_{21}^k & C_{22}^k & C_{26}^k \\ C_{16}^k & C_{26}^k & C_{66}^k \end{bmatrix} dz$$

$$\tilde{\mathbf{B}} = \sum_{k=1}^{N_L} \int_{A_k} z \begin{bmatrix} 0 & 0 & C_{13}^k \\ 0 & 0 & C_{23}^k \\ 0 & 0 & C_{36}^k \end{bmatrix} dz \quad \tilde{\mathbf{D}} = \sum_{k=1}^{N_L} \int_{Ak} z^2 \begin{bmatrix} 0 & 0 & C_{13}^k \\ 0 & 0 & C_{23}^k \\ 0 & 0 & C_{36}^k \end{bmatrix} dz$$

$$\tilde{\mathbf{H}} = \sum_{k=1}^{N_L} \int_{A_k} z \begin{bmatrix} C_{44}^k & C_{45}^k \\ C_{45}^k & C_{55}^k \end{bmatrix} dz \quad \tilde{\mathbf{N}} = \sum_{k=1}^{N_L} \int_{Ak} z^2 \begin{bmatrix} C_{44}^k & C_{45}^k \\ C_{45}^k & C_{55}^k \end{bmatrix} dz \tag{3.60}$$

Substituting into Equation 10.20 the definitions reported in Equation 3.59 and remembering the definition of the strain components, it is possible to write the governing equations for a multilayered plate in terms of the displacement variables

$$\mathbf{Ku} = \mathbf{p} \rightarrow \begin{bmatrix} K_{11} & K_{12} & K_{13} & K_{14} & K_{15} & K_{16} \\ K_{21} & K_{22} & K_{23} & K_{24} & K_{25} & K_{26} \\ K_{31} & K_{32} & K_{33} & K_{34} & K_{35} & K_{36} \\ K_{41} & K_{42} & K_{43} & K_{44} & K_{45} & K_{46} \\ K_{51} & K_{52} & K_{53} & K_{54} & K_{55} & K_{56} \\ K_{61} & K_{62} & K_{63} & K_{64} & K_{65} & K_{66} \end{bmatrix} \begin{Bmatrix} u_{x0} \\ u_{y0} \\ u_{z0} \\ u_{x1} \\ u_{y1} \\ u_{z1} \end{Bmatrix} = \begin{Bmatrix} 0 \\ 0 \\ -p \\ 0 \\ 0 \\ -p\frac{h_k}{2} \end{Bmatrix} \tag{3.61}$$

where $\mathbf{K}$ is a differential operator. In a similar manner, the boundary conditions can be computed as

$$\mathbf{\Pi u} = \mathbf{\Pi \overline{u}} \rightarrow$$

$$\begin{bmatrix} \Pi_{11} & \Pi_{12} & \Pi_{13} & \Pi_{14} & \Pi_{15} & \Pi_{16} \\ \Pi_{21} & \Pi_{22} & \Pi_{23} & \Pi_{24} & \Pi_{25} & \Pi_{26} \\ \Pi_{31} & \Pi_{32} & \Pi_{33} & \Pi_{34} & \Pi_{35} & \Pi_{36} \\ \Pi_{41} & \Pi_{42} & \Pi_{43} & \Pi_{44} & \Pi_{45} & \Pi_{46} \\ \Pi_{51} & \Pi_{52} & \Pi_{53} & \Pi_{54} & \Pi_{55} & \Pi_{56} \\ \Pi_{61} & \Pi_{62} & \Pi_{63} & \Pi_{64} & \Pi_{65} & \Pi_{66} \end{bmatrix} \begin{Bmatrix} u_{x0} \\ u_{y0} \\ u_{z0} \\ u_{x1} \\ u_{y1} \\ u_{z1} \end{Bmatrix} = \begin{bmatrix} \Pi_{11} & \Pi_{12} & \Pi_{13} & \Pi_{14} & \Pi_{15} & \Pi_{16} \\ \Pi_{21} & \Pi_{22} & \Pi_{23} & \Pi_{24} & \Pi_{25} & \Pi_{26} \\ \Pi_{31} & \Pi_{32} & \Pi_{33} & \Pi_{34} & \Pi_{35} & \Pi_{36} \\ \Pi_{41} & \Pi_{42} & \Pi_{43} & \Pi_{44} & \Pi_{45} & \Pi_{46} \\ \Pi_{51} & \Pi_{52} & \Pi_{53} & \Pi_{54} & \Pi_{55} & \Pi_{56} \\ \Pi_{61} & \Pi_{62} & \Pi_{63} & \Pi_{64} & \Pi_{65} & \Pi_{66} \end{bmatrix} \begin{Bmatrix} \overline{u}_{x0} \\ \overline{u}_{y0} \\ \overline{u}_{z0} \\ \overline{u}_{x1} \\ \overline{u}_{y1} \\ \overline{u}_{z1} \end{Bmatrix} \tag{3.62}$$

where $\overline{\mathbf{u}}$ is the displacement function defined at the boundary Γ. The passages for the definition of the above introduced operators is given in Appendix 10.

3.5.3 Governing equations in terms of fundamental nuclei

In the following it is demonstrated that it is possible to express the governing equations in terms of fundamental nuclei, that is it is possible to express the plate governing equations reported in eq.s 10.34 as

$$\begin{bmatrix} \mathbf{K}^{00} & \mathbf{K}^{01} \\ \mathbf{K}^{10} & \mathbf{K}^{11} \end{bmatrix} \cdot \begin{Bmatrix} u_{x0} \\ u_{y0} \\ u_{z0} \\ u_{x1} \\ u_{y1} \\ u_{z1} \end{Bmatrix} = \begin{Bmatrix} 0 \\ 0 \\ -p \\ 0 \\ 0 \\ -p\frac{h}{2} \end{Bmatrix} \tag{3.63}$$

where $\mathbf{K}^{00}$, $\mathbf{K}^{01}$, $\mathbf{K}^{10}$ and $\mathbf{K}^{11}$ are 3×3 differential operators. The upper scripts 0 and 1 refer to the expansion order employed in the definition of the displacement field, in this case 0 refers to the constant term of the displacement field and 1 refers to the linear term of the expansion. In the following, these upper scripts are labeled as τ and s. In an explicit way it is

$$\begin{array}{c} \\ 1 \\ \\ z \\ \\ \end{array} \begin{array}{c} \begin{array}{ccc} 1 & & z \end{array} \\ \begin{bmatrix} K_{11}^{00} & K_{12}^{00} & K_{13}^{00} & K_{11}^{01} & K_{11}^{01} & K_{11}^{01} \\ K_{21}^{00} & K_{22}^{00} & K_{23}^{00} & K_{21}^{01} & K_{22}^{01} & K_{23}^{01} \\ K_{31}^{00} & K_{32}^{00} & K_{33}^{00} & K_{31}^{01} & K_{32}^{01} & K_{33}^{01} \\ K_{11}^{10} & K_{12}^{10} & K_{13}^{10} & K_{11}^{11} & K_{12}^{11} & K_{13}^{11} \\ K_{21}^{10} & K_{22}^{10} & K_{23}^{10} & K_{21}^{11} & K_{22}^{11} & K_{23}^{11} \\ K_{31}^{10} & K_{32}^{10} & K_{33}^{10} & K_{31}^{11} & K_{32}^{11} & K_{33}^{11} \end{bmatrix} \end{array} \begin{Bmatrix} u_{x0} \\ u_{y0} \\ u_{z0} \\ u_{x1} \\ u_{y1} \\ u_{z1} \end{Bmatrix} = \begin{Bmatrix} 0 \\ 0 \\ -p \\ 0 \\ 0 \\ -p\frac{h}{2} \end{Bmatrix} \tag{3.64}$$

The equation reported in 10.37 can be written in a unified manner by means of a fundamental nucleus. All the passages are not reported in this chapter for the sake of brevity, they are reported in the Appendix 10. In that Appendix it is shown how it is possible to define the fundamental nucleus for the theory reported in this chapter and how it is possible to extend it to any order plate theory. The fundamental nucleus for any order plate theory is defined for the generic k layer of a multilayered plate as

$$\begin{aligned}
K_{11}^{k\tau s} =& C_{11}^k E_{\tau s}\partial_{,xx} + C_{66}^k E_{\tau s}\partial_{,yy} + 2C_{16}^k E_{\tau s}\partial_{,xy} - C_{55}^k E_{\tau_{,z}s_{,z}} \\
K_{12}^{k\tau s} =& C_{16}^k E_{\tau s}\partial_{,xx} + C_{26}^k E_{\tau s}\partial_{,yy} + (C_{66}^k E_{\tau s} + C_{12}^k E_{\tau s})\partial_{,xy} - C_{45}^k E_{\tau_{,z}s_{,z}} \\
K_{13}^{k\tau s} =& (C_{13}^k E_{\tau_{,z}s} - C_{55}^k E_{\tau s_{,z}})\partial_{,x} + (C_{36}^k E_{\tau_{,z}s} - C_{45}^k E_{\tau s_{,z}})\partial_{,y} \\
K_{21}^{k\tau s} =& C_{16}^k E_{\tau s}\partial_{,xx} + C_{26}^k E_{\tau s}\partial_{,yy} + (C_{12}^k E_{\tau s} + C_{66}^k E_{\tau s})\partial_{,xy} - C_{45}^k E_{\tau_{,z}s_{,z}} \\
K_{22}^{k\tau s} =& C_{66}^k E_{\tau s}\partial_{,xx} + C_{22}^k E_{\tau s}\partial_{,yy} + 2C_{26}^k E_{\tau s}\partial_{,xy} - C_{44}^k E_{\tau_{,z}s_{,z}} \\
K_{23}^{k\tau s} =& (C_{36}^k E_{\tau_{,z}s} - C_{45}^k E_{\tau s_{,z}})\partial_{,x} + (C_{23}^k E_{\tau_{,z}s} - C_{44}^k E_{\tau s_{,z}})\partial_{,y} \\
K_{31}^{k\tau s} =& (C_{55}^k E_{\tau_{,z}s} - C_{13}^k E_{\tau s_{,z}})\partial_{,x} + (C_{45}^k E_{\tau_{,z}s} - C_{36}^k E_{\tau s_{,z}})\partial_{,y} \\
K_{32}^{k\tau s} =& (C_{45}^k E_{\tau_{,z}s} - C_{36}^k E_{\tau s_{,z}})\partial_{,x} + (C_{44}^k E_{\tau_{,z}s} - C_{23}^k E_{\tau s_{,z}})\partial_{,y} \\
K_{33}^{k\tau s} =& C_{55}^k E_{\tau s}\partial_{,xx} + C_{44}^k E_{\tau s}\partial_{,yy} + 2C_{45}^k E_{\tau s}\partial_{,xy} - C_{33}^k E_{\tau_{,z}s_{,z}}
\end{aligned} \tag{3.65}$$

Similar passages can be applied to the differential operator $\mathbf{\Pi}^{k\tau s}$, the result is

$$\begin{aligned}
\Pi_{11}^{k\tau s} =& E_{\tau s}(C_{11}^k\partial_{,x} + C_{16}^k\partial_{,y}) + E_{\tau s}(C_{16}^k\partial_{,x} + C_{66}^k\partial_{,y}) \\
\Pi_{12}^{k\tau s} =& E_{\tau s}(C_{16}^k\partial_{,x} + C_{12}^k\partial_{,y}) + E_{\tau s}(C_{26}^k\partial_{,y} + C_{66}^k\partial_{,x}) \\
\Pi_{13}^{k\tau s} =& C_{13}^k E_{\tau_{,z}s} + C_{36}E_{\tau_{,z}s} \\
\Pi_{21}^{k\tau s} =& E_{\tau s}(C_{21}^k\partial_{,x} + C_{26}^k\partial_{,y}) + E_{\tau s}(C_{16}^k\partial_{,x} + C_{66}^k\partial_{,y}) \\
\Pi_{22}^{k\tau s} =& E_{\tau s}(C_{26}^k\partial_{,x} + C_{22}^k\partial_{,y}) + E_{\tau s}(C_{26}^k\partial_{,y} + C_{66}^k\partial_{,x}) \\
\Pi_{23}^{k\tau s} =& C_{23}^k E_{\tau_{,z}s} + C36E_{\tau_{,z}s} \\
\Pi_{31}^{k\tau s} =& C_{45}^k E_{\tau_{,z}s} + C_{55}^k E_{\tau_{,z}s} \\
\Pi_{32}^{k\tau s} =& C_{44}^k E_{\tau_{,z}s} + C_{54}^k E_{\tau_{,z}s} \\
\Pi_{33}^{k\tau s} =& E_{\tau s}(C_{45}^k\partial_{,x} + C_{44}^k\partial_{,y}) + E_{\tau s}(C_{55}^k\partial_{,x} + C_{54}^k\partial_{,y})
\end{aligned} \tag{3.66}$$

The meaning of $E_{\tau s}$, $E_{\tau_{,z}s}$, $E_{\tau s_{,z}}$ and $E_{\tau_{,z}s_{,z}}$ is reported in the Appendix 10.

3.5.4 Conclusion

The equation reported in 10.48 show that it is possible to write the equilibrium equations in a such a way it is not necessary to derive these ones whenever a new displacement field is assumed. The same passages can be repeated for the shell case and for multifield problems. The results reported in this chapter can be considered as preparatory to the introduction of the Carrera Unified Formulation (CUF). In the next chapter, it is introduced a compact notation to define any expansion order displacement field. The fundamental nucleus is defined by means of this notation and some results of multilayered and multifiled plate and shells will be discussed. In the following, the closed-form Navier type solutions are considered.

Chapter 4

Unified Formulation

The Carrera Unified Formulation (CUF) is introduced in this chapter. This theory is developed by considering two different schemes (Equivaletn Single Layer (ELS) and Layer Wise (LW)) and two different variational statements (the Principle of Virtual Variation (PVD) and the Reissner Mixed Variational Theorem (RMVT)). The CUF is employed to obtain the governing equation for multifiled problems for plates, taking into consideration the PVD variational statement. The thermal and piezomechanical problems are considered.

4.1 Unified Formulation, an introduction

Improvement of the classical theories for plate ans shells can be obtained by increasing the expansion order of the displacement components in the thickness direction z; these models are defined as *refined*. A model can be implemented according to two different approaches, Equivalent Single Layer (ESL) and Layer Wise approach (LW). According to ESL approach a heterogeneous multilayered plate is analyzed considering a single equivalent lamina. In this case the number of unknowns does not depend on the number of layers. Classical theories, i.e. CLT and FSDT, can be classified as ESL theories. According to LW approach each layer of a multilayered plate/shell is separately considered. In this case the number of unknowns depends on the number of the layers considered. The Carrera Unified Formulation makes it possible to obtain the refined models for plates and shells in a unified manner according to both ESL and LW schemes; the governing equations can be written in terms of few fundamental nuclei whose form does not depend on the particular expansion order adopted. Considering

a generic bidimensional structure whose reference system is $\alpha - \beta - z$, according to the CUF the displacement field can be described as:

$$\mathbf{u}(\alpha, \beta, z) = F_\tau(z) \cdot \mathbf{u}_\tau(\alpha, \beta) \qquad \tau = 0, 2, \ldots, N \tag{4.1}$$

where $\mathbf{u}$ is the displacement vector $(u_\alpha \; u_\beta \; u_z)$ whose components are the displacements along the α, β, z reference axes. F_τ are the expansion functions and functions $\mathbf{u}_\tau = (u_{\tau\alpha}, \; u_{\tau\beta}, \; u_{\tau z})$ are the displacement variables; N is the expansion order.

4.2 ESL and LW schemes

The expansion functions F_τ can be defined on the overall thickness of the plate/shell or for each k-layer. In the former case Equivalent Single Layer (ESL) approach is followed and in the latter case a Layer Wise (LW) approach is used. Examples of ESL and LW schemes for plates are reported in Fig.s 4.1(a) and 4.1(b) respectively: a transverse section of a multilayered plate is reported, the number of layers is equal to N_L. A generic displacement component distribution is presented according to linear and higher order expansion of both methods. In the case an ESL scheme is adopted the location of the point P on the total thickness is z_P (Fig. 4.1(a)) while for LW scheme the point P is defined according to the local k-layer reference system labeled in the figure as x_k, y_k, ζ_k (Fig. 4.1(b)). In the following ESL and LW approaches are discussed in detail. References on the CUF implemented according to the ESL and LW schemes can be found in [18].

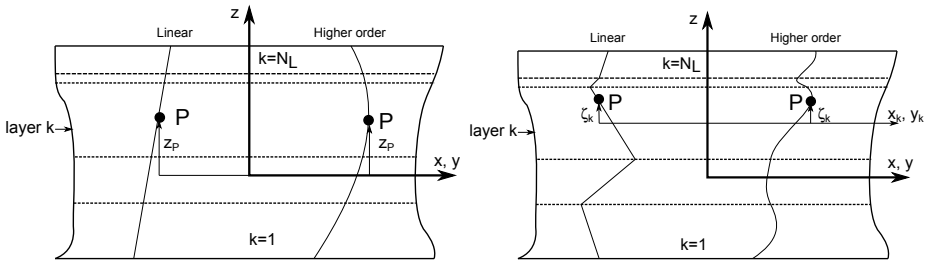

(a) Equivalent Single Layer scheme (b) Layer Wise scheme

Figure 4.1: Linear and higher order ESL and LW examples for plate analysis.

4.2.1 Equivalent Single Layer theory

According to ESL scheme the behavior of a multilayered structure is analyzed considering it as a single equivalent lamina. In this case F_τ functions are the Taylor expansions of z defined as $F_\tau = z^{\tau-1}$. In the following the ESL models are synthetically indicated as EDN, where N is the expansion order and D indicates that the theory is a displacement formulation. In addition, the ESL models are denoted with EMN if the RMVT variational statement is employed ("M" means mixed). An example of an ED4 displacement field for a plate is reported in the following

$$\begin{aligned} u_x &= u_{x_0} + z\,u_{x_1} + z^2\,u_{x_2} + z^3\,u_{x_3} + z^4\,u_{x_4} \\ u_y &= u_{y_0} + z\,u_{y_1} + z^2\,u_{y_2} + z^3\,u_{y_3} + z^4\,u_{y_4} \\ u_z &= u_{z_0} + z\,u_{z_1} + z^2\,u_{z_2} + z^3\,u_{z_3} + z^4\,u_{z_4} \end{aligned} \tag{4.2}$$

In Fig. 4.2, the displacement field computed by means of an ED4 models is reported for a three layered structure.

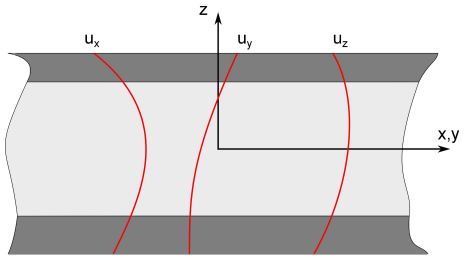

Figure 4.2: Displacement field for ED4 model.

As mentioned in [49], classical models such as CLT and FSDT can be considered special cases of full linear expansion (ED1) since CLT/FSDT displacement variables are

$$\begin{aligned} u_x &= u_{x_0} + z\,u_{x_1} \\ u_y &= u_{y_0} + z\,u_{y_1} \\ u_z &= u_{z_0} \end{aligned} \tag{4.3}$$

A penalty technique can be employed to obtain these models. In addition the penalty technique has to be used in order to impose the condition $\gamma_{xz} = \gamma_{yz} = 0$ for the CLT model. The first order models based on ESL scheme present the so called *thickness locking* (TL), i.e. the simplified kinematic assumptions in the plate analysis does not permit to thin plate theories analysis to lead to 3D solution in thin plate problems. In [50] the authors analyze and propose some solutions for this problem.

4.2.2 Layer Wise theory

According to Layer Wise scheme the displacement field exhibits only C_0-continuity through the laminate thickness. LW models can be conveniently built by using Legendre's polynomials expansion in each layer. The displacement field is described as

$$\mathbf{u}^k = F_t \cdot \mathbf{u}_t^k + F_b \cdot \mathbf{u}_b^k + F_r \cdot \mathbf{u}_r^k = F_\tau \mathbf{u}_\tau^k \qquad \tau = t, b, r \;\; r = 2, 3, \ldots, N \qquad k = 1, 2, \ldots, N_l \tag{4.4}$$

where k is the generic k-layer of a plate/shell and N_l is the number of the layers. Subscripts t and b correspond to the top and the bottom of a layer. Functions F_τ depend on a coordinate ζ_k, its range is $-1 \leq \zeta_k \leq 1$; its representation is reported in Fig. 4.1(b). The extremal values -1 and 1 are reached at the bottom and at the top of the layer. Functions F_τ derive from the Legendre's polynomials according to the following equations.

$$F_t = \frac{P_0 + P_1}{2} \qquad F_b = \frac{P_0 - P_1}{2} \qquad F_r = P_r - P_{r-2} \qquad r = 2, 3, \ldots, N \tag{4.5}$$

The Legendre's polynomials used for fourth order theory are:

$$P_0 = 1 \quad P_1 = \zeta_k \quad P_2 = \frac{3\zeta_k^2 - 1}{2} \quad P_3 = \frac{5\zeta_k^3 - 3\zeta_k}{2} \quad P_4 = \frac{35\zeta_k^4}{8} - \frac{15\zeta_k^2}{4} + \frac{3}{8} \tag{4.6}$$

LW models ensure the compatibility of displacement at the interfaces 'zig-zag' effects by definition, that is

$$\mathbf{u}_t^k = \mathbf{u}_b^{k+1} \qquad k = 1, \ldots, N_l - 1 \tag{4.7}$$

In the following LW models are denoted by the acronym as LDN, where N is the expansion order. In addition, the LW models are denoted with LMN if the RMVT variational statement is employed. "M" means mixed. An example of LD4 layer displacement field for a plate is

$$\begin{aligned} u_x^k &= F_t\, u_{xt}^k + F_2\, u_{x2}^k + F_3\, u_{x3}^k + F_4\, u_{x4}^k + F_b\, u_{xb}^k \\ u_y^k &= F_t\, u_{yt}^k + F_2\, u_{y2}^k + F_3\, u_{y3}^k + F_4\, u_{y4}^k + F_b\, u_{yb}^k \\ u_z^k &= F_t\, u_{zt}^k + F_2\, u_{z2}^k + F_3\, u_{z3}^k + F_4\, u_{z4}^k + F_b\, u_{zb}^k \end{aligned} \tag{4.8}$$

In Fig. 4.3 the displacement field computed by means of an ED4 models is reported for a three layered structure.

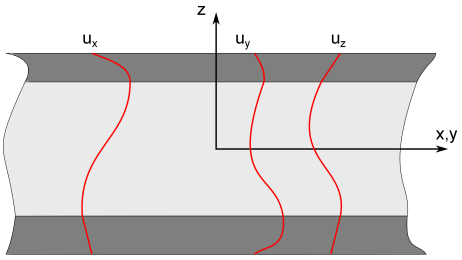

Figure 4.3: Displacement field for LD4 model.

4.3 Governing equations - the PVD case

In this section the refined models obtained by means of the Principle of the Virtual Variation (PVD) are reported. A complete introduction to the PVD and the use of the CUF can be found in [51]. Mechanical case are described for the plate and the shell, and multifield models (i.e. thermal and piezoelectric) for plate are reported. In the following, the attention has been here restricted to the case of closed form solution related to simply supported orthotropic rectangular plates, loaded by a transverse distribution of harmonic loadings. The following properties hold

$$C_{16} = C_{26} = C_{36} = C_{45} = 0 \tag{4.9}$$

In this case the displacement are therefore express in the following harmonic form:

$$\begin{aligned} u^k_{x_\tau} &= \hat{U}^k_{x_\tau} \cos\left(\frac{m\pi_k}{a_k}\right) \sin\left(\frac{n\pi y_k}{b_k}\right) \\ u^k_{y_\tau} &= \hat{U}^k_{y_\tau} \sin\left(\frac{m\pi x_k}{a_k}\right) \cos\left(\frac{n\pi y_k}{b_k}\right) \\ u^k_{z_\tau} &= \hat{U}^k_{z_\tau} \sin\left(\frac{m\pi x_k}{a_k}\right) \sin\left(\frac{n\pi y_k}{b_k}\right) \end{aligned} \qquad \begin{aligned} k &= 1, N_l \\ \tau &= 1, N \end{aligned} \tag{4.10}$$

where $\hat{U}^k_{x_\tau}$, $\hat{U}^k_{y_\tau}$ and $\hat{U}^k_{z_\tau}$ are the amplitudes, m and n are the number of waves (they range from 0 to ∞) and a_k and b_k are the dimensions of the plate. The same solution can be applied to ESL approach, in this case displacement variables appears without superscript k. The transverse pressure acting on the plate is defined as

$$p = p^0_z \sin\left(\frac{m\pi x_k}{a_k}\right) \sin\left(\frac{n\pi y_k}{b_k}\right) \tag{4.11}$$

In the case of shell analysis, the Equations 4.57 become

$$\begin{array}{ll} u^k_{\alpha_\tau} = \hat{U}^k_{\alpha_\tau} \cos\left(\frac{m\pi_k}{a_k}\right) \sin\left(\frac{n\pi\beta_k}{b_k}\right) & k = 1, N_l \\ u^k_{\beta_\tau} = \hat{U}^k_{\beta_\tau} \sin\left(\frac{m\pi\alpha_k}{a_k}\right) \cos\left(\frac{n\pi\beta_k}{b_k}\right) & \tau = 1, N \\ u^k_{z_\tau} = \hat{U}^k_{z_\tau} \sin\left(\frac{m\pi\alpha_k}{a_k}\right) \sin\left(\frac{n\pi\beta_k}{b_k}\right) & \end{array} \tag{4.12}$$

and the transverse pressure load is

$$p = p^0_z \sin\left(\frac{m\pi\alpha_k}{a_k}\right) \sin\left(\frac{n\pi\beta_k}{b_k}\right) \tag{4.13}$$

4.3.1 Plate mechanical analysis

The analysis of a multilayered plate can be conducted by means of the Principle of Virtual Displacement (PVD) which states that:

$$\sum_{k=1}^{N_L} \delta\, L^k_{int} = \sum_{k=1}^{N_L} \delta\, L^k_{ext} \tag{4.14}$$

The virtual variation is denoted as δ and the number of the layers is N_L. The term δL_{ext} denotes the virtual variation of energy of the applied loads, while δL_{int} denotes the virtual variation of the internal strain energy. The virtual variation of the strain energy can be computed in a explicit form as

$$\delta\, L^k_{int} = \int_{V_K} \left(\delta \boldsymbol{\epsilon}^{k^T}_p \cdot \boldsymbol{\sigma}^k_p + \delta \boldsymbol{\epsilon}^{k^T}_n \cdot \boldsymbol{\sigma}^k_n \right) dV_k \tag{4.15}$$

where V_K is the domain of the generic k layer. Considering the strain-stress and the strain-displacement relations, and employing the CUF it is possible to write the governing equations for the plate as

$$\sum_{k=1}^{N_L} \int_{\Omega_k} \delta \mathbf{u}^k_s \, \boldsymbol{K}^{k\tau s}_{uu} \mathbf{u}^k_\tau d\Omega_k + \sum_{k=1}^{N_L} \int_{\Gamma_k} \delta \mathbf{u}^k_s \boldsymbol{\Pi}^{k\tau s}_{uu} \mathbf{u}^k_\tau d\Gamma_k = \sum_{k=1}^{N_L} \int_{\Omega_k} \delta \mathbf{u}_s \, \mathbf{p} \, d\Omega_k \tag{4.16}$$

The definition of the fundamental nuclei $\mathbf{K}^{k\tau s}_{uu}$ and $\boldsymbol{\Pi}^{k\tau s}_{uu}$ is reported in the following:

$$\begin{aligned}\mathbf{K}_{uu}^{\tau\, s} = &\Big\{(-\mathbf{D}_p)^T \left[\mathbf{C}_{pp}^k E_{\tau s}\, \mathbf{D}_p + \mathbf{C}_{pn}^k E_{\tau s}\mathbf{D}_{n\Omega} + \mathbf{C}_{pn}^k E_{\tau_{,z} s}\right] + \\ &(-\mathbf{D}_{n\Omega})^T \left[\mathbf{C}_{np}^k E_{\tau s}\mathbf{D}_p + \mathbf{C}_{nn}^k E_{\tau s}\mathbf{D}_{n\Omega} + \mathbf{C}_{nn}^k E_{\tau_{,z} s}\right] + \\ &+ \left[\mathbf{C}_{np}^k E_{\tau s_{,z}}\mathbf{D}_p + \mathbf{C}_{nn}^k E_{\tau s_{,z}}\mathbf{D}_{n\Omega} + \mathbf{C}_{nn}^k E_{\tau_{,z} s_{,z}}\right]\Big\} \qquad (4.17)\\ \mathbf{\Pi}_{uu}^{k\,\tau\, s} = &\Big\{(\mathbf{I}_p)^T \left[\mathbf{C}_{pp}^k E_{s\tau}\, \mathbf{D}_p + \mathbf{C}_{pn}^k E_{s\tau}\mathbf{D}_{n\Omega} + \mathbf{C}_{pn}^k E_{s\tau_{,z}}\right] + \\ &+ (\mathbf{I}_{n\Omega})^T \left[\mathbf{C}_{np}^k E_{s\tau}\mathbf{D}_p + \mathbf{C}_{nn}^k E_{s\tau}\mathbf{D}_{n\Omega} + \mathbf{C}_{nn}^k E_{s\tau_{,z}}\right]\Big\} \qquad (4.18)\end{aligned}$$

The development of all passages is herein omitted for sake of brevity; details can be found in the Appendix 11. The static response of a plate subjected to a transverse pressure distribution can be computed by solving the system

$$\begin{aligned}\delta\mathbf{u}_s^{k^T} &: \mathbf{K}_{uu}^{\tau s}\cdot\mathbf{u}_\tau^k = \mathbf{P}_{u\tau}^\tau \\ \delta\mathbf{u}_s^{k^T} &: \mathbf{\Pi}_{uu}^{k\tau s}\mathbf{u}_\tau^k = \mathbf{\Pi}_{uu}^{k\tau s}\overline{\widehat{\mathbf{u}}}_\tau^k \qquad (4.19)\end{aligned}$$

$\mathbf{P}_{u\tau}^\tau$ is the external load. The fundamental nucleus, $\mathbf{K}_{uu}^{\tau s}$ is assembled through the depicted indexes, τ and s, which consider the order of the expansion in z for the displacements. Superscript k denotes the assembly on the number of layers. If the Navier closed-form solution is considered, the displacement field is expressed as in Equations 4.10 and a transverse pressure is considered as defined in Equation 4.11. The definition of the components of the operator $\mathbf{K}_{uu}^{k\tau s}$ for the Navier closed form solution case is reported in the Appendix 11.

4.3.2 Mechanical shell analysis

The coordinate frame adopted is presented in Fig. 2.2 for a single layer of a shell. The definitions of some operators used in the followings were introduced in chapter 2. The strain-displacement relations can be written as

$$\boldsymbol{\epsilon}_p^k = \mathbf{D}_p\mathbf{u}^k + \mathbf{A}_p^k\mathbf{u}^k \qquad \boldsymbol{\epsilon}_n^k = \mathbf{D}_{n\Omega}\mathbf{u}^k + \mathbf{A}_n^k\mathbf{u}^k + \mathbf{D}_{nz}^k\mathbf{u}^k \qquad (4.20)$$

where

$$\boldsymbol{\epsilon}_p^k = [\epsilon_{\alpha\alpha}\ \epsilon_{\beta\beta}\ \epsilon_{\alpha\beta}] \qquad \boldsymbol{\epsilon}_n^k = [\epsilon_{\alpha z}\ \epsilon_{\beta z}\ \epsilon_{zz}] \qquad (4.21)$$

The stress - strain relation is defined by means of the Hooke's law

$$\boldsymbol{\sigma}^k = \mathbf{C}\boldsymbol{\epsilon}^k \quad \rightarrow \quad \begin{array}{l} \boldsymbol{\sigma}_p^k = \mathbf{C}_{pp}\boldsymbol{\epsilon}_p^k + \mathbf{C}_{pn}\boldsymbol{\epsilon}_n^k \\ \boldsymbol{\sigma}_n^k = \mathbf{C}_{np}\boldsymbol{\epsilon}_p^k + \mathbf{C}_{nn}\boldsymbol{\epsilon}_n^k \end{array} \tag{4.22}$$

The governing equations are obtained via the Principle of Virtual Displacement (PVD):

$$\sum_{k=1}^{N_l} \int_{\Omega_k} \int_{A_k} \left(\delta\boldsymbol{\epsilon}_p^{k^T} \sigma_p^k + \delta\boldsymbol{\epsilon}_n^{k^T} \sigma_n^k \right) d\Omega_k \, dz = \sum_{k=1}^{N_l} \delta L_e^k \tag{4.23}$$

The governing equations for a multilayered shell can be written in a similar manner as the governing equations for the multilayered plated, i.e.

$$\sum_{k=1}^{N_L} \int_{\Sigma_k} \delta\mathbf{u}_s^k \, \boldsymbol{K}_{uu}^{k\tau s} \mathbf{u}_\tau^k d\Omega_k + \sum_{k=1}^{N_L} \int_{\Gamma_k} \delta\mathbf{u}_s^k \boldsymbol{\Pi}_{uu}^{k\tau s} \mathbf{u}_\tau^k d\Gamma_k = \sum_{k=1}^{N_L} \int_{\Omega_k} \delta\mathbf{u}_s \, \mathbf{p} \, d\Omega_k \tag{4.24}$$

in this case it is

$$\begin{aligned} \mathbf{K}_{uu}^{\tau\, s} = \Big\{ & (-\mathbf{D}_p + \mathbf{A}_p)^T \left[\mathbf{C}_{pp}^k E_{s\tau} \, \mathbf{D}_p + \mathbf{C}_{pp}^k E_{s\tau} \, \mathbf{A}_p + \mathbf{C}_{pn}^k E_{s\tau} \mathbf{D}_{n\Omega} + \mathbf{C}_{pn}^k E_{s\tau_{,z}} + \mathbf{C}_{pn}^k E_{s\tau} \mathbf{A}_n \right] \\ & + (-\mathbf{D}_{n\Omega} + \mathbf{A}_n)^T \left[\mathbf{C}_{pn}^{k^T} E_{s\tau} \mathbf{D}_p + \mathbf{C}_{pn}^{k^T} E_{s\tau} \mathbf{A}_p + \mathbf{C}_{nn}^k E_{s\tau} \mathbf{D}_{n\Omega} + \mathbf{C}_{nn}^k E_{s\tau} \mathbf{A}_n + \mathbf{C}_{nn}^k E_{s\tau_{,z}} \right] \\ & + \left[\mathbf{C}_{pn}^{k^T} E_{s_{,z}\tau} \mathbf{D}_p + \mathbf{C}_{pn}^{k^T} E_{s_{,z}\tau} \mathbf{A}_p + \mathbf{C}_{nn}^k E_{s_{,z}\tau} \mathbf{D}_{n\Omega} + \mathbf{C}_{nn}^k E_{s_{,z}\tau} \mathbf{A}_n + \mathbf{C}_{nn}^k E_{s_{,z}\tau_{,z}} \right] \Big\} \, H_\alpha^k \, H_\beta^k \end{aligned} \tag{4.25}$$

and for boundary condition it is

$$\begin{aligned} \boldsymbol{\Pi}_{uu}^{k\,\tau\, s} = \Big\{ & (\mathbf{I}_p)^T \left[\mathbf{C}_{pp}^k E_{s\tau} \, \mathbf{D}_p + \mathbf{C}_{pp}^k E_{s\tau} \, \mathbf{A}_p + \mathbf{C}_{pn}^k E_{s\tau} \mathbf{D}_{n\Omega} + \mathbf{C}_{pn}^k E_{s\tau} \mathbf{A}_n + \mathbf{C}_{pn}^k E_{s\tau_{,z}} \right] \\ & + (\mathbf{I}_{n\Omega})^T \left[\mathbf{C}_{pn}^{k^T} E_{s\tau} \mathbf{D}_p + \mathbf{C}_{pn}^{k^T} E_{s\tau} \mathbf{A}_p + \mathbf{C}_{nn}^k E_{s\tau} \mathbf{D}_{n\Omega} + \mathbf{C}_{nn}^k E_{s\tau} \mathbf{A}_n + \mathbf{C}_{nn}^k E_{s\tau_{,z}} \right] \Big\} \, H_\alpha^k \, H_\beta^k \end{aligned} \tag{4.26}$$

The static response of a shell subjected to a transverse pressure distribution can be computed by solving the system

$$\begin{array}{l} \delta\mathbf{u}_s^{k^T} : \mathbf{K}_{uu}^{\tau s} \cdot \mathbf{u}_\tau^k = \mathbf{P}_{u\tau}^\tau \\ \delta\mathbf{u}_s^{k^T} : \boldsymbol{\Pi}_{uu}^{k\tau s} \mathbf{u}_\tau^k = \boldsymbol{\Pi}_{uu}^{k\tau s} \overline{\hat{\mathbf{u}}}_\tau^k \end{array} \tag{4.27}$$

$\mathbf{P}_{u\tau}^{\tau}$ is the external load. The fundamental nucleus, $\mathbf{K}_{uu}^{\tau s}$ is assembled through the depicted indexes, τ and s, which consider the order of the expansion in z for the displacements. Superscript k denotes the assembly on the number of layers. In the following, Navier closed form solution for shells (see equations 4.12 and 4.13) are employed. Details on the analysis of shells by means of the CUF are reported in [20].

4.3.3 Thermal stress analysis

The thermal stress analysis reported in this thesis is based on the assumption that the temperature distribution can be considered as an external load. Another possible way to include the effect of the temperature distribution in the structural analysis is the fully coupled approach. This approach makes it possible to describe the mutual effect of the temperature distribution and deformation field [52]. This type of analysis analysis considers both temperature and displacement fields as primary variables in the governing equations. The use of the fully coupled approach for thermo-mechanical analysis of plates in the frame of CUF theory can be found in [53]. In the following, the temperature distribution is assumed a-priori. The temperature distribution is defined as

$$\theta(x, y, z) = \theta_z \sin\left(\frac{m\pi x}{a}\right) \sin\left(\frac{n\pi y}{b}\right) \tag{4.28}$$

where θ_z denotes a temperature distribution along the thickness direction. The function θ_z can be defined a-priori or computed by means of the Fourier differential equation. In the former case, θ_z can be defined as a linear function

$$\theta_z = \theta_0 \frac{2\,z}{h} + \overline{\theta}_0 \tag{4.29}$$

Parameters θ_0 and $\overline{\theta}_0$ have to be defined according to the desired top and bottom temperature values. The total thickness of the plate is h. A synthetic representation of the linear assumed temperature distribution is reported in Fig. 4.4

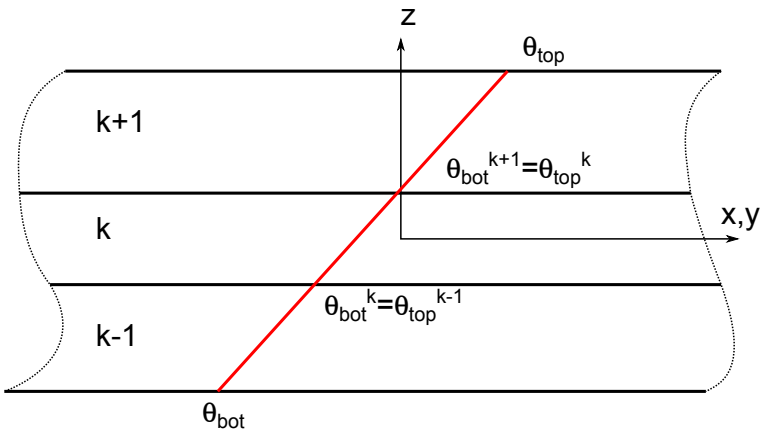

Figure 4.4: Temperature profile distribution.

The governing equations for the thermal plate analysis obtained by means of the PVD are:

$$\sum_{k=1}^{N_l} \int_{\Omega_k} \int_{A_k} \left[\delta \boldsymbol{\epsilon}_p^{k^T} \boldsymbol{\sigma}_p^k + \delta \boldsymbol{\epsilon}_n^{k^T} \boldsymbol{\sigma}_n^k \right] dz \, d\Omega_k = \sum_{k=1}^{N_L} \delta \, L_{ext}^k \tag{4.30}$$

where N_l defines the number of layers of the shell and δ denotes the virtual variation. $\int_{A_k} dz$ indicates the integration along the cross sectional area of a generic k-the layer and Ω_k is the plan area of a k layer. In Equation 4.30 stresses $\boldsymbol{\sigma}_p$ and $\boldsymbol{\sigma}_n$ are considered as the sum of the mechanical (m) and thermal (t) contributions, i.e.

$$\boldsymbol{\sigma}_p = \boldsymbol{\sigma}_{pH}^k - \boldsymbol{\sigma}_{pT}^k \qquad \boldsymbol{\sigma}_n = \boldsymbol{\sigma}_{nH}^k - \boldsymbol{\sigma}_{nT}^k \tag{4.31}$$

The subscript H denotes the stresses defined according to the Hooke's law, while the subscript T denotes the stresses derived from the temperature distribution. The thermal stresses are defined as in Section 2.3. Dividing the strain and stress components into in-plane (p) and out-of-plane (n) components, the thermal stresses can be written for a generic layer k as

$$\begin{aligned} \boldsymbol{\sigma}_{pT}^k &= \mathbf{C}_{pp}^k \, \boldsymbol{\alpha}_p^k \, \theta + \mathbf{C}_{pn}^k \, \boldsymbol{\alpha}_p^k \, \theta \\ \boldsymbol{\sigma}_{nT}^k &= \mathbf{C}_{pn}^k \, \boldsymbol{\alpha}_n^k \, \theta + \mathbf{C}_{nn}^k \, \boldsymbol{\alpha}_n^k \, \theta \end{aligned} \tag{4.32}$$

where θ is the temperature distribution and $\boldsymbol{\alpha}_p^k$ is the in-plane thermal expansion coefficient (the components are $\left[\alpha_x^k \; \alpha_y^k \; 0\right]$) and $\boldsymbol{\alpha}_n^k$ is the out-of-plane thermal expansion coefficient (the components are $\left[0 \; 0 \; \alpha_z^k\right]$). The PVD for the thermal stress analysis of a plate can be written as

$$\sum_{k=1}^{N_l} \int_{\Gamma_k} \delta \mathbf{u}_s^{k^T} \left\{ \mathbf{\Pi}_{uu}^{k\tau s} \mathbf{u}_\tau^k + \mathbf{\Pi}_{u\theta}^{k\tau s} \theta_z \right\} \mathbf{u}_\tau^k d\Gamma_k - \sum_{k=1}^{N_l} \int_{\Omega_k} \delta \mathbf{u}_s^{k^T} \left\{ \mathbf{K}_{uu}^{k\tau s} \mathbf{u}_\tau^k + \mathbf{K}_{u\theta}^{k\tau s} \theta_z \right\} \mathbf{u}_\tau^k d\Omega_k = \sum_{k=1}^{N_l} \int_{\Omega_k} \delta \mathbf{u}_s^{k^T} \mathbf{P}_{u\tau}^k \tag{4.33}$$

Operators $\mathbf{K}_{uu}^{k\tau s}$ and $\mathbf{\Pi}_{uu}^{k\tau s}$ have been already defined in the section related to the plate mechanical stress analysis. The definitions of the operators $\mathbf{K}_{u\theta}^{k\tau s}$ and $\mathbf{\Pi}_{\theta\theta}^{k\tau s}$ are reported in the following:

$$\begin{aligned} \mathbf{K}_{u\theta}^{k\tau\, s} =& \mathbf{D}_p^T \boldsymbol{\lambda}_p^k \left(\int_{A_k} F_s \theta_z^k dz \right) + \mathbf{D}_{n\Omega}^T \boldsymbol{\lambda}_n^k \left(\int_{A_k} F_s \theta_z^k dz \right) + \boldsymbol{\lambda}_n^k \left(\int_{A_k} F_{s,z} \theta_z^k dz \right) \\ \mathbf{\Pi}_{u\theta}^{k\,\tau\, s} =& \mathbf{I}_p^T \boldsymbol{\lambda}_p^k \left(\int_{A_k} F_s \theta_z^k dz \right) + \mathbf{I}_{n\Omega}^T \boldsymbol{\lambda}_n^k \left(\int_{A_k} F_s \theta_z^k dz \right) \end{aligned} \tag{4.34}$$

where $\boldsymbol{\lambda}_p$ and $\boldsymbol{\lambda}_n$ are defined as:

$$\boldsymbol{\lambda}_p = \begin{bmatrix} \lambda_1 \\ \lambda_2 \\ \lambda_6 \end{bmatrix} = \mathbf{C}_{pp} \boldsymbol{\alpha}_p^k + \mathbf{C}_{pn} \boldsymbol{\alpha}_n^k \qquad \boldsymbol{\lambda}_n = \begin{bmatrix} 0 \\ 0 \\ \lambda_3 \end{bmatrix} = \mathbf{C}_{np} \boldsymbol{\alpha}_p^k + \mathbf{C}_{nn} \boldsymbol{\alpha}_n^k \tag{4.35}$$

Vectors $\boldsymbol{\lambda}_p$ and $\boldsymbol{\lambda}_n$ express the partial coupling between the mechanical field and the temperature. The static response of a plate subjected to a temperature distribution can be computed by solving the following equations system

$$\mathbf{K}_{uu}^{k\tau s} \mathbf{u}_\tau^k = -\mathbf{K}_{u\theta}^{k\tau s} \theta_\tau^k + \mathbf{P}_{us}^k \tag{4.36}$$

with the related boundary conditions on edge Γ^k

$$\mathbf{\Pi}_{uu}^{k\tau s} \mathbf{u}_\tau^k + \mathbf{\Pi}_{u\theta}^{k\tau s} \theta_z = \mathbf{\Pi}_{uu}^{k\tau s} \overline{\mathbf{u}}_\tau^k + \mathbf{\Pi}_{u\theta}^{k\tau s} \overline{\theta}_z \tag{4.37}$$

If the Navier closed form solution is employed, the definition of the operators $\mathbf{K}_{uu}^{k\tau s}$ has been already defined in the Appendix 11. More details on the thermal stress analysis performed by means of the CUF are reported in [54].

4.3.4 Piezoelectric mechanic plate

A piezoelectric plate is a multilayered plate which has N_L layers and some of them can have piezoelectric properties, that is they can show a deformation state under the effect of an applied electrical potential. Conversely under the effect of a mechanical load the piezoelectric layers present a potential distribution. The equilibrium equations are developed according to a Cartesian reference system, reported in Fig. 2.4. Stresses and the electric field coupling effect in a generic k-layer is sustained by the direct and converse piezoelectric effect and is defined according to the IEEE standard [46] and reported in 2.4. In the following the electric potential distribution is expressed according to a Layer Wise form distribution, that is

$$\Phi = F_t\Phi_t + F_r\Phi_r + F_b\Phi_b = F_\tau\Phi_\tau \qquad \tau = t, r, b \; r = 2, 3, 4 \tag{4.38}$$

The continuity of the potential distribution at the layers interfaces has to be imposed:

$$\Phi_t^k = \Phi_b^{k+1} \qquad k = 1, \cdots, N_L - 1 \tag{4.39}$$

The potential distribution is a scalar quantity, but for implementation reasons it is convenient to define it as a vector, i.e., $\mathbf{\Phi}^k = \left[\Phi^k \; \Phi^k \; \Phi^k\right]$. In this case, the electric field strength can be expressed as

$$\mathbf{E}^k = \mathbf{D}_e\mathbf{\Phi}^k \tag{4.40}$$

where

$$\mathbf{D}_e = \begin{bmatrix} -\partial_{,x} & 0 & 0 \\ 0 & -\partial_{,y} & 0 \\ 0 & 0 & -\partial_{,z} \end{bmatrix} = \underbrace{\begin{bmatrix} -\partial_{,x} & 0 & 0 \\ 0 & -\partial_{,y} & 0 \\ 0 & 0 & 0 \end{bmatrix}}_{\mathbf{D}_{e\Omega}} + \underbrace{\begin{bmatrix} 0 & 0 & 0 \\ 0 & 0 & 0 \\ 0 & 0 & -\partial_{,z} \end{bmatrix}}_{\mathbf{D}_{ez}} \tag{4.41}$$

The PVD applied to a piezoelectric plate becomes

$$\sum_{k=1}^{N_L} \int_{V_k} \left(\delta\boldsymbol{\epsilon}_p^{k^T} \cdot \boldsymbol{\sigma}_p^k + \delta\boldsymbol{\epsilon}_n^{k^T} \cdot \boldsymbol{\sigma}_n^k - \delta\mathbf{E}^{k^T} \; \tilde{\mathbf{D}}^k \right) dV = \sum_{k=1}^{N_L} \delta \, L_{ext}^k \tag{4.42}$$

Remembering the definition of the operators reported in equation 4.42 it is possible to write

$$\sum_{k=1}^{N_l}\int_{\Omega_k}\Big\{(\mathbf{D}_p\delta\mathbf{u}_\tau^\tau)^T F_\tau\left[\left(\mathbf{C}_{pp}^k\mathbf{D}_p+\mathbf{C}_{pn}^k\mathbf{D}_n\right)F_s\mathbf{u}_s^k-\mathbf{e}_p^k\mathbf{D}_eF_s\Phi_s^k\right]+$$
$$+\left(\mathbf{D}_n\delta\mathbf{u}_\tau^k\right)^T F_\tau\left[\left(\mathbf{C}_{np}^k\mathbf{D}_p+\mathbf{C}_{nn}D_n\right)F_s\mathbf{u}_s^k-\mathbf{e}_n^{k^T}\mathbf{D}_eF_s\Phi_s^k\right]-$$
$$-\left(\mathbf{D}_e\delta\Phi_\tau^k\right)^T F_\tau\left[\left(\mathbf{e}_p^k\mathbf{D}_p+\mathbf{e}_n^k\mathbf{D}_n\right)F_s\mathbf{u}_s^k+\boldsymbol{\varepsilon}^k\mathbf{D}_eF_s\Phi^k\right]\Big\}\,dV=\sum_{k=1}^{N_L}\delta\,L_{ext}^k \quad (4.43)$$

Considering the integration by parts theorem, the PVD for a piezoelectric plate can be written as

$$\sum_{k=1}^{N_l}\int_{\Gamma_k}\left\{\delta\mathbf{u}_s^{k^T}\left(\mathbf{\Pi}_{uu}^{k\tau s}\mathbf{u}_\tau^k+\mathbf{\Pi}_{ue}^{k\tau s}\mathbf{\Phi}_\tau^k\right)+\delta\mathbf{\Phi}_\tau^k\left(\mathbf{\Pi}_{eu}^{k\tau s}\mathbf{u}_\tau^k+\mathbf{\Pi}_{ee}^{k\tau s}\mathbf{\Phi}_\tau^k\right)\right\}d\Gamma_k-$$
$$\sum_{k=1}^{N_l}\int_{\Omega_k}\left\{\delta\mathbf{u}_s^{k^T}\left(\mathbf{K}_{uu}^{k\tau s}\mathbf{u}_\tau^k+\mathbf{K}_{ue}^{k\tau s}\mathbf{\Phi}_\tau^k\right)+\delta\mathbf{\Phi}_\tau^k\left(\boldsymbol{K}_{eu}^{k\tau s}\mathbf{u}_\tau^k+\boldsymbol{K}_{ee}^{k\tau s}\mathbf{\Phi}_\tau^k\right)\right\}d\Omega_k=\sum_{k=1}^{N_L}\delta\,L_{ext}^k \quad (4.44)$$

The development of these equation is herein omitted for sake of brevity. Further details are reported in [55] and in the book [56]. The static response of a piezoelectric plate subjected to a transverse pressure distribution and/or a electric potential distribution can be computed by solving the following equations:

$$\begin{aligned}
\delta\mathbf{u}_s^k &: \mathbf{K}_{uu}^{k\tau s}\mathbf{u}_\tau^k+\mathbf{K}_{ue}^{k\tau s}\mathbf{\Phi}_\tau^k=\mathbf{P}_{u\tau}^k\\
\delta\mathbf{\Phi}_s^k &: \boldsymbol{K}_{eu}^{k\tau s}\mathbf{u}_\tau^k+\boldsymbol{K}_{ee}^{k\tau s}\mathbf{\Phi}_\tau^k=0\\
\delta\mathbf{u}_s^k &: \mathbf{\Pi}_{uu}^{k\tau s}\mathbf{u}_\tau^k+\mathbf{\Pi}_{ue}^{k\tau s}\mathbf{\Phi}_\tau^k=\mathbf{\Pi}_{uu}^{k\tau s}\hat{\mathbf{u}}_\tau^k+\mathbf{\Pi}_{ue}^{k\tau s}\hat{\mathbf{\Phi}}_\tau^k\\
\delta\mathbf{\Phi}_s^k &: \mathbf{\Pi}_{eu}^{k\tau s}\mathbf{u}_\tau^k+\mathbf{\Pi}_{ee}^{k\tau s}\mathbf{\Phi}_\tau^k=\mathbf{\Pi}_{eu}^{k\tau s}\hat{\mathbf{u}}_\tau^k+\mathbf{\Pi}_{ee}^{k\tau s}\hat{\mathbf{\Phi}}_\tau^k
\end{aligned} \quad (4.45)$$

The attention has been here restricted to the case of closed form solution related to simply supported, cross-ply orthotropic rectangular plates loaded by a transverse distribution of harmonic loadings. The displacement have been already defined in Equation 4.10 and the potential function Φ^k is therefore express in the following harmonic form:

$$\Phi_\tau^k=\hat{\Phi}_\tau^k\cdot\sin\left(\frac{m\pi x_k}{a_k}\right)\sin\left(\frac{n\pi y_k}{b_k}\right) \quad (4.46)$$

where $\hat{\Phi}_\tau^k$ is the amplitude. Two different configurations are considered: sensor and actuator configurations. When a sensor configuration is considered, a transverse pressure is applied to the top surface of the plate and a potential distribution is generated. The potential at the top and at the bottom is set to zero. When an actuator configuration is considered the deformation state of a plate is originated by the imposition of a potential distribution: the value of the potential is set to 1 V at the top and to 0 V at the bottom of the plate. A transverse pressure is considered for the sensor configuration, and its expression is reported in Equation 4.11. The electric load employed in the actuator configuration is expressed in Equation and 4.46. The reference system layout and the representation of the two configurations are reported in Figure 4.5.

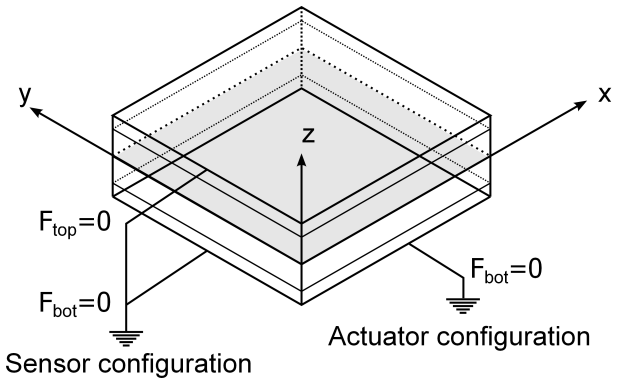

Figure 4.5: Active and sensor plate configuration.

4.4 The governing equations - the RMVT case

In this section, the definition of the fundamental nuclei for multilayered plate models based on the RMVT variational statement. This variational statement is employed in order to obtain the equilibrium equations and the relative boundary conditions for a multilayered the plate considering a transverse pressure distribution. A complete introduction to the RMVT and the use of the CUF can be found in [51]. According to the Reissner Mixed Variational Theorem (RMVT), the transverse stress components (i.e. σ_{xz}, σ_{yz} and σ_{zz}) are assumed. Considering the CUF these variables are defined as

$$\boldsymbol{\sigma}_{nM}(z,y,z) = \begin{bmatrix} \sigma_{xzM}(z,y,z) \\ \sigma_{yzM}(z,y,z) \\ \sigma_{zzM}(z,y,z) \end{bmatrix} = F_\tau(z) \begin{bmatrix} \sigma_{xzM\tau}(x,y) \\ \sigma_{yzM\tau}(x,y) \\ \sigma_{zzM\tau}(x,y) \end{bmatrix} \qquad \tau = 1,2,\ldots,N+1 \tag{4.47}$$

The subscript M is for "model". An appropriate form of the Hooke's law is required since the transverse stresses are assumed. The following mixed form is then employed:

$$\begin{aligned} \boldsymbol{\sigma}_{pH} =& \tilde{\mathbf{C}}^k_{pp}\boldsymbol{\epsilon}^k_{pG} + \tilde{\mathbf{C}}^k_{pn}\boldsymbol{\sigma}^k_{nM} \\ \boldsymbol{\epsilon}_{nH} =& \tilde{\mathbf{C}}^k_{np}\boldsymbol{\epsilon}^k_{pG} + \tilde{\mathbf{C}}^k_{nn}\boldsymbol{\sigma}^k_{nM} \end{aligned} \tag{4.48}$$

The new elastic coefficient matrices are

$$\tilde{\mathbf{C}}^k_{pp} = \mathbf{C}^k_{pp} - \mathbf{C}^k_{pn}\mathbf{C}^{k^{-1}}_{nn}\mathbf{C}^k_{np} \qquad \tilde{\mathbf{C}}^k_{pn} = \mathbf{C}^k_{pn}\mathbf{C}^{k^{-1}}_{nn} \qquad \tilde{\mathbf{C}}^k_{np} = -\mathbf{C}^{k^{-1}}_{nn}\mathbf{C}^k_{np} \qquad \tilde{\mathbf{C}}^k_{nn} = \mathbf{C}^{k^{-1}}_{nn} \tag{4.49}$$

In the case of RMVT approach, the variational statement becomes

$$\sum_{k=1}^{N_L} \int_{\Omega_k}\int_{A_k} \left[\delta\boldsymbol{\epsilon}^T_{pG}\boldsymbol{\sigma}_{pH} + \delta\boldsymbol{\epsilon}^T_{nG}\boldsymbol{\sigma}_{nM} + \delta\boldsymbol{\sigma}^T_{nM}\left(\boldsymbol{\epsilon}_{nG} - \boldsymbol{\epsilon}_{nH}\right)\right] dA_k d\Omega_k = \sum_{k=1}^{N_L} \int_{\Omega_k}\int_{A_k} \delta\mathbf{u}^T\,\mathbf{p}\,dA_k\,d\Omega_k \tag{4.50}$$

The "mixed" term $\delta\boldsymbol{\sigma}^T_{nM}\left(\boldsymbol{\epsilon}_{nG} - \boldsymbol{\epsilon}_{nH}\right)$ enforces the compatibility of the transverse strain components $\boldsymbol{\epsilon}_n$. In the following, the subscript G indicates the strain obtained by means of the differenatial operators defined in Equations 2.36 and 2.37 and the subscript H indicates the stresses obtained by means of the Hooke's law.

The governing equations for the plate analysis can be obtained from Equation 4.50 by substituting the definition of the displacement field, the transverse stress components and and computing the stress by means of the modified Hooke's law. The development of all passages is herein omitted for sake of brevity; details can be found in the already mentioned CUF works and books. The static response of a multilayered plate can be evaluated by solving the equation:

$$\sum_{k=1}^{N_L}\int_{\Gamma_k}\delta\mathbf{u}_s^{kT}\left\{\mathbf{I}_p^T\tilde{\mathbf{C}}_{pp}^k E_{\tau\,s}\mathbf{D}_p\mathbf{u}_\tau^k+\mathbf{I}_p^T\tilde{\mathbf{C}}_{pn}^k E_{\tau\,s}\boldsymbol{\sigma}_{n\tau}^k+\mathbf{I}_{n\Omega}^T E_{\tau\,s}\boldsymbol{\sigma}_{n\tau}\right\}d\Gamma_k-$$
$$\sum_{k=1}^{N_L}\int_{\Omega_k}\left\{\delta\mathbf{u}_s^{kT}\left[\mathbf{D}_p^T\tilde{\mathbf{C}}_{pp}^k E_{\tau\,s}\left(\mathbf{D}_p\mathbf{u}_\tau^k\right)+\mathbf{D}_p^T\tilde{\mathbf{C}}_{pn}^k E_{\tau\,s}\boldsymbol{\sigma}_{n\tau}^k+\mathbf{D}_{n\Omega}^T E_{\tau\,s}\boldsymbol{\sigma}_{n\tau}+E_{\tau\,s,z}\boldsymbol{\sigma}_{n\tau}\right]+\right.$$
$$\left.+\delta\boldsymbol{\sigma}_{ns}^T\left[\mathbf{D}_{n\Omega}E_{\tau\,s}\mathbf{u}_\tau^k+E_{\tau,z\,s}\mathbf{u}_\tau^k-\tilde{\mathbf{C}}_{np}^k E_{\tau\,s}\left(\mathbf{D}_p\mathbf{u}_\tau^k\right)^k-\tilde{\mathbf{C}}_{nn}^k E_{\tau\,s}\boldsymbol{\sigma}_{n\tau}^k\right]\right\}d\Omega_k=$$
$$\sum_{k=1}^{N_L}\int_{\Omega_k}\int_{A_k}\delta\left(F_s\mathbf{u}_s\right)^T\,\mathbf{p}\,dA_k\,d\Omega_k \tag{4.51}$$

In a synthetic way, it is possible to write the equilibrium equations as

$$\begin{aligned}\mathbf{K}_{uu}^{k\tau s}\mathbf{u}_\tau^k+\mathbf{K}_{u\sigma}^{k\tau s}\boldsymbol{\sigma}_\tau^k&=\mathbf{p}^k\\ \mathbf{K}_{\sigma u}^{k\tau s}\mathbf{u}_\tau^k+\mathbf{K}_{\sigma\sigma}^{k\tau s}\boldsymbol{\sigma}_\tau^k&=0\end{aligned} \tag{4.52}$$

with boundary conditions

$$\boldsymbol{\Pi}_u^{k\tau s}\mathbf{u}_\tau^k+\boldsymbol{\Pi}_\sigma^{k\tau s}\boldsymbol{\sigma}_{n\tau}^k=\boldsymbol{\Pi}_u^{k\tau s}\overline{\mathbf{u}}_\tau^k+\boldsymbol{\Pi}_\sigma^{k\tau s}\overline{\boldsymbol{\sigma}}_{n\tau}^k \tag{4.53}$$

The introduced differential arrays are given by the following relations

$$\begin{aligned}\mathbf{K}_{uu}^{k\tau s}&=-\mathbf{D}_p^T\tilde{\mathbf{C}}_{pp}^k\mathbf{D}_pE_{\tau s}\\ \mathbf{K}_{u\sigma}^{k\tau s}&=-\mathbf{D}_p^T\tilde{\mathbf{C}}_{pn}^kE_{\tau s}+\mathbf{I}E_{\tau s,z}-\mathbf{D}_{n\Omega}^TE_{\tau s}\\ \mathbf{K}_{\sigma u}^{k\tau s}&=\mathbf{D}_{n\Omega}E_{\tau s}+\mathbf{I}E_{\tau_{,z}s}-\tilde{\mathbf{C}}_{np}^k\mathbf{D}_pE_{\tau s}\\ \mathbf{K}_{\sigma\sigma}^{k\tau s}&=-\tilde{\mathbf{C}}_{nn}^kE_{\tau s}\\ \boldsymbol{\Pi}_u^{k\tau s}&=\mathbf{I}_p^T\tilde{\mathbf{C}}_{pp}^k\mathbf{D}_pE_{\tau s}\\ \boldsymbol{\Pi}_\sigma^{k\tau s}&=\mathbf{I}_p^T\tilde{\mathbf{C}}_{pn}^kE_{\tau s}+\mathbf{I}_{n\Omega}^TE_{\tau s}\end{aligned} \tag{4.54}$$

$\mathbf{I}$ is the operator

$$\mathbf{I}=\begin{bmatrix}1&0&0\\0&1&0\\0&0&1\end{bmatrix} \tag{4.55}$$

The solution of the system of equations reported in 4.52 is performed expressing the stress variables in function of the displacement variables, i.e.

$$\begin{aligned}
&\boldsymbol{\sigma}_{\tau}^{k} = -\left(\mathbf{K}_{\sigma\sigma}^{k\tau s}\right)^{-1}\left(\mathbf{K}_{\sigma u}^{k\tau s}\mathbf{u}_{\tau}^{k}\right) \\
&\mathbf{K}_{uu}^{k\tau s}\mathbf{u}_{\tau}^{k} - \mathbf{K}_{u\sigma}^{k\tau s}\left(\mathbf{K}_{\sigma\sigma}^{k\tau s}\right)^{-1}\left(\mathbf{K}_{\sigma u}^{k\tau s}\mathbf{u}_{\tau}^{k}\right) = \mathbf{P}^{k} \\
\rightarrow &\left[\mathbf{K}_{uu}^{k\tau s} - \mathbf{K}_{u\sigma}^{k\tau s}\left(\mathbf{K}_{\sigma\sigma}^{k\tau s}\right)^{-1}\mathbf{K}_{\sigma u}^{k\tau s}\right]\mathbf{u}_{\tau}^{k} = \mathbf{P}^{k}
\end{aligned} \tag{4.56}$$

The attention has been here restricted to the case of closed form solution related to simply supported orthotropic rectangular plates, loaded by a transverse distribution of harmonic loadings. In this case, the displacement are therefore express in the harmonic form reported in Equation 11.26. In addition, the transverse stresses are expressed in a similar manner, i.e.

$$\begin{aligned}
\sigma_{xz\tau}^{k} &= \hat{\sigma}_{xz\tau}^{k}\cos\left(\tfrac{m\pi x_k}{a_k}\right)\sin\left(\tfrac{n\pi y_k}{b_k}\right) \qquad k = 1, N_l \\
\sigma_{yz\tau}^{k} &= \hat{\sigma}_{yz\tau}^{k}\sin\left(\tfrac{m\pi x_k}{a_k}\right)\cos\left(\tfrac{n\pi y_k}{b_k}\right) \qquad \tau = 1, N \\
\sigma_{zz\tau}^{k} &= \hat{\sigma}_{zz\tau}^{k}\sin\left(\tfrac{m\pi x_k}{a_k}\right)\sin\left(\tfrac{n\pi y_k}{b_k}\right)
\end{aligned} \tag{4.57}$$

where $\hat{\sigma}_{xz\tau}^{\tau}$, $\hat{\sigma}_{yz\tau}^{\tau}$ and $\hat{\sigma}_{zz\tau}^{\tau}$ are the amplitudes, m and n are the number of waves (they range from 0 to ∞) and a_k and b_k are the dimensions of the plate. The same solution can be applied to ESL approach, in this case displacement variables appears without superscript k.

4.5 Fundamental Nuclei Assembly

Once the fundamental nuclei for a plate under exam are obtained, the same has to be assembled. The assembly procedure depends on the type of scheme assumed. In the following, the fundamental nuclei definition for the ESL and LW schemes are reported.

4.5.1 Equivalent Single Layer

In the following it is described how it is possible to write the governing equations obtained by means of UF for a multilayered plate. Let's consider a two layers plate. The virtual variation of the internal work for such a plate can be computed as

$$\delta L_{int} = \delta L_{int}^{1} + \delta L_{int}^{2} \tag{4.58}$$

the upper scripts 1 and 2 refer to the first and second layer; for each layer it is possible to write

$$\delta L^1_{int} = \delta \mathbf{u}^T_{\tau_1} \mathbf{K}_1 \mathbf{u}_{\tau_1} \qquad \delta L^2_{int} = \delta \mathbf{u}^T_{\tau_2} \mathbf{K}_2 \mathbf{u}_{\tau_2} \tag{4.59}$$

$\mathbf{K}_1$ and $\mathbf{K}_2$ are the obtained from the UF for each layer. Since an ESL scheme is used it is possible to define $\mathbf{u}_{\tau_1} = \mathbf{u}_{\tau_2} = \mathbf{u}_\tau$ so in this case it is

$$\delta L_{int} = \delta \mathbf{u}^T_\tau \left(\mathbf{K}_1 + \mathbf{K}_2 \right) \mathbf{u}_\tau \tag{4.60}$$

It is possible to conclude that when ESL scheme is adopted to analyze a multilayered plate the governing equations for the overall plate can be obtained just summing all terms of the matrices obtained by means of UF for each layer. A graphic representation of the matrix assembly for the ESL scheme is reported in the following. A third order expansion is considered (i.e. ED3 model). The displacement variables of the first layer are represented by means of the symbol ▲, while the displacement variables of the second layer are represented by means of the symbol □. The matrix $\mathbf{K}^{1\,33}_{uu}$ and $\mathbf{K}^{2\,33}_{uu}$ are

▲	▲	▲	▲	▲	▲	▲	▲	▲
▲	▲	▲	▲	▲	▲	▲	▲	▲
▲	▲	▲	▲	▲	▲	▲	▲	▲
▲	▲	▲	▲	▲	▲	▲	▲	▲
▲	▲	▲	▲	▲	▲	▲	▲	▲
▲	▲	▲	▲	▲	▲	▲	▲	▲
▲	▲	▲	▲	▲	▲	▲	▲	▲
▲	▲	▲	▲	▲	▲	▲	▲	▲

Table 4.1: Representation of the matrix $\mathbf{K}^{1\,33}_{uu}$.

□	□	□	□	□	□	□	□	□
□	□	□	□	□	□	□	□	□
□	□	□	□	□	□	□	□	□
□	□	□	□	□	□	□	□	□
□	□	□	□	□	□	□	□	□
□	□	□	□	□	□	□	□	□
□	□	□	□	□	□	□	□	□
□	□	□	□	□	□	□	□	□

Table 4.2: Representation of the matrix $\mathbf{K}^{2\,33}_{uu}$.

The matrix $\mathbf{K}_{uu}^{1\,33} + \mathbf{K}_{uu}^{2\,33}$ is then

▲+□	▲+□	▲+□	▲+□	▲+□	▲+□	▲+□	▲+□	▲+□
▲+□	▲+□	▲+□	▲+□	▲+□	▲+□	▲+□	▲+□	▲+□
▲+□	▲+□	▲+□	▲+□	▲+□	▲+□	▲+□	▲+□	▲+□
▲+□	▲+□	▲+□	▲+□	▲+□	▲+□	▲+□	▲+□	▲+□
▲+□	▲+□	▲+□	▲+□	▲+□	▲+□	▲+□	▲+□	▲+□
▲+□	▲+□	▲+□	▲+□	▲+□	▲+□	▲+□	▲+□	▲+□
▲+□	▲+□	▲+□	▲+□	▲+□	▲+□	▲+□	▲+□	▲+□
▲+□	▲+□	▲+□	▲+□	▲+□	▲+□	▲+□	▲+□	▲+□

Table 4.3: Representation of the matrix $\mathbf{K}_{uu}^{1\,33} + \mathbf{K}_{uu}^{2\,33}$.

4.5.2 Layer Wise

The analysis of a multilayered plate by means of LW starts from the evaluation of the virtual variation of the internal work of each layer; considering a plate made of two layer it is

$$\delta L_{int} = \delta L_{int}^1 + \delta L_{int}^2 \tag{4.61}$$

the upper scripts 1 and 2 refer to the first and second layer; for each layer it is possible to write

$$\delta L_{int}^1 = \delta \mathbf{u}_{\tau_1}^T \mathbf{K}_1 \mathbf{u}_{\tau_1} \qquad \delta L_{int}^2 = \delta \mathbf{u}_{\tau_2}^T \mathbf{K}_2 \mathbf{u}_{\tau_2} \tag{4.62}$$

$\mathbf{K}_1$ and $\mathbf{K}_2$ are the obtained from the UF for each layer. Since a LW scheme is used the displacement variables of each layer can be grouped into common (c) and proper (p) displacement variables; in the former group there are the displacement variables which satisfy the condition $\mathbf{u}_{top}^{k+1} = \mathbf{u}_{bot}^{k}$, in the latter there are the variables which describe the displacement field of the two layer. In this case the δL_{int} is

$$\delta L_{int} = \delta \mathbf{u}_{\tau_1^p}^T \mathbf{K}_1 \mathbf{u}_{\tau_1^p} + \delta \mathbf{u}_{\tau_2^p}^T \mathbf{K}_2 \mathbf{u}_{\tau_2^p} + \delta \mathbf{u}_{\tau^c}^T \left(\mathbf{K}_1 + \mathbf{K}_2\right) \mathbf{u}_{\tau^c} \tag{4.63}$$

A graphic representation of the matrix assembly for the LW scheme is reported in the following. A third order expansion is considered (i.e. LD3 model). The displacement variables of the first layer are represented by means of the symbol ▲, while the displacement variables of the second layer are represented by means of the symbol □. The matrix $\mathbf{K}_{uu}^{1\,33}$ and $\mathbf{K}_{uu}^{2\,33}$ are

▲	▲	▲	▲	▲	▲	▲	▲	▲
▲	▲	▲	▲	▲	▲	▲	▲	▲
▲	▲	▲	▲	▲	▲	▲	▲	▲
▲	▲	▲	▲	▲	▲	▲	▲	▲
▲	▲	▲	▲	▲	▲	▲	▲	▲
▲	▲	▲	▲	▲	▲	▲	▲	▲
▲	▲	▲	▲	▲	▲	▲	▲	▲
▲	▲	▲	▲	▲	▲	▲	▲	▲

Table 4.4: Representation of the matrix $\mathbf{K}_{uu}^{1\,33}$.

□	□	□	□	□	□	□	□	□
□	□	□	□	□	□	□	□	□
□	□	□	□	□	□	□	□	□
□	□	□	□	□	□	□	□	□
□	□	□	□	□	□	□	□	□
□	□	□	□	□	□	□	□	□
□	□	□	□	□	□	□	□	□
□	□	□	□	□	□	□	□	□

Table 4.5: Representation of the matrix $\mathbf{K}_{uu}^{2\,33}$.

The matrix $\mathbf{K}_{uu}^{1\,33} + \mathbf{K}_{uu}^{2\,33}$ is then

▲	▲	▲	▲	▲	▲	▲	▲	▲	0	0	0	0	0	0
▲	▲	▲	▲	▲	▲	▲	▲	▲	0	0	0	0	0	0
▲	▲	▲	▲	▲	▲	▲	▲	▲	0	0	0	0	0	0
▲	▲	▲	▲	▲	▲	▲	▲	▲	0	0	0	0	0	0
▲	▲	▲	▲	▲	▲	▲	▲	▲	0	0	0	0	0	0
▲	▲	▲	▲	▲	▲	▲	▲	▲	0	0	0	0	0	0
▲	▲	▲	▲	▲	▲	▲+□	▲+□	▲+□	□	□	□	□	□	□
▲	▲	▲	▲	▲	▲	▲+□	▲+□	▲+□	□	□	□	□	□	□
▲	▲	▲	▲	▲	▲	▲+□	▲+□	▲+□	□	□	□	□	□	□
0	0	0	0	0	0	□	□	□	□	□	□	□	□	□
0	0	0	0	0	0	□	□	□	□	□	□	□	□	□
0	0	0	0	0	0	□	□	□	□	□	□	□	□	□
0	0	0	0	0	0	□	□	□	□	□	□	□	□	□
0	0	0	0	0	0	□	□	□	□	□	□	□	□	□
0	0	0	0	0	0	□	□	□	□	□	□	□	□	□

Table 4.6: Representation of the matrix $\mathbf{K}_{uu}^{1\,33} + \mathbf{K}_{uu}^{2\,33}$.

4.6 Unified formulation - numerical results

In this chapter, it is reported a comparison of the results obtained by means of the CUF formulation for multilayered plates and shells with the analytical solution available in the open literature. Mechanical and multifield problems are considered, in particular the results computed by means of the LD4, ED4 and LM4 models are described. These comparisons are shown in order to prove that LD4, LM4 and ED4 models can provide accurate reference solutions to the axiomatic/asymptotic technique. In the following, all results are presented in a non-dimensional form, that is

Mechanical stress plate analysis:

$$\begin{aligned} \overline{u}_z =& \frac{100\, u_z\, E_T}{\overline{p}_z\, (a/h)^4} \qquad \overline{\sigma}_{xx/yy/xy} = \frac{\sigma_{xx/yy/xy}}{\overline{p}_z\, (a/h)^2} \\ \overline{\sigma}_{xz/yz} =& \frac{\sigma_{xz/yz}}{\overline{p}_z\, (a/h)} \qquad \overline{\sigma}_{zz} = \frac{\sigma_{zz}}{\overline{p}_z\, (a/h)} \end{aligned} \tag{4.64}$$

Mechanical stress shell analysis:

$$\begin{aligned} \overline{u}_z =& \frac{u_z\, 10\, E_L\, h^3}{p_0\, R_\beta^4} \qquad \overline{\sigma}_{\alpha\alpha/\beta\beta/\alpha\beta} = 10\, \frac{\sigma_{\alpha\alpha/\beta\beta/\alpha\beta}}{p_0\, (R_\beta/h)^2} \\ \overline{\sigma}_{\alpha z/\beta\, z} =& 10\, \frac{\sigma_{\alpha z/\beta\, z}}{p_0\, (R_\beta/h)} \qquad \overline{\sigma}_{zz} = \frac{\sigma_{zz}}{p_0} \end{aligned} \tag{4.65}$$

Thermal stress plate analysis:

$$\begin{aligned} \overline{u}_x =& \frac{u_x}{h\, \alpha_L\, T_0\, (a/h)} \qquad \overline{u}_z = \frac{u_z}{h\, \alpha_L\, T_0\, (a/h)^2} \\ \overline{\sigma}_{ij} =& \frac{\sigma_{ij}}{E_T\, \alpha_L\, T_0} \end{aligned} \tag{4.66}$$

Results for the piezo - electric plate are reported in dimensional form. The transverse pressure distribution, the temperature distribution and the potential distribution are expressed as

$$p_z = \hat{p}_z^0 \sin\left(\frac{m\,x}{a}\right) \sin\left(\frac{n\,y}{b}\right) \qquad \text{plate mechanical analysis} \tag{4.67}$$

$$p_z = \hat{p}_z^0 \sin\left(\frac{m\,\alpha}{a}\right) \sin\left(\frac{n\,\beta}{b}\right) \qquad \text{shell mechanical analysis} \tag{4.68}$$

$$T = \hat{T}_0(z) \sin\left(\frac{m\,x}{a}\right) \sin\left(\frac{n\,y}{b}\right) \qquad \text{thermal stress plate analysis} \tag{4.69}$$

$$\Phi = \hat{\Phi}_0 \sin\left(\frac{m\,x}{a}\right) \sin\left(\frac{n\,y}{b}\right) \qquad \text{plate piezo-mechanic analysis} \tag{4.70}$$

Parameters m and n are specified for each case presented.

4.6.1 Mechanical plate analysis

Aluminum plate

A square plate made of aluminum is considered, material characteristics are $E = 73 \times 10^9$ Pa and $\nu = 0.34$. Two length-to-thickness ratios (a/h) were considered, 100 (thin plate) and 2 (thick plate). In Table 4.7 results are reported from CLT, FSDT, ED4 and LD4 models. 3D analytical results were obtained as reported in [57], [58] and [59]. As well-known, refined models such as ED4 and LD4 are needed to properly detect transversal stresses σ_{xz}, σ_{yz} and σ_{zz} and to analyze thick plates. CLT and FSDT models offer a good evaluation of displacement u_z and in-plane tension σ_{xx} for thin plates.

a/h		$\overline{u}_z$	$\overline{\sigma}_{xx}$	$\overline{\sigma}_{yz}$	$\overline{\sigma}_{zz}$
100	3D	2.7248	0.2037	0.2387	0.0100
	CLT	2.7237	0.2037	-	-
	FSDT	2.7251	0.2037	0.1592	-
	ED4	2.7248	0.2037	0.2387	0.0100
	LD4	2.7248	0.2037	0.2387	0.0100
2	3D	7.3826	0.3145	0.2277	0.5000
	CLT	2.7238	0.2037	-	-
	FSDT	6.1178	0.2037	0.1592	-
	ED4	7.3811	0.3165	0.2306	0.5082
	LD4	7.3811	0.3165	0.2306	0.5082

Table 4.7: Isotropic square plate. Reference solution from [58] and [59].

Symmetric laminated plate

The assessment for the laminated plate are reported in Table 4.8 and it proves that LD4 model offers results that are in excellent agreement with the exact solutions available in the open literature. The exact solutions are taken from [60] and [61], and the material properties are $E_L/E_T = 25$, $G_{LT}/E_T = 0.5$, $G_{TT}/E_T = 0.2$, $\nu_{LT} = \nu_{TT} = 0.25$.

				$a/h = 100$				
				3-plies laminate				
	$\overline{\sigma}_{xx}(z = \pm h/2)$		$\overline{\sigma}_{yy}(z = \pm h/6)$		$\overline{\sigma}_{xz}(z = 0)$	$\overline{\sigma}_{yz}(z = 0)$	$\overline{\sigma}_{xy}(z = \pm h/2)$	
Ref. [60]	± 0.539		0.181		0.395	0.0828	∓ 0.0213	
LD4	± 0.539		0.181		0.395	0.0828	∓ 0.0214	
LM4	± 0.539		0.181		0.395	0.0828	∓ 0.0214	
				5-plies laminate				
	$\overline{\sigma}_{xx}(z = \pm h/2)$		$\overline{\sigma}_{yy}(z = \pm h/3)$		$\overline{\sigma}_{xz}(z = 0)$	$\overline{\sigma}_{yz}(z = 0)$	$\overline{u}_z(z = 0)$	
Ref. [61]	± 0.539		± 0.360		0.272	0.205	1.006	
LD4	± 0.539		± 0.360		0.272	0.206	1.006	
LM4	± 0.539		± 0.360		0.272	0.206	1.006	
				$a/h = 4$				
				3-plies laminate				
	$\overline{\sigma}_{xx}(z = \pm h/2)$		$\overline{\sigma}_{yy}(z = \pm h/6)$		$\overline{\sigma}_{xz}(z = 0)$	$\overline{\sigma}_{yz}(z = 0)$	$\overline{\sigma}_{xy}(z = \pm h/2)$	
Ref. [60]	0.801	-0.755	0.534	-0.556	0.256	0.2172	-0.0511	0.0505
LD4	0.801	-0.755	0.534	-0.556	0.256	0.2180	-0.0511	0.0505
LM4	0.801	-0.755	0.534	-0.556	0.256	0.2180	-0.0511	0.0505
				5-ply laminate				
	$\overline{\sigma}_{xx}(z = \pm h/2)$		$\overline{\sigma}_{yy}(z = \pm h/3)$		$\overline{\sigma}_{xz}(z = 0)$	$\overline{\sigma}_{yz}(z = 0)$	$\overline{u}_z(z = 0)$	
Ref. [61]	0.685	-0.651	0.633	-0.626	0.238	0.229	4.291	
LD4	0.685	-0.651	0.634	-0.626	0.238	0.229	4.291	
LM4	0.685	-0.651	0.634	-0.626	0.238	0.229	4.291	

Table 4.8: Stresses and displacement for a 3-layers and 5-layer simply supported laminated plates. Material properties: $E_L/E_T = 25$, $G_{LT}/E_T = 0.5$, $G_{TT}/E_T = 0.2$, $\nu_{LT} = \nu_{TT} = 0.25$.

4.6.2 Mechanical shell analysis

The assessment herein proposed is based in the work reported in [62]. The material properties are $E_L/E_T = 25$, $\nu = 0.25$, $G_{LT}/E_T = G_{TT}/E_T = 0.5$, $G_{Lz}/E_T = 0.2$. The dimensions of the shell are $a = 4\,R_\beta$ and $b = 2\,\pi\,R_\beta$, the transverse pressure load is applied internally. In Table 4.9 the assessment of LD4 model is conducted and it is shown that this model is on excellent agreement with the reference solution.

	$\overline{u}_z$	$\overline{\sigma}_{\alpha\alpha}$	$\overline{\sigma}_{\beta\beta}$	$\overline{\sigma}_{\alpha\beta}$	$\overline{\sigma}_{\alpha z}$	$\overline{\sigma}_{\beta z}$	$\overline{\sigma}_{zz}$
				1 Ply, 90°			
	$(z=0)$	$(z=\mp h/2)$	$(z=\mp h/2)$	$(z=\mp h/2)$	$(z=0)$	$(z=0)$	$(z=0)$
				$R_\beta/h=4$			
Ref. [62]	2.783	−0.2295	−6.969	−0.0840	0.0987	−2.990	−0.69
		0.0981	4.859	0.0925			
LD4	2.767	−0.2454	−6.836	−0.0831	0.0993	−3.125	−0.71
		0.0861	4.776	0.0919			
				$R_\beta/h=100$			
Ref. [62]	0.5170	0.0288	−3.876	−0.0447	0.0393	−3.859	−10.13
		0.1190	3.843	0.0161			
LD4	0.5170	0.0288	−3.876	−0.0447	0.0393	−3.860	−10.13
		0.1190	3.843	0.0161			
				2 Ply, 90°/0°			
	$(z=0)$	$(z=\mp h/2)$	$(z=\mp h/2)$	$(z=\mp h/2)$	$(z=-h/4)$	$(z=h/4)$	$(z=h/4)$
				$R_\beta/h=4$			
Ref. [62]	6.100	−0.9610	−1.789	−0.2812	0.2758	−4.440	−0.70
		0.2120	10.31	0.2007			
LD4	6.100	−0.9614	−1.789	−0.2812	0.2762	−4.499	−0.70
		0.2088	10.30	0.2007			
				$R_\beta/h=100$			
Ref. [62]	1.367	2.300	−0.5759	−0.3452	−0.1512	−2.972	−7.71
		0.1871	5.560	−0.1817			
LD4	1.367	2.300	−0.5759	−0.3452	−0.1512	−2.972	−7.71
		0.1871	5.560	−0.1819			
				3 Ply, 90°/0°/90°			
	$(z=0)$	$(z=\mp h/2)$	$(z=\mp h/2)$	$(z=\mp h/2)$	$(z=-h/6)$	$(z=0)$	$(z=0)$
				$R_\beta/h=4$			
Ref. [62]	4.009	−0.2701	−9.323	−0.1609	0.1736	−2.349	−0.62
		0.1270	6.545	0.1081			
LD4	4.009	−0.2721	−9.324	−0.1609	0.1737	−2.349	−0.62
		0.1267	6.549	0.1081			
				$R_\beta/h=100$			
Ref. [62]	0.4715	0.0018	−3.507	−0.1038	0.1223	−3.127	−8.30
		0.0838	3.507	−0.0478			
LD4	0.4715	0.0018	−3.504	−0.1038	0.1223	−3.127	−8.30
		0.0838	3.504	−0.0478			

Table 4.9: Static response analysis of a laminated orthotropic shell. Reference solution from [62]. Geometry and load data: $a = 4\,R_\beta$, $b = 2\,\pi\,R_\beta$, $m = 1$, $n = 4$.

4.6.3 Thermal stress plate analysis

The assessment of LD4 model for the thermal analysis is reported in Tables 4.10, considering a thermal load. The reference solution is reported in the works [36]. The material properties are $E_1 = 25$ GPa, $E_2 = E_3 = 1$ GPa, $G_{13} = G_{12} = 0.5$ GPa, $G_{23} = 0.2$ GPa, $\nu = 0.25$ and $\alpha_{2,3}/\alpha_1 = 1125$. The ply sequence is $0°/90°/0°$. It is possible to note the excellent agreement with the exact solutions: this agreement makes the LD4 model the best choice as a reference solution for all the subsequent

analyses.

			Cilindrical thermal load		
	$\overline{u}_x(z=\mp h/2)$	$\overline{u}_z(z=\mp h/2)$	$\overline{\sigma}_{xx}(z=\mp h/6)$	$\overline{\sigma}_{xz}(z=\mp h/6)$	$\overline{\sigma}_{zz}(z=\mp h/6)$
			$a/h=4$		
Ref. [36]	± 7.470	18.32	± 372.3	2.830	± 1.748
LD4	± 7.470	18.32	± 372.3	2.806	± 1.748
			$a/h=100$		
Ref. [36]	± 4.449	2.855	± 371.4	0.2987	0.0018
LD4	± 4.449	2.855	± 371.4	0.2987	0.0018
			Bisinusoidal thermal load		
	$\overline{u}_x(z=\mp h/2)$	$\overline{u}_z(z=\mp h/2)$	$\overline{\sigma}_{xx}(z=\pm h/2)$	$\overline{\sigma}_{xz}(z=\mp h/6)$	$\overline{\sigma}_{zz}(z=\mp h/6)$
			$a/h=4$		
Ref. [36]	± 18.11	42.69	± 1183	84.81	± 0.5786
LD4	± 18.11	42.69	± 1183.2	84.81	± 0.5783
			$a/h=100$		
Ref. [36]	± 16.00	10.26	± 965.4	7.073	$\pm 0.1738\times 10^{-5}$
LD4	± 16.00	10.26	± 965.4	7.073	$\pm 0.1739\times 10^{-5}$

Table 4.10: Stresses and displacement for a 3-layers symmetric laminated plate under thermal load. Material properties: $E_L/E_T = 25$, $G_{LT}/E_T = 0.5$, $G_{TT}/E_T = 0.2$, $\nu_{LT} = \nu_{TT} = 0.25$, $\alpha_T/\alpha_L = 1125$.

4.6.4 Piezoelectric plate analysis

Herein, an assessment of the LD4 model is carried out for the piezoelectric case with respect the case analyzed in [63]. The LD4 model assessment considers a four layers laminated plate: the two piezoelectric layers are located at the top and the bottom. The elastic materials properties are: $E_1 = 132.38 \times 10^9$ Pa, $E_2 = E_3 = 10.756 \times 10^9$ Pa, $G_{12} = G_{13} = 5.6537 \times 10^9$ Pa, $G_{23} = 3.606 \times 10^9$ Pa, $\nu_{12} = \nu_{13} = 0.24$, $\nu_{23} = 0.49$, $\epsilon_{11} = 3.098966 \times 10^{-11}$ F/m, $\varepsilon_{22} = \varepsilon_{33} = 2.6562563 \times 10^{-11}$ F/m. The total thickness of these layers is equal to $h = 0.8 \cdot h_{\mathrm{TOT}}$ and the ply sequence is $90°/0°$. The piezoelectric layers are made of PZT-4 and its properties are: $E_1 = E_2 = 81.3 \times 10^9$ Pa, $E_3 = 64.5 \times 10^9$ Pa, $\nu_{12} = 0.329$, $\nu_{13} = \nu_{23} = 0.432$, $G_{44} = G_{55} = 25.6 \times 10^9$, $G_{66} = 30.6 \times 10^9$, $e_{31} = e_{32} = -5.20$ C/m^2, $e_{33} = 15.08$ C/m^2, $e_{24} = e_{15} = 12.72$ C/m^2, $\varepsilon_{11}/\varepsilon_0 = \varepsilon_{22}/\varepsilon_0 = 1475$, $\varepsilon_{33}/\varepsilon_0 : 1300$. ε_0 is the vacuum permittivity, which is equal to 8.854187×10^{-12} F/m. The thickness is $h = 0.1 \cdot h_{\mathrm{TOT}}$ per each piezoelectric layer. The results are reported in Table 4.11 and in Table 4.12 for sensor and actuator configurations. It is possible to note that the LD4 model offers a good agreement with the exact solution and for this reason it is used as reference solution for the axiomatic / asymptotic analysis.

z	$u_x \times 10^{12}, [m]$		Φ, [V]		$\sigma_{zz} \times 10, [Pa]$		$\mathcal{D}_z \times 10^{13}, [C/m^2]$	
	3D [63]	LD4	3D [63]	LD4	3D [63]	LD4	3D [63]	LD4
0.500	-47.549	-47.552	0.0000	0.0000	10.000	10.000	160.58	160.58
0.475	-41.425	-41.428	0.0189	0.0189	9.9657	9.9657	149.35	149.35
0.450	-35.424	-35.427	0.0358	0.0352	9.8682	9.8683	117.23	117.23
0.425	-29.531	-29.533	0.0488	0.0488	9.7154	9.7155	66.568	66.566
0.400	-23.732	-23.733	0.0598	0.0599	9.5151	9.5153	-0.3382	-0.3348
0.300	-10.480	-10.477	0.0589	0.0590	8.5199	8.5196	-0.1276	-0.1277
0.200	0.1413	0.1411	0.0589	0.0589	7.3747	7.3757	0.0813	0.0813
0.100	9.8917	9.8880	0.0596	0.0596	6.1686	6.1678	0.2913	0.2914
0.000	20.392	20.394	0.0611	0.0611	4.9831	4.9855	0.5052	0.5053
-0.100	24.768	24.771	0.0634	0.0634	3.8045	3.8052	0.7259	0.7261
-0.200	29.110	21.291	0.0665	0.0666	2.6137	2.6131	0.9563	0.9565
-0.300	33.819	33.822	0.0706	0.0706	1.4821	1.4823	1.1995	1.1997
-0.400	39.309	39.313	0.0756	0.0756	0.4868	0.4867	1.4587	1.4590
-0.425	44.492	44.495	0.0602	0.0602	0.2845	0.2844	-58.352	-58.350
-0.450	49.772	49.776	0.0425	0.0425	0.1312	0.1311	-103.66	-103.67
-0.475	55.163	55.167	0.0224	0.0225	0.0340	0.0340	-132.40	-132.40
-0.500	60.678	60.682	0.0000	0.0000	0.0000	0.0000	-142.46	-142.46

Table 4.11: Piezo-mechanic static response of a piezoelectric plate. Analytical solution from [63] for sensor configuration - $a/h = 4$. Material properties reported in [63].

LD4 model proved to offer solutions in agreement with the analytical solutions available in the literature. The comparisons shown in this section prove that it possible to employ the solutions offered by LD4, LM4 and ED4 models as a reference solution in the following axiomatic/asymptotic analyses.

z	$u_x \times 10^{12}, [m]$		$\Phi, [V]$		$\sigma_{zz} \times 10^3, [Pa]$		$\sigma_{xz} \times 10^3, [Pa]$	
	3D [63]	LD4	3D [63]	LD4	3D [63]	LD4	3D [63]	LD4
0.500	-32.764	-32.765	1.0000	1.0000	0.0000	0.0000	0.0000	0.0000
0.475	-23.349	-23.350	0.9971	0.9972	-0.8333	-0.8300	41.457	41.457
0.450	-13.973	-13.974	0.9950	0.9951	-2.8471	-2.8399	64.626	64.629
0.425	-4.6174	-4.6180	0.9936	0.9936	-5.3241	-5.3140	69.556	69.558
0.400	4.7356	4.7352	0.9929	0.9931	-7.5482	-7.5339	56.259	56.034
0.300	2.9808	2.9801	0.8415	0.8416	-12.957	-12.927	19.082	19.152
0.200	1.7346	1.7346	0.7014	0.7015	-15.245	-15.260	-4.5693	-4.6376
0.100	0.8008	0.8014	0.5707	0.5708	-15.510	-15.479	-18.203	-18.130
0.000	0.0295	0.0297	0.4476	0.4477	-14.612	-14.629	-23.866	-23.863
-0.100	-0.4404	-0.4401	0.3305	0.3306	-12.524	-12.512	-25.282	-25.271
-0.200	-0.8815	-0.8811	0.2179	0.2179	-9.2558	-9.2602	-25.633	-25.625
-0.300	-1.3206	-1.3202	0.1081	0.1082	-5.5018	-5.4906	-24.994	-24.984
-0.400	-1.7839	-1.7834	-0.0010	-0.0010	-1.8733	-1.8958	-23.379	-23.376
-0.425	-2.0470	-2.0464	-0.0009	-0.0010	-1.1074	-1.1066	-18.888	-18.881
-0.450	-2.3140	-2.3134	-0.0008	-0.0008	-0.5162	-0.5157	-13.501	-13.497
-0.475	-2.5856	-2.5849	-0.0004	-0.0004	-0.1351	-0.1350	-7.2092	-7.2064
-0.500	-2.8625	-2.8618	0.0000	0.0000	0.0000	0.0000	0.0000	0.0000

Table 4.12: Piezo-mechanic static response of a piezoelectric plate. Analytical solution from [63] for actuator configuration - $a/h = 4$. Material properties reported in [63].

Part II

Axiomatic/Asymptotic Analysis - plate and shell, mechanical and multifield analysis

Chapter 5

Axiomatic/asymptotic technique

In this chapter the axiomatic / asymptotic technique is introduced. This method makes it possible to evaluate the "best" reduced models for a given problem. This technique is based on the evaluation of the relevance of each term of a model: a term is deactivated and the error due to its deactivation is measured with respect to a reference solution. A term is considered as non-relevant if the error due to its deactivation is below an a-priori defined threshold. Different parameters are considered, such as length-to-thickness and radius-to-thickness ratios and different material properties. In addition, the several criteria to measure the error are defined and their influence on terms selection is considered. This technique is applied to refined models for multifield analysis, i.e. thermal stress analysis and piezoelectric plate analysis, and to mixed models (RMVT).

The analysis of plates and shells is based on a number of models. The solution of 3D elasticity equations offers the most accurate evaluation of the elastic response, but the computational cost can be significantly high. As an alternative, a 2D approach can be used. In the field of 2D approaches for plate analysis, the first model that was developed was the Kirchoff-Love model ([4], [5]). According to this model, the thickness strain and the transverse shear deformations are neglected. Better accuracy in the plate response analysis can be obtained if at least one of Kirchhoff's hypotheses is removed. For example, a constant through-the-thickness transverse shear deformation can be taken into consideration. This is the case of the Reissner-Mindlin theories ([64], [65]), also known as the First-Order Shear Deformation Theory (FSDT). Further improvements have been introduced in Vlasov's ([66]) or Hildebrand-Reissner-Thomas's theories ([67]), which are based on higher-order expansions of the displacement components on the reference surface. The transverse stress and displacement components

in a multilayer plate/shell are continuous functions along the z direction; these significant particular features of layered structures were defined as C_z^0-requirement in [6]. The continuous displacement field is defined as the Zig-Zag effect (ZZ), and the transverse stress continuity at the interfaces is defined as Interlaminar-Continuity (IC). These two particular features make classical models inefficient for the analysis of multilayered plates, since they were originally developed for metallic one-layered plates. Moreover, classical models can be inaccurate for thick plate analysis.

It is possible to affirm that a way to overcome the limitations of the classical plate and shells theories is to employ refined theories, i.e. to consider in the formulation higher order terms. In this sense the CUF was introduced since it is possible to construct any order theory in an unified manner. The equilibrium equations can be written according to few fundamental nuclei whose form does not depend on either the order of the introduced approximations or on the choices made for the base functions in the thickness direction.

Are all model terms necessary? It is a legitimate question since under some conditions some classical models are able to provide results similar to the ones of the refined theories. It is plausible to think that under some conditions it is possible to ignore some terms of a refined theory without loosing accuracy. In this case, it is possible to provide an accurate analysis with a lower computational cost.

The axiomatic/asymptotic technique, introduced by Carrera and Petrolo [49, 68], makes it possible to define the non-relevant terms of a model for a specific problem and to discard them. This method is based on a preliminary axiomatic choice of a refined model obtained through the CUF and then the effectiveness of each higher-order term is evaluated against a reference solution. Those variables whose influence can be neglected are retained. This leads to the development of reduced models whose accuracies are equivalent to those of full higher-order models. The influence of each term can be evaluated for different values of geometrical and material parameters, such as the thickness-to-length ratio or the orthotropic ratio in order to obtain asymptotic-like results.

In this thesis, ESL models for plates and shells are analyzed by means of this technique and the axiomatic/asymptotic technique is extended to LW models for multilayered plates and shells. The effectiveness of the model variables is defined by means of different criteria and their influence on the term selection process is analyzed. In addition, this technique is applied to the analysis of thermal- and piezo-mechanical problems for multilayered plates, for both ESL and LW models. Moreover, the axiomatic/asymptotic technique is adopted for the first time for the analysis of multilayered plate models based on the RMVT statements (both ESL and LW approaches). The quest of the terms relevance is conducted trying to answer to the following ques-

tions:

- which parameter influence the relevance of terms of a refined models?
- which is the best criterium to evaluate the error?
- which is the influence of the type of load?

5.1 Displacement variables effectiveness evaluation

The CUF approach offers the possibility to perform an accurate plate or shell analysis since it is possible to include in the displacement field higher order terms. The price to pay is a higher computational cost than classical formulations. In order to preserve the accuracy of a high order model and to lower the computational cost it is possible to employ the axiomatic/asymptotic approach which aims to evaluate the effectiveness of each term. This method consists of the following steps:

1. plate parameters such as the geometry, boundary conditions, loadings, materials and layer layouts, are fixed;
2. a set of output parameters is chosen, such as displacement or stress components;
3. a starting theory is fixed (axiomatic part), that is the displacement variables to be analyzed are defined;
4. a reference solution is defined (in the present work LD4/LM4 approaches are adopted, since these fourth order model offers an excellent agreement with the three-dimensional solutions);
5. the CUF is used to generate the governing equations for the theories considered;
6. the effectiveness of each term of the adopted expansion is evaluated by measuring the error due to its deactivation; a term is considered as non-effective if its error is below an a-priori defined threshold (asymptotic part);
7. the most suitable structural model for a given structural problem is then obtained discarding the non-effective displacement variables.

The effectiveness of each displacement variable is computed considering stress / displacement component according to some specific criteria. The results are reported by means of a synthetic representation, which is introduced in the following. An example of LD4 model for a two layers shell is presented:

$$\begin{aligned}
u_\alpha =& F_b^1 u_{\alpha b}^1 + F_2^1\ u_{\alpha 2}^1 + F_3^1\ u_{\alpha 3}^1 + F_4^1\ u_{\alpha 4}^1 + F_t^1\ u_{\alpha t}^1 + F_b^2 u_{\alpha b}^2 + F_2^2\ u_{\alpha 2}^2 + F_3^2\ u_{\alpha 3}^2 + F_4^2\ u_{\alpha 4}^2 + F_t^2\ u_{\alpha t}^2 \\
u_\beta =& F_b^1 u_{\beta b}^1 + F_2^1\ u_{\beta 2}^1 + F_3^1\ u_{\beta 3}^1 + F_4^1\ u_{\beta 4}^1 + F_t^1\ u_{\beta t}^1 + F_b^2 u_{\beta b}^2 + F_2^2\ u_{\beta 2}^2 + F_3^2\ u_{\beta 3}^2 + F_4^2\ u_{\beta 4}^2 + F_t^2\ u_{\beta t}^2 \\
u_z =& F_b^1 u_{z b}^1 + F_2^1\ u_{z 2}^1 + F_3^1\ u_{z 3}^1 + F_4^1\ u_{z 4}^1 + F_t^1\ u_{z t}^1 + F_b^2 u_{z b}^2 + F_2^2\ u_{z 2}^2 + F_3^2\ u_{z 3}^2 + F_4^2\ u_{z 4}^2 + F_t^2\ u_{z t}^2
\end{aligned} \tag{5.1}$$

Its synthetic representation is reported in Table 5.1:

■	▲	▲	▲	■	▲	▲	▲	■
■	▲	▲	▲	■	▲	▲	▲	■
■	▲	▲	▲	■	▲	▲	▲	■

Table 5.1: Representation of the full model .

The terms $F_t^1\ u_{\alpha t}^1 + F_b^2 u_{\alpha b}^2$, $F_t^1\ u_{\beta t}^1 + F_b^2 u_{\beta b}^2$ and $F_t^1\ u_{z t}^1 + F_b^2 u_{z b}^2$ are synthetically denoted by the term ■ at the middle of Table 5.1. In the following, all terms ■ located in the middle of a Table like 5.1, denotes synthetically the sum of the top and bottom term of two adjacent layers (this convention holds for electric potential and stress distribution, examples are given in the following). The legend is reported in Table 5.2:

Active term	Inactive term	Non-deactivable term
▲	△	■

Table 5.2: Symbols to indicate the status of a displacement variable.

If the term $u_{\alpha 2}^2$ is deactivated the model obtained is

$$\begin{aligned}
u_\alpha =& F_b^1 u_{\alpha b}^1 + F_2^1\ u_{\alpha 2}^1 + F_3^1\ u_{\alpha 3}^1 + F_4^1\ u_{\alpha 4}^1 + F_t^1\ u_{\alpha t}^1 + F_b^2 u_{\alpha b}^2 + \quad\quad + F_3^2\ u_{\alpha 3}^2 + F_4^2\ u_{\alpha 4}^2 + F_t^2\ u_{\alpha t}^2 \\
u_\beta =& F_b^1 u_{\beta b}^1 + F_2^1\ u_{\beta 2}^1 + F_3^1\ u_{\beta 3}^1 + F_4^1\ u_{\beta 4}^1 + F_t^1\ u_{\beta t}^1 + F_b^2 u_{\beta b}^2 + F_2^2\ u_{\beta 2}^2 + F_3^2\ u_{\beta 3}^2 + F_4^2\ u_{\beta 4}^2 + F_t^2\ u_{\beta t}^2 \\
u_z =& F_b^1 u_{z b}^1 + F_2^1 u_{z 2}^1 + F_3^1\ u_{z 3}^1 + F_4^1\ u_{z 4}^1 + F_t^1\ u_{z t}^1 + F_b^2 u_{z b}^2 + F_2^2\ u_{z 2}^2 + F_3^2\ u_{z 3}^2 + F_4^2\ u_{z 4}^2 + F_t^2\ u_{z t}^2
\end{aligned} \tag{5.2}$$

The response given by the model reported in eq. 5.2 is compared with the reference solution according to a criterium and if the error introduced by the deactivation of the term $u^2_{\alpha 2}$ is below an a priori threshold the term is discarded. In order to show synthetically the results a graphical representation is proposed:

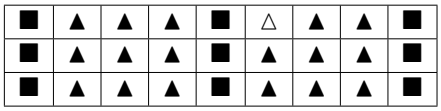

Table 5.3: Representation of the reduced model .

In the case of a piezoelectric plate analysis the synthetic representation of the reduced models has to incorporate the potential distribution, an example is given in the following. The complete model for a two piezoelectric plate is

$$\begin{aligned}
u_x &= F_t\, u^1_{xt} + F_2\, u^1_{x2} + F_3\, u^1_{x3} + F_4\, u^1_{x4} + F_b\, u^1_{xb} + F_t\, u^2_{xt} + F_2\, u^2_{x2} + F_3\, u^2_{x3} + F_4\, u^2_{x4} + F_b\, u^2_{xb} \\
u_y &= F_t\, u^1_{yt} + F_2\, u^1_{y2} + F_3\, u^1_{y3} + F_4\, u^1_{y4} + F_b\, u^1_{yb} + F_t\, u^2_{yt} + F_2\, u^2_{y2} + F_3\, u^2_{y3} + F_4\, u^2_{y4} + F_b\, u^2_{yb} \\
u_z &= F_t\, u^1_{zt} + F_2\, u^1_{z2} + F_3\, u^1_{z3} + F_4\, u^1_{z4} + F_b\, u^1_{zb} + F_t\, u^2_{zt} + F_2\, u^2_{z2} + F_3\, u^2_{z3} + F_4\, u^2_{z4} + F_b\, u^2_{zb} \\
\Phi &= F_t\, \Phi^1_t + F_2\, \Phi^1_2 + F_3\, \Phi^1_3 + F_4\, \Phi^1_4 + F_b\, \Phi^1_b + F_t\, \Phi^2_t + F_2\, \Phi^2_2 + F_3\, \Phi^2_3 + F_4\, \Phi^2_4 + F_b\, \Phi^2_b
\end{aligned} \tag{5.3}$$

The full model can be represented as reported in Table 5.4 and it is labeled as "Full model". If terms u^2_{x2}, u^1_{y4}, u^1_{z3}, u^2_{x2}, Φ^1_1, Φ^2_1 are discarded, the reduced model becomes:

$$\begin{aligned}
u_x &= F_t\, u^1_{xt} + F_2\, u^1_{x2} + F_3\, u^1_{x3} + F_4\, u^1_{x4} + F_b\, u^1_{xb} + F_t\, u^2_{xt} + \quad\; + F_3\, u^2_{x3} + F_4\, u^2_{x4} + F_b\, u^2_{xb} \\
u_y &= F_t\, u^1_{yt} + F_2\, u^1_{y2} + F_3\, u^1_{y3} + \quad\; + F_b\, u^1_{yb} + F_t\, u^2_{yt} + F_2\, u^2_{y2} + F_3\, u^2_{y3} + F_4\, u^2_{y4} + F_b\, u^2_{yb} \\
u_z &= F_t\, u^1_{zt} + F_2\, u^1_{z2} + \quad\; + F_4\, u^1_{z4} + F_b\, u^1_{zb} + F_t\, u^2_{zt} + F_2\, u^2_{z2} + F_3\, u^2_{z3} + F_4\, u^2_{z4} + F_b\, u^2_{zb} \\
\Phi &= F_t\, \Phi^1_t + \quad\; + F_3\, \Phi^1_3 + F_4\, \Phi^1_4 + F_b\, \Phi^1_b + F_t\, \Phi^2_t + \quad\; + F_3\, \Phi^2_3 + F_4\, \Phi^2_4 + F_b\, \Phi^2_b
\end{aligned} \tag{5.4}$$

In the following, the terms for LW models are denoted as u^k_{ji}/Φ^k_i, where j is a main direction ($x,\ y,\ z$ in the case of plate or $\alpha\ \beta\ z$ for shells), i is the expansion order and k denotes the displacement variable related to the generic k-layer. The layers are enumerated starting from the bottom plate/shell. It should to be marked that when the axiomatic/asymptotic technique is applied to LW model the terms $\mathbf{u}^k_t$ and $\mathbf{u}^k_b$ cannot be suppressed since they are fundamental to impose the continuity condition

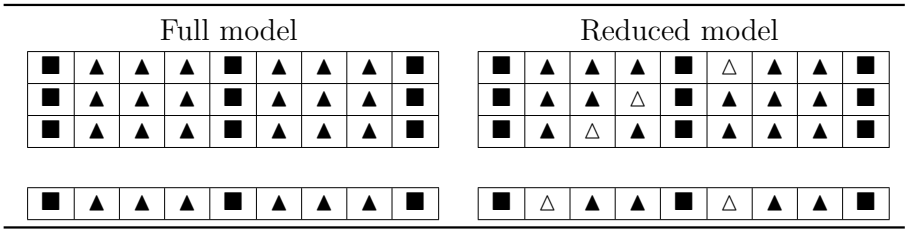

Table 5.4: Representation of a full and reduced kinematics models. Terms u^2_{x2}, u^1_{y4}, u^1_{z3}, u^2_{x2}, Φ^1_1, Φ^2_1 terms are deactivated.

on the displacement, that is $\mathbf{u}^k_t = \mathbf{u}^{k+1}_b$. The same fact holds for the potential variables $\Phi^k_t = \Phi^{k+1}_b$ and for the stress variables or the RMVT variational statements (in this case it is $\boldsymbol{\sigma}^k_t = \boldsymbol{\sigma}^{k+1}_b$). The reduced models for the RMVT approach are presented in a similar manner as in 5.4. As an example the reduced RMVT model for a plate

$$
\begin{aligned}
u_x &= F_t\,u^1_{xt} + F_2\,u^1_{x2} + \quad\; + F_4\,u^1_{x4} + F_b\,u^1_{xb} + F_t\,u^2_{xt} + F_2\,u^2_{x2} + F_3\,u^2_{x3} + F_4\,u^2_{x4} + F_b\,u^2_{xb}\\
u_y &= F_t\,u^1_{yt} + F_2\,u^1_{y2} + F_3\,u^1_{y3} + F_4\,u^1_{y4} + F_b\,u^1_{yb} + F_t\,u^2_{yt} + F_2\,u^2_{y2} + F_3\,u^2_{y3} + F_4\,u^2_{y4} + F_b\,u^2_{yb}\\
u_z &= F_t\,u^1_{zt} + F_2\,u^1_{z2} + F_3\,u^1_{z3} + F_4\,u^1_{z4} + F_b\,u^1_{zb} + F_t\,u^2_{zt} + F_2\,u^2_{z2} + F_3\,u^2_{z3} + F_4\,u^2_{z4} + F_b\,u^2_{zb}\\
\sigma_{xz} &= F_t\,\sigma^1_{xz\,t} + F_2\,\sigma^1_{xz\,2} + F_3\,\sigma^1_{xz\,3} + F_4\,\sigma^1_{xz\,4} + F_b\,\sigma^1_{xz\,b} + F_t\,\sigma^2_{xz\,t} + F_2\,\sigma^2_{xz\,2} + F_3\,\sigma^2_{xz\,3} + F_4\,\sigma^2_{xz\,4} + F_b\,\sigma^2_{xz\,b}\\
\sigma_{yz} &= F_t\,\sigma^1_{yz\,t} + F_2\,\sigma^1_{yz\,2} + F_3\,\sigma^1_{yz\,3} + F_4\,\sigma^1_{yz\,4} + F_b\,\sigma^1_{yz\,b} + F_t\,\sigma^2_{yz\,t} + F_2\,\sigma^2_{yz\,2} + \quad\; + F_4\,\sigma^2_{yz\,4} + F_b\,\sigma^2_{yz\,b}\\
\sigma_{zz} &= F_t\,\sigma^1_{zz\,t} + F_2\,\sigma^1_{zz\,2} + F_3\,\sigma^1_{zz\,3} + F_4\,\sigma^1_{zz\,4} + F_b\,\sigma^1_{zz\,b} + F_t\,\sigma^2_{zz\,t} + F_2\,\sigma^2_{zz\,2} + F_3\,\sigma^2_{zz\,3} + F_4\,\sigma^2_{zz\,4} + F_b\,\sigma^2_{zz\,b}
\end{aligned}
\tag{5.5}
$$

can be represented as

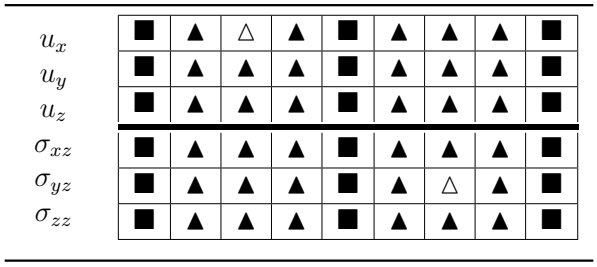

The deactivation of a term is obtained by means of the penalty technique. An example is reported in Fig. 5.1.

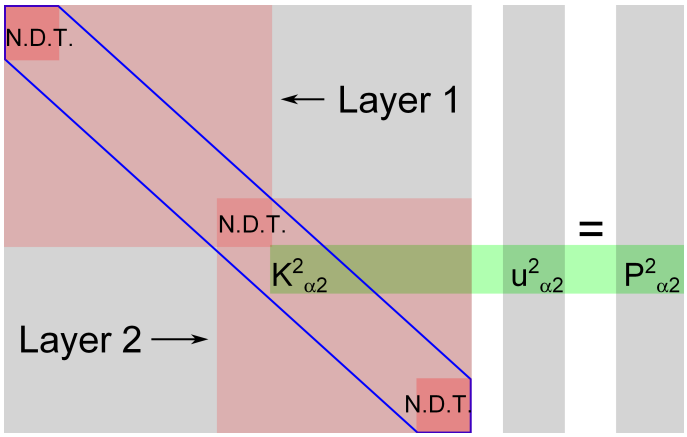

Figure 5.1: Deactivation of a generic term, LW approach.

The Figure depicts synthetically the matrix of the fundamental nuclei assembled considering the Navier closed form solutions. In this case, the LW scheme applied to the two-layer shell is considered (see Equation 5.2). The acronym "N.D.T." means "Non Deactivable Terms", i.e. the terms that cannot be deactivated since the continuity on the displacement components at the layers interface is imposed (it should be underlined that the non deactivable terms exist whenever a LW scheme is adopted). The relevance of the displacement variable $u^2_{\alpha 2}$ can be computed by suppressing it, in the case herein reported it leads to

$$\lim_{K^2_{\alpha 2}\to\infty} u^2_{\alpha 2} \approx \lim_{K^2_{\alpha 2}\to\infty} \frac{P^2_{\alpha 2}}{K^2_{\alpha 2}} = 0 \tag{5.6}$$

The limit operation proposed in Equation 5.6 is obtained by setting the term of the matrix considered (in this case the term $K^2_{\alpha 2}$) to a very high value: in the analyses proposed in the following this value is equal to 10^{31}.

5.2 Description of the error criteria

The error introduced by the terms deactivation is computed as

$$e = 100 \left| 1 - \frac{Q_P}{Q_P^{Ref}} \right| \tag{5.7}$$

Q_P represents the value of the quantity under exam (stress/displacement component) when the term analyzed is suppressed; Q_P is computed at the point P which is

located on the thickness direction. Q_P^{ref} is the reference value of the same quantity at the same point P. The positions of the points on which the errors are evaluated define the criterium employed.

Criterium **C1** is used when stress and displacement components are evaluated at $[a/2, b/2, h/2]$ for u_z, $\sigma_{\alpha\,\alpha}$ (in-plane shell stress) /σ_{xx} (in-plane plate stress), and σ_{zz}, at $[0, b/2, 0]$ for $\sigma_{\alpha\,z}$ (out-of-plane shell stress) /σ_{xz} (out-of-plane plate stress) and electric potential Φ, and at $[a/2, 0, 0]$ for $\sigma_{\beta\,z}$ (out-of-plane shell stress) / σ_{yz} (out-of-plane plate stress). Criterium **C2** is used when the error on the stress and displacement components is computed considering their absolute maximum values. In this case the position of the points is not known a priori. According to criterium **C3** the error on stress/displacement components is computed at the middle of each layer. Criterium **C4** evaluates the error at the points located at the interfaces of the layers and criterium **C5** computes the error at the interfaces and at the middle of each layer. In order to explain how the above mentioned criteria work an example is offered in Fig. 5.2 for C2 and C5 criteria. A section of a two layer shell is represented and the points on which C2 and C5 criteria operate are reported. The points on which the error is computed when C2 criterium is used depends on where the maximum value of stress/displacement component is located. In the following, a variable is considered as relevant if the error obtained by its suppression is greater than 0.05%.

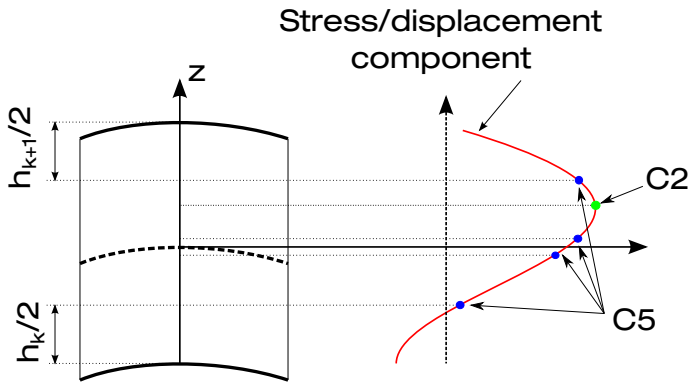

Figure 5.2: Point locations, error criteria C2 and C5

5.3 Parameters in the evaluation

As reported in the works [49, 69] the axiomatic/asymptotic analysis is affected to a great extent by the problem considered. The axiomatic/asymptotic analyses reported hereafter consider the influence of several parameters, in particular:

Geometry in the case of a plate the length-to-thickness ratio (a/h) is considered and in the case of shell radius-to-thickness ration (R/h) is considered;

Material isotropic and orthotropic materials are considered;

Load the type of load influence the number and the order of the retained terms. A transverse pressure load, a temperature distribution and a potential distribution for a piezoelectric plate are contemplated. In some cases, the influence of load shape is analyzed by varying the number of half-waves along the main direction.

In the following, the results include in some case "COMBINED" reduced models, i.e. reduced models obtained including all relevant variables of the displacement/stress components analyzed.

Chapter 6

Axiomatic/asymptotic analysis, results

Results of the axiomatic/asymptotic technique are reported in this chapter. The analyses deal about plates and shells considering ESL and LW approaches. The influence of the geometry and the material properties are analyzed: it is demonstrated that these parameters have an important role in the process of the selection of terms. In addition, multifield problems are taken into consideration: it is intended to demonstrate the influence of the thermal and electric loads on the process of selection of terms with respect to the mechanical load. Navier-like closed-form solutions are employed, so simply supported boundary condition is considered. This choice has been made in order to obtain quickly results and so to be able to focus on different aspects of this technique, e.g. the analysis of the term relevance of a model for a plate subjected to mechanical and thermal loads.

6.1 Plate models analysis, mechanical load

The analysis of the relevance of the terms is performed for a metallic plate subjected to a transverse pressure distribution whose expression is reported in Equation 4.67. The material is aluminum whose properties are $E = 73 \times 10^9$ Pa and $\nu = 0.34$. Two length-to-thickness ratios (a/h) are considered, 100 (thin plate) and 2 (thick plate). The following analyses are related with ESL models, the reference values employed in the axiomatic/asymptotic analysis are reported in Table 4.7. 3D analytical results were obtained as reported in [57], [58] and [59]. In the following, criterion C1 is employed. As well-known, refined models, such as ED4, are needed to properly detect transverse

stresses σ_{xz}, σ_{yz} and σ_{zz} and to analyze thick plates. Table 4.7 shows that ED4 model is in good agreement with 3D results. This reason makes ED4 models suitable as reference solution for the influence analysis of each displacement variable. Firstly, ED1 model is considered: in Table 6.1 the error committed by the deactivation of ED1 terms are reported for a thin plate ($a/h = 100$)

	u_z	σ_{xx}	σ_{xz}	σ_{yz}	σ_{zz}
△ ▲ / ▲ ▲ / ▲ ▲	0.00	0.00	33.33	33.33	-2.13×10^5
▲ ▲ / △ ▲ / ▲ ▲	0.00	0.00	33.33	33.33	-2.13×10^5
▲ ▲ / ▲ ▲ / △ ▲	100.00	100.00	100.00	100.00	50.00
▲ △ / ▲ ▲ / ▲ ▲	99.9	99.97	-33.29	99.96	-56.17
▲ ▲ / ▲ △ / ▲ ▲	99.9	99.92	99.96	-33.29	-56.17
▲ ▲ / ▲ ▲ / ▲ △	0.00	0.00	33.33	33.33	-2.13×10^5

Table 6.1: Error for ED1 model for isotropic plate, $a/h = 100$. ED4 as reference solution.

It is possible to note that the relevance of a term is different according to the quantity analyzed, e.g. if term u_{x1} is deactivated, u_z displacement and σ_{xx} stress do not show any degradation while σ_{xz}, σ_{yz} and σ_{zz} stresses deviate totally from the reference solution. In the following, reduced ED1, ED2, ED3 and ED4 models are reported.

a/h	u_z	σ_{xx}	σ_{xz}	σ_{yz}	σ_{zz}	COMBINED
			ED1			
100	M_e : 3/6 	M_e : 3/6 	M_e : 6/6 	M_e : 6/6 	M_e : 6/6 	M_e : 6/6 
2	M_e : 3/6 	M_e : 6/6 	M_e : 6/6 	M_e : 6/6 	M_e : 6/6 	M_e : 6/6 
			ED2			
100	M_e : 4/9 	M_e : 4/9 	M_e : 9/9 	M_e : 9/9 	M_e : 7/9 	M_e : 9/9 
2	M_e : 9/9 	M_e : 9/9 	M_e : 9/9 	M_e : 9/9 	M_e : 9/9 	M_e : 9/9 
			ED3			
100	M_e : 4/12 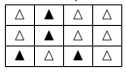	M_e : 4/12 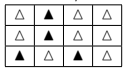	M_e : 4/12 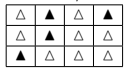	M_e : 4/12 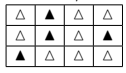	M_e : 12/12 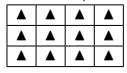	M_e : 12/12 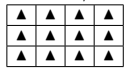
2	M_e : 12/12 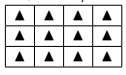	M_e : 12/12 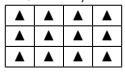	M_e : 12/12 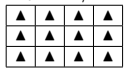	M_e : 12/12 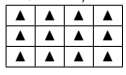	M_e : 12/12 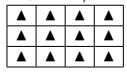	M_e : 12/12 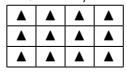
			ED4			
100	M_e : 4/15 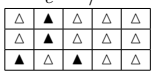	M_e : 4/15 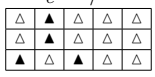	M_e : 5/15 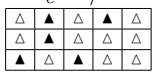	M_e : 5/15 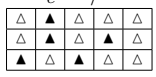	M_e : 4/15	M_e : 8/15
2	M_e : 13/15	M_e : 14/15	M_e : 7/15	M_e : 8/15	M_e : 13/15	M_e : 15/15

Table 6.2: Reduced ESL models for isotropic plate. Tolerance on error: 0.05%, ED4 model is the reference solution.

The results show that more terms can be discarded if a thin geometry is considered. In addition it is worth noting that ED1, ED2 and ED3 models show no reduction of terms in the case of a thick plate. An interesting fact can be noted for u_z displacement

and σ_{xx} stress: ED1, ED2, ED3 and ED4 models present some common active terms, i.e. u_{z0}, u_{x1} and u_{y1}, when a thin plate is considered. In addition only u_{z2} is retained when ED2, ED3 and ED4 models are considered. It means that an ED2 model is enough accurate to evaluate u_z displacement and σ_{xx} stress. ED4 is the only refined model which presents some retained terms when a thick plate is considered. It is possible to note that the ED1 reduced models for displacement u_z and stress σ_{xx} are similar to CLT and FSDT theories in the case of a thin plate. Differently form CLT and FSDT models, u_{x0} and u_{y0} terms are excluded: this fact suggest that the computational cost of CLT and FSDT theories can be reduced for the case under exam. In Figure 6.1 stresses σ_{xz} and σ_{zz} vs. z are reported; results are obtained by means of ED4 reduced combined model.

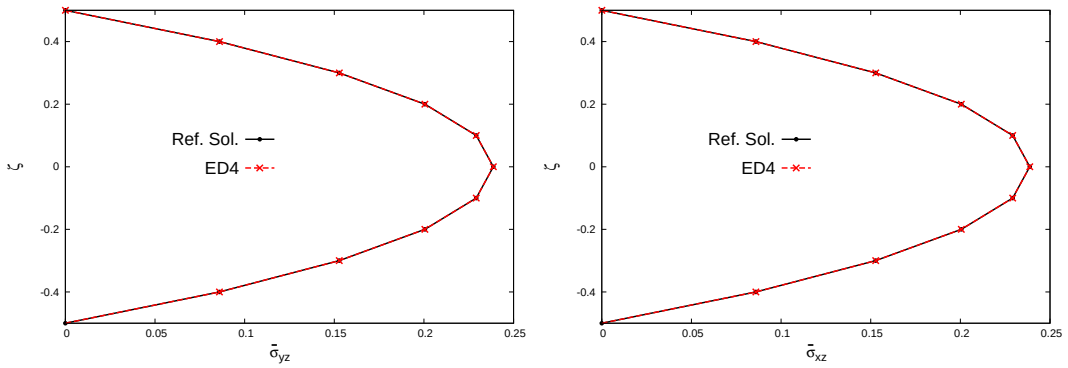

(a) Stress $\overline{\sigma}_{yz}$. (b) Stress $\overline{\sigma}_{zz}$

Figure 6.1: $\overline{\sigma}_{yz}$ and $\overline{\sigma}_{zz}$ vs z. Isotropic plate, $a/h = 100$.

It can be noted that the stress distribution is computed in agreement with the reference solution, although the reduced models are constructed considering the error on the displacement/stress component at only on point.

The number of half-waves of the transverse pressure load is another aspect that can affect the selection of terms process. The following analyses consider the metallic plate under the effect of a pressure with different number of half-waves, as reported in Table 6.3:

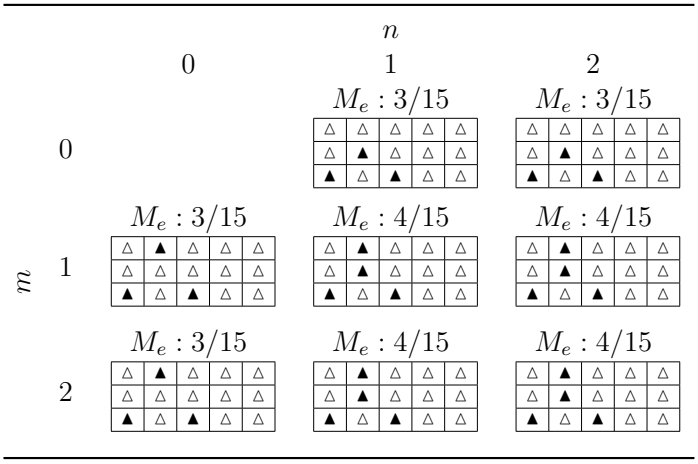

Table 6.3: Reduced ESL models for isotropic plate, a/h=100 - displacement u_z. ED4 model is the reference solution, influence of the load shape

The case $m = n = 0$ is not reported since it has no meaning. It can be noted that as m is equal to 0, all the terms related with the x directions are excluded. A similar observation can be made when n is 0, in this case the terms related with the y direction are not retained. It is interesting to note that the reduced models for the thin plate seem to not be affected by the number of half-waves. The reduced models for $m = 1, 2$ and $n = 1, 2$ are the same. The reduced models obtained for $m = 0$ and $n = 0$ can be considered as particular cases of the models obtained for m and n different from 0, as a matter of fact, these models can be obtained by suppressing term u_{x2} for $m = 0$ and term u_{y2} for $n = 0$. In general, the number of half-waves has a significant influence on the selection of terms process. The results obtained for the isotropic plate show that:

1. the through-the-thickness distribution are correctly computed, although the reduced models are derived through the evaluation of variables on given points;

2. the number of terms necessary to detect the solution increases as the a/h decreases (thicker plates), i.e. more unknown variables are needed;

3. terms u_{z1}, u_{z3}, u_{x2} and u_{y2} are relevant in most of the reduced models for thin plate;

4. the number of half-waves of the transverse pressure load has a significant influence. The absence of a half-wave along a main direction (x or y) leads to the exclusion the terms related with that direction.

Further results on this topic can be found in [69].

6.2 Shell models analysis, mechanical load

The axiomatic/asymptotic technique is applied to ESL and LW models considering an asymmetric laminated shell. Material properties and the geometric parameters were already defined for the LD4 model assessment (see chapter 4.6). The stacking sequence is $90°/0°$. The radius-to-thickness ratios (R_β/h) considered are equal to 4 and 100, each layer has the same thickness. The pressure is applied internally and it is $m = 1$ and $n = 4$ (see Equation 4.68).

As first, ESL models are examined and the results are reported in Table 6.4. It is found that the term reduction is effective when displacement u_z is retained. It is possible to observe that the reduced models ED1, ED2, ED3 and ED4 for displacement u_z for the thin shell case, present all terms in commons. It can be noted that ED3 and ED4 reduced models do not present any additional higher-order terms than ED2 reduced model. It is possible to conclude that for this particular case, the use of any higher-order displacement variables except u_{z3} does not improve the accuracy. It should be noted that these reduced models have the same terms of the classic models (CLT and FSDT), but in addition a parabolic term (u_{z3}) is present.

	ED1		ED2		ED3		ED4	
R_β/h	4	100	4	100	4	100	4	100
M_e	6/6	5/6	9/9	6/9	12/12	6/12	15/15	7/15
C1, C2	▲▲ ▲▲ ▲▲	▲▲ ▲▲ ▲△	▲▲▲ ▲▲▲ ▲▲▲	▲▲△ ▲▲△ ▲△▲	▲▲▲▲ ▲▲▲▲ ▲▲▲▲	▲▲△△ ▲▲△△ ▲△▲△	▲▲▲▲▲ ▲▲▲▲▲ ▲▲▲▲▲	▲▲△△△ ▲▲△△△ ▲△▲△△

Table 6.4: Reduced ESL models for laminated asymmetric shell, variable u_z. LD4 model results used as reference, C1 and C2 criteria adopted.

The axiomatic/asymptotic technique is applied to LW models and the results are reported in Table 6.5:

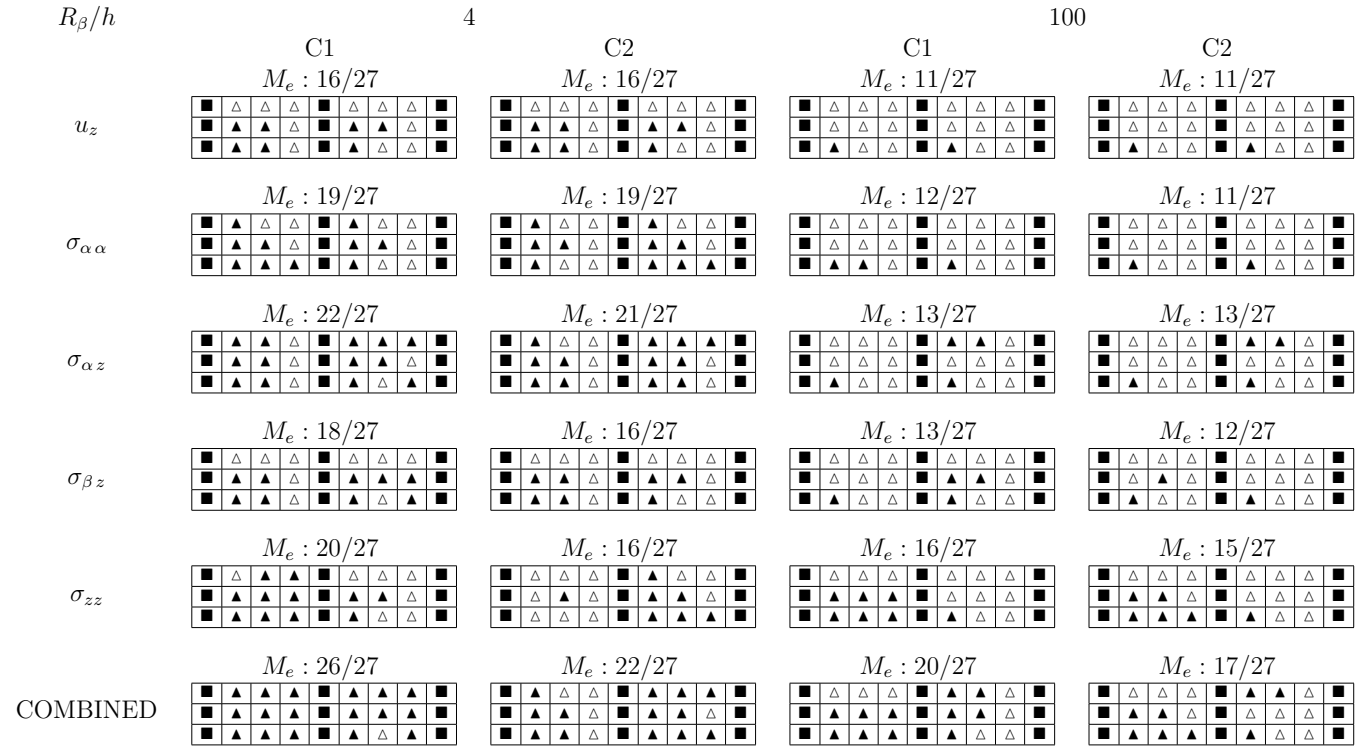

Table 6.5: LD4 reduced models for asymmetric shell. LD4 model results as reference solution.

It is possible to note that more terms are discarded when thin shells are considered. In particular the reduced models for displacement u_z and stress $\sigma_{\alpha\alpha}$ have the same retained terms as LD2 and LD3 models when criterium C2 is employed. It is possible to affirm that for this particular case, good accuracies can be obtained by using second- and third-order variables u_{z2} and u_{z3}. It can be noted that the use of different criteria leads to consider different terms: the reported data suggest that the use of C2 criterium leads to less terms than C1 criterium for both thick and thin shell case. In Fig. 6.2 the stress components distribution along the thickness are reported. It is possible to note that reduced models obtained by means of C1 and C2 criteria are able to detect the correct value at the reference point although the distribution along the thickness differs from the reference solution.

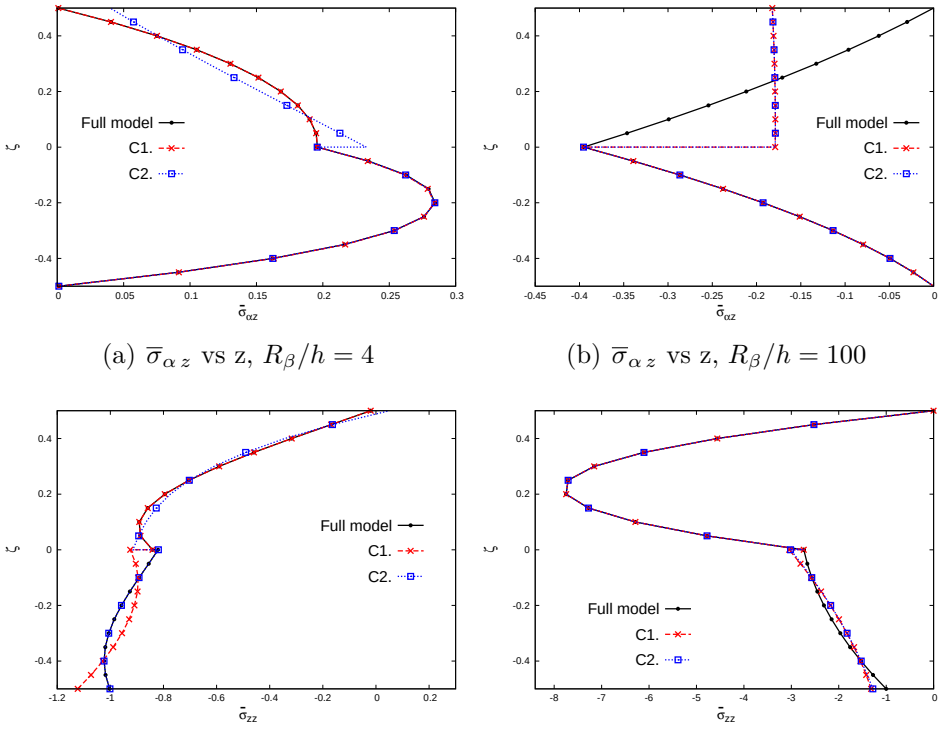

(a) $\overline{\sigma}_{\alpha\, z}$ vs z, $R_\beta/h = 4$

(b) $\overline{\sigma}_{\alpha\, z}$ vs z, $R_\beta/h = 100$

(c) $\overline{\sigma}_{zz}$ vs z, $R_\beta/h = 4$

(d) $\overline{\sigma}_{zz}$ vs z, $R_\beta/h = 100$

Figure 6.2: Asymmetric shell, LD4 reduced combined model.

As noted in Fig. 6.2 the proposed reduced models are able to detect the proper stress/displacement value at the reference point but the distribution may differ from the reference solution. A possible way to improve the evaluation of the distribution along the thickness is to employ different criteria to measure the error. The effect of the criteria on the retained terms is analyzed and the results for the asymmetric shell are reported in Table 6.6 and in Fig. 6.3.

R_β/h	4	100
C3	M_e : 18/27 	M_e : 14/27 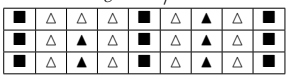
C4	M_e : 22/27 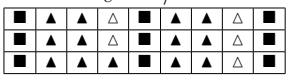	M_e : 20/27 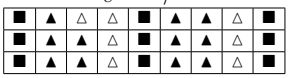
C5	M_e : 22/27 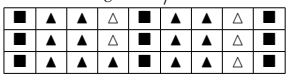	M_e : 20/27 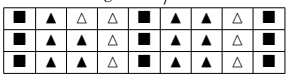

Table 6.6: Reduced LD4 combined models according to several error criteria for asymmetric shell.

Only reduced combined models are reported. The most relevant differences are obtained considering the C3 and C4 criteria, the use C5 criterium does not lead to consider any further terms than C4 criterium. In order to observe these models offer a satisfactory distibution, in Fig. 6.3 stress $\sigma_{\alpha z}$ vs z is reported:

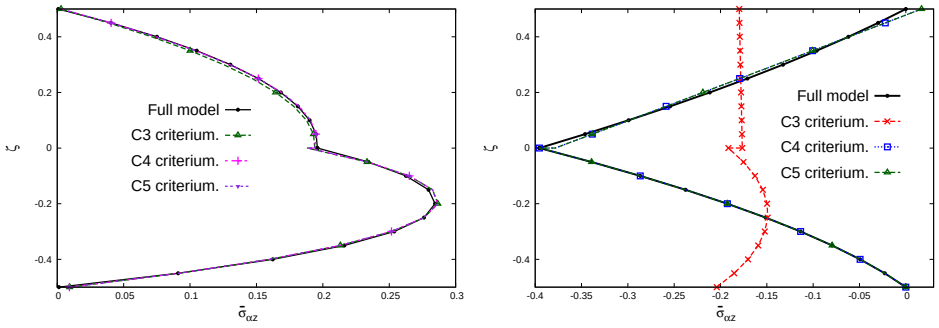

(a) $\overline{\sigma}_{\alpha\, z}$ vs z, $R_\beta/h = 4$ (b) $\overline{\sigma}_{\alpha\, z}$ vs z, $R_\beta/h = 100$

Figure 6.3: Asymmetric shell, LD4 reduced combined model according to several error criteria.

It is possible to note that the best results are obtained by means of the C4 and C5 criterium. Results reported in Table 6.6 once again confirm that reduced models for thick shells require more displacement variables than for the thin shell case. In addition it is possible to note that for a thin shell the fourth order terms (for both layers, $u^{(1)}_{x4}$, $u^{(1)}_{y4}$, $u^{(1)}_{z4}$ and $u^{(2)}_{x4}$, $u^{(2)}_{y4}$, $u^{(2)}_{z4}$) are totally excluded. The $\sigma_{\alpha z}$ stress distribution reported

in Fig. 6.3 highlights that for an asymmetric shell the evaluation of the error at the interfaces of the layers (C4 criterium) makes it possible to construct valid reduced models. The analyses herein conducted showed that:

- the geometry (R_β/h) and material properties influence the relevance of each term of the model, in particular reduced models for thick shells in general require more displacement variables than reduced models for thin shells;
- LW models offer a better analysis of static response compared to ESL models and show a more significant terms reduction with respect to ESL models;
- the adopted criterium influence the number and the order of the retained displacement variables; in addition results suggest that the computation of the error at the interfaces of the layers makes it possible to construct reduced models which offer a distribution that is substantially in agreement with the reference solution.

Further results on the axiomatic/asymptotic technique applied to multilayered shells can be found in [70]. Similar conclusions were drawn in [49] and in [69], which dealt with the reduced models for simply supported plates. In accordance with these works, it was found that geometry and material properties play an important role in the selection of the terms that have to be discarded. In addition the conclusion reported in [71] is confirmed: an improvement of the solution offered by the reduced models can be achieved evaluating the error at several points along the thickness.

6.3 Plate models analysis, thermal load

Reduced models for the thermal and mechanical stress analysis of plates are reported hereafter. Thermal and transverse pressure distributions are considered, their expressions are reported in Equations 4.67 and 4.69, respectively. The analyses herein reported consider an a-priori assumed linear distribution of the temperature, see Equation 4.29, and a temperature profile obtained from the solution of the conductivity equations.

The axiomatic/asymptotic analysis has been performed considering a symmetric laminated plate (ply sequence $0°/90°/0°$); the material properties are the same as those adopted for the LD4 model assessment (chapter 4.6). The reference values employed in the axiomatic/asymptotic technique are reported in Table 6.7, where thermal and mechanical loads are considered. The temperature values at the top and at the bottom of the plate are $T_{top} = 1.0$ K and $T_{bot} = -1.0$ K, respectively. The results are reported

according to Equations 4.66 and 4.64. It is interesting to note that the ED4 model does not provide solutions that are in agreement with the reference solution for the out-of-plane stress and displacement components. This fact is particularly clear when a thick plate is considered. In the same table, the results obtained for an effective temperature are reported:

		$\overline{\sigma}_{xx}(z=h/2)$	$\overline{\sigma}_{xz}(z=0)$	$\overline{u}_x(z=h/2)$	$\overline{u}_z(z=h/2)$
			$a/h=100$		
LD4	M	0.5393	0.3947	-6.7802×10^{-3}	0.4347
ED4		0.5392	0.2806	-6.7791×10^{-3}	0.4342
LD4	TH-A	965.37	6.1875	−15.9983	10.2598
ED4		965.26	4.7748	−15.9970	10.2529
LD4	TH-C	964.55	6.1845	−15.9880	10.2532
ED4		964.45	4.7723	−15.9868	10.2463
			$a/h=4$		
LD4	M	0.801	0.2559	-9.69426×10^{-3}	2.1216
ED4		0.786	0.2050	-9.51403×10^{-3}	2.0083
LD4	TH-A	1183.2	62.1210	−18.1082	42.6862
ED4		1187.8	60.0510	−18.2001	42.0481
LD4	TH-C	795.90	53.2600	−13.3929	32.1159
ED4		789.45	48.9100	−13.4541	31.5658

Table 6.7: Stresses and displacement for the symmetric laminated plate, mechanical (M) and thermal (TH-A, TH-C) load.

ED4 models have been investigated, and the reduced models are reported in Table 6.8 for the thermal and mechanical cases.

u_x	σ_{xx}
$a/h=100$	
M_e : 5/15	M_e : 5/15
△ ○ ▲ ● △ ○ ▲ ● △ ○	△ ○ ▲ ● △ ○ ▲ ● △ ○
△ ○ ▲ ● △ ○ △ ○ △ ○	△ ○ ▲ ● △ ○ △ ○ △ ○
▲ ● △ ○ ▲ ● △ ○ △ ○	▲ ● △ ○ ▲ ● △ ○ △ ○

Table 6.8: Reduced models, ED4 model - symmetric laminated plate. Symbols ▲ and △ refer to the thermal load. Symbols ● and ○ to the mechanical load.

It can again be confirmed that the analysis of a thick plate requires a greater computation effort than the analysis of a thin plate. The analyses have proved that a reduction of terms is possible for thin plate analysis, but for only some cases. It can be noted that the reduced models for thermal and mechanical stress analysis do not show any differences. The axiomatic/asymptotic analysis has been also carried out for

LD4 models, and the results are reported in Tables 6.9 for the thermal and mechanical loads.

	$a/h = 100$	$a/h = 4$
u_x	$M_e^{\blacktriangle}$: 15/39 - $M_e^{\bullet}$: 12/39	$M_e^{\blacktriangle}$: 22/39 - $M_e^{\bullet}$: 20/39
u_z	$M_e^{\blacktriangle}$: 15/39 - $M_e^{\bullet}$: 12/39	$M_e^{\blacktriangle}$: 22/39 - $M_e^{\bullet}$: 20/39
σ_{xx}	$M_e^{\blacktriangle}$: 16/39 - $M_e^{\bullet}$: 13/39	$M_e^{\blacktriangle}$: 22/39 - $M_e^{\bullet}$: 21/39
σ_{xz}	$M_e^{\blacktriangle}$: 16/39 - $M_e^{\bullet}$: 13/39	$M_e^{\blacktriangle}$: 23/39 - $M_e^{\bullet}$: 21/39
COMBINED	$M_e^{\blacktriangle}$: 17/39 - $M_e^{\bullet}$: 14/39	$M_e^{\blacktriangle}$: 23/39 - $M_e^{\bullet}$: 22/39

Table 6.9: Reduced models, LD4 model - symmetric laminated plate. Symbols ▲ and △ refer to the thermal load. Symbols • and ○ to the mechanical load.

Again in this case, the thick plate has a greater computational cost than the thin plate analysis. In this case, different terms have been selected for both thick and thin geometries, according to the type of load. In particular, it can be noted that, in general, the reduced models for the mechanical analysis have a lower computational cost than the reduced models for the thermal stress analysis. It is worth noting that fourth-order terms are not included in any of the reduced models. In general, second- and third-order term are employed. The displacement and stress distributions are reported in Fig.s 6.4, 6.5 and 6.6. Reduced models have been employed.

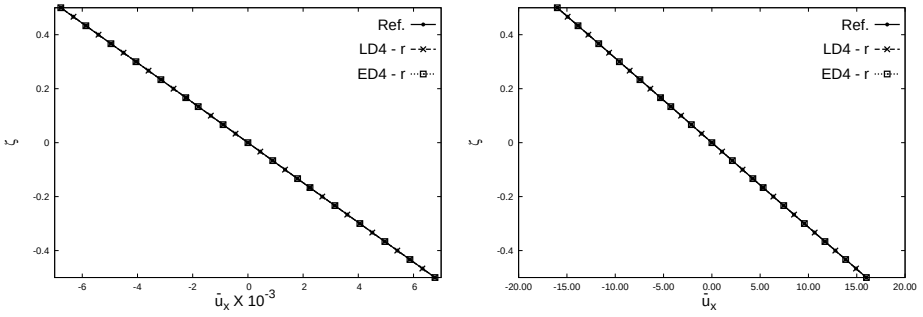

(a) Mechanic (b) Thermal

Figure 6.4: Symmetric laminated plate, $a/h = 100$ - displacement $\overline{u}_x$ vs z.

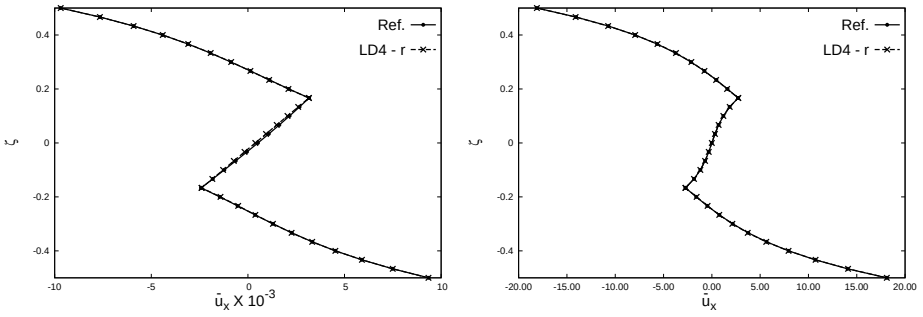

(a) Mechanic (b) Thermal

Figure 6.5: Symmetric laminated plate, $a/h = 4$ - displacement $\overline{u}_x$ vs z.

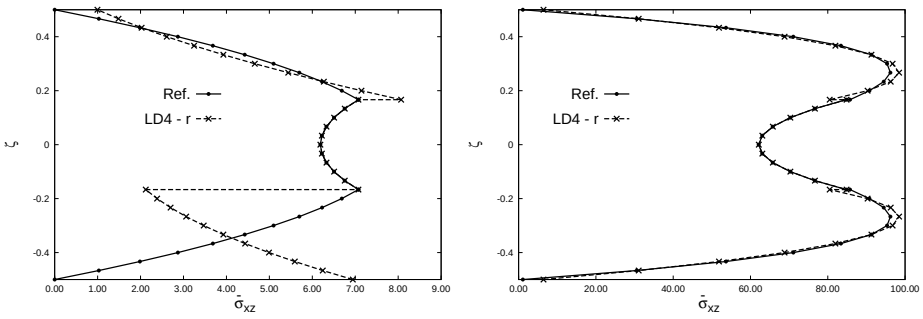

(a) $a/h = 100$ (b) $a/h = 4$

Figure 6.6: Symmetric laminated plate, thermal load - stress $\overline{\sigma}_{xz}$ vs z.

It is interesting to note that in all of the cases, the stress/displacement component values have been are correctly detected although, in some cases, the distribution deviates significantly from the reference solution. It is possible to conclude that:

- in general, thick plate analysis has a higher computational cost than thin plate analysis;
- it is difficult to perform the term reduction process in the case of ED4 model. The reduced models for the thick plate analysis do not show any term reduction, and only a few stress/displacement components present reduced models in the case of thin plate analysis;
- the type of load affects the retained variables;
- symmetric plate LD4 reduced models do not include fourth-order terms in the cases herein reported; in the case of an antisymmetric plate, this kind of term is only included when a thermal stress analysis is considered.

Results of the axiomatic/asymptotic analysis applied to refined plate model can be found in [72] and in [73].

6.4 Plate models analysis, electric load

Axiomatic/asymptotic analysis is herein conducted considering a laminate plate with two piezoelectric layers. Its properties and geometry have been already introduced when the assessment of LD4 model for the piezo-mechanic analysis has been performed.

The reference values of all quantities are not reported for the sake of brevity in Tables 6.10 and 6.11. Only few values for displacement u_z, potential Φ and stress σ_{zz} are reported for both sensor and actuator configurations, respectively.

	$a/h = 4$			$a/h = 100$		
z	$u_z \times 10^9, [m]$	$\Phi \times 10^2, [V/m]$	$\sigma_{zz}, [Pa]$	$u_z \times 10^4, [m]$	$\Phi, [V/m]$	$\sigma_{zz}, [Pa]$
	LD4					
-0.5	0.2843	0.0000	0.0000	0.4675	0.0000	0.0000
-0.4	0.2877	0.7562	0.0487	0.4675	4.5821	0.0457
0.0	0.3003	0.6109	0.4982	0.4675	4.5804	0.5000
0.4	0.3176	0.5985	0.9515	0.4675	4.5802	0.9544
0.5	0.3153	0.0000	1.0000	0.4675	0.0000	1.0000
	ED4					
-0.5	0.2707	0.0000	0.1608	0.4673	0.0000	29.052
-0.4	0.2741	0.7831	0.0519	0.4674	4.5709	-42.987
0.0	0.2859	0.6128	0.5482	0.4674	4.5690	-12.572
0.4	0.3005	0.5758	3.3692	0.4674	4.5686	-19.560
0.5	0.2985	0.0000	-0.7427	0.4673	0.0000	-29.649

Table 6.10: Piezo-mechanic static response of a square laminated plate, sensor configuration.

	$a/h = 4$			$a/h = 100$		
z	$u_z \times 10^{11}, [m]$	$\Phi, [V/m]$	$\sigma_{zz} \times 10^3, [Pa]$	$u_z \times 10^{11}, [m]$	$\Phi, [V/m]$	$\sigma_{zz} \times 10^6, [Pa]$
	L4					
-0.5	-1.4246	0.000	0.0000	-1.3432	0.0000	0.0000
-0.4	-1.4415	-1.0391×10^{-4}	-1.8958	-1.3471	2.3089×10^{-4}	0.2152
0.0	-1.4707	0.4477	-14.629	-1.3493	0.4999	1.0592
0.4	-1.3955	0.9929	-7.5339	-1.3514	0.9998	0.2002
0.5	-1.6058	1.0000	0.0000	-1.3556	1.0000	0.0000
z	$u_z \times 10^{11}, [m]$	$\Phi, [V/m]$	$\sigma_{zz}, [Pa]$	$u_z \times 10^{11}, [m]$	$\Phi, [V/m]$	$\sigma_{zz} \times 10^3, [Pa]$
	ED4					
-0.5	-3.3720	0.0000	0.9952	-3.2203	0.000	-7.1137
-0.4	-3.4004	-4.5484×10^{-4}	-0.6361	-3.2240	2.3272×10^{-4}	12.091
0.0	-3.5675	0.4481	0.0679	-3.2282	0.4999	0.8525
0.4	-3.2947	0.9942	-0.0156	-3.2317	0.9998	-3.5903
0.5	-3.5348	1.0000	1.4086	-3.2358	1.0000	-6.5019

Table 6.11: Piezo-mechanic static response of a square laminated plate, actuator configuration.

The ED4 model is analyzed and the results are presented in Table 6.12; it is possible

to observe that, as already noted for the metallic plate, the type of configuration adopted influences the displacement/stress components which take advantage of term reduction technique.

a/h	4	100
	Sensor configuration	
u_z	$M_e : 32/32$ 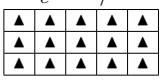	$M_e : 13/32$ 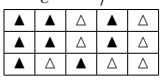
		
	Actuator configuration	
Φ	$M_e : 29/32$ 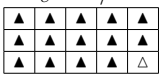	$M_e : 5/32$ 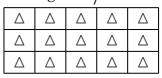
		

Table 6.12: Reduced ED4 models for laminated plate.

In addition, it is possible to note that thick plate analysis is more critical than thin plate analysis, since more displacement variables are required. It is interesting to note that the potential distribution for a thin laminate plate in actuator configuration can be computed with an acceptable accuracy by means of a linear model (only Φ_t^k and Φ_b^k are involved). It is possible to state that, similarly to the isotropic core case, the potential distribution tends to be quasi uncoupled. The displacement u_z and potential Φ distribution with the thickness direction are reported in Figure 6.7. The reduced models proposed in Table 6.12 are employed.

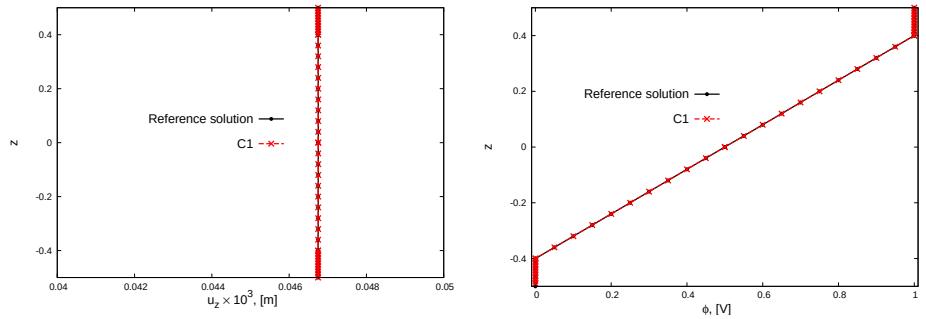

(a) Displacement u_z - sensor configuration.

(b) Potential Φ - actuator configuration.

Figure 6.7: Displacement u_z and potential Φ vs z evaluated by means of E4 reduced model for the laminated plate, $a/h = 100$.

In both cases, it is possible to note the good agreement of the solution offered by the reduced models with the reference solution. In the following, LD4 models is analyzed. The reduced LD4 models for sensor and actuator configurations are reported in Tables 6.13 and 6.14, respectively.

a/h	4	100
u_z	M_e : 28/68	M_e : 24/68
σ_{xx}	M_e : 31/68	M_e : 25/68
σ_{xz}	M_e : 32/68	M_e : 26/68
σ_{yz}	M_e : 31/68	M_e : 26/68
σ_{zz}	M_e : 23/68	M_e : 23/68
Φ	M_e : 34/68	M_e : 24/68
COMBINED	M_e : 40/68	M_e : 31/68

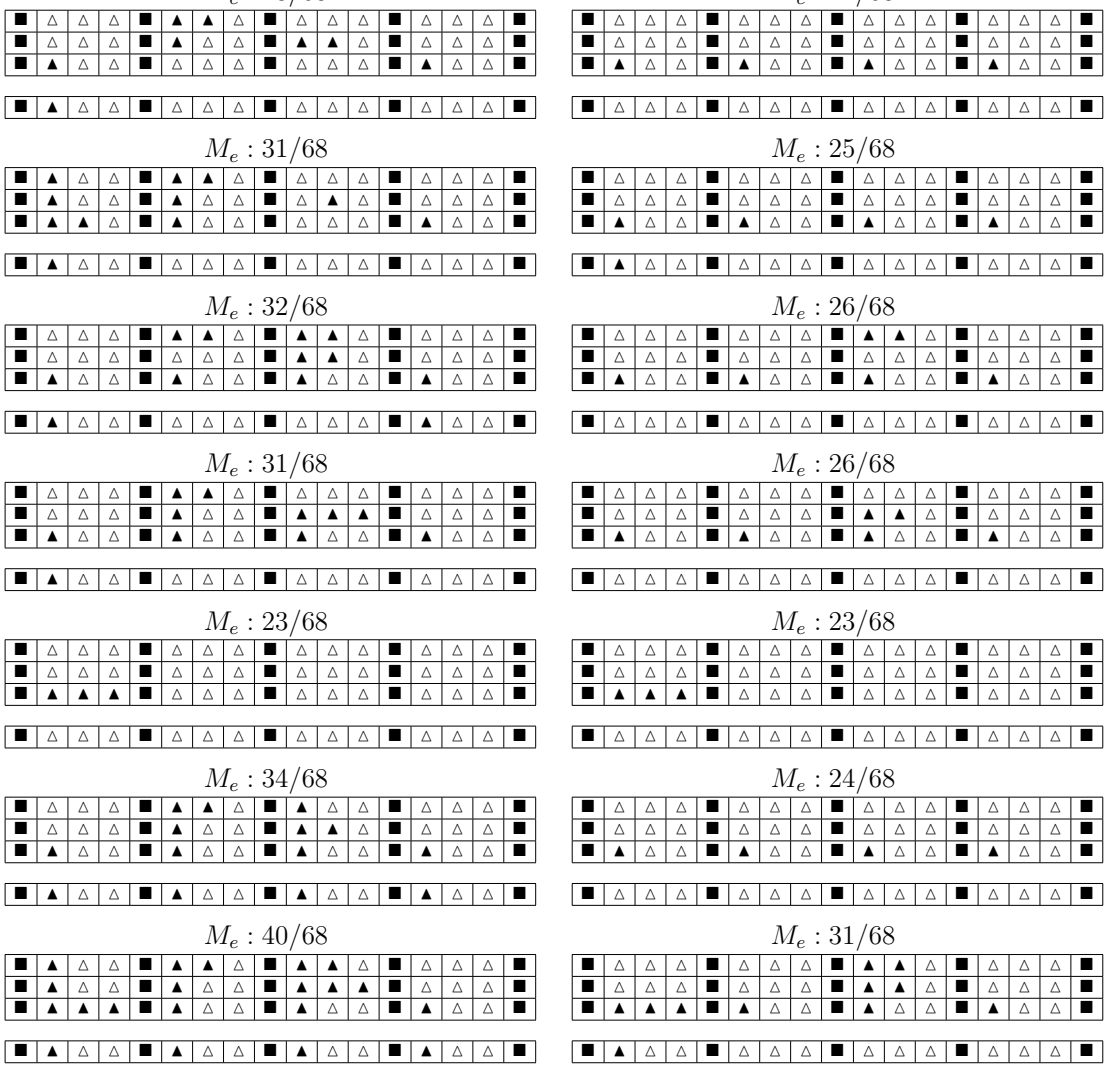

Table 6.13: Reduced LD4 model for laminated plate - sensor configuration.

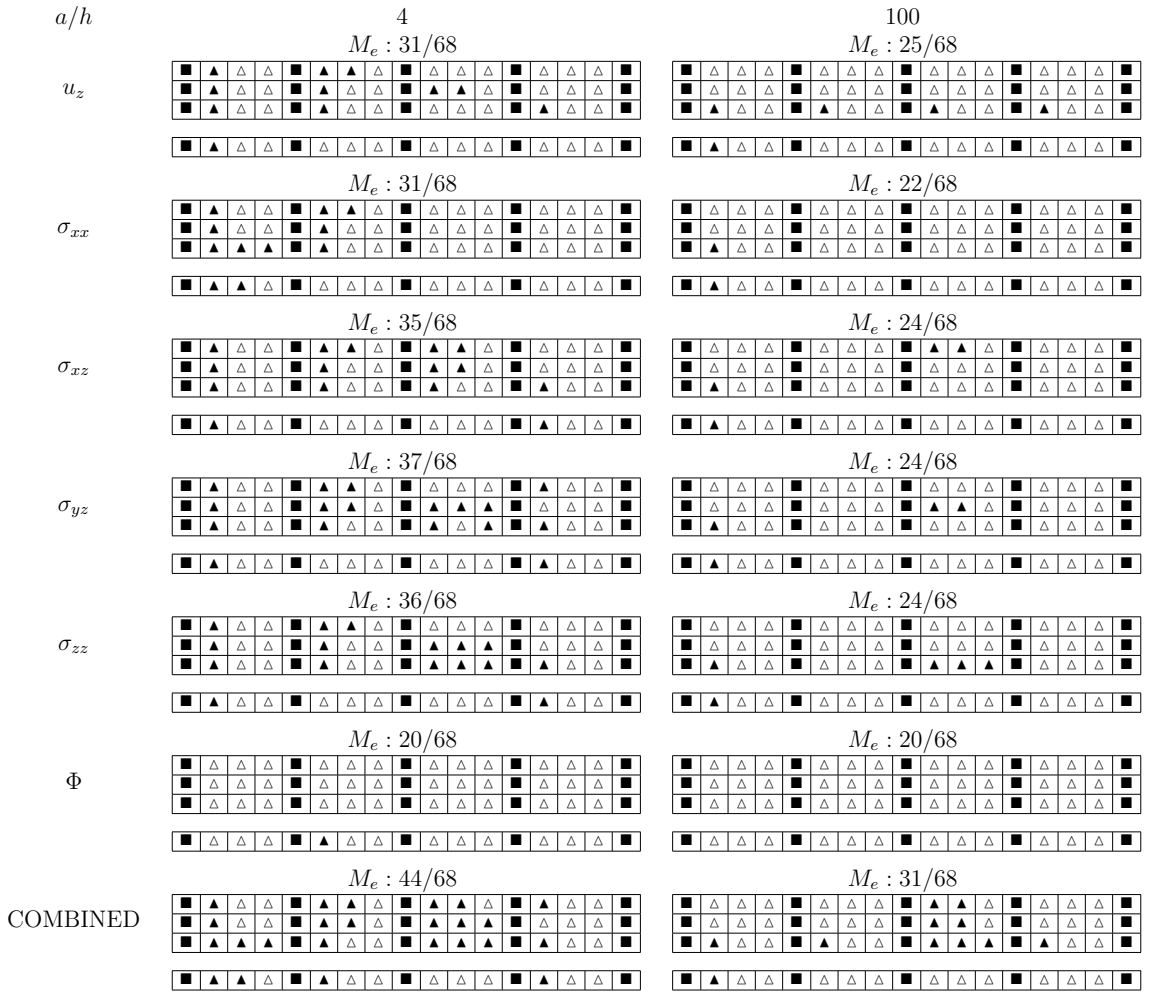

Table 6.14: Reduced LD4 model for laminated plate - actuator configuration.

Firstly, it can be noted that when sensor configuration is considered (Table 6.13) the analysis of a thick plate requires more displacement variables than the analysis of a thin plate. In addition, the reduced combined model for a thick plate has more than the 50% of the terms while the same model for a thin plate has less than the 50% of the displacement variables. It is possible to note that the two types of configurations lead to different reduced models: differences exist in terms of number and order of the retained terms. As an example, it is possible to note the relevance of terms u^1_{x1}, u^1_{y1} and u^1_{y1} (i.e. the terms u_{x1}, u_{y1} and u_{y1} related with the first layer) in the case of the reduced model for the displacement u_z, in thick plate case. It should be underlined

that, as already reported for the isotropic core plate, the potential distribution Φ, when actuator configuration is considered, has only the terms related with the top and bottom functions (F_t^k and F_b^k, see Table 6.14). This observation holds for thick and thin geometries. It is worth noting that the fourth-order terms are rarely included in all problems, as already underlined for the isotropic core plate. The distributions of the stress σ_{zz} and potential Φ along the thickness direction for the sensor configuration computed by means of the reduced combined models of Table 6.13 are reported in Fig. 6.8.

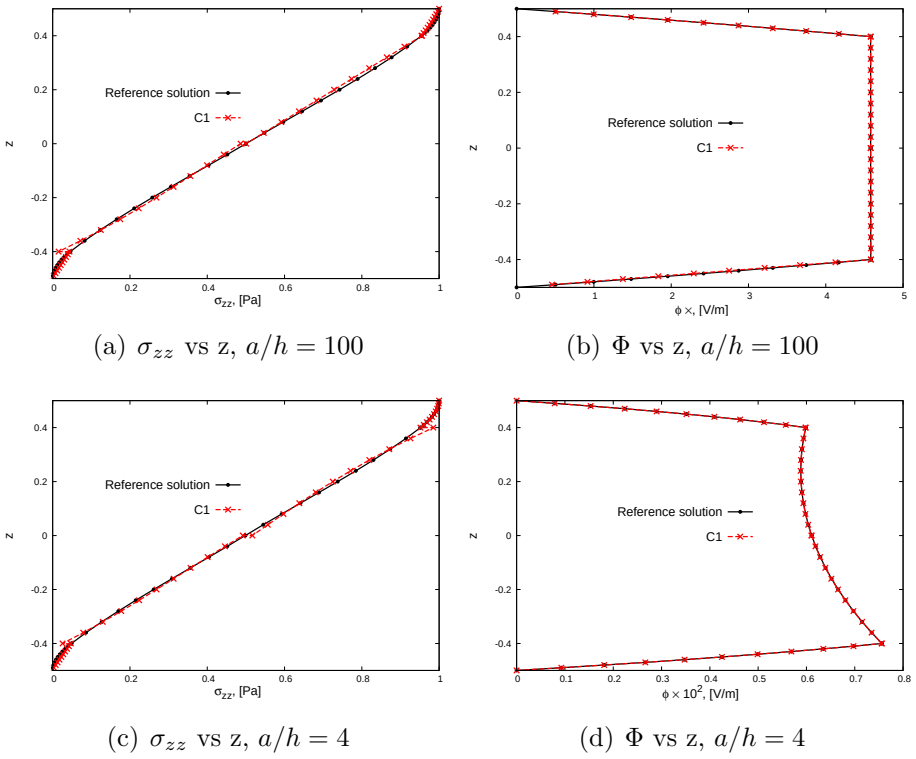

(a) σ_{zz} vs z, $a/h = 100$ (b) Φ vs z, $a/h = 100$

(c) σ_{zz} vs z, $a/h = 4$ (d) Φ vs z, $a/h = 4$

Figure 6.8: LD4 reduced model for laminated plate - sensor configuration.

It is possible to observe the good agreement with the reference solution. In addition, the distribution of the stress σ_{zz} and displacement u_z with the thickness direction for the actuator configuration are reported in Fig. 6.9. In this case, the reduced combined models employed to compute these quantities are in Table 6.14. It can be noted that the values are correctly computed (i.e. the accuracy is within the a-priori threshold) at the error criterium points although, in some case, the distribution may differ from

the reference solution.

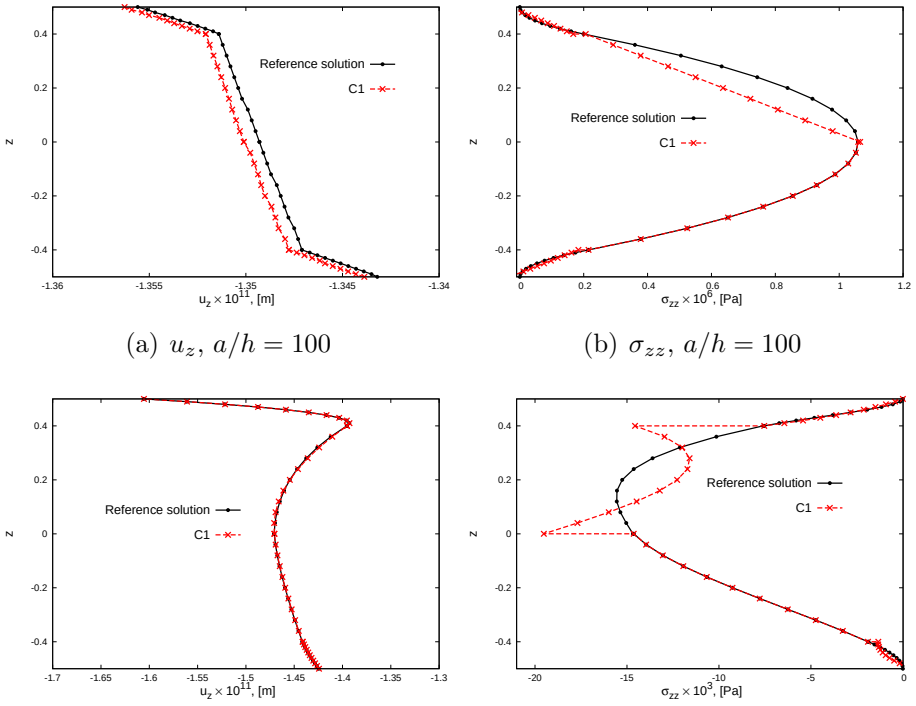

(a) u_z, $a/h = 100$ (b) σ_{zz}, $a/h = 100$

(c) u_z vs z , $a/h = 4$ (d) σ_{zz} vs z , $a/h = 4$

Figure 6.9: LD4 reduced model for laminated plate - actuator configuration.

The results reported for the piezoelectric plate showed that:

1. thick plate analysis is more crtical than thin plate analysis, since more terms are required. This is valid for both types of configurations;

2. the relevance of the terms is influenced by the type of the configuration considered, in other words reduced models for sensor configuration are different from the reduced models for actuator configuration;

3. the description of the potential distribution in the thickness direction for a thin isotropic and laminated plate can be performed considering a quasi decoupled model, that is, only Φ_t and Φ_b can be retained;

In-depth analyses on the piezo-electric plate are reported in the work [74].

6.5 Analysis of refined models for plates, RMVT statement

The analysis of the relevance of the terms of refined and mixed models for plate is performed considering a bimetallic plate. The top layer of this plate is titanium ($E =$ 114 GPa, $\nu = 0.3$) and the bottom layer is aluminum ($E = 70.3$ GPa, $\nu = 0.33$). The reference results employed in the axiomatic/asymptotic analysis are reported in Table 6.15.

	$\overline{\sigma}_{xx}(z = \pm h/2)$	$\overline{\sigma}_{xz}(z = 0)$	$\overline{\sigma}_{yz}(z = 0)$	$\overline{u}_z(z = h/2)$
		$a/h = 100$		
LM4	0.2236	−0.1810	0.2355	0.2355	2.2073
LD4	0.2236	−0.1810	0.2355	0.2355	2.2073
EM4	0.2244	−0.1803	0.2316	0.2316	2.2072
ED4	0.2246	−0.1804	0.1846	0.1845	2.2072
		$a/h = 4$		
LM4	0.2520	−0.1830	0.2306	0.2307	2.9079
LD4	0.2520	−0.1830	0.2306	0.2306	2.9079
EM4	0.2514	−0.1840	0.2287	0.2286	2.8982
ED4	0.2521	−0.1845	0.1823	0.1822	2.8945

Table 6.15: Stresses and displacement for a bimetallic laminated plate.

Both results offered by ESL and LW schemes are reported, considering both the PVD and the RMVT variational statements. It is possible to note that the LD4 model offer results in agreement with the reference solution (LM4). The results offered by the EM4 show differences with respect to the LW model. This difference becomes significant when a thick plate is considered. The displacement and stress component values computed by means of the ED4 model are in agreement when u_z and σ_{xx} are evaluated for a thin plate. The values of the σ_{xz} and σ_{yz} stresses present a significant deviation from the reference results for both thick and thin plate case.

Firstly, the analysis of the relevance of the terms is perfomed for the EM4 and ED4 models. The results are reported in Table 6.16.

In the same Table, the error computed by these models is reported. The results show that some term can be discarded only when the displacement u_z is considered for a thin plate. In addition, it is interesting to note that the retained displacement variables are the same for both models. In particular, the reduced models show that a linear expansion is needed for the displacements u_x and u_y, while the displacement u_z can be properly analyzed by means of a second order expansion. It is possible to note that the stress variables are not included in the EM4 model, except for the top

	EM4	ED4
	$a/h = 100$	
M_e	16/42	M_e : 7/15
Error	0.0406%	0.0458%
	$a/h = 4$	
M_e	42/42	M_e : 15/15
Error	0.3305%	0.4596%

Table 6.16: Reduced EM4 and ED4 models for bimetallic plate - displacement u_z.

and bottom stress variables. The displacement u_z is computed by means of the model reported in Table 6.16 and the results are reported in Figure 6.10. It can be noted that both models offer a good accuracy, in particular the reduced EM4 model offer a better accuracy than the reduced ED4 model.

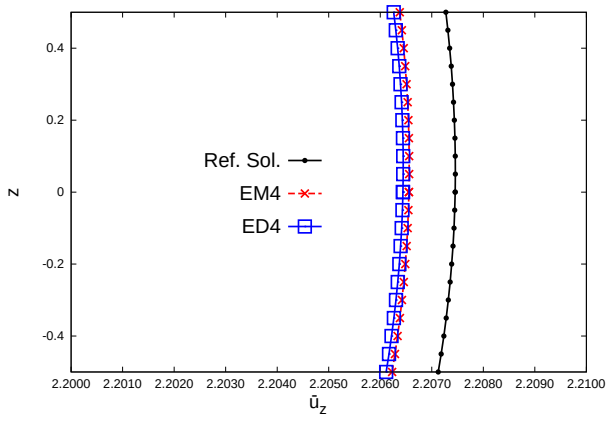

Figure 6.10: Displacement u_z distribution along the thickness, EM4 model - 2 layers metallic plate, $a/h = 100$.

The axiomatic/asymptotic technique is extended to LM4 and LD4 models. The

results are reported in Table 6.17 and 6.18, for LM4 and LD4 models, respectively.

	$a/h = 100$	$a/h = 4$
u_z	M_e : 20/54	M_e : 30/54
σ_{xx}	M_e : 20/54	M_e : 40/54
σ_{xz}	M_e : 28/54	M_e : 40/54
σ_{yz}	M_e : 28/54	M_e : 41/54
COMBINED	M_e : 34/54	M_e : 50/54

Table 6.17: Reduced LM4 model for the bimetallic plate.

	$a/h = 100$	$a/h = 4$
	M_e : 11/27	M_e : 17/27
u_z	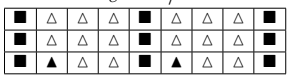	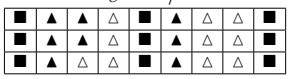
	M_e : 11/27	M_e : 19/27
σ_{xx}	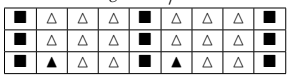	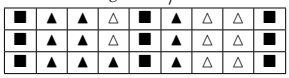
	M_e : 13/27	M_e : 20/27
σ_{xz}	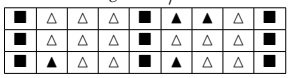	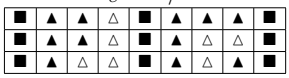
	M_e : 13/27	M_e : 20/27
σ_{yz}		
	M_e : 15/27	M_e : 24/27
COMBINED		

Table 6.18: Reduced LD4 models for the bimetallic plate.

These Tables report the reduced models for the displacement/stress components and the COMBINED models, which reports all the active terms from the previous displacement/stress components. As a general observation, it is possible to note that both LM4 and LD4 models require more active terms when a thick plate is analyzed rather than for a thin plate. In particular, it can be observed that the reduced models for the displacement u_z require the same displacement variables for both LM4 and LD4 models, for the thick and thin plate cases. In general, the reduced models for the evaluation of the out-of-plane stresses present different displacement variables according to the variational statement employed. It is possible to note that the reduced combined model present more than the 50% of the active variables for both thick and thin geometry. Instead, the reduced combined model for the LD4 model has less than the 50% of the active terms when a thin plate is conisdered. In the case of a thick plate, more than half terms are required for a thick plate. This fact was already noted in [69] for the LD4 reduced models. An example of stress computation perfomed by means of these reduced models is reported in Figure 6.11, where the distribution of the stress σ_{xz} along the thickness direction is computed by means of the reduced combined models.

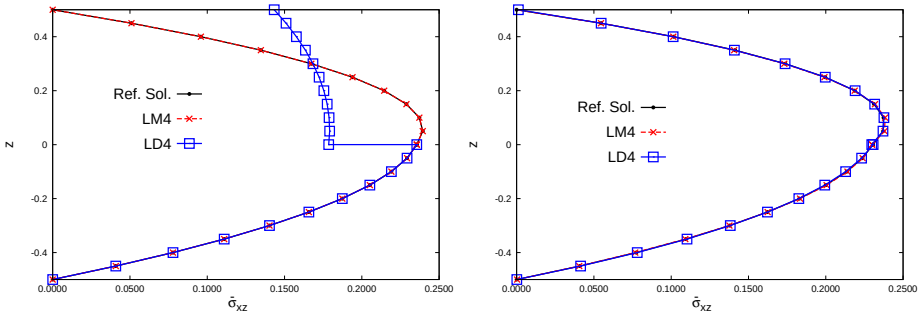

(a) $a/h = 100$ (b) $a/h = 4$

Figure 6.11: Stress σ_{xz} distribution along the thickness - 2 layers metallic plate.

It interesting to note that the reduced LM4 models offer a satisfactory distribution in both of cases while, the reduced LD4 models for the thin plat case presents a significant discontinuity at the interfaces. This was noted in [69] and in that occasion different criteria were proposed in order to obtain better satisfactory distributions. In this case, it is possible to affirm that distributions in agreement with the reference solution can be obtained for refined models based on RMVT variational statement just by computing the error at one point. An interesting fact is reported in Figure 6.12.

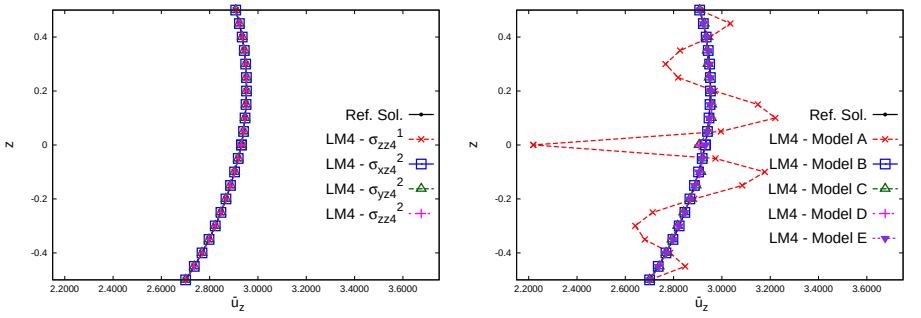

(a) Variable deactivation influence (b) Accuracy of models A, B, C and D (see Table 6.19)

Figure 6.12: Displacement u_z distribution along the thickness - 2 layers metallic plate, $a/h = 4$. σ_{zz4}^{1}, σ_{xz4}^{2}, σ_{yz4}^{2}, and σ_{zz4}^{2} in the legend of Figure 6.12(a) are the stress variables suppressed. Models A, B, C, D and E are reported in Table 6.17.

The displacement u_z distribution along the thickness direction for the thick plate

case is reported in Figure 6.12(a) computed by deactivating the stress variables σ^1_{zz4}, σ^2_{xz4}, σ^2_{yz4}, and σ^2_{zz4} one by one and it is possible that any error is present. It seems that these terms are not influent, as a matter of fact the reduced combined model of Table 6.17 (and reported as model A in Table 6.19) shows that these variables are not included.

Model		Error	M_e
A	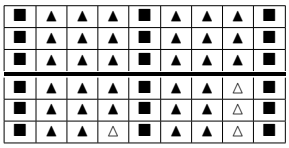	0.0132 %	50/54
B	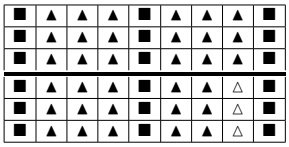	0.0 %	51/54
C	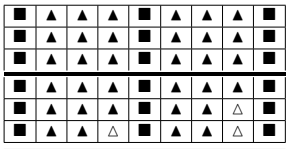	-4.6274×10^{-4} %	51/54
D	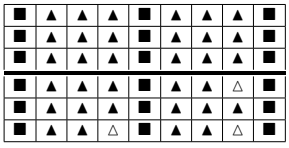	-4.6274×10^{-4} %	51/54
E	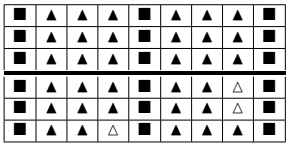	0.0 %	51/54

Table 6.19: Reduced LM4 model for the bimetallic plate, displacement u_z.

The displacement u_z is computed by means of this reduced combined model and it is reported in Figure 6.12(b): the displacement is correctly computed at $z = h/2$ but the overall distribution significantly differs from the reference solution. In this case it is possible to affirm that in some case the simultaneous deactivation of variables that do not contribute to the analysis may lead to a not correct evaluation of the quantity considered for the axiomatic/asymptotic technique. This fact is confirmed by considering the models labels as B, C, D, and E reported in Table 6.19: these models are obtained from the model A by reactivating one by one the excluded terms. The error reported next to these models and the displacement u_z distribution computed

by these models and reported in Figure 6.12(b) leads to the conclusion that in some case effective reduced models cannot be obtained just by deactivating the not relevant terms, but by evaluating the accuracy of an entire sequence of active/not-active terms. An example of this type of analysis is reported in the work [75], where the authors employ a genetic algorithm to the axiomatic/asymptotic technique in order to detect the reduced models which offer the lowest possible error. It is possible to conclude:

- the selection of terms can be applied to ESL models for only some stress/displacement component, e.g. stress σ_{xx}. In addition, the cases herein reported showed that the reduced models based on both PVD and RMVT variational statements have the same active displacement variables;

- the reduced models for the LW models present more active terms when a thick plate is considered. In addition, LD4 models for thin plate has less than the 50% of active terms, while the reduced models for the thick plate case has more terms. In general, the reduced LM4 models have more than the 50% of active terms for both thick and thin plate case;

- in some case, the deactivation of all variables which seem to not contribute to the plate analysis does not lead to an accurate evaluation of the plate response.

Further cases are considered in the work [76].

6.6 Conclusions

The results reported in this chapter are related with the analysis of refined and mixed theories for simply supported multilayered plates; isotropic and orthotropic materials have been considered. The axiomatic/asymptotic analysis has been employed in order to discard not necessary terms from refined models obtained by means of CUF. All analyses considered Navier-like closed-form solutions. The equivalent Single Layer (ESL) and Layer Wise (LW) approaches were considered and the influence of specific parameters - length-to-thickness ratio a/h and the ply stacking sequence - were investigated. In addition, the influence of different error criteria have been analyzed and the influence of the type of load on the terms selection process was investigated. The axiomatic/asymptotic technique was employed by considering two different variational statements: the PVD and the RMVT. The analyses herein conducted make it possible to conclude that:

1. LW models offer a better analysis of static response compared to ESL models and show a more significant terms reduction with respect to ESL models. The results showed that the distribution of the out-of-plane displacement and in-plane stress of a thin isotropic single layer plate can be correctly predicted by means of an ESL model if only the plate displacement field contains the linear variables for displacements u_x and u_y and the second order term for the displacement u_z; furthermore, it has been demonstrated that the correct computation of out-of-plane stress require the inclusion of a third order term in addition to the previous ones;

2. the set of effective terms can be influenced to a great extent by the displacement/stress component to be accounted for and by the geometrical and material characteristics; in general, thick plate reduced models have a higher computational cost than thin plate reduced models;the present methodology leads to a significant reduction of the number of unknowns variables in a LW model;

3. the number of half-waves load influences the number and the order of the retained terms for the reduced plate models for mechanical analysis, in particular in the case of thick plates; the absence of any half-wave along a main direction (x or y) lead to the exclusion of the terms related with that direction;

4. the adopted criterium influence the number and the order of the retained displacement variables. In addition, the proposed criteria makes it possible to compute correctly the displacement/stress component values at the reference points, although the distribution along the thickness direction may differ from the reference solution; a possibility to improve the computation of the distribution may come form the use of different criteria; the results have demonstrated that satisfactory distributions can be computed if the error is computed at the the interfaces of the layers in the case of laminated and sandwich plates;

5. in the case of shell analysis, the geometry (R_β/h) influences the relevance of each term of the model, in particular reduced models for thick shells require in general more displacement variables than reduced models for thin shells;

6. the type of load in general may influence the displacement variable retained in a refined model, as proved the analysis of refined models for the thermal and mechanical stress analysis. The results showed that the correct evaluation of the displacement/stress distribution for thin multilayered plate subjected to a temperature distribution requires at least a second order term for the out-of-plane

displacement (u_z) for a LW model. In the case a thick geometry is considered, third order terms have to be included in a LW model. In general it is possible to note that the fourth order terms are seldomly included in the LW models, even for thick plate geometry;

7. in the case of piezoelectric plate analysis, the relevance of the terms is influenced by the type of the configuration considered, in other words reduced models for the sensor problem are different from the reduced models for the actuator problem; it has been noted that the description of the potential distribution in the thickness direction for a thin isotropic and laminated plate can be performed considering a quasi decoupled model, that is, only Φ_t and Φ_b can be retained;

8. the axiomatic/asymptotic technique applied to mixed models obtained by means of the RMVT variational statement showed that the reduced refined models for the thick plates require more variables than the thin plate case; in particular, the reduced LW models obtained by means of the RMVT statement require more variables than the models obtained by means of the PVD statement;

9. in the case of RMVT models for plates, the selection of terms can be applied to ESL models for only some stress/displacement component, e.g. displacement u_z. In addition, the reduced models based on the PVD and on the RMVT have the same active displacement variable;

10. when the RMVT variational statement is considered, the exclusion of all variables which seem to not contribute to the plate analysis does not lead to an accurate evaluation of the plate response.

Part III

Best Theory Diagram - plate and shell, mechanical and multifield analysis

Chapter 7

Best Theory Diagram

In this chapter, the Best Theory Diagrams (BTDs) are described. These graphs make it possible to represent in a synthetic way the "best" reduced models, i.e. the reduced refined models which offer the highest accuracy with the lowest computational cost. The definition of such curves is obtained by means of the axiomatic/asymptotic technique: in this case, the effectiveness of an entire active/non-active terms combination is considered and not the effectiveness of the single term. A genetic algorithm is employed, since a large number of combination should be analyzed. This genetic algorithm was inspired directly from the work of C. Darwin: the sequence of active/non-active terms are considered as the genoma of an individual (in this case, reduced models) and the best individuals/models are selected and mutated.

7.1 Best Theory Diagram, an introduction

It is possible to associate to each reduced refined model the number of the active terms and its error computed with respect to a reference solution. This information are susceptible of an interesting graphical representation as reported in Fig. 7.1.

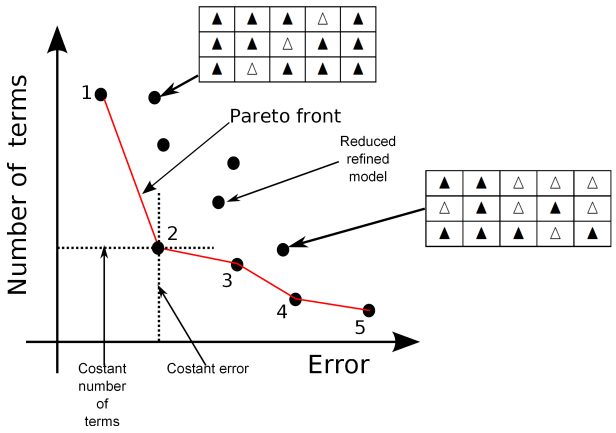

Figure 7.1: Example of representation of the errors of all possible refined models terms combinations.

The error values are reported on the abscissa and the number of active terms is reported on the ordinate. Each black dot represents a reduced refined model and its position on the Cartesian plane is defined considering its error and the number of the active terms. In addition the synthetic representation of the active/non-active terms is reported for some reduced models. Considering all models, it is possible to note that some of them present the lowest error for a given number of active terms. These models are labeled in Fig. 7.1 as 1, 2, 3, 4, 5 and they represent a Pareto front for the considered problems. This Pareto front is defined in this work as the Best Theory Diagram. The existence of such curve was already demonstrated in the work reported in [75]. This curve can be constructed for several problems, for example considering several type of materials, geometries and boundary conditions. Moreover the informations reported synthetically in a BTD makes it possible to evaluate the minimum number of terms, N_{min}, that have to be used in order to achieve a desired accuracy. A BTD for a specific problem is obtained by means of the Axiomatic/Asymptotic technique. The algorithm employed to generate a BTD is the following

1. plate parameters such as the geometry, boundary conditions, loadings, materials and layer layouts, are fixed;

2. a set of output parameters is chosen, such as displacement or stress components;

3. a starting theory is fixed (axiomatic part), that is the displacement variables to be analyzed are defined;

4. a reference solution is defined (in the present work LD4/LM4 approaches are adopted, since these fourth order model offers an excellent agreement with the three-dimensional solutions);

5. the CUF is used to generate the governing equations for the theories considered;

6. a genetic algorithm is employed in order to obtain the reduced refined models belonging to the BTD.

7.2 BTD construction by means of genetic algorithms

The number of all possible combinations of active/not-active terms for a given refined model is equal to 2^M where M is the term model number. In the case of an ESL model, M can be computed as $M = (N+1)\,3$. In the case of a LW model the displacement variables related with the top and bottom of each layer must be included due to the continuity condition of the displacement field, so the number M is computed as

$$M = 3\,(N-1)\;N_L \tag{7.1}$$

As the expansion order increases the number of the combinations to consider also increases. In this case the computational cost required for the BTD construction can be very significant. In order to construct a BTD with a minimal computation effort a different strategy has to be employed; for this purpose in this work a genetic approach is used and its implementation is discussed in the following. It should be mentioned that the BTDs are constructed considering the effectiveness of an entire active/non-active term combination. This strategy is employed since the definition of a BTD by assuming an a-priori error threshold may lead to the exclusion of some "best" model which can be in neighborhood of the chosen threshold. This situation is depicted in Figure 7.2

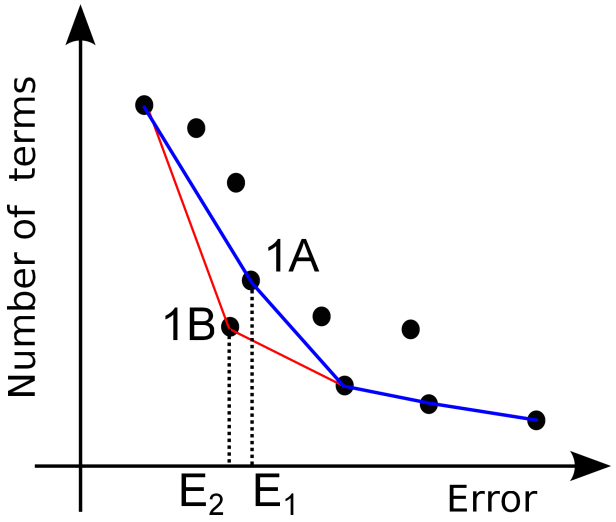

Figure 7.2: Best Theory Diagram definition.

The model 1A is defined by assuming an a-priori threshold (E_1), while the model 1B is defined by considering all possible active/non-active term combination and its error with respect the reference solution is equal to E_2. It can be noted that assuming a-priori the error threshold may lead to the exclusion of reduced models with better accuracy. In the case of BTD definition, the error of a reduced model is an output parameter.

The genetic algorithms are inspired by the evolution theory explained in "The origin of species", written by Darwin ([77]). In nature, weak and unfit individuals within their environment are faced with extinction by natural selection. The strong ones have a greater opportunity to pass their genes down to future generations via reproduction. In the long run, the species carrying the correct combination in their genes become dominant in their population. Sometimes, during the slow process of evolution, random changes may occur in the genes. If these changes provide additional advantages within the challenge of survival, new species evolve from the old ones. Unsuccessful changes are eliminated by natural selection. In genetic algorithm terminology, a solution vector $\boldsymbol{x} \in \boldsymbol{X}$, where $\boldsymbol{X}$ is the solution space, is called *individual* or *chromosome*. Individuals are made of discrete units called *genes*. Each gene controls one or more features of the individual. The present genetic algorithm use the *mutation* operator to generate new solutions from existing ones. The mutation operator introduce random changes into the characteristics of the chromosome. Mutation is generally applied at gene level. In the multi-objective optimization genetic algorithm each individual has a fitness value based on its rank in the population, not its actual objective function value. The population

is ranked according to the dominance rule reported in [78]. A synthetic representation of the dominance of a generic model/individual k is depicted in Figure7.3

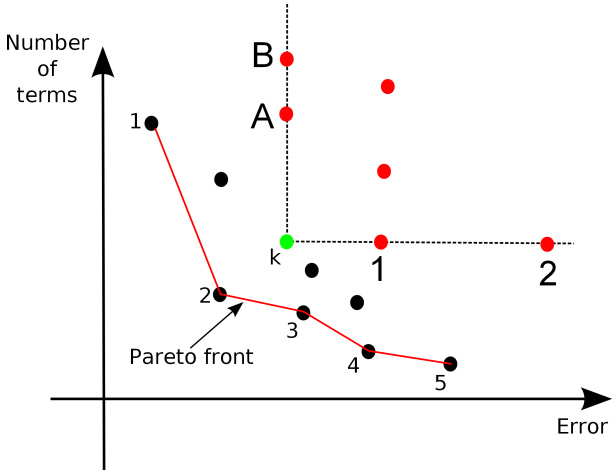

Figure 7.3: Dominance of the model k.

The model k dominates over the red models included in the part of the plane marked with the dotted lines. This part of plane is defined by the models with the same accuracy of the model k but with the higher computational cost (in the Figure, models A and B), and the models with the same computational cost of models k but with lower accuracy (in the Figure, models 1 and 2). The fitness of each chromosome is evaluated through the following formula:

$$r_i(\boldsymbol{x}_i, t) = 1 + nq(\boldsymbol{x}_i, t) \tag{7.2}$$

where $nq(\boldsymbol{x}_i, t)$ is the number of solutions dominating by solution $\boldsymbol{x}_i$ at generation t. A lower rank corresponds to a better solution.
The genetic algorithm employed in this work is similar to the algorithm described in [75], but with some differences which will be described in the following. Each plate theory has been considered as an individual. The genes are the terms of the expansion and each gene can be active or not active, the deactivation of a term is obtained by exploiting a penalty technique. A synthetic representation of this is reported in Fig. 7.4.

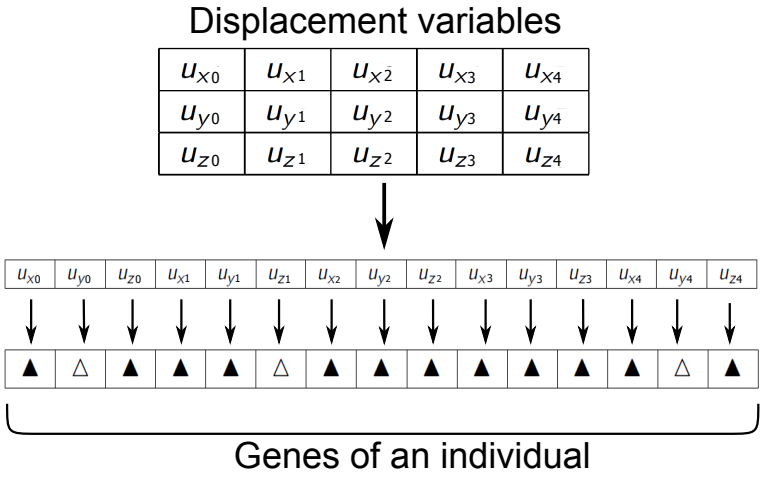

Figure 7.4: Displacement variables of a refined model and genes of an individual.

The meaning of the symbols ▲ and △ is reported in Table 5.2. Each individual is therefore described by the number of active terms and its error computed with respect to a reference solution. Through these two parameters it is possible to apply the dominance rule in order to evaluate the individuals fitness. The generation of the new population considered in this work is different than the one described in [75]: in that work a new individual was originated by exchanging parts of the chromosomes of the best individual. In this work, the generation of new refined theories starting from a generic population is inspired to the reproduction of bacteria. The best individuals of a population are detected and a number of copies are created according to their dominance and then, a number of mutations are applied in order to vary the set of new individuals. This modification has been implemented since the BTD for large models (i.e. models with a considerable number of variables such as LW models for multylayered plate/shell) were not detected correctly.

The purpose of this analysis is to find the individuals which belong to the Pareto front, that is the subset of individuals which are dominated by no other individual. The number of the individuals of the initial population and the number of iterations depend on the specific problem under examination. As an example in some simple problems, e.g. thin isotropic plate analyzed by means of ED4 model, an initial guess population of 400 individuals was considered. In this case only 10 iterations were necessary to obtain the BTD. On the other hand, in the case of a LM4 models for a 3-layered plate an initial guess population of 32000 individuals were necessary. The number of required iterations to obtain the BTD was equal to 50. These parameters have been defined for each problem analyzed by a trial-and-error process. The error

of the reduced models with respect to a reference solution is evaluated through the following formula:

$$e = 100 \, \frac{\sum_{i=1}^{N_p} |Q^i - Q^i_{\text{ref}}|}{\max Q_{\text{ref}}} \cdot \frac{1}{N_p} \tag{7.3}$$

where Q is the entity under exam (stress/displacement component) and N_p is the number of points along the thickness on which the entity Q is computed. The use of this criterium for the evaluation of the accuracy of a reduced model was adopted since it was intended to provide a number of reduced refined models for bidimensional structures able to computed correctly the displacement/stress components distribution along all the thickness direction.

The originality of this work consists of the new kind of genetic algorithm (i.e. how the new individuals are created starting form an initial population) and the extension of BTD definition to the multifield problems (thermal and piezo-electrical) for plates. In addition, the BTD has been obtained for refined models based on the RMVT statement. It should be mentioned that the algorithm adopted in this thesis included the evaluation of the thickness locking phenomenon for ESL models whose displacement u_z expansion is truncated to the first order (models based on PVD statement).

Chapter 8

Best Theory Diagram, results

Best Plate Theory Diagrams (BTDs) are reported in this chapter for the static analysis of metallic and laminated composite plates and shells. The theories that belong to the BTD are obtained by means of the Axiomatic/Asymptotic technique, and a genetic algorithm is employed to obtain the BTD. The Carrera Unified Formulation (CUF) is employed to obtain refined models; Equivalent Single Layer (ESL) and Layer Wise (LW) kinematics are considered. Closed-form, Navier - type solutions are employed, and attention is therefore restricted to simply-supported plates. As in the case of the axiomatic/asymptotic technique, the Navier - type solutions have been chosen in order to obtain quickly the results and to be able to focus on different aspects, as the influence of the type of load on the definition of the BTD. The influence of various geometries, material properties and layouts are evaluated, and their influence on the BTD is analyzed. Furthermore, some known theories are compared with the BTD curve. The results suggest that the BTD and the CUF can be considered as tools to evaluate any structural theory against a reference solution. BTDs are reported also for multifield analyses, i.e. for refined models related to thermal stress analysis and piezoelectric plate analysis. The influence of geometrical and material parameters is evaluated for the multifield case. In addition, in some case the BTDs are obtained considering different displacement and stress components in order to highlight their influence on the definition of the BTDs.

8.1 Best Theory Diagram for plates - mechanical analysis

In this section, BTDs for the mechanical plate stress analysis are reported. In all cases the acting load is a transverse pressure applied to the top surface of a plate, see Equation 4.67. In the following, parameters m and n are equal to 1. The reference system layout is reported in Fig. 2.4. All the reduced models are developed for stress σ_{xx}, which is computed at [a/2, b/2, z] with $-\frac{h}{2} \leq z \leq \frac{h}{2}$, where h is the total thickness of the plate. Axiomatic/asymptotic analyses have been conducted for a metallic plate, whose material properties are $E = 73$ GPa and $\nu = 0.34$ (aluminum). The length-to-thickness ratios (a/h) are equal to 5 and 50.

First, an ED4 model assessment was performed considering an aluminum plate. The results are reported in Table 8.1; the three-dimensional exact elasticity results are obtained as in [79, 80].

a/h	100	10	5	2
Ref. [79, 80]	0.2037	0.2068	0.2168	0.3145
ED4	0.2037	0.2068	0.2168	0.3165

Table 8.1: ED4 model assessment, reference solution reported in [79, 80]. Stress $\overline{\sigma}_{xx}(z = \pm h/2)$, simply supported metallic plate under mechanical load, $\overline{\sigma}_{xx} = \frac{\sigma_{xx}}{p_z\,(a/h)^2}$

It is possible to note that the results offered by the ED4 model are in excellent agreement with the reference solution. This makes the ED4 model suitable for the computation of the reference solution of the axiomatic/asymptotic analysis for the case under examination.

The first method that was used to build the BTD is based on the evaluation of all the possible combinations given by the 15 terms of an ED4 model, that is, $2^{15} = 32768$ theories; Fig. 8.1(a) shows the error of each theory.

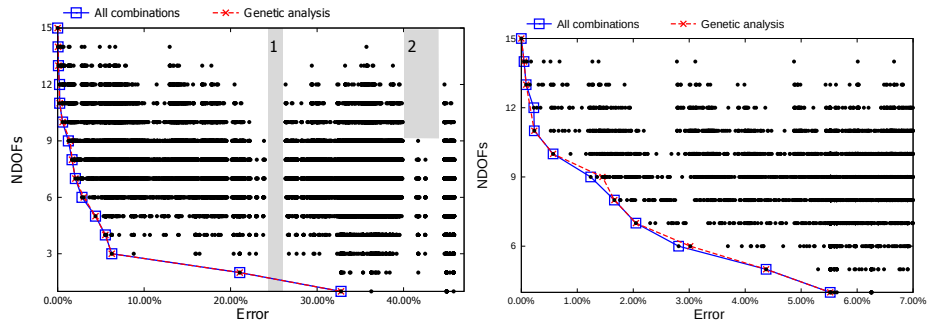

(a) BTD, assessment (b) BTD, assessment - zoom

Figure 8.1: Genetic algorithm assessment, ED4 reduced models - metallic plate, $a/h = 2.5$

It is possible to note that some empty regions are present, and these regions are labeled as 1 and 2 in the figure. In this case, it is possible to state that the construction of reduced refined models is not always possible: no term combinations are present for some errors and term number intervals. The BTD is given by those combinations (i.e. plate theories) which, for a given error, require the lowest number of unknown variables. Two BTDs are shown in Fig. 8.1, where the "All Combinations" BTD was built by evaluating all the 2^{15} combinations. The "Genetic" curve was built by exploiting a genetic algorithm. The genetic algorithm for the axiomatic/asymptotic technique evaluates around 400 individuals for 10 generations: this means that only about 4000 out of 32768 theories have to be evaluated. It is possible to note that almost all the models on the Pareto front are detected.

The influence of the plate geometry on BTD construction was considered, and the results are reported in Fig. 8.2.

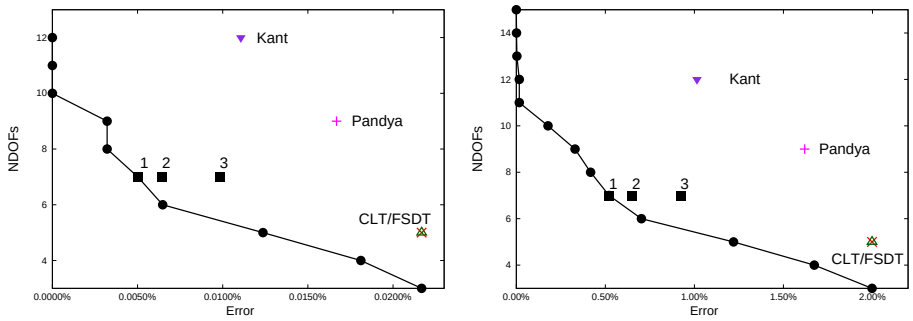

(a) BTD, $a/h = 50$. (b) BTD, $a/h = 5$

Figure 8.2: Best Plate Theory Diagram (BTD) for a simply supported metallic plate - ED4 reduced models

The curves suggest that, as a metallic plate becomes thinner, the BTD tends to be defined in a smaller region of the error/number-of-variable plane (E/NoVs plane). In addition, it is possible to note that the BTD distribution becomes steeper as the plate becomes thinner. Four classical theories from bibliography are also reported in the same graphs, that is, the CLT and FSDT theories and the theories of Pandya ([81]) and Kant ([82]). As the plate becomes thinner (i.e. ratio a/h increases), the accuracy of the classical models increases. It is worth noting that none of the four models lie on the BTD: this means that either the accuracy of the classical models can be achieved with fewer unknown variables, or that it is possible to obtain a better accuracy with the same number of variables. It can be noted that, for the thin plate case ($a/h = 50$), the best accuracy is given by a 13-term theory, that is, two terms in a ED4 model are not effective for the particular problem considered. In addition, the accuracy offered by 10, 11 and 12 term models is almost equal to the accuracy offered by the 13-term theory. The synthetic representation of the classical models and the models belonging to the BTD with the same number of terms are reported in Table 8.2 with their accuracy:

	$a/h = 50$			$a/h = 5$		
Kant	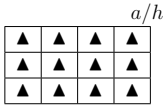	$M_e : 12/15$	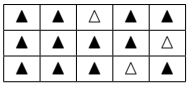	Kant	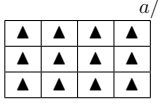	$M_e : 12/15$	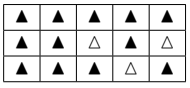
Error	0.0111%		7.138×10^{-8}%		1.0146%		0.0165 %
Pandya	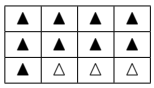	$M_e : 9/15$	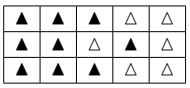	Pandya	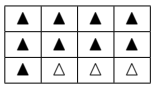	$M_e : 9/15$	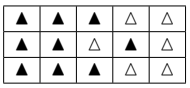
Error	0.0167%		3.2123×10^{-3}%		1.6193%		0.3297%
CLT/FSDT		$M_e : 5/15$	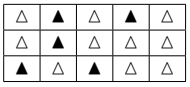	CLT/FSDT		$M_e : 5/15$	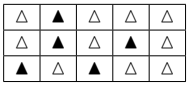
Error	0.0217%		0.0167%		1.9977%		1.60691%

Table 8.2: Reduced model for an isotropic plate, ED4 models - genetic approach.

The results show how the accuracy of the classical models can be improved. As an example, the accuracy of CLT/FSDT models for the cases herein considered can be improved by neglecting the constant terms u_{x0} and u_{y0} and considering a parabolic term for the displacement u_z and a third order term (u_{x3} for the thin plate case and u_{y3} for the thick plate case). It is possible to conclude that, in general, the geometry of a plate influences the improvement process of classical models. It is interesting to note that the improved Pandya models related to the thin and thick plates corresponds, but different accuracy are obtained. Anyway, the results indicate that in general the improvement of the classical models can be obtained if higher expansion terms are considered for the displacement u_z component (see Pandya and CLT/FSDT models).

The graphs of Figure 8.2 show that, by keeping the number of active terms constant, it is possible to detect different plate theories that compute the required output with a different approximation. These models are labeled 1,2, and 3 (Fig. 8.2). Models 1, 2 and 3 and their errors are reported in Table 8.3.

	1	2	3	M_E
		$a/h = 50$		
	▲▲△△△ △▲△▲△ ▲▲▲△△	▲▲△△△ △▲△△▲ ▲▲▲△△	△▲△△△ ▲▲△▲△ ▲▲▲△△	7/15
Error	$5.0143 \times 10^{-3}\,\%$	$9.8327 \times 10^{-3}\,\%$	$2.0822 \times 10^{-2}\,\%$	
		$a/h = 5$		
	▲▲△▲▲ △▲△△△ ▲▲△△△	▲▲▲△△ ▲▲△△△ ▲▲△△△	△▲▲△△ △▲△▲△ ▲▲▲△△	7/15
Error	$0.5212\,\%$	$0.9225\,\%$	$1.8596\,\%$	

Table 8.3: Reduced models for a simply supported isotropic plate, ED4 reduced models.

It is possible to note that, for moderately thick and thin plates, the models that offer the lowest possible error have the same term arrangement. In addition, the models that belong to the BTD (models 1) have the terms u_{x0}, u_{z0}, u_{x1}, u_{y1} and u_{z1} in common. It is worth noting that, for a given plate geometry, the relevance of a term cannot be predicted easily: as an example, considering the models labeled 1 and 2 and 3 for $a/h = 5$, the term u_{x2} is included when the error is equal to 0.9225%, and is not included when the error is equal to 0.5212%, but when the error is equal to 1.8596%, this term is again included. The σ_{xx} distributions along the thickness are reported for different plate thickness in Fig. 8.3.

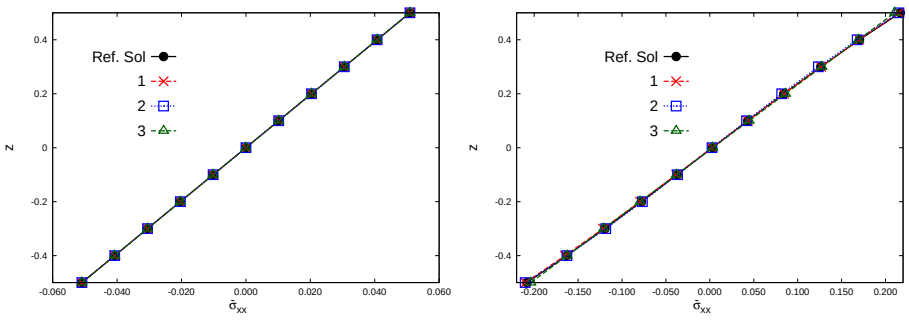

(a) $a/h = 50$. (b) $a/h = 5$

Figure 8.3: Stress σ_{xx} distribution for metallic plate, ED4 reduced models - reduced models from Table 8.3.

The evaluation of the σ_{xx} stress is performed by means of the reduced models reported in Table 8.3. It can be noted that the stress distributions computed by

means of the reduced models, which belong to the BTD (i.e. the models labeled as 1), are in agreement with the reference solution. Moreover, it is possible to state that, for a given error interval, as a plate becomes thinner, different reduced models are able to compute the stress distribution within the imposed accuracy. The results herein reported for the metallic plate suggest that

- for a given theory and problem, it is possible to define a BTD that is a set of reduced models which offer the lowest possible error with respect to a reference solution;
- a genetic algorithm makes it possible to construct a BTD with a lower computational cost;
- it is difficult to predict the relevant terms for a given problem;
- in most cases, the BTD models allow one to obtain better accuracies than classical models with the same number of variables, or to have the same accuracy with fewer variables.

Further results on this topic are reported in the work [83].

8.2 Best Theory Diagram for shells - mechanical analysis

Hereafter, a metallic shell is considered and the BTDs for this case are proposed. The shell considered has dimensions $a = R_\beta/10$, $b = R_\beta\,\pi/3$ and thick and thin geometry are considered (R_β/h equal to 4 and 100, respectively). The material properties are $E = 73\ 10^9$ Pa and $\nu = 0.34$. Some values of the displacement u_z and stress $\sigma_{\alpha\alpha}$ evaluated by means of the ED4 model are reported in Table 8.4.

$\overline{u}_z(z=0)$	$\overline{\sigma}_{\alpha\,\alpha}(z=\mp h/2)$	$\overline{u}_z(z=0)$	$\overline{\sigma}_{\alpha\,\alpha}(z=\mp h/2)$
ED4			
$R_\beta/h=100$		$R_\beta/h=4$	
1.6669	−2.5757	2.1132	−3.3236
	2.5504		2.7882

Table 8.4: Static response analysis of an isotropic shell.

Firstly, the BTD are constructed considering all possible combinations, which are $2^{15} = 32768$. The error is computed considering the stress $\sigma_{\alpha\alpha}$ and the position of the all combinations in the E/NDOFs plane are reported in Figure 8.4.

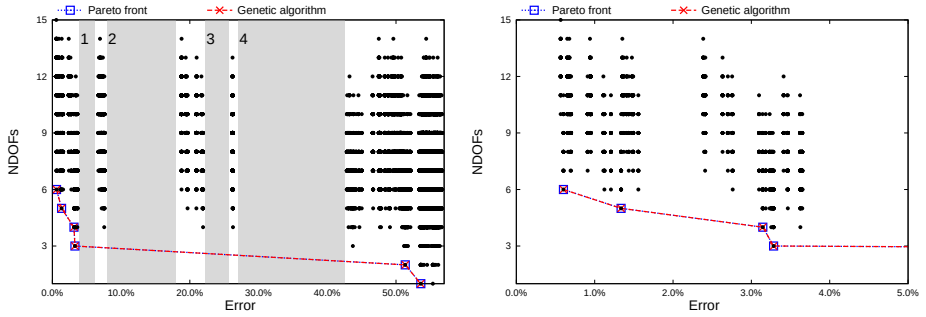

(a) All combinations (b) All combinations - zoom

Figure 8.4: All combinations, ED4 model - metallic shell, $R_\beta/h = 4$.

The Pareto front is obtained by considering the reduced model which offer the lowest possible error for a given number of active terms. Once these models are detected, the Pareto front is defined: the models which offer a lower accuracy with respect the models with a lower number of terms are excluded. The BTD obtained by means of the genetic approach is reported in the same Figure: it can be noted that the proposed algorithm is able to detect all the models that belong on the Pareto curve. It should be underlined that the BTDs do not include any reduced model with more than 6 terms. The reason is that the models with more than 6 terms have the same error as the 6-term model but a higher computational cost (see Figure 8.4(b)). Another interesting fact is that empty regions are present: it means that for some specific combinations of number of terms and error it is not possible to create any reduced models (see regions labeled as 1, 2, 3 and 4 in Figure 8.4). The genetic algorithm proved to be a valid means to obtain the BTDs.

It is interesting to compare the accuracies of some well-known models with the accuracy of the models which belong to the BTD for the case in exam. The accuracies of the CLT, FSDT and Pandya models are reported in the E/NDOFs plane as depicted in Figure 8.5 with the BTDs for the thin and thick shells.

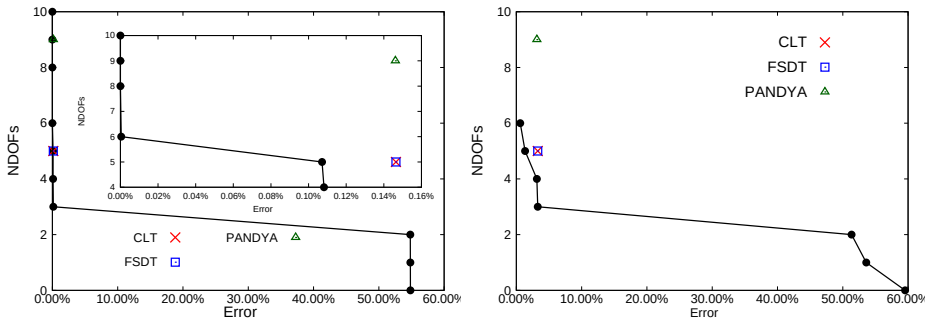

(a) $R_\beta/h = 100$ (b) $R_\beta/h = 4$

Figure 8.5: BTD for metallic shell - ED4 model. Different theories considering $\sigma_{\alpha\alpha}$.

It is possible to note that the error committed by these models is higher than the error of the models which belong to the BTD. This difference is particular clear when a thick shell is considered. This means that the accuracy of the classical models can be improved. An in-depth analysis of these model is reported in Table 8.5, where classical and BTD models are reported with their relative error: it is intended to understand how to improve the accuracies of the classical models.

	$R_\beta/h = 100$			
	Pandya	M_e : 9/15 - 9T	CLT/FSDT	M_e : 5/15 - 5T
	▲ ▲ ▲ ▲ ▲ ▲ ▲ ▲ ▲ △ △ △	△ △ △ △ △ ▲ ▲ △ ▲ ▲ ▲ ▲ ▲ ▲ ▲	▲ ▲ ▲ ▲ ▲ △	△ △ △ △ △ ▲ ▲ △ ▲ △ ▲ ▲ △ △ △
Error	1.6074 %	3.9210×10^{-6} %	0.1465 %	0.1072 %
	$R_\beta/h = 4$			
	Pandya	M_e : 6/15 - 6T	CLT/FSDT	M_e : 5/15 - 5T
	▲ ▲ ▲ ▲ ▲ ▲ ▲ ▲ ▲ △ △ △	△ △ △ △ △ ▲ ▲ △ △ △ ▲ ▲ ▲ ▲ △	▲ ▲ ▲ ▲ ▲ △	△ △ △ △ △ ▲ ▲ △ △ △ ▲ △ ▲ ▲ △
Error	3.1428 %	0.6014 %	3.2831 %	1.3366 %

Table 8.5: Reduced model for an isotropic shell, ED4 models - genetic approach.

As an example, the accuracy of the Pandya model for the thin shell can be significantly improved by considering the fourth-order terms along the β and z directions, and neglecting all terms which belong to the α direction. It is interesting to note that in the case of the thick shell it is not possible to improve the Pandya model. The

BTD presents the 6-term model (see Figure 8.5): the 6-term model is able to provide a higher accuracy than the Pandya model, as reported in the Table 8.5. This means that in some cases classical models cannot be improved and better results can be obtained with reduced models with a lower number of terms than the classical models. The stress $\sigma_{\alpha\alpha}$ distribution along the thickness direction is reported in Figure 8.6: FSDT and Pandya models are considered.

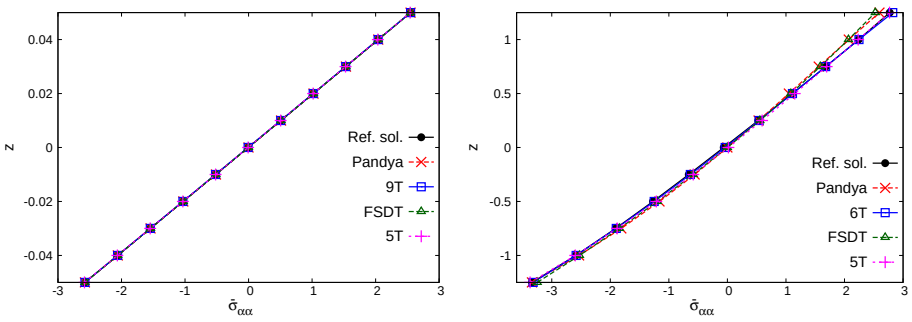

(a) $R_\beta/h = 100$. (b) $R_\beta/h = 4$.

Figure 8.6: Stress distribution for metallic shell, ED4 reduced models.

In the same Figure, the stress distribution is computed by means of the reduced refined models 9T, 6T and 5T reported in Table 8.5. The distribution computed with the BTD model is more accurate than the distribution computed by means of the classical models. In addition, it is possible to note in the case of thin shell all the models offer distributions that are in agreement with the reference solution. It is possible to affirm that in the case of a thin shell, for a given error interval more reduced models are available than in the thick shell case.

It should be noted that in general the displacement variables related with the α direction are in general excluded. The reason can be that the transverse load has no half-wave along α direction. The results of the analysis of the influence of the load shape on the selection of terms is reported in Figure 8.7: in this Figure the BTDs are obtained considering for the shell under examination two different transverse pressures whose parameters are $m = 0$, $n = 1$ and $m = 1$, $n = 1$.

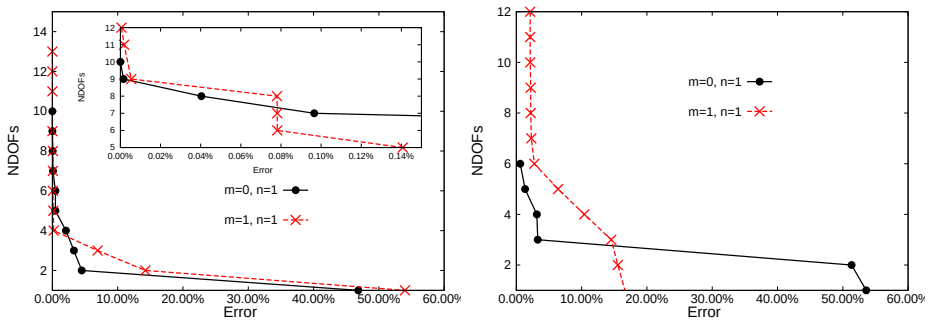

(a) $R_\beta/h = 100$. (b) $R_\beta/h = 4$.

Figure 8.7: BTD for metallic shell - ED4 model. Influence of the load shape.

It can be noted that the BTDs are affected to a great extent by the load distribution, in particular the BTDs for $m = 0$ and $n = 1$ has a steeper trend than the BTDs for $m = 1$ and $n = 1$. A detailed analysis of the influence of the load shape on the retained terms is reported in Table 8.6, where some models of the BTD of Figure 8.7 are reported. These models seem to assess this initial hypothesis, although the 6-term model for the thick shell case contradicts this conclusion.

	$m = 0,\ n = 1$	$m = 1,\ n = 1$
	$R_\beta/h = 100$	
M_e	6/15	6/15
	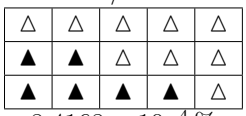	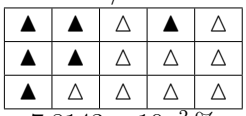
Error	$8.4168 \times 10^{-4}\,\%$	$7.8143 \times 10^{-2}\,\%$
	$R_\beta/h = 4$	
M_e	6/15	6/15
	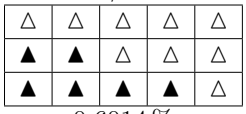	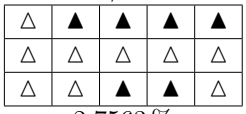
Error	0.6014 %	2.7563 %
M_e		12/15
		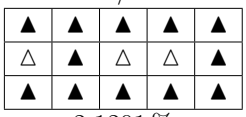
Error		2.1201 %

Table 8.6: Reduced model for an isotropic shell, ED4 models - load shape influence. L4 model as reference solution.

As a matter of fact, all terms of the β direction are excluded although n is not null. Anyway, the 12-term reduced model which belong to the BTD of Figure 8.7 ($m = n = 1$ case, thick geometry) reported in the same Table show that the terms of α, β and z direction are included. It is possible to affirm that, in general, the shape of the load influence the relevance of the terms of a refined model. In particular, in some cases the absence of the half-waves along a direction may lead to the exclusion of the terms related with that direction.

The curvature of the shell may affect the relevance of the terms, as reported in Figure 8.8. These BTDs are obtained considering the same geometry and the same material as the case reported in Table 8.4, but the curvature is variated according to the ratio R'_β/R_β, where R_β is the curvature of the case reported in Table 8.4 and R'_β is the curvature of the case considered.

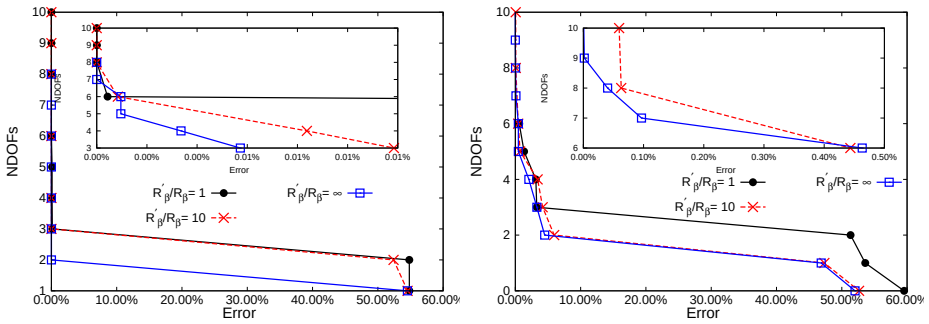

(a) Thin shell case. (b) Thick shell case.

Figure 8.8: BTD for metallic shell - ED4 model. Influence of radius R_β.

Two cases are considered (see Table 8.7): "thick shell case" corresponds to the $R_\beta/h = 4$ case reported in Table 8.4, and "thin shell case" corresponds to the $R_\beta/h = 100$ case reported in Table 8.4. The BTD reported in Figure 8.8 show that as the curvature tends to infinity (plate case), in general the BTD tends to lower error values. Some reduced models which belong to the BTD are reported in Table 8.7.

	$R'_\beta/R_\beta = 1$	$R'_\beta/R_\beta = 10$	$R'_\beta/R_\beta \to \infty$
	Thin shell case		
M_e	8/15	8/15	8/15
	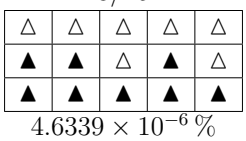	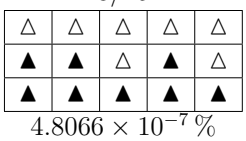	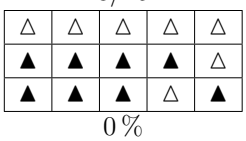
Error	$4.6339 \times 10^{-6}\,\%$	$4.8066 \times 10^{-7}\,\%$	$0\,\%$
	Thick shell case		
M_e	6/15	6/15	6/15
	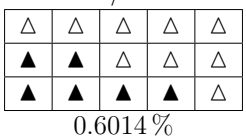	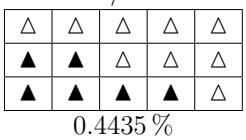	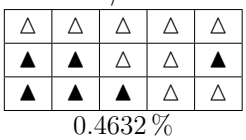
Error	$0.6014\,\%$	$0.4435\,\%$	$0.4632\,\%$
M_e	5/15	5/15	5/15
	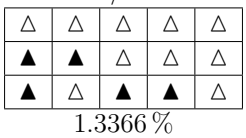	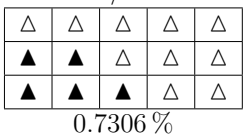	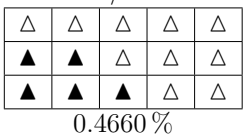
Error	$1.3366\,\%$	$0.7306\,\%$	$0.4660\,\%$

Table 8.7: Reduced model for an isotropic shell, ED4 models - radius influence. L4 model as reference solution.

The curvature affects the retained terms, although it is lower than the influence of the geometry (R_β/h) or shape of the load (m, n). As a matter of fact, the reduced models for the thin shell case do not show any difference when R'_β/R_β ratio is equal to 1 and 10. The same observation holds when a thick shell is considered (R'_β/R_β equal to 1 and 10). It can be noted that when $R'_\beta/R_\beta \to \infty$ the reduced model for the thin shell case is in total agreement with the reference solution. It is possible to say that for this particular case 7 terms in the ED4 model are not necessary. It is possible to note, as already underlined for the thin shell case, some reduced model are not affected by the variation of the curvature. The results demonstrated that:

1. the creation of the BTDs is affected to a great extent by the geometry of the shell (thick / thin shell, curvature), the material properties and by the quantity considered (displacement/stress component);

2. it is not always possible to construct reduced models for a given number-of-terms and error;

3. the curvature affects the creation of a BTD but not in the same intensity as the radius-to-thickness ratio;

4. another factor that influence the creation of a BTD is the shape of the load, i.e. the number of half-waves along the main direction; in particular, in some cases the absence of the half-waves along a direction may lead to the exclusion of the terms related with that direction;

5. the accuracies of some well-known models (CLT, FSDT and Pandya) is lower than the models reported in the BTDs, in particular for the thick shell geometry.

8.3 Best Theory Diagram for multifield plate analysis

Best Theory Diagrams (BTDs) for simply supported multilayered plate are reported in the following considering separately a pure transverse pressure distribution, a temperature distribution and the effect of an electric potential distribution. The mathematical expressions of these loads are reported in Equations 4.67, 4.69 and 4.70, respectively. The number of the half-waves m and n are equal to 1 and the pressure distribution is applied to the top surface of the plate. The BTDs for the thermal case are obtained by considering a temperature distribution defined as in the Equations 4.69 and 4.29. In the cases herein considered, the top and bottom temperatures (t_{top}, t_{bot}) are equal to 1 and -1, respectively. The BTDs for the piezoelectric case are defined by analyzing two different configurations: the sensor and actuator configurations. In the case of a sensor configuration, a transverse pressure is applied to the top surface of the plate and a potential distribution is evaluated. The potential at the top and at the bottom is set to zero. In the case of an actuator configuration, a potential distribution is applied to the plate and the value of the potential is set to 1 V at the top and to 0 V at the bottom. In the case of sensor distribution, the pressure is assumed as in Equation 4.67. The BTDs reported in this chapter are obtained for both ESL and LW schemes. The reference system layout and the representation of the two configurations are reported in Figure 4.5. In the following, $\overline{\Phi}$ is set equal to 1. The definition of a BTD is possible if a reference solution is available. The BTDs reported in this section are based on the solution computed by means of the LD4, since in the chapter 4.6 this model proved to be in excellent agreement with the analytical solutions of the open literature. The BTD reported in this work are related to a 4-layers plate. The top and bottom layers are made of PZT-4, whose properties were already introduced for the LD4 model assessment (chapter 4.6). The thermal expansion coefficients are $\alpha_1 = \alpha_2 = 3.8 \times 10^{-6}$ and $\alpha_3 = 1.7 \times 10^{-6}$. The second and third layers of the plate are made of the same elastic material considered during the assessment, the thermal expansion coefficients

are equal to $\alpha_1 = -1. \times 10^{-6}$, $\alpha_2 = \alpha_3 = 10. \times 10^{-6}$. All the four layers have the same thickness, and it is equal to to 1/4 of the total plate thickness. This particular plate configuration has been considered in order to create for the same plate, the BTDs for each multifield problem analyzed.

Firstly, few values of the stress and displacement components related to the plate considered are reported in Tables 8.8, 8.9, 8.10 and 8.11 for the mechanical, thermal and piezoelectric loads. The results are computed by means of the LD4 and ED4 models. It can be noted that in general the solutions offered by the LD4 and ED4 models are in good agreement when a thin plate is considered.

	$a/h = 100$		$a/h = 4$		$a/h = 100$		$a/h = 4$	
	LD4				ED4			
z	$\overline{u}_z$	$\overline{\sigma}_{xx}$	$\overline{u}_z$	$\overline{\sigma}_{xx}$	$\overline{u}_z$	$\overline{\sigma}_{xx}$	$\overline{u}_z$	$\overline{\sigma}_{xx}$
-0.5	0.3963	-0.2328	0.9744	-0.2881	0.3957	-0.2304	0.7917	-0.3116
-0.4	0.3963	-0.1888	0.9915	-0.1828	0.3957	-0.1895	0.8063	-0.1705
0.0	0.3964	-0.0017	1.0336	0.0100	0.3958	-0.0019	0.8481	-0.0398
0.4	0.3963	0.1629	1.0782	0.2080	0.3957	0.1635	0.8653	0.1964
0.5	0.3963	0.2069	1.0662	0.3230	0.3957	0.2043	0.8538	0.3408

Table 8.8: Mechanic static response of a square laminated plate.

	$a/h = 100$		$a/h = 4$		$a/h = 100$		$a/h = 4$	
	LD4				ED4			
z	$\overline{u}_z$	$\overline{\sigma}_{xx}$	$\overline{u}_z$	$\overline{\sigma}_{xx}$	$\overline{u}_z$	$\overline{\sigma}_{xx}$	$\overline{u}_z$	$\overline{\sigma}_{xx}$
-0.5	0.4927	136.0200	0.5636	133.5900	0.4894	130.6500	0.5426	132.5100
-0.4	0.4927	102.8600	0.5445	99.8270	0.4894	104.6700	0.5238	104.1500
0.0	0.4926	-4.0093	0.4742	-3.4198	0.4893	-4.0312	0.4814	-3.7648
0.4	0.4927	-162.5700	0.5445	-159.3700	0.4894	-158.1200	0.5238	-157.4100
0.5	0.4927	-195.7300	0.5636	-190.3900	0.4894	-183.7100	0.5426	-184.8000

Table 8.9: Thermal static response of a square laminated plate.

	$a/h = 100$		$a/h = 4$	
z	$\sigma_{xx} \times 10^4, [Pa]$	$\Phi, [V/m]$	$\sigma_{xx} \times 10^{-4}, [Pa]$	$\Phi, [V/m]$
	LD4			
-0.5	-0.24970	0.0000	-5.2226	0.00000
-0.4	-0.20186	3.0819	-3.2037	0.00646
0.0	-0.00147	6.4150	0.1701	0.00865
0.4	0.17977	3.0802	3.5513	0.00519
0.5	0.22761	0.0000	5.7604	0.00000
	ED4			
-0.5	-0.24934	0.0000	-5.4224	0.00000
-0.4	-0.20200	3.0830	-3.1613	0.00609
0.0	-0.00166	6.4088	0.0827	0.00953
0.4	0.17985	3.0821	3.2304	0.00538
0.5	0.22710	0.0000	4.6103	0.00000

Table 8.10: Piezo-mechanic static response of a square laminated plate, sensor configuration.

	$a/h = 100$		$a/h = 4$	
z	$\sigma_{xx}, [Pa]$	$\Phi, [V/m]$	$\sigma_{xx}, [Pa]$	$\Phi, [V/m]$
	LD4			
-0.5	-0.02659	0.00000	1.04780	0.00000
-0.4	-0.02736	0.00035	0.53439	-0.00091
0.0	0.00246	0.49993	-0.09214	0.45799
0.4	-0.02859	0.99961	-0.08477	0.97355
0.5	-0.02604	0.00000	1.33300	0.10000
	ED4			
-0.5	-0.03304	0.00000	2.06260	0.00000
-0.4	-0.02559	0.00034	1.05410	-0.00179
0.0	0.00013	0.49993	-0.20510	0.45939
0.4	-0.02780	0.99961	-0.01939	0.97425
0.5	-0.03504	0.10000	1.06870	1.00000

Table 8.11: Piezo-mechanic static response of a square laminated plate, actuator configuration.

8.3.1 BTDs for the ESL scheme

Once the reference solutions are introduced, it is possible to define the BTDs for the multifield plate analysis. ESL approach is considered, and the BTDs for the ED4 model are reported in Figures 8.9 and 8.10 for the thin and thick geometry, respectively.

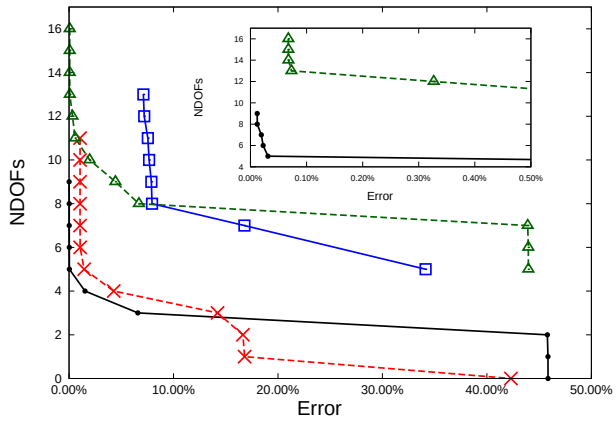

Figure 8.9: BTDs for ED4 model - mechanical, thermal and piezoelectric load cases, $a/h = 100$ - stress σ_{xx}.

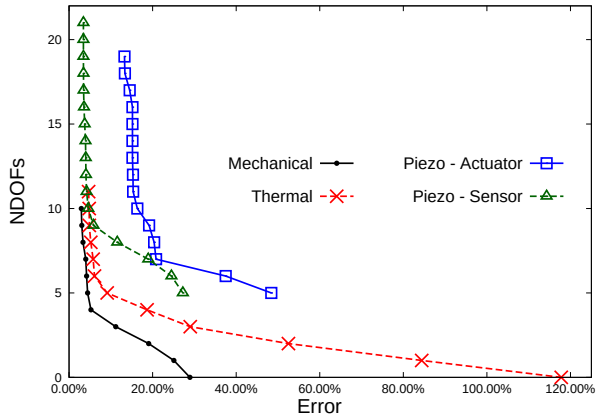

Figure 8.10: BTDs for ED4 model - mechanical, thermal and piezoelectric load cases, $a/h = 4$ - stress σ_{xx}.

These curves are defined considering the in-plane stress σ_{xx}. It can be noted that in general the reduced refined models for the piezoelectric case have a higher computational cost than the reduced models for the mechanical and thermal case, since the variables of the electric potential are retained. It can be noted that the BTDs for the thermal and mechanical case have the same accuracy when a thin plate is considered, and the BTDs for the piezoelectric case present a significant difference between the sensor and actuator configuration. The BTD for the sensor configuration have better accuracy than the BTD for the actuator configuration. This fact holds for the thick

and thin plate cases. It is possible to note that the BTD for the mechanical case offer the best accuracy. It is interesting to note that in the case of the thin plate geometry, the highest error is equal to 50% while in the case of thick plate geometry this value is equal to 120%.

The synthetic representation of some of the reduced models which belong to the BTDs of Figures 8.9 and 8.10, are reported in Table 8.12 for the thin plate case and in Table 8.13 for the thick plate case.

	Mechanical load		Thermal load
	$M_e = 9/15$		$M_e = 9/15$
			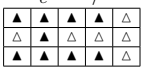
Error	1.0498 %		0.0120%
		Piezoelectric load	
	Sensor		Actuator
	$M_e = 10/32$		$M_e = 10/32$
			
Error	1.9703 %		7.6621 %

Table 8.12: Reduced ED4 model for laminated plate - Multifield cases, $a/h = 100$.

	Mechanical load		Thermal load
	$M_e = 10/15$		$M_e = 10/15$
			
Error	2.9268 %		4.8339%
		Piezoelectric load	
	Sensor		Actuator
	$M_e = 10/32$		$M_e = 10/32$
			
Error	4.5933 %		16.3465 %

Table 8.13: Reduced ED4 model for laminated plate - Multifield cases, $a/h = 4$.

It is possible to note that for a given number of terms and stress component, the retained variables are different as a different type of load is considered. It should be mentioned that the reduced refined models for BTDs related to the the mechanical and thermal case present common active displacement variables for the particular problem

considered (variables u_{x0}, u_{x1}, u_{x2}, u_{x3}, u_{x4}, u_{y1}, u_{z0}, u_{z1} and u_{z2} are present in all models), while the reduced refined models for the piezoelectric case are quite different from the previous cases. In addition, the reduced refined models for the piezoelectric case are different as the sensor or actuator configuration are employed. The stress σ_{xx} distribution is evaluated by means of the reduced models of the BTDs for the thick plate case, and the result is reported in Figure 8.11. It is possible to note that the solutions proposed are in good agreement with the reference solution.

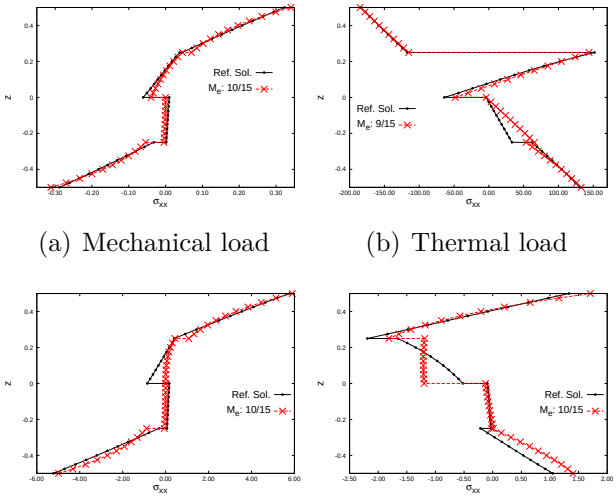

(a) Mechanical load (b) Thermal load

(c) Piezoelectric load - sensor (d) Piezoelectric load - actuator

Figure 8.11: Stress σ_{xx} distribution along the thickness. ED4 model, $a/h = 4$.

An in-depth analysis of the difference between the BTDs for the piezoelectric plate models for sensor and actuator configurations is carried out and the results are reported in Figure 8.12.

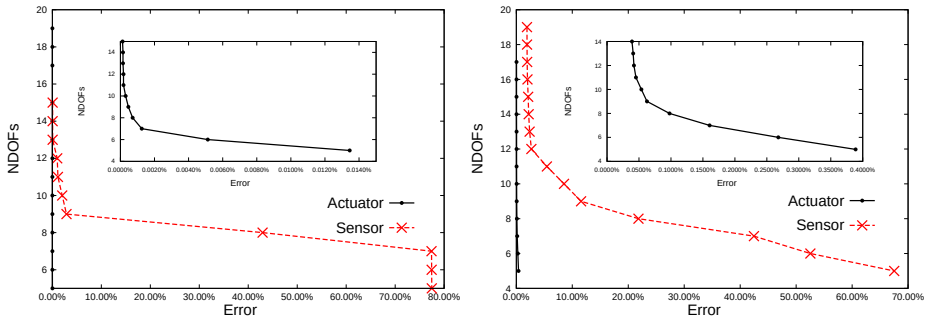

(a) $a/h = 100$ (b) $a/h = 4$

Figure 8.12: BTD for ED4 model - piezoelectric load case, Φ.

These BTDs are constructed considering the potential distribution Φ. The results show that the reduced models for the actuator configuration offer better accuracy than the reduced models for the sensor configuration. It should be mentioned the fact that the accuracy of the models for the BTDs related to the sensor configuration are very similar for both thin and thick plate geometry. On the contrary, the accuracy of the refined models related to the actuator plate configuration is higher in the case of the thin geometry than in the case of the thick geometry. The synthetic representation of the models are reported in Table 8.14 for the thin and thick plate case. The models reported in this Table have the same number of active terms (10/32).

	Sensor	Actuator
	$a/h = 100$	
	$M_e = 10/32$ 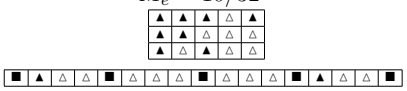	$M_e = 10/32$ 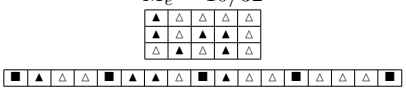
Error	$5.4769 \times 10^{-2}\,\%$	$1.2699 \times 10^{-4}\,\%$
	$a/h = 4$	
	$M_e = 10/32$ 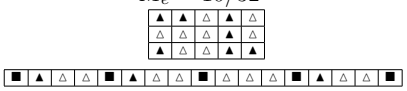	$M_e = 10/32$ 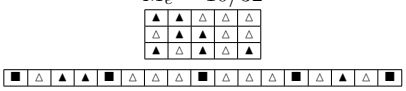
Error	$2.1203\,\%$	$15.1653\,\%$

Table 8.14: Reduced ED4 model for laminated plate - Piezoelectric plate case, potential Φ.

It can be noted that the configuration has a significant relevance in the selection of the relevant terms: all the models reported in Table have different activated terms.

The results show in addition that all the reported models include higher order terms for the displacement u_z. The potential distributions computed by means of the reduced model which belong to the BTDs just reported are depicted in Figures 8.13.

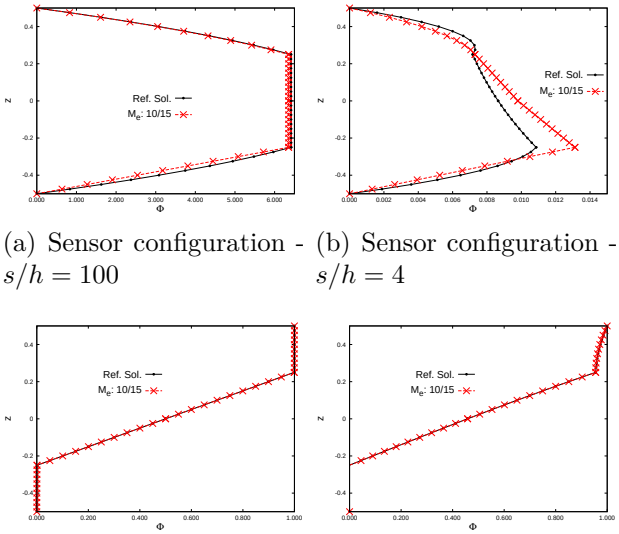

(a) Sensor configuration - $s/h = 100$

(b) Sensor configuration - $s/h = 4$

(c) Actuator configuration - $s/h = 100$

(d) Actuator configuration - $s/h = 4$

Figure 8.13: Potential Φ distribution along the thickness. ED4 model.

In general, the reduced models make it possible to computed solution that are in good agreement with the reference solution. In particular, it is possible to note that better accuracy are obtained for the actuator configuration. The results related to the ED4 models showed that

- the geometry and the type of load affect the process of selection of the terms;
- in general, the BTDs related to the mechanical load offer the better accuracy, while the lowest accuracy has been registered for the BTDs related to the piezoelectric plate case (actuator configuration);
- in some case, the reduced refined models for mechanical and thermal stress analysis have in common several displacement variables.

8.3.2 BTDs for the LW scheme

The definition of BTDs is performed also for LD4 models, and the results are reported in Figures 8.14 and 8.15 for the thin and thick plate, respectively. The stress σ_{xx} distribution is considered for the definition of these curves.

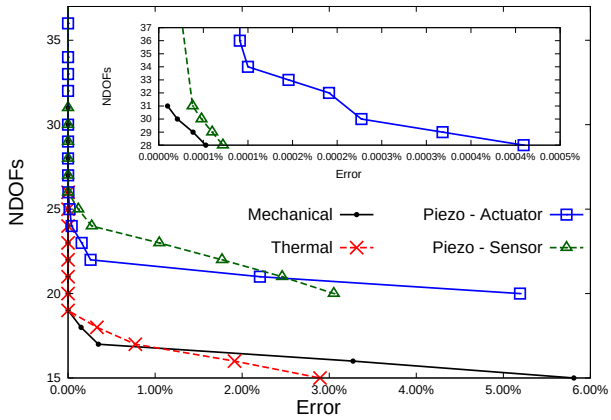

Figure 8.14: BTDs for LD4 model - mechanical, thermal and piezoelectric load cases, $a/h = 100$.

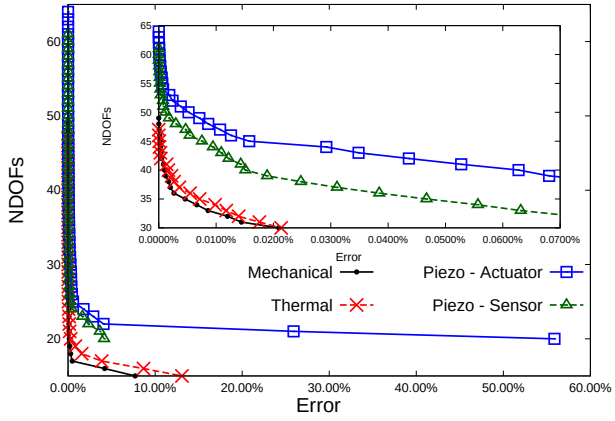

Figure 8.15: BTDs for LD4 model - mechanical, thermal and piezoelectric load cases, $a/h = 4$.

It is possible to note that the reduced models which belong to the BTDs for the mechanical and thermal load present around the same accuracy. The highest computational cost is registered for the BTDs related with the piezo electric plate case, since

the potential distribution variables are included in the model. In particular, it can be noted that in the case of the thick plate piezo electric plate, considering the actuator configuration, the highest error is equal to the 60%. In addition, it is possible to note that the BTD related with the mechanical case have more reduced models than the BTD related with the temperature distribution when a thin plate is considered. This difference can be noted also for the BTDs obtained for the piezo electric plate case, considering the thin and thick geometry.

The synthetic representation of the models of those BTDs are reported in Tables 8.15 and 8.16, respectively.

	Mechanical load	Thermal load
	$M_e = 25/51$	$M_e = 25/51$
		
Error	$1.1752 \times 10^{-4}\,\%$	$3.6136 \times 10^{-6}\,\%$
	Piezoelectric load	
	Sensor	Actuator
	$M_e = 25/68$	$M_e = 25/68$
	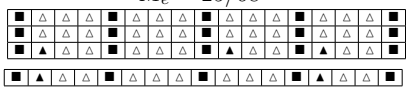	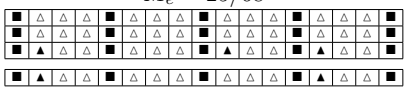
Error	$0.1173\,\%$	$1.7808 \times 10^{-2}\,\%$

Table 8.15: Reduced LD4 model for laminated plate - Multifield cases, $a/h = 100$.

	Mechanical load	Thermal load
	$M_e = 25/51$	$M_e = 25/51$
	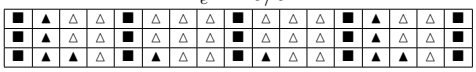	
Error	$7.6734 \times 10^{-2}\,\%$	$5.1093 \times 10^{-2}\,\%$
	Piezoelectric load	
	Sensor	Actuator
	$M_e = 25/68$	$M_e = 25/68$
	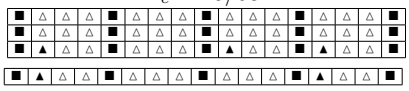	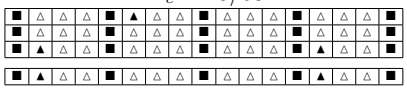
Error	$0.2847\,\%$	$0.5683\,\%$

Table 8.16: Reduced LD4 model for laminated plate - Multifield cases, $a/h = 4$.

It is interesting to note that in some case, the reduced refined model for the piezoelectric case have the same retained terms for both configurations, as reported for the

thin plate case. This fact is no longer valid when a thick plate is considered. It is possible to note that for the case herein considered, the reduced refined models which belong to the BTD for the mechanical and thermal load are different. The results reported in both tables show that the accuracy of the models related with the mechanical and thermal load is higher than the accuracy of the models related with the piezoelectric case for the same number of active terms (25). The stress distribution for the the reduced models reported in Table 8.16 are depicted in Figure 8.16. It is possible to note that the reduced models makes it possible to compute the stress distribution in good agreement with the reference solution.

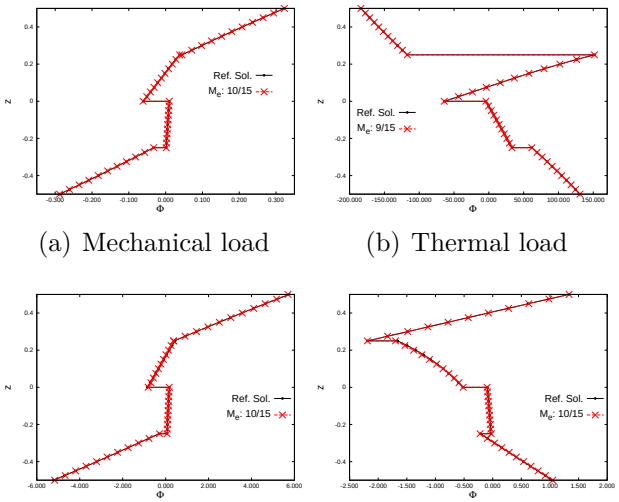

(a) Mechanical load (b) Thermal load

(c) Piezoelectric load - sensor (d) Piezoelectric load - actuator

Figure 8.16: Stress σ_{xx} distribution along the thickness. LD4 model, $a/h = 4$.

The influence on the selection of terms for the electric potential Φ analysis of the piezoelectric plate configuration is analyzed. The results are depicted in Figure 8.17.

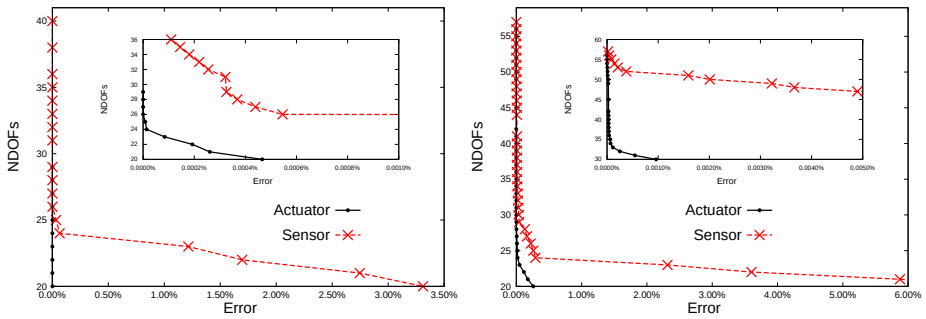

(a) $a/h = 100$ (b) $a/h = 4$

Figure 8.17: BTD for LD4 model - piezoelectric load case, Φ.

As already noted for the ED4 model, the accuracy offered by the reduced model for the actuator configuration is higher than the accuracy offered by the reduced model for the sensor actuator. Anyway, the lowest accuracy is obtained for the thick plate case for the sensor configuration and it is equal to the 6%. The related synthetic representations of some models which belong to these BTDs are reported in Table 8.17.

	Sensor	Actuator
	$a/h = 100$	
	$M_e = 29/68$	$M_e = 29/68$
	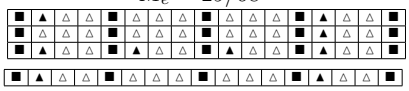	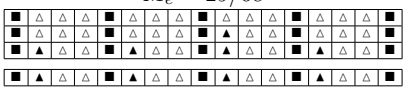
Error	$3.2581 \times 10^{-4}\,\%$	$2.2727 \times 10^{-9}\,\%$
	$a/h = 4$	
	$M_e = 30/68$	$M_e = 30/68$
	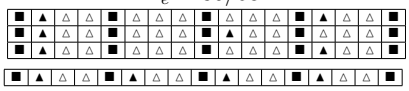	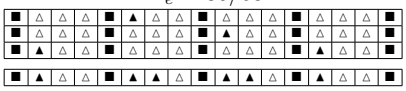
Error	$3.7704 \times 10^{-2}\,\%$	$9.5918 \times 10^{-4}\,\%$

Table 8.17: Reduced LD4 model for laminated plate - Piezoelectric load, Φ.

The models reported in that Table show that the type of configuration influence to a great extent the selection of the terms. In addition, it is possible to note that high accuracy in the potential distribution analysis can be achieved by employing only second order terms, as reported for the thin actuator plate case (error equal to

2.2727×10^{-9} %). The potential distributions computed with these reduced models are depicted in Figure 8.18.

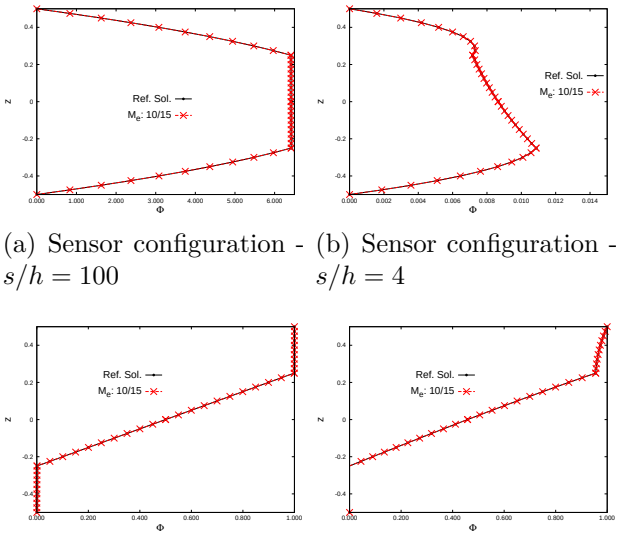

(a) Sensor configuration - $s/h = 100$

(b) Sensor configuration - $s/h = 4$

(c) Actuator configuration - $s/h = 100$

(d) Actuator configuration - $s/h = 4$

Figure 8.18: Potential Φ distribution along the thickness for LD4 model.

It is possible to note that the accuracy of these models is particularly good. Differently from the ED4 models case, the potential distribution computed for the thick and thin plate in the sensor configuration, present a better agreement with the reference solution than in the case of the ED4 models. The BTDs reported in this section for the multifield case related to multilayered plate showed that

1. the type of load and the geometry influence to a great extent the selection of the relevant terms for both LW and ESL approaches; in addition, the type of load influence the number of the models for a given problem;

2. the accuracy of the LW models related to the mechanical and thermal loads cases are very similar;

3. the accuracy of the models related to the piezoelectric case are influenced by the type of the configuration considered (actuator or sensor); in general, the models related to the actuator configuration are more accurate than the models for the sensor configuration;

4. in some case, a reduced model can be employed to analyze both sensor and actuator configuration but with different accuracy.

8.4 Best Theory Diagram for refined and mixed plate models

Best Theory Diagram, are reported in this section for multilayered plate models based on PVD and RMVT variational statement. In all cases the acting load is a transverse pressure applied to the top surface of a plate, and their load is defined as in Equation 4.67. In the following analyses it is $m = n = 1$. The reference system layout is reported in Fig. 2.4. All the reduced models are developed for stress components σ_{xx} and σ_{xz}, which are computed at [a/2, b/2, z] with $-\frac{h}{2} \leq z \leq \frac{h}{2}$, where h is the total thickness of the plate. The reference solutions for the definition of the BTDs curves is computed by means of the LM4 model since the solutions computed by means of this model are in excellent agreement with the analytical solutions reported in the literature as reported in the chapter 4.6.

Firstly, some reference values employed in the term relevance analysis are reported in Table 8.18. As already noted for the bimetallic plate, the LW models offer solution that are in agreement with each other. The solution offered by the ESL models differ from each other, but the solution offered by the EM4 is closer to the reference solution than the solution offered by the ED4 model.

	$\overline{\sigma}_{xx}(z = \pm h/2)$		$\overline{\sigma}_{xz}(z = 0)$
	$a/h = 100$		
LM4	± 0.539		0.395
LD4	± 0.539		0.395
EM4	± 0.539		0.301
ED4	± 0.539		0.281
	$a/h = 4$		
LM4	0.801	-0.755	0.256
LD4	0.801	-0.755	0.256
EM4	0.791	-0.745	0.219
ED4	0.786	-0.740	0.205

Table 8.18: Stresses and displacement for a 3-layers simply supported laminated plates.

The BTDs for the ESL models are reported in Figures 8.19 and 8.20 for both thin and thick plate geometry, respectively.

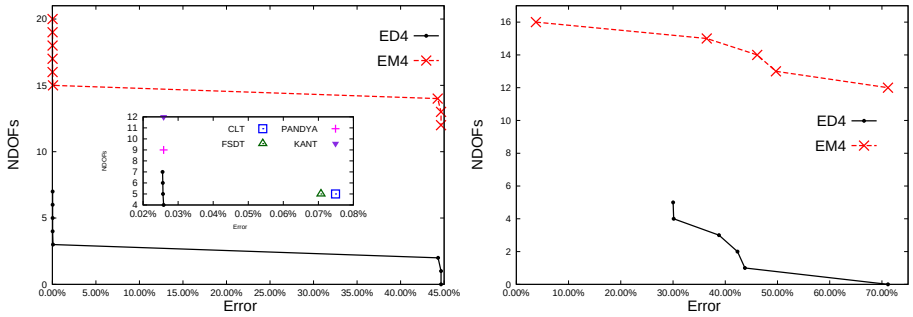

(a) σ_{xx} (b) σ_{xz}

Figure 8.19: BTD for the symmetric laminated layers plate, $a/h = 100$. ESL scheme, stress σ_{xz} and σ_{xx}.

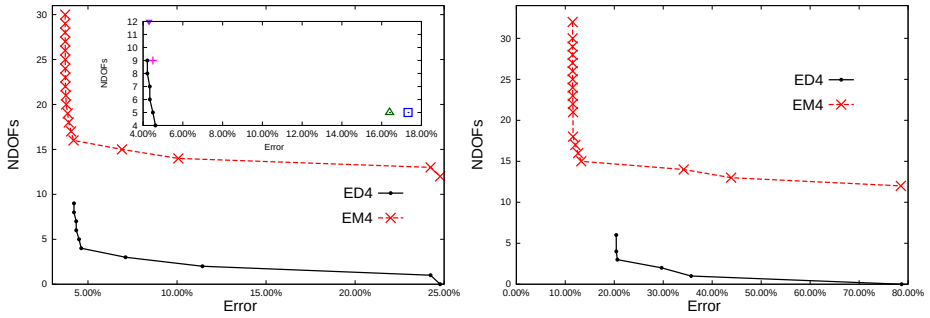

(a) σ_{xx} (b) σ_{xz}

Figure 8.20: BTD for the symmetric laminated layers plate, $a/h = 4$. ESL scheme, stress σ_{xz} and σ_{xx}.

Both variational statement have been considered and in-plane σ_{xx} and out-of-plane σ_{xz} stresses have been considered. It is possible to note that the accuracy of the models which belong to the BTD for the in-plane stress are similar for both ED4 and EM4 models, although the computational cost is higher for the EM4 reduced models than for the ED4 reduced models. It is possible to note that better accuracy for the σ_{xz} stress analysis can be obtained by means of the reduced EM4 models. Figures 8.20 8.19 and show that it is possible to define a transition error point. This point divides the Cartesian plane on which the BTD belongs to into two regions: one where, for a given accuracy, the PVD based models are advantageous and one where, for a given accuracy, RMVT based models are advantageous. This point corresponds to the highest accuracy

achieved by the PVD based models and its value changes with the stress components considered and the geometry: in Figure 8.19, this point corresponds to the 7- and 5-terms models for stresses σ_{xx} and σ_{xz}, respectively, while in Figure 8.20, this point corresponds to the 9- and 6-terms models for stresses σ_{xx} and σ_{xz}, respectively. The synthetic representations of the models which are in the neighborhood of this point are reported in Table 8.19.

	σ_{xx}		σ_{xz}	
	EM4	ED4	EM4	ED4
	$a/h = 100$			
M_e	16/54	7/15	16/54	5/15
	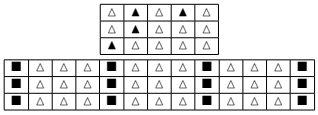		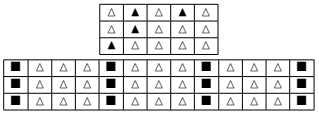	
Error	$1.9947 \times 10^{-2}\%$	$2.5555 \times 10^{-2}\%$	3.7482%	30.0212%
	$a/h = 4$			
M_e	16/54	9/15	16/54	6/15
	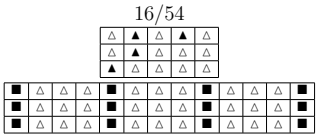		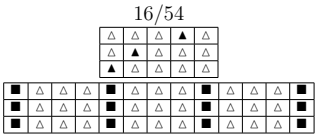	
Error	4.1879%	4.2142%	13.2624%	20.4033%

Table 8.19: Reduced EM4 and ED4 models for symmetric laminated plate.

It is possible to note that the order of the displacement variables retained is different as PVD or RMVT statement is employed. In addition, it can be noted that any stress variable is retained except the top and bottom stress variables. It is possible to conclude that the accuracy of an ED4 can be increased by considering a linear stress distribution along the thickness direction. Higher accuracy can be achieved considering higher stress variables order. In addition, in Figure 8.21 the stress σ_{xz} distribution along the thickness is computed by means of the reduced models reported in the previous Table. As already note for the isotropic plate, better accuracy is obtained when EM4 model is considered. In particular, the reduced EM4 model offers the best accuracy when a thin plate is considered.

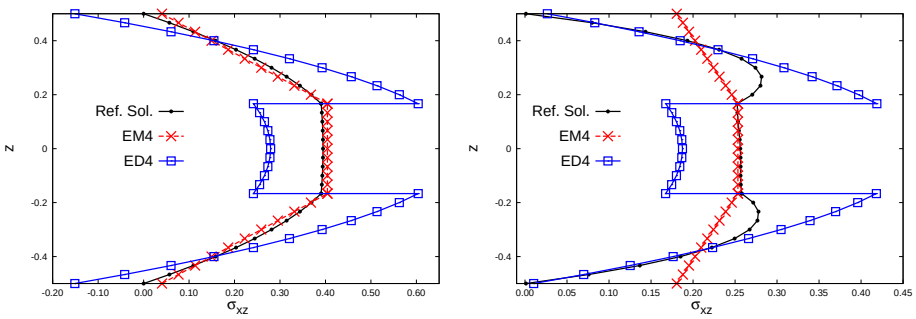

(a) $a/h = 100$ (b) $a/h = 4$

Figure 8.21: Stress σ_{xz} and distribution along the thickness - symmetric laminated plate, ESL scheme.

The accuracies of the classical models are reported in the same Figures for the BTDs obtained for the stress σ_{xx}: it is possible to note that in general the accuracy of these models can be improved. This fact is underlined in Table 8.20, where the synthetic representations the models which belong to the BTD are reported.

	$a/h = 100$		$a/h = 4$	
	Kant	$M_e : 7/15$	Kant	$M_e : 9/15$
Error	$2.5866 \times 10^{-2}\,\%$	$2.5555 \times 10^{-2}\,\%$	$4.3015\,\%$	$4.2142\,\%$
	Pandya	$M_e : 7/15$	Pandya	$M_e : 9/15$
Error	$2.5859 \times 10^{-2}\,\%$	$2.5555 \times 10^{-2}\,\%$	$4.4958\,\%$	$4.2142\,\%$
	FSDT	$M_e : 5/15$	FSDT	$M_e : 5/15$
Error	$7.0737 \times 10^{-2}\,\%$	$2.5682 \times 10^{-2}\,\%$	$16.3979\,\%$	$4.4952\,\%$

Table 8.20: Reduced models for symmetric laminated plate - stress σ_{xx}.

The results reported in the Table show that in some case better accuracy can be achieved by employing refined models with a lower number of terms than the classical models. This is the case of the Kant model for the thin plate case. In addition, those model show that the accuracy of a model can be improved by considering higher order

terms in lieu of the constant/linear term, this is the case of the FSDT model for the thin and thick plate.

The BTDs for the LW scheme are obtained considering thin and thick plate for both variational statements. The results are reported in Figures 8.22 and 8.23.

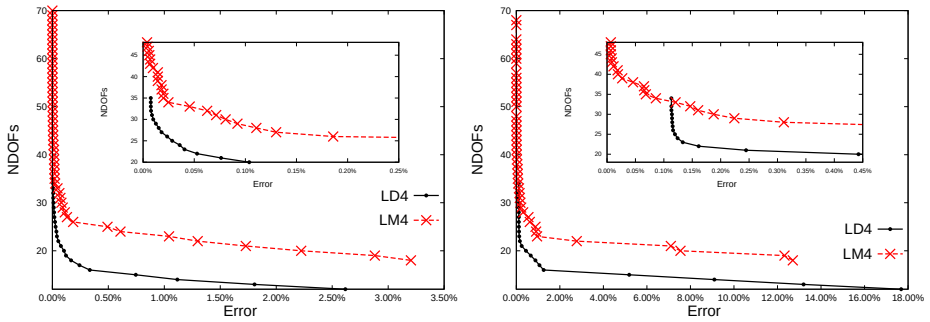

(a) σ_{xx} (b) σ_{xz}

Figure 8.22: BTD for the symmetric laminated plate, $a/h = 100$. LW scheme, stress σ_{xz} and σ_{xx}.

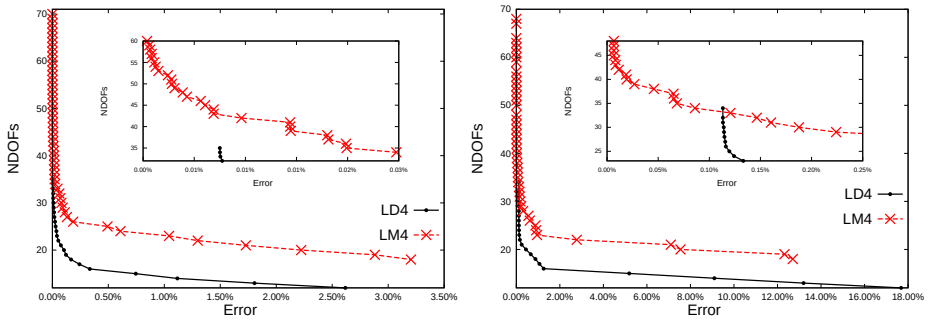

(a) σ_{xx} (b) σ_{xz}

Figure 8.23: BTD for the symmetric laminated plate, $a/h = 4$. LW scheme, stress σ_{xz} and σ_{xx}.

As already noted for the ESL models and for the LW models for the bimetallic plate case, it is possible to note that the transition error point exist: this point is different for the BTDs for stress σ_{xx} and σ_{xz}. The position of this point seems not to be influenced by the geometry in the case of stress σ_{xz}. On the contrary, the BTDs for stress σ_{xx} show

that the position of the transition point is influenced by the geometry. The synthetic representations of the models which are in the neighborhood of the transition point are reported in Table 8.21.

	LM4	LD4
	$a/h = 100$	
M_e	48/78	29/39
	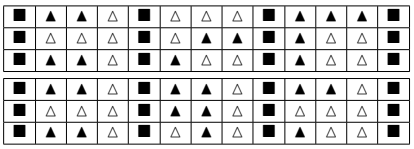	
Error	$5.6194 \times 10^{-9}\%$	$5.6194 \times 10^{-9}\%$
	$a/h = 4$	
M_e	65/78	35/39
	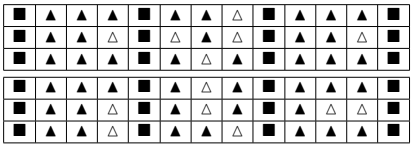	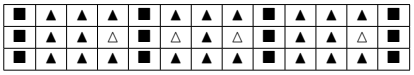
Error	$6.0806 \times 10^{-4}\%$	$7.4997 \times 10^{-3}\%$
	σ_{xz}	
	LM4	LD4
	$a/h = 100$	
M_e	39/78	28/39
	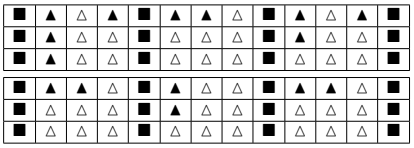	
Error	$2.4478 \times 10^{-5}\%$	$8.1782 \times 10^{-5}\%$
	$a/h = 4$	
M_e	40/78	34/39
	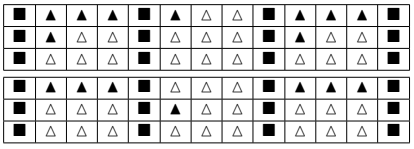	
Error	$8.5945 \times 10^{-3}\%$	0.1132%

Table 8.21: Reduced LM4 and LD4 models for symmetric laminated plate.

In general, it is possible to note that the displacement variables retained in the

reduced LM4 and LD4 models are different. In addition, the number and the order of the retained stress and displacement variables are different for a given reduced LM4 model. The reduced LW model reported in Table 8.21 are employed to analyze the stress σ_{xz} distribution along the thickness, for both thin and thick plate case. The results are reported in Figure 8.24. It is possible to note that solution offered by these models are in excellent agreement with the reference solution.

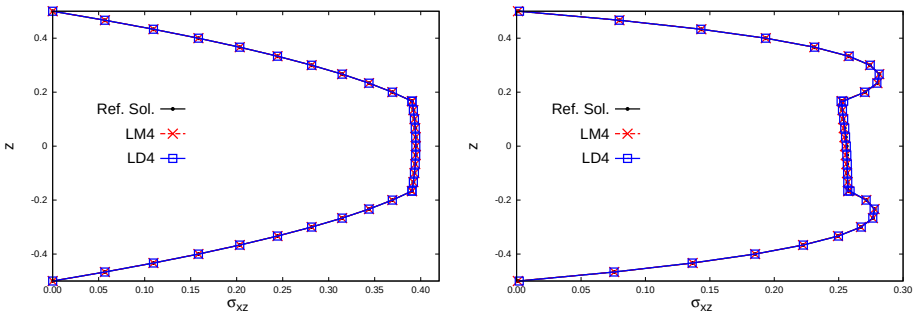

(a) $a/h = 100$ (b) $a/h = 4$

Figure 8.24: Stress σ_{xz} and distribution along the thickness - symmetric laminated plate, LW scheme.

The BTDs reported in this section for the refined and mixed models showed that

1. the geometry and the type of material influences the definition of the BTDs;
2. the displacement variables retained in the ED4/LD4 models are different from the displacement variables of the EM4/LM4 models in terms of order for a given accuracy; in addition, the order of the stress variables is different from the order of the displacement variables for an EM4/LM4 model;
3. for all cases it is possible to define a transition error point: refined models based on PVD can be employed for plate analysis in lieu of mixed models based on RMVT statement; lower error can be obtained if mixed models are employed; the position of this point is influenced by the geometry and the material properties.

8.5 Conclusions

Best Theory Diagrams for plates and shells were reported in this chapter. These curves were obtained by means of the axiomatic/asymptotic technique: differently from the

chapter 6, the reduced refined models were obtained by considering the accuracy of an entire sequence of active/non-active model terms. A genetic algorithm was employed to generate and evaluate these combinations. In the case of plates, the multifield problem was considered: BTDs are reported for the same type of plate but considering a pressure distribution, a temperature distribution and an electric potential distribution. The best models were reported for ESL and LW schemes. The governing equations for the above mentioned problems were obtained by means of the CUF, which makes it possible to defined the equilibrium equations in terms of few fundamental nuclei whose form does not depend on the particular expansion order employed. Analytical solution (Navier-type) was employed: the use of such solution made it possible in some cases to present the accuracy of all possible term combination and to assess the genetic algorithm. The influence on the terms selection was analyzed considering several geometries (length-to-thickness ratio, a/h) and material properties. The following conclusions may be drawn:

1. for a given model, plate/shell geometry and material configuration it is possible to identify a number of reduced models which present the lowest possible error; in other words for a given problem and terms expansion it is possible to define a Pareto front, which in this work was defined as Best Theory Diagram; in addition, the curvature of a shell affects the creation of a BTD but not in the same intensity as the radius-to-thickness ratio;

2. for a given plate problem as a/h parameter varies, the reduced models on the BTD curve may present some common retained terms; in addition it is proven that for a given problem and for a given number of active terms as the error changes the terms arrangement changes;

3. the axiomatic/asymptotic technique conducted by means of the genetic algorithm is able to detect all or almost reduced models which belong to the BTD;

4. in the case of ED4 models, it was discovered that it is not always possible to construct a reduced model for a given error and terms number interval;

5. classical and refined models reported in the literature are accurate, although according to the data reported in the BTD higher accuracies can be achieved;

6. the reduced models which belong to the BTD are different for a given problem and for a given number of terms;

7. in some cases, some models for a given geometry can be employed to evaluate both displacement or stress component but with different accuracy.

8. the type of load and the geometry influence to a great extent the selection of the relevant terms for both LW and ESL approaches; in addition, the type of load influence the number of the models for a given problem;

9. the accuracy of the LW models related to the mechanical and thermal loads cases are very similar;

10. the accuracy of the models related to the piezoelectric case are influenced by the type of the configuration considered (actuator or sensor); in general, the models related to the actuator configuration are more accurate than the models for the sensor configuration; in some case, a reduced model can be employed to analyze both sensor and actuator configuration but with different accuracy;

11. the displacement variables retained in the ED4/LD4 models are different from the displacement variables of the EM4/LM4 models in terms of order for a given accuracy; in addition, the order of the stress variables is different from the order of the displacement variables for an EM4/LM4 model;

12. in the case of the BTDs related to refined and advanced plate models it is possible to define a transition error point: refined models based on PVD can be employed for plate analysis in lieu of advanced models based on RMVT statement; lower error can be obtained if advanced models are employed; the position of this point is influenced by the geometry and the material properties.

Part IV

Conclusions

Chapter 9

Conclusions

An extensive analysis of refined models for plates and shells has been reported in this thesis. The purpose of the work described in this thesis is to decrease the computational cost of refined plate/shell models without loosing accuracy in the plate/shell response analysis. The axiomatic/asymptotic technique has been employed for this purpose. The refined models have been obtained by means of the Carrera Unified Formulation and both the Principle of Virtual Displacement (PVD) and the Reissner Mixed Variational Theorem (RMVT) have been employed to derive the governing equations. Navier-like closed form solutions has been employed, and for this reason simply supported isotropic and orthotropic plates and shells has been considered. The refined models analyzed have been implemented according to the schemes known as Equivalent Single Layer and Layer Wise. In some case, the accuracy of the reduced refined models have been compared to the refined models available in the open scientific literature.

A detailed description of the axiomatic/asymptotic technique is reported in chapter 5. The methodology employed to measure the relevance of all terms is reported and all criteria employed to measure the error are described. The results for the axiomatic/asymptotic analyses are reported in chapter 6, where plates and shells models are considered. It has been demonstrated that the term selection process is affected to a great extent by the problem considered: the load shape, the geometry and the material properties are all important parameters. In addition, the effect of the error computation has been analyzed by means of several criteria defined as C3, C4 and C5. These criteria are defined in the same chapter. It has been proved that an improvement of the stress/displacement distribution computation can be obtained if a proper criterium is used. In the same chapter, multifiled problems have been considered: reduced models for plates are reported considering a transverse pressure distribution,

a temperature distribution and a electric potential distribution. It has been demonstrated that, as for the previous cases, geometry configuration and material properties play an important role in the term selections. In addition, the type of load influences the process of term selection: the reduced models present some differences in terms of order and number of variables involved. This difference can be relevant if thick plates are considered. As last analyses, reduced ESL and LW models based on the RMVT variational principle have been reported for a bimetallic plate. The results have shown that reduced ESL models based on RMVT and PVD have the same active displacement variables. In particular, it has been demonstrated that in some cases the deactivation of all variables which seem to not contribute to the plate analysis does not lead to an accurate evaluation of the plate response. In general, the results have shown that it is difficult to define a-priori the relevance of a term of a model for a specific problem.

In this work, Best Theory Diagrams for plates and shells have been reported. These curves represents in a synthetic manner the relation between the number of terms and the error committed by the reduced models. In chapter 7 the algorithm employed to obtain these curves is described. A genetic algorithm has been employed in order to discover the combination that can offer the lowest possible error for a given number of terms. This kind of approach has been inspired by Darwin's observations he made in "The Origin of Species": an individual is subjected to a process of natural selection, which permits the survival of the individuals which fit the best to their environment. In this case a plate/shell theory has been considered as an individual and its performances have been evaluated with respect a reference solution. The use of Navier-like closed form solution has made it possible to assess the genetic algorithm in use since, in this case, it is possible to evaluate a large number of combinations in a reasonable time. In addition, the genetic analysis of refined models have required a low computational time. The BTDs have been reported for plate and shell mechanical stress analysis, and for multifield problems related to multilayered plate. In addition, BTDs for refined/advance plate models (i.e. models based on the PVD and RMVT variational statements) have been considered.

In chapter 8, the Best Theory Diagrams (BTDs) have been reported for multilayered plates and shells, and for multifield problems related to plates. In addition, BTDs have been reported for models developed according to the PVD and RMVT variational statements. The accuracy of the reduced refined models has been compared with the results offered by some refined models available in the open scientific literature. The results showed that in most cases the response of these classical models can be improved either by considering a lower number of terms or by considering different order terms in the expansion. BTDs for shell models have been considered, and the role of the curvature has been discussed and different BTDs have been reported considering

different parameters. It has been proved that for a given geometrical, material and load parameters the presence of a curvature makes to consider different terms than a plate configuration; in addition, the radius length has no effect on the retained terms. A remarkable results has been obtained when considering the accuracy of all possible active/non-active term combinations for ESL scheme (plate and shell case): it is not always possible to define a reduced model for a given accuracy interval and number of terms. Multifield refined models have been investigated by means of the genetic algorithm and BTD have been reported. The results related to the multifield plate analysis demonstrated that the type of load and the geometry influence to a great extent the definition of a BTD for both LW and ESL approaches. It was noted that the accuracy of the LW models related to the mechanical and thermal loads cases are very similar. Moreover, the analysis of refined model plate for the piezoelectric analysis showed that the accuracy of these models is influenced by the type of the configuration considered (actuator or sensor). BTDs for refined theories have been also reported: it was intended to point out the differences between BTDs based on PVD and on RMVT for multilayered plate analysis. It has been noted that, in general, the displacement variables retained in the ED4/LD4 models are different from the displacement variables of the EM4/LM4 models in terms of order for a given accuracy. In addition, for all cases it is possible to define a transition error point. This point divides the Cartesian plane on which the BTD belongs to into two regions: one where, for a given accuracy, the PVD based models are advantageous and one where, for a given accuracy, RMVT based models are advantageous. This point corresponds to the highest accuracy achieved by the PVD based models and its value changes with the stress components considered and the geometry.

All analyses pointed out that the relevance of a term or the best model for a given problem cannot be determined a-priori. In this work the axiomatic/asymptotic technique proved to be a valuable means in order to define the best plate/shell theory for a given case. An extension of the present work can consider different boundary conditions. In addition, these works can be used to implement a neuronal network able to learn how to define the best model for a given problem, offering the possibility to achieve a good accuracy with respect to the 3D analytical solutions but with a lower computational cost than the refined full models.

Part V

Appendices

Chapter 10

Appendix 1: equilibrium equations for refined plate model

The equilibrium equations for a plate obtained by considering a refined plate models are reported in this Appendix. The introduction of additional terms in a plate displacement field can improve its analysis. A non-classical displacement field can be defined as:

$$\begin{aligned} u_x(x,y,z) &= u_{x0}(x,y) + z u_{x1}(x,y) \\ u_y(x,y,z) &= u_{y0}(x,y) + z u_{y1}(x,y) \\ u_z(x,y,z) &= u_{z0}(x,y) + z u_{z1}(x,y) \end{aligned} \tag{10.1}$$

In this case, the strain-displacement relation can be defined synthetically as

$$\begin{aligned} \epsilon_{xx} &= \epsilon^0_{xx} + z\epsilon^1_{xx} & \epsilon_{yy} &= \epsilon^0_{yy} + z\epsilon^1_{yy} & \gamma_{xy} &= \gamma^0_{xy} + z\gamma^1_{xy} \\ \gamma_{yz} &= \gamma^0_{yz} + z\gamma^1_{yz} & \gamma_{xz} &= \gamma^0_{xz} + z\gamma^1_{xz} & \epsilon_{zz} &= \epsilon^1_{zz} \end{aligned} \tag{10.2}$$

where

$$\begin{aligned} \epsilon^0_{xx} &= u_{x0,x} & \epsilon^1_{xx} &= u_{x1,x} \\ \epsilon^0_{yy} &= u_{y0,y} & \epsilon^1_{yy} &= u_{y1,y} \\ \gamma^0_{xy} &= u_{x0,y} + u_{y0,x} & \gamma^1_{xy} &= u_{x1,y} + u_{y1,x} \\ \gamma^0_{yz} &= u_{z0,y} + u_{y1} & \gamma^1_{yz} &= u_{z1,y} \\ \gamma^0_{xz} &= u_{z0,x} + u_{x1} & \gamma^1_{xz} &= u_{z1,x} \\ \epsilon^0_{zz} &= u_{z1} & \epsilon^1_{zz} &= 0 \end{aligned} \tag{10.3}$$

In the following it is convenient to group the stress and strain quantities into two distinct sets, that is *in-plane*, denoted as p, and the *out-of-plane* quantities, denoted as n. In this case it is

$$\begin{aligned}\boldsymbol{\epsilon}_p &= \{\epsilon_{xx} \quad \epsilon_{yy} \quad \gamma_{xy}\} \quad \boldsymbol{\sigma}_p = \{\sigma_{xx} \quad \sigma_{yy} \quad \gamma_{xy}\} \\ \boldsymbol{\epsilon}_n &= \{\epsilon_{xz} \quad \epsilon_{yz} \quad \gamma_{zz}\} \quad \boldsymbol{\sigma}_n = \{\sigma_{xz} \quad \sigma_{yz} \quad \gamma_{zz}\}\end{aligned} \tag{10.4}$$

The in-plane and out-of-plane quantities are referred to the surface Ω depicted in Figure 2.4. Considering a generic k layer of a multilyaered plate Hooke's law defines the stress-strain relation, othotropic materials are considered:

$$\boldsymbol{\sigma}^k_{pp} = \mathbf{C}^k_{pp}\boldsymbol{\epsilon}_p + \mathbf{C}^k_{pn}\boldsymbol{\epsilon}_n \tag{10.5}$$
$$\boldsymbol{\sigma}^k_{nn} = \mathbf{C}^k_{pn}\boldsymbol{\epsilon}_p + \mathbf{C}^k_{nn}\boldsymbol{\epsilon}_n \tag{10.6}$$
$$\tag{10.7}$$

that is

$$\begin{aligned}\left\{\begin{array}{c}\sigma^k_{xx}\\ \sigma^k_{yy}\\ \sigma^k_{xy}\end{array}\right\} &= \left[\begin{array}{ccc}C^k_{11} & C^k_{12} & C^k_{16}\\ C^k_{21} & C^k_{22} & C^k_{26}\\ C^k_{16} & C^k_{26} & C^k_{66}\end{array}\right]\cdot\left\{\begin{array}{c}\epsilon_{xx}\\ \epsilon_{yy}\\ \gamma_{xy}\end{array}\right\} + \left[\begin{array}{ccc}0 & 0 & C^k_{13}\\ 0 & 0 & C^k_{23}\\ 0 & 0 & C^k_{36}\end{array}\right]\cdot\left\{\begin{array}{c}\gamma_{xx}\\ \gamma_{yz}\\ \epsilon_{zz}\end{array}\right\} \\ \left\{\begin{array}{c}\sigma^k_{xz}\\ \sigma^k_{yz}\\ \sigma^k_{zz}\end{array}\right\} &= \left[\begin{array}{ccc}0 & 0 & 0\\ 0 & 0 & 0\\ C^k_{13} & C^k_{23} & C^k_{36}\end{array}\right]\cdot\left\{\begin{array}{c}\epsilon_{xx}\\ \epsilon_{yy}\\ \gamma_{xy}\end{array}\right\} + \left[\begin{array}{ccc}C^k_{55} & C^k_{45} & 0\\ C^k_{44} & C^k_{44} & 0\\ 0 & 0 & C^k_{33}\end{array}\right]\cdot\left\{\begin{array}{c}\gamma_{xx}\\ \gamma_{yz}\\ \epsilon_{zz}\end{array}\right\}\end{aligned} \tag{10.8}$$

10.1 Governing equations

The governing equations for a plate are obtained by means of the Principle of the Virtual Displacement (PVD) which states

$$\delta L_{int} = \delta L_{ext} \tag{10.9}$$

that is

$$\sum_{k=1}^{N_L}\int_{\Omega_k}\int_{A_k}\left(\delta\boldsymbol{\epsilon}_p^T\boldsymbol{\sigma}^k_p + \delta\boldsymbol{\epsilon}_n^T\boldsymbol{\sigma}^k_n\right)dV = \sum_{k=1}^{N_L}\delta L^k_{ext} \tag{10.10}$$

N_L is the number of the layers of the plate under exam. Transverse plate section is denoted as A_k. The virtual variation of the external applied loadings is written as

$\sum_{k=1}^{N_L} \delta L_{ext}$ and the virtual variation of the internal strain energy is denoted as δL_{int}. Upper script T denotes the transposition operation. Considering each component of stress and strain it is possible to write:

$$\sum_{k=1}^{N_L} \int_{\Omega_k} \int_{A_k} \left(\delta\epsilon_{xx}\sigma^k_{xx} + \delta\epsilon_{yy}\sigma^k_{yy} + \delta\gamma_{xy}\sigma^k_{xy} + \delta\gamma_{yz}\sigma^k_{yz} + \delta\gamma_{xz}\sigma^k_{xz} + \delta\epsilon_{zz}\sigma^k_{zz} \right) d\Omega_k = \sum_{k=1}^{N_L} \delta L^k_{ext} \tag{10.11}$$

Remembering how the strain relations are defined it is possible to write

$$\sum_{k=1}^{N_L} \int_{\Omega_k} \int_{A_k} \left(\delta\epsilon^0_{xx}\sigma^k_{xx} + z\,\delta\epsilon^1_{xx}\sigma^k_{xx} + \delta\epsilon^{0\,k}_{yy}\sigma^k_{yy} + z\,\delta\epsilon^1_{yy}\sigma^k_{yy} + \delta\gamma^0_{xy}\sigma^k_{xy} + z\,\delta\gamma^1_{xy}\sigma^k_{xy} + \right.$$
$$\left. \delta\gamma^0_{yz}\sigma^k_{yz} + z\,\delta\gamma^1_{yz}\sigma^k_{yz} + \delta\gamma^0_{xz}\sigma^k_{xz} + z\,\delta\gamma^1_{xz}\sigma^k_{xz} + \delta\epsilon^0_{zz}\sigma^k_{zz} \right) d\Omega_k = \sum_{k=1}^{N_L} \delta L^k_{ext} \tag{10.12}$$

defining

$$\left\{ \begin{array}{c} N_{xx} \\ N_{yy} \\ N_{xy} \end{array} \right\} = \sum_{k=1}^{N_L} \int_{A_k} \left[\begin{array}{c} \sigma^k_{xx} \\ \sigma^k_{yy} \\ \sigma^k_{xy} \end{array} \right] dz \qquad \left\{ \begin{array}{c} N_{yz} \\ N_{xz} \\ N_{zz} \end{array} \right\} = \sum_{k=1}^{N_L} \int_{A_k} \left[\begin{array}{c} \sigma^k_{yz} \\ \sigma^k_{xz} \\ \sigma^k_{zz} \end{array} \right] dz \tag{10.13}$$

$$\left\{ \begin{array}{c} M_{xx} \\ M_{yy} \\ M_{xy} \end{array} \right\} = \sum_{k=1}^{N_L} \int_{A_k} z \left[\begin{array}{c} \sigma^k_{xx} \\ \sigma^k_{yy} \\ \sigma^k_{xy} \end{array} \right] dz \qquad \left\{ \begin{array}{c} M_{yz} \\ M_{xz} \end{array} \right\} = \sum_{k=1}^{N_L} \int_{A_k} z \left[\begin{array}{c} \sigma^k_{yz} \\ \sigma^k_{xz} \end{array} \right] dz \tag{10.14}$$

Applying the integration by parts, the PVD can be written as

$$\int_\Gamma \left[\delta u_{x0} \left(\overline{N}_{xx} n_x + \overline{N}_{xy} n_y \right) + \delta u_{y0} \left(\overline{N}_{yy} n_x + \overline{N}_{xy} n_y \right) + \delta u_{z0} \left(\overline{N}_{yz} n_x + \overline{N}_{xz} n_y \right) + \right.$$
$$\left. + \delta u_{x1} \left(\overline{M}_{xx} n_x + \overline{M}_{xy} n_y \right) + \delta u_{y1} \left(\overline{M}_{yy} n_x + \overline{M}_{xy} n_y \right) + \delta u_{z1} \left(\overline{M}_{yz} n_x + \overline{M}_{xz} n_y \right) \right] d\Gamma_k -$$
$$\int_\Omega \left[\delta u_{x0} \left(N_{xx,x} + N_{xy,y} \right) + \delta u_{y0} \left(N_{yy,y} + N_{xy,x} \right) + \delta u_{z0} \left(N_{yz,y} + N_{xz,x} \right) + \right.$$
$$+ \delta u_{x1} \left(M_{xx,x} + M_{xy,y} - N_{xz} \right) + \delta u_{y1} \left(M_{yy,y} + M_{xy,x} - N_{yz} \right)$$
$$\left. + \delta u_{z1} \left(M_{yz,y} + M_{xz,x} - N_{zz} \right) \right] d\Omega_k = \sum_{k=1}^{N_L} \delta L^k_{ext} \tag{10.15}$$

It has bee assumed that $\Omega_k = \Omega$ and $\Gamma_k = \Gamma$, where Ω and Γ denote the midsurface and boundary of plate, respectively. Virtual work of the external loadings is now evaluated. A general pressure distribution is considered:

$$\sum_{k=1}^{N_L} \delta L_{ext}^k = \int_\Omega \delta \mathbf{u}^T \cdot \mathbf{p}\, d\Omega_k = \int_{\Omega_k} \left(\delta u_x \cdot p_x + \delta u_y \cdot p_y + \delta u_z \cdot p_z\right) d\Omega \tag{10.16}$$

The attention is restricted to a pressure applied to the top of the plate, that is

$$\sum_{k=1}^{N_L} \delta L_{ext}^k = \int_\Omega \delta u_z \cdot p_z d\Omega_k = \int_{\Omega_k} \left(\delta u_z(x,y,h/2) \cdot p_z^{top}\right) d\Omega_k \tag{10.17}$$

Upper script *top* indicates the top pressure transverse distribution. Remembering how u_z is defined it is

$$\delta L_{ext} = \int_\Omega \left(\delta u_{z0} \cdot p_z^{top} + \delta u_{z1} \cdot p_z^{top} \frac{h}{2}\right) d\Omega \tag{10.18}$$

The PVD now becomes

$$\begin{aligned}
&\int_\Gamma \left[\delta u_{x0}\left(\overline{N}_{xx}n_x + \overline{N}_{xy}n_y\right) + \delta u_{y0}\left(\overline{N}_{yy}n_x + \overline{N}_{xy}n_y\right) + \delta u_{z0}\left(\overline{N}_{yz}n_x + \overline{N}_{xz}n_y\right) + \right. \\
&\quad \left. + \delta u_{x1}\left(\overline{M}_{xx}n_x + \overline{M}_{xy}n_y\right) + \delta u_{y1}\left(\overline{M}_{yy}n_x + \overline{M}_{xy}n_y\right) + \delta u_{z1}\left(\overline{M}_{yz}n_x + \overline{M}_{xz}n_y\right)\right] d\Gamma - \\
&\int_\Omega \left[\delta u_{x0}\left(N_{xx,x} + N_{xy,y}\right) + \delta u_{y0}\left(N_{yy,y} + N_{xy,x}\right) + \delta u_{z0}\left(N_{yz,y} + N_{xz,x}\right) + \right. \\
&\quad + \delta u_{x1}\left(M_{xx,x} + M_{xy,y} - N_{xz}\right) + \delta u_{y1}\left(M_{yy,y} + M_{xy,x} - N_{yz}\right) + \\
&\quad \left. + \delta u_{z1}\left(M_{yz,y} + M_{xz,x} - N_{zz}\right)\right] d\Omega_k = -\int_{\Omega_k} \left(\delta u_{z0} \cdot p_z^{top} + \delta u_{z1} \cdot p_z^{top} \frac{h}{2}\right) d\Omega
\end{aligned} \tag{10.19}$$

Considering a transverse pressure distribution at the top surface of the place the equilibrium equations of the plate are:

$$\begin{aligned}
\delta u_{x0}: &\quad N_{xx,x} + N_{xy,y} = 0 \\
\delta u_{y0}: &\quad N_{yy,y} + N_{xy,x} = 0 \\
\delta u_{z0}: &\quad N_{yz,y} + N_{xz,x} + p = 0 \\
\delta u_{x1}: &\quad M_{xx,x} + M_{xy,y} - N_{xz} = 0 \\
\delta u_{y1}: &\quad M_{yy,y} + M_{xy,x} - N_{yz} = 0 \\
\delta u_{z1}: &\quad M_{xz,x} + M_{yz,y} - N_{zz} + p\tfrac{h}{2} = 0
\end{aligned} \tag{10.20}$$

and the related boundary conditions are

$$\begin{array}{ll} \delta u_{x0}: & \overline{N}_{xx}n_x + \overline{N}_{xy}n_y = 0 \\ \delta u_{y0}: & \overline{N}_{yy}n_x + \overline{N}_{xy}n_y = 0 \\ \delta u_{z0}: & \overline{N}_{yz}n_x + \overline{N}_{xz}n_y = 0 \\ \delta u_{x1}: & \overline{M}_{xx}n_x + \overline{M}_{xy}n_y = 0 \\ \delta u_{y1}: & \overline{M}_{yy}n_x + \overline{M}_{xy}n_y = 0 \\ \delta u_{z1}: & \overline{M}_{yz}n_x + \overline{M}_{xz}n_y = 0 \end{array} \tag{10.21}$$

10.2 Internal forces and momenta in terms of displacement variables

In the following the internal forces and momenta introduced are expressed in terms of displacement variables for a generic multilayer plate. The internal forces are:

$$\begin{aligned} \left\{ \begin{array}{c} N_{xx} \\ N_{yy} \\ N_{xy} \end{array} \right\} &= \sum_{k=1}^{N_L} \int_{A_k} \left[\begin{array}{c} \sigma_{xx}^k \\ \sigma_{yy}^k \\ \sigma_{xy}^k \end{array} \right] dz = \sum_{k=1}^{N_L} \int_{A_k} \left(\left[\begin{array}{ccc} C_{11}^k & C_{12}^k & C_{16}^k \\ C_{21}^k & C_{22}^k & C_{26}^k \\ C_{16}^k & C_{26}^k & C_{66}^k \end{array} \right] \cdot \left\{ \begin{array}{c} \epsilon_{xx}^k \\ \epsilon_{yy}^k \\ \gamma_{xy}^k \end{array} \right\} + \right. \\ &\left. + \left[\begin{array}{ccc} 0 & 0 & C_{13}^k \\ 0 & 0 & C_{23}^k \\ 0 & 0 & C_{36}^k \end{array} \right] \cdot \left\{ \begin{array}{c} \gamma_{xx}^k \\ \gamma_{yz}^k \\ \epsilon_{zz}^k \end{array} \right\} \right) dz = \\ &\sum_{k=1}^{N_L} \int_{A_k} \left(\mathbf{C}_{pp}^k \cdot \left\{ \begin{array}{c} u_{x0,x} \\ u_{y0,y} \\ u_{x0,y} + u_{y0,x} \end{array} \right\} + z\, \mathbf{C}_{pp}^k \cdot \left\{ \begin{array}{c} u_{x1,x} \\ u_{y1,y} \\ u_{x1,y} + u_{y1,x} \end{array} \right\} + \right. \\ &\left. + \mathbf{C}_{pn}^k \cdot \left\{ \begin{array}{c} u_{z0,x} + u_{x1} \\ u_{z0,y} + u_{y1} \\ u_{x1} \end{array} \right\} + z\, \mathbf{C}_{pn}^k \cdot \left\{ \begin{array}{c} u_{z1,x} \\ u_{z1,y} \\ 0 \end{array} \right\} \right) dz \end{aligned} \tag{10.22}$$

defining

$$\begin{aligned} \mathbf{A} &= \sum_{k=1}^{N_L} \int_{A_k} \left[\begin{array}{ccc} C_{11}^k & C_{12}^k & C_{16}^k \\ C_{21}^k & C_{22}^k & C_{26^k} \\ C_{16}^k & C_{26}^k & C_{66}^k \end{array} \right] dz \qquad \mathbf{B} = \sum_{k=1}^{N_L} \int_{Ak} z \left[\begin{array}{ccc} C_{11}^k & C_{12}^k & C_{16}^k \\ C_{21}^k & C_{22}^k & C_{26}^k \\ C_{16}^k & C_{26}^k & C_{66}^k \end{array} \right] dz \\ \tilde{\mathbf{A}} &= \sum_{k=1}^{N_L} \int_{A_k} \left[\begin{array}{ccc} 0 & 0 & C_{13}^k \\ 0 & 0 & C_{23}^k \\ 0 & 0 & C_{36}^k \end{array} \right] dz \qquad \tilde{\mathbf{B}} = \sum_{k=1}^{N_L} \int_{Ak} z \left[\begin{array}{ccc} 0 & 0 & C_{13}^k \\ 0 & 0 & C_{23}^k \\ 0 & 0 & C_{36}^k \end{array} \right] dz \end{aligned} \tag{10.23}$$

it is

$$\mathbf{N}_p = \mathbf{A}\boldsymbol{\epsilon}_p^0 + \mathbf{B}\boldsymbol{\epsilon}_p^1 + \tilde{\mathbf{A}}\boldsymbol{\epsilon}_n^0 + \tilde{\mathbf{B}}\boldsymbol{\epsilon}_n^1 \tag{10.24}$$

$$\begin{aligned}
\left\{ \begin{array}{c} N_{xz} \\ N_{yz} \\ N_{zz} \end{array} \right\} &= \sum_{k=1}^{N_L} \int_{A_k} \left[\begin{array}{c} \sigma_{xz}^k \\ \sigma_{yz}^k \\ \sigma_{zz}^k \end{array} \right] dz = \sum_{k=1}^{N_L} \int_{A_k} \left(\left[\begin{array}{ccc} 0 & 0 & 0 \\ 0 & 0 & 0 \\ C_{13}^k & C_{23}^k & C_{36}^k \end{array} \right] \cdot \left\{ \begin{array}{c} \epsilon_{xx}^k \\ \epsilon_{yy}^k \\ \gamma_{xy}^k \end{array} \right\} + \right. \\
&\left. + \left[\begin{array}{ccc} C_{44}^k & C_{45}^k & 0 \\ C_{45}^k & C_{55}^k & 0 \\ 0 & 0 & C_{33}^k \end{array} \right] \cdot \left\{ \begin{array}{c} \gamma_{xx}^k \\ \gamma_{yz}^k \\ \epsilon_{zz}^k \end{array} \right\} \right) dz \\
&= \sum_{k=1}^{N_L} \int_{A_k} \left(\mathbf{C}_{np}^k \cdot \left\{ \begin{array}{c} u_{x0,x} \\ u_{y0,y} \\ u_{x0,y} + u_{y0,x} \end{array} \right\} + z\, \mathbf{C}_{np}^k \cdot \left\{ \begin{array}{c} u_{x1,x} \\ u_{y1,y} \\ u_{x1,y} + u_{y1,x} \end{array} \right\} + \right. \\
&\left. + \mathbf{C}_{nn}^k \cdot \left\{ \begin{array}{c} u_{z0,x} + u_{x1} \\ u_{z0,y} + u_{y1} \\ u_{x1} \end{array} \right\} + z\, \mathbf{C}_{nn}^k \cdot \left\{ \begin{array}{c} u_{z1,x} \\ u_{z1,y} \\ 0 \end{array} \right\} \right) dz
\end{aligned} \tag{10.25}$$

defining

$$\begin{aligned}
\mathbf{E} &= \sum_{k=1}^{N_L} \int_{A_k} \left[\begin{array}{ccc} 0 & 0 & 0 \\ 0 & 0 & 0 \\ C_{13}^k & C_{23}^k & C_{36}^k \end{array} \right] dz \qquad \mathbf{F} = \sum_{k=1}^{N_L} \int_{Ak} z \left[\begin{array}{ccc} 0 & 0 & 0 \\ 0 & 0 & 0 \\ C_{13}^k & C_{23}^k & C_{36}^k \end{array} \right] dz \\
\tilde{\mathbf{E}} &= \sum_{k=1}^{N_L} \int_{A_k} \left[\begin{array}{ccc} C_{44}^k & C_{45}^k & 0 \\ C_{45}^k & C_{55}^k & 0 \\ 0 & 0 & C_{33}^k \end{array} \right] dz \qquad \tilde{\mathbf{F}} = \int_{Ak} z \left[\begin{array}{ccc} C_{44}^k & C_{45}^k & 0 \\ C_{45}^k & C_{55}^k & 0 \\ 0 & 0 & C_{33}^k \end{array} \right] dz
\end{aligned} \tag{10.26}$$

it is

$$\mathbf{N}_n = \mathbf{E}\boldsymbol{\epsilon}_p^0 + \mathbf{F}\boldsymbol{\epsilon}_p^1 + \tilde{\mathbf{E}}\boldsymbol{\epsilon}_n^0 + \tilde{\mathbf{F}}\boldsymbol{\epsilon}_n^1 \tag{10.27}$$

$$\left\{ \begin{array}{c} M_{xx} \\ M_{yy} \\ M_{xy} \end{array} \right\} = \sum_{k=1}^{N_L} \int_{A_k} z \left[\begin{array}{c} \sigma_{xx}^k \\ \sigma_{yy}^k \\ \sigma_{xy}^k \end{array} \right] dz = \sum_{k=1}^{N_L} \int_{A_k} \left(z \left[\begin{array}{ccc} C_{11}^k & C_{12^k} & C_{16}^k \\ C_{21}^k & C_{22}^k & C_{26}^k \\ C_{16}^k & C_{26}^k & C_{66}^k \end{array} \right] \cdot \left\{ \begin{array}{c} \epsilon_{xx}^k \\ \epsilon_{yy}^k \\ \gamma_{xy}^k \end{array} \right\} + \right.$$
$$\left. z \left[\begin{array}{ccc} 0 & 0 & C_{13}^k \\ 0 & 0 & C_{23}^k \\ 0 & 0 & C_{36}^k \end{array} \right] \cdot \left\{ \begin{array}{c} \gamma_{xx}^k \\ \gamma_{yz}^k \\ \epsilon_{zz}^k \end{array} \right\} \right) dz$$
$$= \sum_{k=1}^{N_L} \int_{A_k} \left(z\, \mathbf{C}_{pp}^k \cdot \left\{ \begin{array}{c} u_{x0,x} \\ u_{y0,y} \\ u_{x0,y} + u_{y0,x} \end{array} \right\} + z^2\, \mathbf{C}_{pp}^k \cdot \left\{ \begin{array}{c} u_{x1,x} \\ u_{y1,y} \\ u_{x1,y} + u_{y1,x} \end{array} \right\} + \right.$$
$$\left. + z\, \mathbf{C}_{pn}^k \cdot \left\{ \begin{array}{c} u_{z0,x} + u_{x1} \\ u_{z0,y} + u_{y1} \\ u_{x1} \end{array} \right\} + z^2\, \mathbf{C}_{pn}^k \cdot \left\{ \begin{array}{c} u_{z1,x} \\ u_{z1,y} \\ 0 \end{array} \right\} \right) dz \tag{10.28}$$

defining

$$\mathbf{B} = \sum_{k=1}^{N_L} \int_{A_k} z \left[\begin{array}{ccc} C_{11}^k & C_{12}^k & C_{16}^k \\ C_{21}^k & C_{22}^k & C_{26}^k \\ C_{16}^k & C_{26}^k & C_{66}^k \end{array} \right] dz \qquad \mathbf{D} = \sum_{k=1}^{N_L} \int_{Ak} z^2 \left[\begin{array}{ccc} C_{11}^k & C_{12}^k & C_{16}^k \\ C_{21}^k & C_{22}^k & C_{26}^k \\ C_{16}^k & C_{26}^k & C_{66}^k \end{array} \right] dz$$
$$\tilde{\mathbf{B}} = \sum_{k=1}^{N_L} \int_{A_k} z \left[\begin{array}{ccc} 0 & 0 & C_{13}^k \\ 0 & 0 & C_{23}^k \\ 0 & 0 & C_{36}^k \end{array} \right] dz \qquad \tilde{\mathbf{D}} = \sum_{k=1}^{N_L} \int_{Ak} z^2 \left[\begin{array}{ccc} 0 & 0 & C_{13}^k \\ 0 & 0 & C_{23}^k \\ 0 & 0 & C_{36}^k \end{array} \right] dz \tag{10.29}$$

it is

$$\mathbf{M}_p = \mathbf{B}\boldsymbol{\epsilon}_p^0 + \mathbf{D}\boldsymbol{\epsilon}_p^1 + \tilde{\mathbf{B}}\boldsymbol{\epsilon}_n^0 + \tilde{\mathbf{D}}\boldsymbol{\epsilon}_n^1 \tag{10.30}$$

$$\left\{ \begin{array}{c} M_{xz} \\ M_{yz} \end{array} \right\} = \sum_{k=1}^{N_L} \int_{A_k} z \left[\begin{array}{c} \sigma_{xz}^k \\ \sigma_{yz}^k \end{array} \right] dz = \sum_{k=1}^{N_L} \int_{A_k} z \left[\begin{array}{cc} C_{44}^k & C_{45}^k \\ C_{45}^k & C_{55}^k \end{array} \right] \cdot \left\{ \begin{array}{c} \gamma_{xx}^k \\ \gamma_{yz}^k \end{array} \right\} dz$$
$$= \sum_{k=1}^{N_L} \int_{A_k} z \left[\begin{array}{cc} C_{44}^k & C_{45}^k \\ C_{45}^k & C_{55}^k \end{array} \right] \cdot \left\{ \begin{array}{c} u_{z0,x} + u_{x1} + z u_{z1,x} \\ u_{z0,y} + u_{y1} + z u_{z1,y} \end{array} \right\} dz =$$
$$= \sum_{k=1}^{N_L} \int_{A_k} z \left[\begin{array}{cc} C_{44}^k & C_{45}^k \\ C_{45}^k & C_{55}^k \end{array} \right] \cdot \left\{ \begin{array}{c} u_{z0,x} + u_{x1} \\ u_{z0,y} + u_{y1} \end{array} \right\} + z^2 \left[\begin{array}{cc} C_{44}^k & C_{45}^k \\ C_{45}^k & C_{55}^k \end{array} \right] \cdot \left\{ \begin{array}{c} z u_{z1,x} \\ z u_{z1,y} \end{array} \right\} dz \tag{10.31}$$

defining

$$\tilde{\mathbf{H}} = \sum_{k=1}^{N_L} \int_{A_k} z \begin{bmatrix} C_{44}^k & C_{45}^k \\ C_{45}^k & C_{55}^k \end{bmatrix} dz \qquad \tilde{\mathbf{N}} = \sum_{k=1}^{N_L} \int_{Ak} z^2 \begin{bmatrix} C_{44}^k & C_{45}^k \\ C_{45}^k & C_{55}^k \end{bmatrix} dz \tag{10.32}$$

it is

$$\mathbf{M}_n = \tilde{\mathbf{H}}\boldsymbol{\epsilon}_n^0 + \tilde{\mathbf{F}}\boldsymbol{\epsilon}_n^1 \tag{10.33}$$

10.3 Equilibrium equations in terms of displacement variables

In the following, the equilibrium equations are written in terms of displacement variables. Substituting into Equations 10.20 the definitions reported in eq.s 10.24, 10.27, 10.30 and 10.33 and remembering the definition of the strains for the case herein reported (see equations 10.2 and 10.3) it is possible to write the governing equations for a multilayered plate in terms of the displacement variables

$$\mathbf{Ku} = \mathbf{p} \rightarrow \begin{bmatrix} K_{11} & K_{12} & K_{13} & K_{14} & K_{15} & K_{16} \\ K_{21} & K_{22} & K_{23} & K_{24} & K_{25} & K_{26} \\ K_{31} & K_{32} & K_{33} & K_{34} & K_{35} & K_{36} \\ K_{41} & K_{42} & K_{43} & K_{44} & K_{45} & K_{46} \\ K_{51} & K_{52} & K_{53} & K_{54} & K_{55} & K_{56} \\ K_{61} & K_{62} & K_{63} & K_{64} & K_{65} & K_{66} \end{bmatrix} \begin{Bmatrix} u_{x0} \\ u_{y0} \\ u_{z0} \\ u_{x1} \\ u_{y1} \\ u_{z1} \end{Bmatrix} = \begin{Bmatrix} 0 \\ 0 \\ -p \\ 0 \\ 0 \\ -p\frac{h_k}{2} \end{Bmatrix} \tag{10.34}$$

where $\mathbf{K}$ is a differential operator. A similar conclusion was reported for the Kirchhoof plate model in equation 3.13 and for the Mindlin model in equation 3.39. The boundary conditions defined in the equations 10.21 can be expressed as

$$\mathbf{\Pi u} = \mathbf{\Pi}\overline{\mathbf{u}} \rightarrow$$

$$\begin{bmatrix} \Pi_{11} & \Pi_{12} & \Pi_{13} & \Pi_{14} & \Pi_{15} & \Pi_{16} \\ \Pi_{21} & \Pi_{22} & \Pi_{23} & \Pi_{24} & \Pi_{25} & \Pi_{26} \\ \Pi_{31} & \Pi_{32} & \Pi_{33} & \Pi_{34} & \Pi_{35} & \Pi_{36} \\ \Pi_{41} & \Pi_{42} & \Pi_{43} & \Pi_{44} & \Pi_{45} & \Pi_{46} \\ \Pi_{51} & \Pi_{52} & \Pi_{53} & \Pi_{54} & \Pi_{55} & \Pi_{56} \\ \Pi_{61} & \Pi_{62} & \Pi_{63} & \Pi_{64} & \Pi_{65} & \Pi_{66} \end{bmatrix} \begin{Bmatrix} u_{x0} \\ u_{y0} \\ u_{z0} \\ u_{x1} \\ u_{y1} \\ u_{z1} \end{Bmatrix} = \begin{bmatrix} \Pi_{11} & \Pi_{12} & \Pi_{13} & \Pi_{14} & \Pi_{15} & \Pi_{16} \\ \Pi_{21} & \Pi_{22} & \Pi_{23} & \Pi_{24} & \Pi_{25} & \Pi_{26} \\ \Pi_{31} & \Pi_{32} & \Pi_{33} & \Pi_{34} & \Pi_{35} & \Pi_{36} \\ \Pi_{41} & \Pi_{42} & \Pi_{43} & \Pi_{44} & \Pi_{45} & \Pi_{46} \\ \Pi_{51} & \Pi_{52} & \Pi_{53} & \Pi_{54} & \Pi_{55} & \Pi_{56} \\ \Pi_{61} & \Pi_{62} & \Pi_{63} & \Pi_{64} & \Pi_{65} & \Pi_{66} \end{bmatrix} \begin{Bmatrix} \overline{u}_{x0} \\ \overline{u}_{y0} \\ \overline{u}_{z0} \\ \overline{u}_{x1} \\ \overline{u}_{y1} \\ \overline{u}_{z1} \end{Bmatrix} \tag{10.35}$$

where $\overline{\mathbf{u}}$ is the displacement function defined at the boundary Γ.

10.4 Governing equations in terms of fundamental nuclei

In the following it is demonstrated that it is possible to express the governing equations in terms of fundamental nuclei, that is it is possible to express the plate governing equations reported in eq.s 10.34 as

$$\begin{bmatrix} \mathbf{K}^{00} & \mathbf{K}^{01} \\ \mathbf{K}^{10} & \mathbf{K}^{11} \end{bmatrix} \cdot \begin{Bmatrix} u_{x0} \\ u_{y0} \\ u_{z0} \\ u_{x1} \\ u_{y1} \\ u_{z1} \end{Bmatrix} = \begin{Bmatrix} 0 \\ 0 \\ -p \\ 0 \\ 0 \\ -p\frac{h}{2} \end{Bmatrix} \tag{10.36}$$

where $\mathbf{K}^{00}$, $\mathbf{K}^{01}$, $\mathbf{K}^{10}$ and $\mathbf{K}^{11}$ are 3×3 differential operators. The upper scripts 0 and 1 refer to the expansion order employed in the definition of the displacement field, in this case it is $0 \to 1$ and $1 \to z$. In the following these upper scripts are labeled as τ and s. In an explicit way it is

$$\begin{array}{c} \\ 1 \\ \\ z \\ \\ \end{array} \begin{array}{c} \begin{array}{ccc} 1 & & \quad z \end{array} \\ \begin{bmatrix} K_{11}^{00} & K_{12}^{00} & K_{13}^{00} & K_{11}^{01} & K_{11}^{01} & K_{11}^{01} \\ K_{21}^{00} & K_{22}^{00} & K_{23}^{00} & K_{21}^{01} & K_{22}^{01} & K_{23}^{01} \\ K_{31}^{00} & K_{32}^{00} & K_{33}^{00} & K_{31}^{01} & K_{32}^{01} & K_{33}^{01} \\ K_{11}^{10} & K_{12}^{10} & K_{13}^{10} & K_{11}^{11} & K_{12}^{11} & K_{13}^{11} \\ K_{21}^{10} & K_{22}^{10} & K_{23}^{10} & K_{21}^{11} & K_{22}^{11} & K_{23}^{11} \\ K_{31}^{10} & K_{32}^{10} & K_{33}^{10} & K_{31}^{11} & K_{32}^{11} & K_{33}^{11} \end{bmatrix} \end{array} \begin{Bmatrix} u_{x0} \\ u_{y0} \\ u_{z0} \\ u_{x1} \\ u_{y1} \\ u_{z1} \end{Bmatrix} = \begin{Bmatrix} 0 \\ 0 \\ -p \\ 0 \\ 0 \\ -p\frac{h}{2} \end{Bmatrix} \tag{10.37}$$

In order to find out how the components of these matrices can be computed let us restrict the attention to the components

$$
\begin{aligned}
K_{11}^{11} =& D_{11}\partial_{,xx} + D_{33}\partial_{,yy} + (D_{13} + D_{31})\partial_{,xy} - \tilde{E}_{11} \\
K_{12}^{11} =& D_{13}\partial_{,xx} + D_{32}\partial_{,yy} + (D_{33} + D_{12})\partial_{,xy} - \tilde{E}_{12} \\
K_{13}^{11} =& (\tilde{B}_{13} - \tilde{F}_{11})\partial_{,x} + (\tilde{B}_{33} - \tilde{F}_{12})\partial_{,y} \\
K_{21}^{11} =& D_{31}\partial_{,xx} + D_{23}\partial_{,yy} + (D_{21} + D_{33})\partial_{,xy} - \tilde{E}_{21} \\
K_{22}^{11} =& D_{33}\partial_{,xx} + D_{22}\partial_{,yy} + (D_{23} + D_{32})\partial_{,xy} - \tilde{E}_{22} \\
K_{23}^{11} =& (\tilde{B}_{33} - \tilde{F}_{21})\partial_{,x} + (\tilde{B}_{23} - \tilde{F}_{22})\partial_{,y} \\
K_{31}^{11} =& (\tilde{H}_{11} - F_{31})\partial_{,x} + (\tilde{H}_{21} - F_{33})\partial_{,y} \\
K_{32}^{11} =& (\tilde{H}_{12} - F_{33})\partial_{,x} + (\tilde{H}_{22} - F_{32})\partial_{,y} \\
K_{33}^{11} =& \tilde{N}_{11}\partial_{,xx} + \tilde{N}_{22}\partial_{,yy} + (\tilde{N}_{12} + \tilde{N}_{21})\partial_{,xy} - \tilde{E}_{33}
\end{aligned}
\tag{10.38}
$$

Remembering the definition of the matrices and considering a k layer plate it is

$$
\begin{aligned}
K_{11}^{k11} =& C_{11}^{k}\left(\int_A z^2 dz\right)\partial_{,xx} + C_{66}^{k}\left(\int_A z^2 dz\right)\partial_{,yy} + (C_{16}^{k}\left(\int_A z^2 dz\right) + C_{16}^{k}\left(\int_A z^2 dz\right))\partial_{,xy} - C_{55}^{k}\left(\int_A 1 dz\right) \\
K_{12}^{k11} =& C_{16}^{k}\left(\int_A z^2 dz\right)\partial_{,xx} + C_{26}^{k}\left(\int_A z^2 dz\right)\partial_{,yy} + (C_{66}^{k}\left(\int_A z^2 dz\right) + C_{12}^{k}\left(\int_A z^2 dz\right))\partial_{,xy} - C_{45}^{k}\left(\int_A 1 dz\right) \\
K_{13}^{k11} =& (C_{13}^{k}\left(\int_A z dz\right) - C_{55}^{k}\left(\int_A z dz\right))\partial_{,x} + (C_{36}^{k}\left(\int_A z dz\right) - C_{45}^{k}\left(\int_A z dz\right))\partial_{,y} \\
K_{21}^{k11} =& C_{16}^{k}\left(\int_A z^2 dz\right)\partial_{,xx} + C_{26}^{k}\left(\int_A z^2 dz\right)\partial_{,yy} + (C_{12}^{k}\left(\int_A z^2 dz\right) + C_{66}^{k}\left(\int_A z^2 dz\right))\partial_{,xy} - C_{45}^{k}\left(\int_A 1 dz\right) \\
K_{22}^{k11} =& C_{66}^{k}\left(\int_A z^2 dz\right)\partial_{,xx} + C_{22}^{k}\left(\int_A z^2 dz\right)\partial_{,yy} + (C_{26}^{k}\left(\int_A z^2 dz\right) + C_{26}^{k}\left(\int_A z^2 dz\right))\partial_{,xy} - C_{44}^{k}\left(\int_A 1 dz\right) \\
K_{23}^{k11} =& (C_{36}^{k}\left(\int_A z dz\right) - C_{45}^{k}\left(\int_A z dz\right))\partial_{,x} + (C_{23}^{k}\left(\int_A z dz\right) - C_{44}^{k}\left(\int_A z dz\right))\partial_{,y} \\
K_{31}^{k11} =& (C_{55}^{k}\left(\int_A z dz\right) - C_{13}^{k}\left(\int_A z dz\right))\partial_{,x} + (C_{45}^{k}\left(\int_A z dz\right) - C_{36}^{k}\left(\int_A z dz\right))\partial_{,y} \\
K_{32}^{k11} =& (C_{45}^{k}\left(\int_A z dz\right) - C_{36}^{k}\left(\int_A z dz\right))\partial_{,x} + (C_{44}^{k}\left(\int_A z dz\right) - C_{23}^{k}\left(\int_A z dz\right))\partial_{,y} \\
K_{33}^{k11} =& C_{55}^{k}\left(\int_A z^2 dz\right)\partial_{,xx} + C_{44}^{k}\left(\int_A z^2 dz\right)\partial_{,yy} + (C_{45}^{k}\left(\int_A z^2 dz\right) + C_{45}^{k}\left(\int_A z^2 dz\right))\partial_{,xy} - C_{33}^{k}\left(\int_A 1 dz\right)
\end{aligned}
\tag{10.39}
$$

Let us define the following quantities

$$\left(E_{\tau s}, E_{\tau_{,z} s_{,z}}\right) = \int_{A_k} (z \cdot z, 1 \cdot 1)\ dz \qquad \tau, s = 0, 1 \tag{10.40}$$

it is possible to write equation 10.39 as

$$\begin{aligned}
K_{11}^{k11} =& C_{11}^k E_{\tau s}\partial_{,xx} + C_{66}^k E_{\tau s}\partial_{,yy} + (C_{16}^k E_{\tau s} + C_{16}^k E_{\tau s})\partial_{,xy} - C_{55}^k \\
K_{12}^{k11} =& C_{16}^k E_{\tau s}\partial_{,xx} + C_{26}^k E_{\tau s}\partial_{,yy} + (C_{66}^k E_{\tau s} + C_{12}^k E_{\tau s})\partial_{,xy} - C_{45}^k E_{\tau_{,z} s_{,z}} \\
K_{13}^{k11} =& (C_{13}^k \left(\int_A z dz\right) - C_{55}^k \left(\int_A z dz\right))\partial_{,x} + (C_{36}^k \left(\int_A z dz\right) - C_{45}^k \left(\int_A z dz\right))\partial_{,y} \\
K_{21}^{k11} =& C_{16}^k E_{\tau s}\partial_{,xx} + C_{26}^k E_{\tau s}\partial_{,yy} + (C_{12}^k E_{\tau s} + C_{66}^k E_{\tau s})\partial_{,xy} - C_{45}^k E_{\tau_{,z} s_{,z}} \\
K_{22}^{k11} =& C_{66}^k E_{\tau s}\partial_{,xx} + C_{22}^k E_{\tau s}\partial_{,yy} + (C_{26}^k E_{\tau s} + C_{26}^k E_{\tau s})\partial_{,xy} - C_{44}^k E_{\tau_{,z} s_{,z}} \\
K_{23}^{k11} =& (C_{36}^k \left(\int_A z dz\right) - C_{45}^k \left(\int_A z dz\right))\partial_{,x} + (C_{23}^k \left(\int_A z dz\right) - C_{44}^k \left(\int_A z dz\right))\partial_{,y} \\
K_{31}^{k11} =& (C_{55}^k \left(\int_A z dz\right) - C_{13}^k \left(\int_A z dz\right))\partial_{,x} + (C_{45}^k \left(\int_A z dz\right) - C_{36}^k \left(\int_A z dz\right))\partial_{,y} \\
K_{32}^{k11} =& (C_{45}^k \left(\int_A z dz\right) - C_{36}^k \left(\int_A z dz\right))\partial_{,x} + (C_{44}^k \left(\int_A z dz\right) - C_{23}^k \left(\int_A z dz\right))\partial_{,y} \\
K_{33}^{k11} =& C_{55}^k E_{\tau s}\partial_{,xx} + C_{44}^k E_{\tau s}\partial_{,yy} + (C_{45}^k E_{\tau s} + C_{45}^k E_{\tau s})\partial_{,xy} - C_{33}^k \left(\int_A 1 z dz\right)
\end{aligned} \tag{10.41}$$

Particular attention has to be put in the definition of the integral term $\int_A z\, dz$. This terms has to be defined as done in eq. 10.40 is such a way to obtain in a unified way the following terms:

$$\begin{aligned}
K_{13}^{k00} =& 0 \quad K_{13}^{k01} = C_{13}^k \left(\int_A 1 dz\right)\partial_{,x} + C_{36}^k \left(\int_A 1 dz\right)\partial_{,y} \quad K_{13}^{k10} = -C_{55}^k \left(\int_A 1 dz\right)\partial_{,x} - C_{45}^k \left(\int_A dz\right)\partial_{,y} \\
K_{13}^{k11} =& (C_{13}^k \left(\int_A z dz\right) - C_{55}^k \left(\int_A z dz\right))\partial_{,x} + (C_{36}^k \left(\int_A z dz\right) - C_{45}^k \left(\int_A z dz\right))\partial_{,y}
\end{aligned} \tag{10.42}$$

$$\begin{aligned}
K_{23}^{k00} =& 0 \quad K_{23}^{k01} = C_{23}^k \left(\int_A 1 dz\right)\partial_{,y} + C_{36}^k \left(\int_A 1 dz\right)\partial_{,x} \quad K_{23}^{k10} = -C_{45}^k \left(\int_A 1 dz\right)\partial_{,x} - C_{44}^k \left(\int_A 1 dz\right)\partial_{,y} \\
K_{23}^{k11} =& (C_{36}^k \left(\int_A z dz\right) - C_{45}^k \left(\int_A z dz\right))\partial_{,x} + (C_{23}^k \left(\int_A z dz\right) - C_{44}^k \left(\int_A z dz\right))\partial_{,y}
\end{aligned} \tag{10.43}$$

$$
\begin{aligned}
K_{31}^{k00} =& 0 \quad K_{31}^{k01} = C_{55}^{k}\left(\int_A 1dz\right)\partial_{,x} + C_{45}^{k}\left(\int_A 1dz\right)\partial_{,y} \quad K_{31}^{k10} = -C_{13}^{k}\left(\int_A 1dz\right)\partial_{,x} - C_{36}^{k}\left(\int_A 1dz\right)\partial_{,y} \\
K_{31}^{k11} =& (C_{55}^{k}\left(\int_A zdz\right) - C_{13}^{k}\left(\int_A zdz\right))\partial_{,x} + (C_{45}^{k}\left(\int_A zdz\right) - C_{36}^{k}\left(\int_A zdz\right))\partial_{,y}
\end{aligned}
\tag{10.44}
$$

$$
\begin{aligned}
K_{32}^{k00} =& 0 \quad K_{32}^{k01} = C_{45}^{k}\left(\int_A 1dz\right)\partial_{,x} + C_{44}^{k}\left(\int_A 1dz\right)\partial_{,y} \quad K_{32}^{k10} = -C_{36}^{k}\left(\int_A 1dz\right)\partial_{,x} - C_{23}^{k}\left(\int_A 1dz\right)\partial_{,y} \\
K_{32}^{k11} =& (C_{45}^{k}\left(\int_A zdz\right) - C_{36}^{k}\left(\int_A zdz\right))\partial_{,x} + (C_{44}^{k}\left(\int_A zdz\right) - C_{23}^{k}\left(\int_A zdz\right))\partial_{,y}
\end{aligned}
\tag{10.45}
$$

A way to obtain in a unified manner the previous terms is to defined the following quantities

$$
\left(E_{\tau,_z s}, E_{\tau s,_z}\right) = \int_{A_k} (1 \cdot z, z \cdot 1)\ dz \qquad \tau, s = 0, 1 \tag{10.46}
$$

It implies that

$$
\begin{aligned}
K_{13}^{k11} =& (C_{13}^{k}E_{\tau,_z s} - C_{55}^{k}E_{\tau s,_z})\partial_{,x} + (C_{36}^{k}E_{\tau,_z s} - C_{45}^{k}E_{\tau s,_z})\partial_{,y} \\
K_{23}^{k11} =& (C_{36}^{k}E_{\tau,_z s} - C_{45}^{k}E_{\tau s,_z})\partial_{,x} + (C_{23}^{k}E_{\tau,_z s} - C_{44}^{k}E_{\tau s,_z})\partial_{,y} \\
K_{31}^{k11} =& (C_{55}^{k}E_{\tau,_z s} - C_{13}^{k}E_{\tau s,_z})\partial_{,x} + (C_{45}^{k}E_{\tau,_z s} - C_{36}^{k}E_{\tau s,_z})\partial_{,y} \\
K_{32}^{k11} =& (C_{45}^{k}E_{\tau,_z s} - C_{36}^{k}E_{\tau s,_z})\partial_{,x} + (C_{44}^{k}E_{\tau,_z s} - C_{23}^{k}E_{\tau s,_z})\partial_{,y}
\end{aligned}
\tag{10.47}
$$

The components of the fundamental nucleus are defined. The differential operator $\mathbf{K}^{k\tau s}$ for a single layer k is now presented:

$$
\begin{aligned}
K_{11}^{k\tau s} =& C_{11}^{k} E_{\tau s} \partial_{,xx} + C_{66}^{k} E_{\tau s} \partial_{,yy} + 2C_{16}^{k} E_{\tau s} \partial_{,xy} - C_{55}^{k} E_{\tau_{,z} s_{,z}} \\
K_{12}^{k\tau s} =& C_{16}^{k} E_{\tau s} \partial_{,xx} + C_{26}^{k} E_{\tau s} \partial_{,yy} + (C_{66}^{k} E_{\tau s} + C_{12}^{k} E_{\tau s}) \partial_{,xy} - C_{45}^{k} E_{\tau_{,z} s_{,z}} \\
K_{13}^{k\tau s} =& (C_{13}^{k} E_{\tau_{,z} s} - C_{55}^{k} E_{\tau s_{,z}}) \partial_{,x} + (C_{36}^{k} E_{\tau_{,z} s} - C_{45}^{k} E_{\tau s_{,z}}) \partial_{,y} \\
K_{21}^{k\tau s} =& C_{16}^{k} E_{\tau s} \partial_{,xx} + C_{26}^{k} E_{\tau s} \partial_{,yy} + (C_{12}^{k} E_{\tau s} + C_{66}^{k} E_{\tau s}) \partial_{,xy} - C_{45}^{k} E_{\tau_{,z} s_{,z}} \\
K_{22}^{k\tau s} =& C_{66}^{k} E_{\tau s} \partial_{,xx} + C_{22}^{k} E_{\tau s} \partial_{,yy} + 2C_{26}^{k} E_{\tau s} \partial_{,xy} - C_{44}^{k} E_{\tau_{,z} s_{,z}} \\
K_{23}^{k\tau s} =& (C_{36}^{k} E_{\tau_{,z} s} - C_{45}^{k} E_{\tau s_{,z}}) \partial_{,x} + (C_{23}^{k} E_{\tau_{,z} s} - C_{44}^{k} E_{\tau s_{,z}}) \partial_{,y} \\
K_{31}^{k\tau s} =& (C_{55}^{k} E_{\tau_{,z} s} - C_{13}^{k} E_{\tau s_{,z}}) \partial_{,x} + (C_{45}^{k} E_{\tau_{,z} s} - C_{36}^{k} E_{\tau s_{,z}}) \partial_{,y} \\
K_{32}^{k\tau s} =& (C_{45}^{k} E_{\tau_{,z} s} - C_{36}^{k} E_{\tau s_{,z}}) \partial_{,x} + (C_{44}^{k} E_{\tau_{,z} s} - C_{23}^{k} E_{\tau s_{,z}}) \partial_{,y} \\
K_{33}^{k\tau s} =& C_{55}^{k} E_{\tau s} \partial_{,xx} + C_{44}^{k} E_{\tau s} \partial_{,yy} + 2C_{45}^{k} E_{\tau s} \partial_{,xy} - C_{33}^{k} E_{\tau_{,z} s_{,z}}
\end{aligned}
\tag{10.48}
$$

Similar passages can be applied to the differential operator $\mathbf{\Pi}$, the result is

$$
\begin{aligned}
\Pi_{11}^{k\tau s} =& E_{\tau s}(C_{11}^{k} \partial_{,x} + C_{16}^{k} \partial_{,y}) + E_{\tau s}(C_{16}^{k} \partial_{,x} + C_{66}^{k} \partial_{,y}) \\
\Pi_{12}^{k\tau s} =& E_{\tau s}(C_{16}^{k} \partial_{,x} + C_{12}^{k} \partial_{,y}) + E_{\tau s}(C_{26}^{k} \partial_{,y} + C_{66}^{k} \partial_{,x}) \\
\Pi_{13}^{k\tau s} =& C_{13}^{k} E_{\tau_{,z} s} + C_{36} E_{\tau_{,z} s} \\
\Pi_{21}^{k\tau s} =& E_{\tau s}(C_{21}^{k} \partial_{,x} + C_{26}^{k} \partial_{,y}) + E_{\tau s}(C_{16}^{k} \partial_{,x} + C_{66}^{k} \partial_{,y}) \\
\Pi_{22}^{k\tau s} =& E_{\tau s}(C_{26}^{k} \partial_{,x} + C_{22}^{k} \partial_{,y}) + E_{\tau s}(C_{26}^{k} \partial_{,y} + C_{66}^{k} \partial_{,x}) \\
\Pi_{23}^{k\tau s} =& C_{23}^{k} E_{\tau_{,z} s} + C_{36} E_{\tau_{,z} s} \\
\Pi_{31}^{k\tau s} =& C_{45}^{k} E_{\tau_{,z} s} + C_{55}^{k} E_{\tau_{,z} s} \\
\Pi_{32}^{k\tau s} =& C_{44}^{k} E_{\tau_{,z} s} + C_{54}^{k} E_{\tau_{,z} s} \\
\Pi_{33}^{k\tau s} =& E_{\tau s}(C_{45}^{k} \partial_{,x} + C_{44}^{k} \partial_{,y}) + E_{\tau s}(C_{55}^{k} \partial_{,x} + C_{54}^{k} \partial_{,y})
\end{aligned}
\tag{10.49}
$$

Chapter 11

Appendix 2: CUF - plate governing equations

The PVD for a multilayered plate can be written as

$$\int_V \left(\delta\boldsymbol{\epsilon}_p\boldsymbol{\sigma}_p + \delta\boldsymbol{\epsilon}_n\boldsymbol{\sigma}_n\right)\, dV = \int_V \delta\mathbf{u}^T\,\mathbf{p}\, dV \tag{11.1}$$

V is the domanin of the plate. Considering a multilayered plate, that is a plate made of N_L layers, the PVD can be written as

$$\sum_{k=1}^{N_L}\int_{\Omega_K}\int_{A_k}\left(\delta\boldsymbol{\epsilon}_p^{k^T}\boldsymbol{\sigma}_p^k + \delta\boldsymbol{\epsilon}_n^{k^T}\boldsymbol{\sigma}_n^k\right)\, dA_k d\Omega_k = \sum_{k=1}^{N_L}\delta L_{ext}^k \tag{11.2}$$

The term $\sum_{k=1}^{N_L}\delta L_{ext}^k$ denotes the virtual variation of the work made by the external loadings on the generic k layer, the operator $\int_{A_k} dA_k$ the integration through the thickness of the k layer and Ω_k the midsurface of a k layer. According to the definitions above mentioned the PVD can be written as

$$\sum_{k=1}^{N_L}\int_{\Omega_K}\int_{A_k}\left[\delta\left(\mathbf{D}_p\mathbf{u}\right)^T\left(\mathbf{C}_{pp}\boldsymbol{\epsilon}_p + \mathbf{C}_{pn}\boldsymbol{\epsilon}_n\right) + \delta\left(\mathbf{D}_n\mathbf{u}\right)^T\left(\mathbf{C}_{np}\boldsymbol{\epsilon}_p + \mathbf{C}_{nn}\boldsymbol{\epsilon}_n\right)\right]\, dA_k d\Omega_k = \sum_{k=1}^{N_L}\delta L_{ext}^k \tag{11.3}$$

that is

$$\sum_{k=1}^{N_L} \int_{\Omega_K} \int_{A_k} \left[\delta \left(\mathbf{D}_p \mathbf{u} \right)^T \left(\mathbf{C}_{pp} \mathbf{D}_p \mathbf{u} + \boldsymbol{\epsilon}_p + \mathbf{C}_{pn} \mathbf{D}_n \mathbf{u} \right) + \delta \left(\mathbf{D}_n \mathbf{u} \right)^T \left(\mathbf{C}_{np} \mathbf{D}_p \mathbf{u} + \mathbf{C}_{nn} \mathbf{D}_n \mathbf{u} \right) \right] dA_k d\Omega_k = \sum_{k=1}^{N_L} \delta L_{ext}^k \tag{11.4}$$

Remembering that $\mathbf{D}_n = \mathbf{D}_{n\Omega} + \mathbf{D}_{nz}$ it is possible to write

$$\sum_{k=1}^{N_L} \int_{\Omega_K} \int_{A_k} \left[\delta \left(\mathbf{D}_p \mathbf{u} \right)^T \left(\mathbf{C}_{pp} \mathbf{D}_p \mathbf{u} + \boldsymbol{\epsilon}_p + \mathbf{C}_{pn} \mathbf{D}_{n\Omega} \mathbf{u} + \mathbf{C}_{pn} \mathbf{D}_{nz} \mathbf{u} \right) + \right.$$
$$\left. + \delta \left(\mathbf{D}_{n\Omega} \mathbf{u} + \mathbf{D}_{nz} \mathbf{u} \right)^T \left(\mathbf{C}_{np} \mathbf{D}_p \mathbf{u} + \mathbf{C}_{nn} \mathbf{D}_{n\Omega} \mathbf{u} + \mathbf{C}_{nn} \mathbf{D}_{nz} \mathbf{u} \right) \right] dA_k d\Omega_k = \sum_{k=1}^{N_L} \delta L_{ext}^k \tag{11.5}$$

that is

$$\sum_{k=1}^{N_L} \int_{\Omega_K} \int_{A_k} \left[\delta \left(\mathbf{D}_p \mathbf{u} \right)^T \left(\mathbf{C}_{pp} \mathbf{D}_p \mathbf{u} + \boldsymbol{\epsilon}_p + \mathbf{C}_{pn} \mathbf{D}_{n\Omega} \mathbf{u} + \mathbf{C}_{pn} \mathbf{D}_{nz} \mathbf{u} \right) + \right.$$
$$+ \delta \left(\mathbf{D}_{n\Omega} \mathbf{u} \right)^T \left(\mathbf{C}_{np} \mathbf{D}_p \mathbf{u} + \mathbf{C}_{nn} \mathbf{D}_{n\Omega} \mathbf{u} + \mathbf{C}_{nn} \mathbf{D}_{nz} \mathbf{u} \right) +$$
$$\left. + \delta \left(\mathbf{D}_{nz} \mathbf{u} \right)^T \left(\mathbf{C}_{np} \mathbf{D}_p \mathbf{u} + \mathbf{C}_{nn} \mathbf{D}_{n\Omega} \mathbf{u} + \mathbf{C}_{nn} \mathbf{D}_{nz} \mathbf{u} \right) \right] dA_k d\Omega_k = \sum_{k=1}^{N_L} \delta L_{ext}^k \tag{11.6}$$

According to the CUF the displacement field can be defined as $\mathbf{u} = F_\tau \mathbf{u}_\tau$, so it is possible to write

$$\sum_{k=1}^{N_L} \int_{\Omega_K} \int_{A_k} \left[\delta \left(\mathbf{D}_p F_s \mathbf{u}_s \right)^T \left(\mathbf{C}_{pp} \mathbf{D}_p F_\tau \mathbf{u}_\tau + \boldsymbol{\epsilon}_p + \mathbf{C}_{pn} \mathbf{D}_{n\Omega} F_\tau \mathbf{u}_\tau + \mathbf{C}_{pn} \mathbf{D}_{nz} F_\tau \mathbf{u}_\tau \right) + \right.$$
$$+ \delta \left(\mathbf{D}_{n\Omega} F_s \mathbf{u}_s \right)^T \left(\mathbf{C}_{np} \mathbf{D}_p F_\tau \mathbf{u}_\tau + \mathbf{C}_{nn} \mathbf{D}_{n\Omega} F_\tau \mathbf{u}_\tau + \mathbf{C}_{nn} \mathbf{D}_{nz} F_\tau \mathbf{u}_\tau \right) +$$
$$\left. + \delta \left(\mathbf{D}_{nz} F_s \mathbf{u}_s \right)^T \left(\mathbf{C}_{np} \mathbf{D}_p F_\tau \mathbf{u}_\tau + \mathbf{C}_{nn} \mathbf{D}_{n\Omega} F_\tau \mathbf{u}_\tau + \mathbf{C}_{nn} \mathbf{D}_{nz} F_\tau \mathbf{u}_\tau \right) \right] dA_k d\Omega_k = \sum_{k=1}^{N_L} \delta L_{ext}^k \tag{11.7}$$

where $\tau, s = 1, N+1$ with N the expansion order adopted. The definition of the differential operator $\mathbf{D}_{nz}$ is reported in eq. 2.37. It is possible to write

$$\begin{aligned}\sum_{k=1}^{N_L}\int_{\Omega_K}\int_{A_k}\Big[&\delta\left(\mathbf{D}_p F_s\mathbf{u}_s\right)^T\left(\mathbf{C}_{pp}\mathbf{D}_p F_\tau\mathbf{u}_\tau+\mathbf{C}_{pn}\mathbf{D}_{n\Omega}F_\tau\mathbf{u}_\tau+\mathbf{C}_{pn}F_{\tau,_z}\mathbf{u}_\tau\right)+\\&+\delta\left(\mathbf{D}_{n\Omega}F_s\mathbf{u}_s\right)^T\left(\mathbf{C}_{np}\mathbf{D}_p F_\tau\mathbf{u}_\tau+\mathbf{C}_{nn}\mathbf{D}_{n\Omega}F_\tau\mathbf{u}_\tau+\mathbf{C}_{nn}F_{\tau,_z}\mathbf{u}_\tau\right)+\\&+\delta\left(F_{s,_z}\mathbf{u}_s\right)^T\left(\mathbf{C}_{np}\mathbf{D}_p F_\tau\mathbf{u}_\tau+\mathbf{C}_{nn}\mathbf{D}_{n\Omega}F_\tau\mathbf{u}_\tau+\mathbf{C}_{nn}F_{\tau,_z}\mathbf{u}_\tau\right)\Big]\,dA_k d\Omega_k=\sum_{k=1}^{N_L}\delta L^k_{ext}\end{aligned} \tag{11.8}$$

that is

$$\begin{aligned}\sum_{k=1}^{N_L}\int_{\Omega_K}\int_{A_k}\Big[&\delta\left(\mathbf{D}_p\mathbf{u}_s\right)^T\left(\mathbf{C}_{pp}\mathbf{D}_p F_sF_\tau\mathbf{u}_\tau+\mathbf{C}_{pn}\mathbf{D}_{n\Omega}F_sF_\tau\mathbf{u}_\tau+\mathbf{C}_{pn}F_sF_{\tau,_z}\mathbf{u}_\tau\right)+\\&+\delta\left(\mathbf{D}_{n\Omega}\mathbf{u}_s\right)^T\left(\mathbf{C}_{np}\mathbf{D}_p F_sF_\tau\mathbf{u}_\tau+\mathbf{C}_{nn}\mathbf{D}_{n\Omega}F_sF_\tau\mathbf{u}_\tau+\mathbf{C}_{nn}F_sF_{\tau,_z}\mathbf{u}_\tau\right)+\\&+\delta\left(\mathbf{u}_s\right)^T\left(\mathbf{C}_{np}\mathbf{D}_p F_{s,_z}F_\tau\mathbf{u}_\tau+\mathbf{C}_{nn}\mathbf{D}_{n\Omega}F_{s,_z}F_\tau\mathbf{u}_\tau+\mathbf{C}_{nn}F_{s,_z}F_{\tau,_z}\mathbf{u}_\tau\right)\Big]\,dA_k d\Omega_k=\sum_{k=1}^{N_L}\delta L^k_{ext}\end{aligned} \tag{11.9}$$

The integration by parts is requested to obtain strong form of the differential equations on Ω_k and boundary conditions on Γ_k (Ω_k and its boundary Γ_k are defined as in Fig. 2.4). For a generic variable $\mathbf{a}_k$, the integration by parts states

$$\int_{\Omega_k}\left(\mathbf{D}_\Omega\delta\mathbf{a}_k\right)^T\mathbf{a}^k d\Omega_k=-\int_{\Omega_k}\delta\mathbf{a}^{k^T}\left(\mathbf{D}^T_\Omega\mathbf{a}^k\right)d\Omega_k+\int_{\Gamma_k}\delta\mathbf{a}^{k^T}\left(\mathbf{I}_\Omega\mathbf{a}^k\right)d\Gamma_k \tag{11.10}$$

where $\Omega = n, np$. In this case it is possible to write the equation for the PVD as

$$\sum_{k=1}^{N_L} \int_{\Omega_K} \int_{A_k} \Big[-\delta \mathbf{u}_s^T \mathbf{D}_p^T \left(\mathbf{C}_{pp} \mathbf{D}_p F_s F_\tau \mathbf{u}_\tau + \mathbf{C}_{pn} \mathbf{D}_{n\Omega} F_s F_\tau \mathbf{u}_\tau + \mathbf{C}_{pn} F_s F_{\tau_{,z}} \mathbf{u}_\tau \right) -$$
$$- \delta \mathbf{u}_s^T \mathbf{D}_{n\Omega}^T \left(\mathbf{C}_{np} \mathbf{D}_p F_s F_\tau \mathbf{u}_\tau + \mathbf{C}_{nn} \mathbf{D}_{n\Omega} F_s F_\tau \mathbf{u}_\tau + \mathbf{C}_{nn} F_s F_{\tau_{,z}} \mathbf{u}_\tau \right) +$$
$$+ \delta \mathbf{u}_s^T \left(\mathbf{C}_{np} \mathbf{D}_p F_{s_{,z}} F_\tau \mathbf{u}_\tau + \mathbf{C}_{nn} \mathbf{D}_{n\Omega} F_{s_{,z}} F_\tau \mathbf{u}_\tau + \mathbf{C}_{nn} F_{s_{,z}} F_{\tau_{,z}} \mathbf{u}_\tau \right) \Big] \, dA_k d\Omega_k +$$
$$+ \sum_{k=1}^{N_L} \int_{\Gamma_K} \int_{A_k} \Big[\delta \mathbf{u}_s^T \mathbf{I}_p^T \left(\mathbf{C}_{pp} \mathbf{D}_p F_s F_\tau \mathbf{u}_\tau + \mathbf{C}_{pn} \mathbf{D}_{n\Omega} F_s F_\tau \mathbf{u}_\tau + \mathbf{C}_{pn} F_s F_{\tau_{,z}} \mathbf{u}_\tau \right) -$$
$$- \delta \mathbf{u}_s^T \mathbf{I}_{n\Omega}^T \left(\mathbf{C}_{np} \mathbf{D}_p F_s F_\tau \mathbf{u}_\tau + \mathbf{C}_{nn} \mathbf{D}_{n\Omega} F_s F_\tau \mathbf{u}_\tau + \mathbf{C}_{nn} F_s F_{\tau_{,z}} \mathbf{u}_\tau \right) \Big] \, dA_k d\Gamma_k = \sum_{k=1}^{N_L} \delta L_{ext}^k \tag{11.11}$$

The meaning of the $\mathbf{I}_p$ and $\mathbf{I}_{np}$ involved is reported in the following:

$$\mathbf{I}_p = \begin{bmatrix} 1 & 0 & 0 \\ 0 & 1 & 0 \\ 1 & 1 & 0 \end{bmatrix} \qquad \mathbf{I}_{n\Omega} = \begin{bmatrix} 0 & 0 & 1 \\ 0 & 0 & 1 \\ 0 & 0 & 0 \end{bmatrix} \tag{11.12}$$

The quantities $\left(E_{\tau s}, E_{\tau_{,z} s}, E_{\tau s_{,z}}, E_{\tau_{,z} s_{,z}} \right)$ are introduced; they are defined as

$$\left(E_{\tau s}, E_{\tau_{,z} s}, E_{\tau s_{,z}}, E_{\tau_{,z} s_{,z}} \right) = \int_{A_k} \left(F_\tau F_s, F_{\tau_{,z}} F_s, F_\tau F_{s_{,z}}, F_{\tau_{,z}} F_{s_{,z}}, \right) \, dA_k \tag{11.13}$$

The PVD can be written as

$$\sum_{k=1}^{N_L} \int_{\Omega_K} \delta \mathbf{u}_s^T \Big[-\mathbf{D}_p^T \left(\mathbf{C}_{pp} \mathbf{D}_p E_{\tau\, s} + \mathbf{C}_{pn} \mathbf{D}_{n\Omega} E_{\tau\, s} + \mathbf{C}_{pn} E_{\tau_{,z}\, s} \right) -$$
$$- \mathbf{D}_{n\Omega}^T \left(\mathbf{C}_{np} \mathbf{D}_p E_{\tau\, s} + \mathbf{C}_{nn} \mathbf{D}_{n\Omega} E_{\tau\, s} + \mathbf{C}_{nn} E_{\tau_{,z}\, s} \right) +$$
$$+ \left(\mathbf{C}_{np} \mathbf{D}_p E_{\tau\, s_{,z}} + \mathbf{C}_{nn} \mathbf{D}_{n\Omega} E_{\tau\, s,z} + \mathbf{C}_{nn} E_{\tau_{,z}\, s_{,z}} \right) \Big] \, \mathbf{u}_\tau d\Omega_k +$$
$$+ \sum_{k=1}^{N_L} \int_{\Gamma_K} \delta \mathbf{u}_s^T \Big[\mathbf{I}_p^T \left(\mathbf{C}_{pp} \mathbf{D}_p E_{\tau\, s} + \mathbf{C}_{pn} \mathbf{D}_{n\Omega} E_{\tau\, s} + \mathbf{C}_{pn} E_{\tau_{,z}\, s} \right) +$$
$$+ \mathbf{I}_{n\Omega}^T \left(\mathbf{C}_{np} \mathbf{D}_p E_{\tau\, s} + \mathbf{C}_{nn} \mathbf{D}_{n\Omega} E_{\tau\, s} + \mathbf{C}_{nn} E_{\tau_{,z}\, s} \right) \Big] \, \mathbf{u}_\tau d\Gamma_k = \sum_{k=1}^{N_L} \delta L_{ext}^k \tag{11.14}$$

Virtual work of the external loadings is now evaluated. The virtual variation of the work for generic layer k can be computed as A general pressure distribution is considered:

$$\delta L_{ext}^k = \int_{\Omega_k} \delta \mathbf{u}^{k^T} \, \mathbf{p} d\Omega_k \tag{11.15}$$

$\delta \mathbf{u}$ is the virtual variation of the displacement vector $\mathbf{u}$ and the components of the vector $\mathbf{p}$ (i.e. p_x, p_y, and p_z) are the load distributions according to the reference system axes x, y and z. It is

$$\delta L_{ext}^k = \int_{\Omega_k} \left(\delta u_x^k \, p_x + \delta u_y^k \, p_y + \delta u_z^k \, p_z \right) \, d\Omega_k \tag{11.16}$$

Remembering how u_z^k is defined according to the CUF it is

$$\begin{aligned} \delta L_{ext}^k &= \int_{\Omega_k} \left[\delta \left(F_s u_{xs}^k \right) \, p_x^{top} + \delta \left(F_s u_{ys}^k \right) \, p_y^{top} + \delta \left(F_s u_{zs}^k \right) \, p_z^{top} \right] \, d\Omega_k \\ &= \int_{\Omega_k} \left[\delta u_{xs}^k \, F_s \, p_x^{top} + \delta u_{ys}^k \, F_s \, p_y^{top} + \delta u_{zs}^k \, F_s \, p_z^{top} \right] \, d\Omega_k \\ &= \int_{\Omega_k} \delta \mathbf{u}_s^{k^T} F_s \left\{ p_x \; p_y \; p_z \right\} \, d\Omega_k \end{aligned} \tag{11.17}$$

In the following a transverse pressure on the top of a plate can be considered; in this case is

$$\delta \, L_{ext}^k = \int_{\Omega_k} \delta \mathbf{u}_s^{k^T} F_s \left(\frac{h_k}{2} \right) \left\{ 0 \; 0 \; p_z^{top} \right\} \, d\Omega_k = \int_{\Omega_k} \delta \mathbf{u}_s^T \mathbf{P}_{u\tau}^k \tag{11.18}$$

where h_k is the thickness of the generic k layer, p_z^{top} is the transverse pressure distribution over the top surface of the plate and $\mathbf{P}_{u\tau}^k = F_s \left(\frac{h_k}{2} \right) \{0 \; 0 \; p_z^{top}\}$. In this case the PVD can be written as

$$\sum_{k=1}^{N_L} \int_{\Omega_k} \delta \mathbf{u}_s^{k^T} \mathbf{K}_{uu}^{\tau s} \mathbf{u}_\tau + \sum_{k=1}^{N_L} \int_{\Gamma_k} \delta \mathbf{u}_s^{k^T} \mathbf{\Pi}_{uu}^{\tau s} \mathbf{u}_\tau = \sum_{k=1}^{N_L} \int_{\Omega_k} \delta \mathbf{u}_s^{k^T} \mathbf{P}_{u\tau}^k \tag{11.19}$$

The governing equations can be synthetically written as

$$\delta \mathbf{u}_s^{k^T} \; : \; \mathbf{K}_{uu}^{\tau s} \mathbf{u}_\tau^k = \mathbf{P}_{u\tau}^\tau \tag{11.20}$$

and the boundary conditions are

$$\delta \mathbf{u}_s^{k^T} \; : \; \mathbf{\Pi}_{uu}^{k\tau s} \mathbf{u}_\tau^k = \mathbf{\Pi}_{uu}^{k\tau s} \overline{\mathbf{u}}_\tau^k \tag{11.21}$$

being

$$\begin{aligned}\mathbf{K}_{uu}^{\tau\, s} = &\Big\{(-\mathbf{D}_p)^T \left[\mathbf{C}_{pp}^k E_{\tau s}\, \mathbf{D}_p + \mathbf{C}_{pn}^k E_{\tau s} \mathbf{D}_{n\Omega} + \mathbf{C}_{pn}^k E_{\tau_{,z} s}\right] + \\ &(-\mathbf{D}_{n\Omega})^T \left[\mathbf{C}_{np}^k E_{\tau s} \mathbf{D}_p + \mathbf{C}_{nn}^k E_{\tau s} \mathbf{D}_{n\Omega} + \mathbf{C}_{nn}^k E_{\tau_{,z} s}\right] + \\ &+ \left[\mathbf{C}_{np}^k E_{\tau s_{,z}} \mathbf{D}_p + \mathbf{C}_{nn}^k E_{\tau s_{,z}} \mathbf{D}_{n\Omega} + \mathbf{C}_{nn}^k E_{\tau_{,z} s_{,z}}\right]\Big\}\end{aligned} \tag{11.22}$$

The fundamental nucleus, $\mathbf{K}_{uu}^{\tau\, s}$ is assembled through the depicted indexes,τ and s, which consider the order of the expansion in z for the displacements. For boundary condition it is

$$\begin{aligned}\mathbf{\Pi}_{uu}^{k\,\tau\, s} = &\Big\{(\mathbf{I}_p)^T \left[\mathbf{C}_{pp}^k E_{s\tau}\, \mathbf{D}_p + \mathbf{C}_{pn}^k E_{s\tau} \mathbf{D}_{n\Omega} + \mathbf{C}_{pn}^k E_{s\tau_{,z}}\right] + \\ &+ (\mathbf{I}_{n\Omega})^T \left[\mathbf{C}_{np}^k E_{s\tau} \mathbf{D}_p + \mathbf{C}_{nn}^k E_{s\tau} \mathbf{D}_{n\Omega} + \mathbf{C}_{nn}^k E_{s\tau_{,z}}\right]\Big\}\end{aligned} \tag{11.23}$$

The terms of the components of the operator $K_{uu}^{\tau s}$ reported in eq. 11.22 are here developed

$$\begin{aligned}
K_{11}^{k\tau s} =& C_{55}^k E_{\tau_{,z} s_{,z}} - E_{\tau s}\partial_{,x}(C_{11}^k \partial_{,x} + C_{16}^k \partial_{,y}) - E_{\tau s}\partial_{,y}(C_{16}^k \partial_{,x} + C_{66}^k \partial_{,y}) \\
K_{12}^{k\tau s} =& C_{54}^k E_{\tau_{,z} s_{,z}} - E_{\tau s}\partial_{,x}(C_{16}^k \partial_{,x} + C_{12}^k \partial_{,y}) - E_{\tau s}\partial_{,y}(C_{26}^k \partial_{,y} + C_{66}^k \partial_{,x}) \\
K_{13}^{k\tau s} =& E_{\tau s_{,z}}(C_{55}^k \partial_{,x} + C_{54}^k \partial_{,y}) - C13 E_{\tau_{,z} s}\partial_{,x} - C_{36}^k E_{\tau_{,z} s}\partial_{,y} \\
K_{21}^{k\tau s} =& C_{45}^k E_{\tau_{,z} s_{,z}} - E_{\tau s}\partial_{,y}(C_{21}^k \partial_{,x} + C_{26}^k \partial_{,y}) - E_{\tau s}\partial_{,x}(C_{16}^k \partial_{,x} + C_{66}^k \partial_{,y}) \\
K_{22}^{k\tau s} =& C_{44}^k E_{\tau_{,z} s_{,z}} - E_{\tau s}\partial_{,y}(C_{26}^k \partial_{,x} + C22 \partial_{,y}) - E_{\tau s}\partial_{,x}(C_{26}^k \partial_{,y} + C_{66}^k \partial_{,x}) \\
K_{23}^{k\tau s} =& E_{\tau s_{,z}}(C_{45}^k \partial_{,x} + C_{44}^k \partial_{,y}) - C_{23}^k E_{\tau_{,z} s}\partial_{,y} - C_{36}^k E_{\tau_{,z} s}\partial_{,x} \\
K_{31}^{k\tau s} =& E_{\tau s_{,z}}(C13 \partial_{,x} + C_{36}^k \partial_{,y}) - C_{45}^k E_{\tau_{,z} s}\partial_{,y} - C_{55}^k E_{\tau_{,z} s}\partial_{,x} \\
K_{32}^{k\tau s} =& E_{\tau s_{,z}}(C_{23}^k \partial_{,y} + C_{36}^k \partial_{,x}) - C_{44}^k E_{\tau_{,z} s}\partial_{,y} - C_{54}^k E_{\tau_{,z} s}\partial_{,x} \\
K_{33}^{k\tau s} =& C33 E_{\tau_{,z} s_{,z}} - E_{\tau s}\partial_{,y}(C_{45}^k \partial_{,x} + C_{44}^k \partial_{,y}) - E_{\tau s}\partial_{,x}(C_{55}^k \partial_{,x} + C_{54}^k \partial_{,y})
\end{aligned} \tag{11.24}$$

considering an orthotropic material it is

$$
\begin{aligned}
K_{11}^{k\tau s} =& - C_{11}^{k} E_{\tau s} \partial_{,x}^{2} - C_{66}^{k} E_{\tau s} \partial_{,y}^{2} + C_{55}^{k} E_{\tau_{,z} s_{,z}} \\
K_{12}^{k\tau s} =& - C_{12}^{k} E_{\tau s} \partial_{,xy}^{2} - C_{66}^{k} E_{\tau s} \partial_{,xy}^{2} \\
K_{13}^{k\tau s} =& C_{55}^{k} E_{\tau s_{,z}} \partial_{,x} - C_{13}^{k} E_{\tau_{,z} s} \partial_{,x} \\
K_{21}^{k\tau s} =& - C_{21}^{k} E_{\tau s} \partial_{,xy}^{2} - C_{66}^{k} E_{\tau s} \partial_{,xy}^{2} \\
K_{22}^{k\tau s} =& - C_{66}^{k} E_{\tau s} \partial_{,x}^{2} - C_{22}^{k} E_{\tau s} \partial_{,y}^{2} + C_{44}^{k} E_{\tau_{,z} s_{,z}} \\
K_{23}^{k\tau s} =& C_{44}^{k} E_{\tau s_{,z}} \partial_{,y} - C_{23}^{k} E_{\tau_{,z} s} \partial_{,y} \\
K_{31}^{k\tau s} =& C_{13}^{k} E_{\tau s_{,z}} \partial_{,x} - C_{55}^{k} E_{\tau_{,z} s} \partial_{,x} \\
K_{32}^{k\tau s} =& C_{23}^{k} E_{\tau s_{,z}} \partial_{,y} - C_{44}^{k} E_{\tau_{,z} s} \partial_{,y} \\
K_{33}^{k\tau s} =& - C_{55}^{k} E_{\tau s} \partial_{,x}^{2} - C_{44}^{k} E_{\tau s} \partial_{,y}^{2} + C_{33}^{k} E_{\tau_{,z} s_{,z}}
\end{aligned}
\tag{11.25}
$$

If a simply supported orthotropic plate is analyzed, the Navier solution can be considered. The components of the vector $\mathbf{u}_{\tau}^{k}$ are defined as

$$
\begin{aligned}
u_{x\tau}^{k} &= \hat{U}_{x\tau} \cos\left(\frac{m\pi\, x}{a}\right) \sin\left(\frac{n\pi\, y}{b}\right) \\
u_{y\tau}^{k} &= \hat{U}_{y\tau} \sin\left(\frac{m\pi\, x}{a}\right) \cos\left(\frac{n\pi\, y}{b}\right) \\
u_{z\tau}^{k} &= \hat{U}_{z\tau} \sin\left(\frac{m\pi\, x}{a}\right) \sin\left(\frac{n\pi\, y}{b}\right)
\end{aligned}
\tag{11.26}
$$

$\hat{U}_{x\tau}$, $\hat{U}_{y\tau}$ and $\hat{U}_{z\tau}$ are the amplitudes, m and n are the number of waves (they go from 0 to ∞) and a and b are the dimensions of the plate. Let us define the quantities

$$
\alpha = \frac{m\,\pi}{a^{k}} \qquad \beta = \frac{n\,\pi}{b^{k}} \tag{11.27}
$$

where a^{k} and b^{k} are the length of the generic k layer. The solution of the equation 11.20 can be obtained by solving the algebraic system

$$
\delta \mathbf{u}_{s}^{k^{T}} \,:\, \mathbf{K}_{uu}^{\tau s} \hat{\mathbf{U}}_{\tau}^{k} = \mathbf{P}_{u\tau}^{\tau} \tag{11.28}
$$

Each term of the fundamental nucleus $\mathbf{K}_{uu}^{\tau s}$ can be expressed as

$$
\begin{aligned}
K_{11}^{k\tau s} =& C_{11}^{k}\, E_{\tau\, s}\alpha^2 + C_{66}^{k}\, E_{\tau\, s}\beta^2 + C_{55}^{k} E_{\tau, z\, s, z} \\
K_{12}^{k\tau s} =& C_{12}^{k}\, E_{\tau\, s}\alpha\beta + C_{66}^{k}\, E_{\tau\, s}\alpha\beta \\
K_{13}^{k\tau s} =& -C_{13}^{k} E_{\tau, z\, s}\alpha + C_{55}^{k} E_{\tau\, s, z}\alpha \\
K_{21}^{k\tau s} =& C_{12}^{k}\, E_{\tau\, s}\alpha\beta + C_{66}^{k}\, E_{\tau\, s}\alpha\beta \\
K_{22}^{k\tau s} =& C_{22}^{k}\, E_{\tau\, s}\beta^2 + C_{66}^{k}\, E_{\tau\, s}\alpha^2 + C_{44}^{k} E_{\tau, z\, s, z} \\
K_{23}^{k\tau s} =& -C_{23}^{k} E_{\tau, z\, s}\beta + C_{44}^{k} E_{\tau\, s, z}\beta \\
K_{31}^{k\tau s} =& C_{55}^{k} E_{\tau, z\, s}\alpha - C_{13}^{k} E_{\tau\, s, z}\alpha \\
K_{32}^{k\tau s} =& C_{44}^{k} E_{\tau, z\, s}\beta - C_{23}^{k} E_{\tau\, s, z}\beta \\
K_{33}^{k\tau s} =& C_{55}^{k}\, E_{\tau\, s}\alpha^2 + C_{44}^{k}\, E_{\tau\, s}\beta^2 + C_{33}^{k} E_{\tau, z\, s, z}
\end{aligned}
\tag{11.29}
$$

The boundary conditions are satisfied since the Navier closed form solution is employed.

Bibliography

[1] Kraus., H. *Thin Elastic Shells.* John Wiley & Sons, 1967.

[2] Cauchy, A. L. "Sur l'équilibre et le mouvement d'une plaque solide". *Exercises de Matematique* , 3:328–355, 1828.

[3] Poisson, S. D. "Memoire sur l'équilibre et le mouvement des corps elastique" *Mémoires de l'Académie Royale des Sciences de l'Institut de France* , 8:51–88, 1829.

[4] Kirchhoff,G. "Uber das gleichgewicht und die bewegung einer elastischen scheibe" *Journal fur reins und angewandte Mathematik* , 40:51–88, 1850. doi: 10.1515/crll.1850.40.51.

[5] Love, A. E. H. *The Mathematical Theory of Elasticity* . Cambridge University Press, Cambridge, 1927.

[6] Carrera, E. C_z^0 requirements - models for the two dimensional analysis of multilayered structures. *Composite Structures*, 37(3-4):373–383, 1997. http://dx.doi.org/10.1016/S0263-8223(98)80005-6.

[7] Ambartsumian., S. A. Contributions to the theory of anisotropic layered shells. *Applied Mechanics Reviews*, 15(4), 1962.

[8] Ambartsumian., S. A. *Theory of Anisotropic Shells.* Fizmatzig, Moskwa, 1961. Translated from Russian, NASA TTF-118.

[9] Ambartsumian., S. A. *Fragments of the Theory of Anisotropic Shells.* World Scientific Publishing Co., Singapore, 1991. Technomic Publishing Company, Translated from Russian, Moskwa.

[10] Grigolyuk, E. I. and Kogan, F.A. The present status of the thoery of multilayered shells. *Prikl. Mekh.*, 8:3–17, 1972.

[11] Kapania, R.K. A review on the analysis of laminated shells. *ASME J. Pressure Vessel Technol.*, 111(2):88–96, 1989. doi: 10.1515/crll.1850.40.51.

[12] Grigolyuk, E. I. and Kulikov, G. M. General directions of the development of theory of shells. *Mechanics of Composite Materials*, 24(2):231–241, 1988. doi: 10.1515/crll.1850.40.51.

[13] Noor, A. K., Burton, W. S., and Bert, C. W. Computational model for sandwich panels and shells. *Applied Mechanics Reviews*, 49(3):155–199, 1996. doi: 10.1115/1.3101923.

[14] Fettahlioglu, O. A. and Steele, C. R. Asymptotic solutions for orthotropic nonhomogeneous shells of revolution. *Journal of Applied Mechanics*, 41(3):753–758, 1974. doi: 10.1115/1.3423383.

[15] Berdichevsky, V. L. Variational-asymptotic method of shell theory construction. *Prikladnaya Matematika i Mekhanika*, 43:664–667, 1979.

[16] Berdichevsky, V. L. and Misyura, V. Effect of accuracy loss in classical shell theory. *Journal of Applied Mechanics*, 59(2):217–223, 1992. doi: 10.1115/1.2899492.

[17] Carrera, E. Developments, ideas and evaluations based upon the Reissner's mixed variational theorem in the modeling of multilayered plates and shells. *Applied Mechanics Reviews*, 54:301–329, 2001.

[18] Carrera, E. Theories and Finite elements for multilayered anisotropic, composite plates and shells. *Archives of Computational Methods in Engineering*, 9:87–140, 2002.

[19] Carrera, E. Historical review of zig-zag theories for multilayered plates and shells. *Applied Mechanics Reviews*, 56:287–308, 2003.

[20] Carrera, E. Theories and Finite elements for multilayered plates and shells: a unified compact formulation with numerical assessment and benchmarking. *Archives of Computational Methods in Engineering*, 10:215–296, 2003.

[21] Reddy, J. N. *Mechanics of Laminated Plates, Theory and Analysis* . CRC Press, Boca Raton, 1997.

[22] Ambartsumian, S. A. Contributions to the theory of anisotropic layered shells. *Applied Mechanics Reviews*, 15(4), 1962.

[23] Librescu, L. and Reddy, J.N. *A critical Review and Generalization of Transverse Shear Deformable Anisotropic Plates, Euromech Colloquium 219, Kassel. Refined Dynamical Theories of Beams, Plates and Shells and Their Applications.* I. Elishakoff and H. Irretier, Springer-Verlag, Berlin, 1986.

[24] Noor, A. K. and Burton,W. S. Assessment of shear deformation theories for multilayered composite plates. *Applied Mechanics Reviews*, 42(1):1–18, 1989. doi: 10.1115/1.3152418.

[25] Hetnarski, R. B. and Eslami, M. R. *Thermal Stresses - Advanced Theory and Applications.* Editors, Barber, J. R., Klarbring, Anders, Vol 158, 2009.

[26] Duhamel, J. M. C. Second memoire sur les phenomenes thermomecaniques *J. de l'Ecole Polytechnique*, Vol. 15(25): 1–57,1837

[27] Navier, C.L.M.H. Memoire sur les lois de l'equilibre et du movement des corps solides elastiques *Mem. Acad. Sci.*, Paris, Vol. 7:375–393, 1827.

[28] Fourier, J.B.J. Theorie analytique de la chaleur *Firmin Didot*,Paris,1822.

[29] Neumann, F. Vorlesung uber die Theorie des Elasticitat der festen Korper und des Lichtathers *Teubner*, Leipzig, 1885.

[30] Almansi, E. Use of the Stress Function in Thermoelasticity *Mem. Reale Accad. Sci. Torino*, Vol 47(2), 1897.

[31] Tedone, O. Allgemeine Theoreme der matematischen Elastizitatslehre (Integrationstheorie) *Encyklopadie der matematischen Wissenschaften*, Vol. 4, Part D, pp. 55–124 and pp. 125–214(second article written with A. Timpe.), 1906.

[32] Voigt, W. Lehrbuch der Kristallphysik *Teubner*, Berlin, 1910.

[33] Tauchert, T.R. . Thermally induced flexure, buckling, and vibration of plates. *Applied Mechanics Reviews*, vol. 44, num. 8, pp. 347–360, 1991.

[34] Noor, A.K. and Burton., W.S. Computational models for high-temperature multilayered composite plates and shells. *Applied Mechanics Reviews*, vol. 12, num. 10, pp. 419–446, 1992.

[35] Argyris,J. and Tenek,L. Recent advances in computational thermostructural analysis of composite plates and shells with strong nonlinearities. *Applied Mechanics Reviews*, vol. 50, num. 5, pp. 285–306, 1997.

[36] Bhaskar, K., Varadan, T.K., and Ali, J.S.M. Thermoelastic solutions for orthotropic and anisotropic composite laminates. *Composites*, vol. 27B, pp. 415–420, 1996.

[37] Murakami, H. Assessment of plate theories for treating the thermomechanical response of layered plates. *Composites Engineering*, vol. 3, num. 2, pp. 137–149, 1993.

[38] Curie, J. and Curie, P. D'eveloppement par compression de l'électricité polaire dans les cristaux hémiédres a faces inclinées. C. R. Acad. Sci. Paris, 91:294–295, 1880.

[39] Cady, W.G. *Piezoelectricity*. Dover, 1964.

[40] Tiersten, H.F. *Linear Piezoelectric Plate Vibrations*. Plenum Press, 1969.

[41] Ikeda, T. *Fundamentals of Piezoelectricity*. Oxford University Press, 1996.

[42] Ahmad, I. Smart structures and materials. in proceedings of us army research office workshop on smart materials, structures and mathematical issues. 1988.

[43] Sirohi, J. and Chopra, I. Fundamental understanding of piezoelectric strain sensors. *J. Intell. Mater. Syst. Struct.*, 11:246–257, 2000.

[44] Saravanos, D. and Heyliger, P. Mechanics and computational models for laminated piezoelectric beams, plates and shells. *Appl Mech Rev*, 52(10):305–320, 1999.

[45] Benjeddou, A. Advances in piezoelectric finite element modeling of adaptive structural elements: a survey. *Computer & Structures*, 76(1-3):347–63, 2000.

[46] A.N.S. Institute. Ieee standard on piezoelectricity. Technical Report NASA CR 4665, IEEE, March 1987.

[47] Cicala, P. Sulla teoria elastica della parete sottile. *Giornale del Genio Civile*, 97(4-6-9):238–256,429–449, 714–723, 1959

[48] Cicala, P. *Systematic Approach to Linear Shell Theory* . Levrotto & Bella, Torino (Italy), 1965.

[49] Carrera, E. and Petrolo, M. "Guidelines and recommendation to construct theories for metallic and composite plates" *AIAA Journal* , 48(12):2852–2866, 2010. doi: 10.2514/1.J050316.

[50] Carrera, E. and Brischetto, S. "Analysis of thickness locking in classical, refined and mixed multilayered plate theories" *Composite Structures* , 82(4):549 – 562, 2008. doi: http://dx.doi.org/10.1016/j.compstruct.2007.02.002.

[51] Carrera, E., Brischetto, S. and Nali, P., "Variational statements and computational models for multifield problems and multilayered structures" *Mechanics of Advanced Materials and Structures* , 15(3):182–198, 2008.

[52] Nowinski, J. L. *Theory of Thermoelasticity with Applications* . Sijthoff and Noordhoff, The Netherlands, 1978.

[53] Carrera, E., Brischetto, S., "Coupled thermo-mechanical analysis of one-layered and multilayered plates" *Composite Structures* , 92:1793–1812, 2010.

[54] Carrera, E. Temperature profile influence on layered plates response considering classical and advanced theories. *AIAA Journal*, vol. 40, num. 9, pp. 1885–1896, 2002.

[55] Ballhause, D. and D'Ottavio, M. and Kroplin, B. and Carrera, E. A unified formulation to assess multilayered theories for piezoelectric plates. *Computer & Structures*, 83:1217–1235, 2005.

[56] Carrera, E., Brischetto, S. and Nali, P. *Plates and Shells for Smart Structures Classical and Advanced Theories for Modeling and Analysis* . Wiley, New Delhi, 2011.

[57] Carrera, E, Giunta,G, and Belouettar,S. A refined beam theory with only displacement variables and deformable cross-section. In *50th AIAA/ASME/ASCE/AHS/ASC Structures, Structural Dynamics, and Materials Conference*, Palm Springs, CA, 4-7 May 2009.

[58] Carrera,E., Giunta, G., and Brischetto, S. Hierarchical closed form solutions for plates bent by localized transverse loadings. *Journal of Zhejiang University Science B*, 8(7):1026–1037, 2007. doi:10.1631/jzus.2007.A1026.

[59] Carrera, E. and Giunta., G. Hierarchical models for failure analysis of plates bent by distributed and localized transverse loadings. *Journal of Zhejiang University Science A*, 9(5):600–613, 2008. doi:10.1631/jzus.A072110.

[60] Pagano, N. J. "Exact solutions for rectangular bidirectional composites and sandwich plate" *Journal of Composites Material* , 4:20–34, 1969.

[61] Pagano, N. J. and Hatfield, S. J. "Elastic Behavior of Multilayered Bidirectional Composites" *AIAA Journal* , 10(7):931–933, 1972

[62] Varadan, T.K. and Bhaskar, K. Bending of laminated orthotropic cylindrical shells - an elasticity approach. *Composite Structures*, 17:141–156, 1991.

[63] Heyliger, P. Static Behavior of Laminated Elastic/Piezoelectric Plates *AIAA Journal*, 32(12):2481–2484, 1994.

[64] Reissner, E. "The effect of transverse shear deformation on the bending of elastic plates" *Journal of Applied Mechanics* , 12:69–76, 1945. doi: 10.1515/crll.1850.40.51.

[65] Mindlin, R. D. "Influence of rotatory inertia and shear in flexural motions of isotropic elastic plates" *Journal of Applied Mechanics* , 18:1031–1036, 1951. doi: 10.1515/crll.1850.40.51.

[66] Vlasov, B. F. "On the equations of bending of plates" *Doklady Akademii Nauk Azerbaidzhanskoi SSR* , 3:955–979, 1957. doi: 10.1515/crll.1850.40.51.

[67] Hildebrand, F.B., Reissner, E. and Thomas, G.B. "Notes in the foundations of the theory of small displacement of orthotropic shells" Technical report, NASA, March.

[68] Carrera, E. and Petrolo, M. "On the effectiveness of higher-order terms in refined beam theories" *Journal of Applied Mechanics* , 78:1–17, 2011.

[69] Petrolo, M. and Lamberti, A. "Axiomatic/asymptotic analysis of refined layer-wise theories for composite and sandwich plates" *Mechanics of Advanced Materials and Structures* , 2013. In press.

[70] Mashat D.S., Carrera, E., Zenkour, A.M., Al Khateeb, S.A. and Lamberti, A. "Evaluation of refined theories for multilayered shells via Axiomatic/Asymptotic method" *Journal of Mechanical Science and Technology* , 38(11): 1–10, 2014. doi: 10.1007/s12206-014-1033-2

[71] Mashat, D.S., Carrera, E., Zenkour, A.M. and Al Khateeb, S.A. "Axiomatic/asymptotic evaluation of multilayered plate theories by using single and multi-points error criteria" *Composite Structures* , 106(0):393–406, 2013. doi: http://dx.doi.org/10.1016/j.compstruct.2013.05.047.

[72] Carrera, E., Cinefra, M., Lamberti, A. and Zenkour, A.M. "Axiomatic/Asymptotic Evaluation of Refined Plate Models for Thermomechanical Analysis" *Journal of Thermal Stresses* , 38(2): 165-187, 2015. doi: 10.1080/01495739.2014.976141.

[73] Cinefra M., Lamberti A., Carrera E. Axiomatic/Asymptotic Analysis of Refined Models for Thermal Stress Analysis of Plates In *11th World Congress on Computational Mechanics WCCM XI, 5th European Conference on Computational Mechanics ECCM V, 6th European Conference on Computational Fluid Dynamics ECFD VI* , Barcelona, Spain, 20-25 July 2014.

[74] Cinefra, M., Lamberti, A., Zenkour, A.M. and Carrera, E. "Axiomatic/asymptotic technique applied to refined theories for piezoelectric plates " *Mechanics of advanced materials and structures* , 0, 1-18, 2014.

[75] Carrera, E. and Miglioretti, F. "Selection of appropriate multilayered plate theories by using a genetic like algorithm" *Composite Structures* , 94(3):1175 – 1186, 2012. doi: http://dx.doi.org/10.1016/j.compstruct.2011.10.013.

[76] Petrolo, M., Cinefra, M., Lamberti, A. and Carrera, E. "Evaluation of Mixed Theories for Laminated Plates through the Axiomatic/Asymptotic Method" *Composites part B: Engineering* , In press.

[77] Darwin, C. R. *On the origin of species by means of natural selection, or the preservation of favored races in the struggle for life.* John Murray, London, 1859.

[78] Fonseca, M. and Fleming, P. "Genetic algorithm for multiobjective optimization: formulation, discussion and generalization" In *Genetic algorithms: proceedings of the fifth international conference* , 1993.

[79] Carrera, E., Giunta, G., and Brischetto, S. Hierarchical closed form solutions for plates bent by localized transverse loadings. *Journal of Zhejiang University Science B*, 8(7):1026–1037, 2007. doi:10.1631/jzus.2007.A1026.

[80] Carrera, E. and Giunta, G. Hierarchical models for failure analysis of plates bent by distributed and localized transverse loadings. *Journal of Zhejiang University Science A*, 9(5):600–613, 2008. doi:10.1631/jzus.A072110.

[81] Pandya, B. and Kant, T. "Finite element analysis of laminated compiste plates using high-order displacement model" *Compos Sci Technol* , 32:137–55, 1988.

[82] Kant, T. and Manjunatha, B. "An unsymmetric FRC laminate C^0 finite element model with 12 degrees of freedom per node" *Eng Comput* , 5(3):292–308, 1988.

[83] Carrera, E., Petrolo, M., Miglioretti, F. and Lamberti, A. "Best Theory Diagram of Metallic and Laminated Composite Plates" *Journal of Composite Material* , In press

[84] Carrera, E., Giunta, G. and Petrolo, M. *Beam Structures, Classical and Advanced Theories* . Wiley, New Delhi, 2011.

[85] Miglioretti, F., Carrera, E. and Petrolo, M. "Accuracy of refined finite elements for laminated plate analysis" *Composite Structures* , 93:1311–1327, 2010. doi: 10.1016/j.compstruct.2010.11.007.

[86] Miglioretti, F., Carrera, E. and Petrolo, M. "Computations and evaluations of higher order theories for free vibration analysis of beams" *Journal of Sound and Vibration* , 331, 2012.

[87] Mashat, D.S., Carrera, E., Zenkour, A.M. and Al Khateeb, S.A. "Use of axiomatic/asymptotic approach to evaluate various refined theories for sandwich shells" *Composite Structures* , 109(0):139–149, 2013. doi: http://dx.doi.org/10.1016/j.compstruct.2013.10.046.